ROYAL INSTITUTE
OF TECHNOLOGY

Geoid Model of Tanzania from Sparse and Varying Gravity Data Density by the KTH Method

Prosper E. Ulotu

Doctoral Dissertation in Geodesy

Royal Institute of Technology (KTH)
Department of Transport and Economics
Division of Geodesy

100 44 Stockholm, Sweden

May, 2009

Prosper E Ulotu Geoid Model of Tanzania from Sparse and Varying Gravity Data Density by the KTH Method

Supervisor:
Prof. Lars E Sjöberg

Faculty Opponent:
Prof. Hossein Nahavandchi
Norwegian University of Science and Technology (NTNU), Norway

Evaluation Committee:
Prof. Artu Ellmann
Tallinn University of Technology, ESTONIA

Prof. Dan Dyrelius
Department of Earth Sciences, Geophysics, Uppsala

Dr. Stig-Göran Mårtensson
University of Gävle, Sweden

Royal Institute of Technology (KTH)
School of Architecture and Built Environment
Department of Transport and Economics
Division of Geodesy
SE 100 44 Stockholm, Sweden

Printed by the Universitetsservice US-AB
Stockholm, 2009

TRITA -TEC-PHD09-002 ◁▷ ISSN 1653-4468 ◁▷ ISBN 978-91-7415-318-7

Abstract

Developed countries are striving to achieve a cm geoid model. Most developing countries/regions think that the situation in their areas does not allow even a few decimetre geoid model. GNSS, which provides us with position, is one of the greatest achievements of the present time. Conversion of ellipsoidal height to orthometric height, which is more useful, requires an accurate geoid model.

In spite of the sparse terrestrial gravity data of variable density, distribution and quality (a typical situation in developing countries), this study set out to develop as accurately as possibly achievable, a high quality geoid model of Tanzania. Literature review of three more preferred geoid methods came to a conclusion, that the Royal Institute of Technology of Sweden (KTH) method of least squares modification of Stokes formula (LSMS) with additive corrections (AC) is the most suitable for this research. However, even with a good method, the accuracy and the quality of a geoid model depend much on the quality of the data.

In this study, a procedure to create a gravity database (GDB) out of sparse data with varying density, distribution and quality has been developed. This GDB is of high density and full coverage, which ensures presence of high and low gravity frequencies, with medium frequencies ranging between fair and excellent. Also an alternative local/regional Global Gravitational Model (GGM) validation method based on quality terrestrial point surface gravity anomaly has been developed. Validation of a GGM using the new approach of terrestrial point gravity and GPS/Levelling, gave the same results. Once satisfactorily proved, the method has extra advantages. The limits of Tanzania GDB (TGDB) are latitudes $15^{\circ}S$ to $4^{\circ}N$ and longitudes $26^{\circ}E$ to $44^{\circ}E$. Cleaning and quality control of the TGDB was based on the cross validation (XV) by the Kriging method and Gaussian distribution of the XV residuals.

The data used in the LSMS with AC to develop a new Tanzania gravimetric geoid model 2008, TZG08, are $1' \times 1'$ clean and statistically tested surface gravity anomalies. 39,677 point gravity in land and 57,723 in the ocean were utilised. Pure satellite ITG-GRACE03S GGM to degree 120 was used to determine modification parameters and long-wavelength component of the geoid model. $3''$ Shuttle Radar Topographic Mission (SRTM) Digital Elevation Model (DEM), ITG-GRACE03S to degree 120 and EIGEN-CG03C to degree 360 combined GGM qualified to patch the data voids in accordance to the method of this research. TZG08 is referred to Geodetic Reference System 1980 (GRS80), and its extents are latitudes $12^{\circ}S$ to $1^{\circ}N$ and longitudes $29^{\circ}E$ to $41^{\circ}E$.

19 GPS/levelling points qualified to assess the overall accuracy of TZG08 as 29.7 cm, and upon approximate removal of GPS and orthometric systematic effects, the accuracy of TZG08 is 27.8 cm. A corrector surface (CS) for conversion of GPS height to orthometric height referred to Tanzania National Height Datum (TNHD) has been created for a part of TZG08. Using the CS and TZG08, orthometric height of Mt. Kilimanjaro is re-established as it was in 1952 to be 5,895 m above the TNHD, which is still the official height of the mountain.

Keywords: Geoid, sparse gravity data, gravity database, GGM validation by gravity, corrector surface, hybrid geoid, KTH-LSMS with AC, Mt. Kilimanjaro, Tanzania.

Dedication

My late dear mother Angelina E Ulotu (1928- 06.01.2009) and brother Leonard E Ulotu (1951-04.01.2009) never got tired praying for my successful end, but GOD ALMIGHTY had better intentions by taking both of them away from this world at the same time when I was at the culmination, it will never be the same again. Ps 89:48, Gn 3:19.

Job 1:21: "Said I was born with nothing, and I will die with nothing. The Lord gave, and now he has taken away. May his name be praised".

Acknowledgement

First and foremost, my profound gratitude is to my sole supervisor Professor Lars E. Sjöberg. His invaluable intellectual guidance, professional discussions and advices, patience, flexibility and availability have been very inspirational and instrumental to the successful end of this study. I feel privileged and honoured to have him as my supervisor.

I am also very grateful to Dr. Jonas Ågren of the National Land Survey of Sweden, for wonderful assistance with the management of SRTM-DEM, KTH-Geolab and many impromptu discussions.

I am deeply indebted to Mr. Erick Asenjo, who has been very helpful with many issues. His assistance with GPS/levelling observations in Tanzania in 2007 and processing at KTH, taking and waiting for me at the Karolinska hospital when I fell sick in July 2008, are just a few clear examples of a dear friend.

I sincerely thank all my former and present staff members and graduate students at the Division of Geodesy for the discussions we had and many other issues, which can not be listed here all. Special thanks go to Dr. Ramin Kiamehr, for introduction to valuable geodetic sites, programs and KTH-Geolab, Dr. Huaan Fan, Dr. Milan Horemuz, Mr. Eshagh Mehdi, Ms. Uliana Danila, Dr. Yuriy Reshetyuk and Ms. W. Solveig.

I am indebted to individuals and institutions which provided me either with data, computer software or information, especially Professor C. C. Tscherning and Dr. R. Forsberg for the Gravsoft package, Dr. Bernard Langellier - BGI for most of the land and sea point gravity data, Dr. Ole Andersen for the KMS02 altimetry data, Professor C.L. Merry - Capetown Univ. for the AGP data and material, Mr. J. Saburi - ARU for most of the gravity data from Tanzania, Professor J. D. Fairhead - GETECH Leeds Univ. for mean gravity anomaly. Also Dr. I. Marobhe - UDSM, Professor E. Calais - Purdue Univ., Professor C. Ebinger - Rochester Univ., Dr. J.G. Olliver - UK, and Mr. W. Shija, Mr. J. Msemwa and Mr. Z.Y. Maselle of the Ministry of Lands Tanzania.

I am very thankful to all my old and new colleagues at the Department of Geomatics - ARU, for physical and moral support, no one mentioned, no one forgotten.

I am very much indebted to Dr. John Lupala, Professor Jackson Msafiri and Professor Dick Urban Vestbro who not only draw my attention to the joint Sida/SAREC-UCLAS programme, but also helped me to get onboard. I highly value the assistance of the former and present Sida/SAREC coordinators and co-coordinator.

Without the financial support from Sida-SAREC of Sweden and my employer ARU, this study would not have become a reality, I am deeply and sincerely grateful.

I sincerely thank my family and relatives for the inspirational moral support and encouragement, especially my dear wife Naomi, my children; Nicole-Neema, Rudolf-Shekia and Harold-Sereki, my long absence must have had a lasting effect on your lives. It is my hope I will have more time with you for you hereafter.

GOD Almighty, you are all LOVE, praise and glory to you most gracious, most merciful in the mighty name of my LORD Jesus Christ. All I can do is to say THANK YOU.

Prosper E. Ulotu
Stockholm, December 2008

Table of Contents

List of Figures

List of Tables

Acronyms

AC	Additive Corrections
AGP	African Geoid Project
AGP2003	African Geoid Model 2003
AGP2006	African Geoid Model 2006
aMSL	above Mean Sea Level
AOI	research Area Of Interest
ARU	Ardhi University
ARUDB	Ardhi University gravity Data Base
AWK/awk	Computer pattern scanning and processing language
Bash/bash	Born again shell; a shell is a command language interpreter
BGI	Bureau Gravimetrique International
BLWN	Band Limited White Noise
BLWN_RD	Composite/combined BLWN and RD
BM	Benchmark
BVP	Boundary Value Problem
CD	Computational Distance
CDC	Committee for Developing Countries
CGIAR	Consultative Group for International Agricultural Research
CHAMP	CHAllenging Mini-satellite Payload
CI, CL	Confidence Interval, Confidence Level
CP	Computation Point
CS	Corrector Surface
CSH/Csh/csh	C++ shell
CSI	Consortium for Spatial Information
CSR	Centre for Space Research
CYGWIN	CYGnus unix solutions for MS WINdows
DEM	Digital Elevation Model
DEMs	Digital Elevation Models
DG	David Gil terrain lister executable code
dg_GGM	Gravity anomaly computed from a GGM
dg_surf	Surface gravity anomaly

dg_surf.res	Residual point surface gravity anomaly
dgL_surf	Land point surface gravity anomaly
dgS_surf	Sea surface gravity anomaly
DLR	German Aerospace Centre
DNSC	Danish National Space Centre
DOS	Disk Operating System
DR-Congo	Democratic Republic of Congo
DTM	Digital Terrain Model
DTMs	Digital Terrain Models
DTU	Technical University of Denmark
DWC/dwc	DownWard Continuation
EARVS	East Africa Rift Valley System
ECAGN	Eastern and Central Africa Gravity Network
ECSAMPC	Eastern, Central and Southern Africa Mineral Prospecting Centre
EGM	Earth Gravity Model
EGM2006	Provisional/preliminary EGM2008 model
EGM2008	Earth Gravity Model 2008
EGM96	Earth Gravity Model 96
EIGEN	European Improved Gravity Earth models using New techniques
ERS	European Remote Sensing satellite
ERS-1, ERS-2	Earth Resource Satellites 1& 2
ESA	European Space Agency
FBM	Fundamental Benchmark
FFT	Fast Fourier Transform
FORTRAN	FORmula TRANslation, a computer programming language
GAWK/gawk	AWK from GNU
GDB	Gravity Data Base
GEOSAT	GEOdetic SATellite of USA Navy Earth observing satellites
GETECH	Global Exploration Technology
GFC	Gravity Field Commission
GFZ	GeoForschungsZentrum
GGM	Global Gravitational Model

GGMs	Global Gravitational Models
GIS	Geographical Information Systems
GLAS	Geoscience Laser Altimeter System
GLOBE	Global Land One-kilometre Base Elevation
GNSS	Global Navigation Satellite Systems
GNU	Gnu's Not Unix
GOCE	Gravity field and steady state Ocean Circulation Explorer
GOT00.2	Goddard Ocean Tide Model
GPS	Global Positioning System
GRACE	Gravity Recovery And Climate Experiment
Gravsoft	Denmark-KMS precise geoid model determination computer package
GRS67	Geodetic Reference System 1967
GRS80	Geodetic Reference System 1980
GSFC	Goddard Space Flight Centre
IAG	International Association of Geodesy
IBM	Intermediate Benchmark
ICESat	Ice, Cloud and land Elevation Satellite
ICGEM	International Centre for Global Earth Models
ID2P	Inverse distance to power
IGF	International Gravity Formula
IGF1967	International Gravity Formula 1967
IGS	International GNSS Stations
IGSN71	International Gravity Standardization Network 1971
ITG	Institute for Theoretical Geodesy, University of Bonn Germany
ITRF	International Terrestrial Reference System
IUGG	International Union of Geophysics and Geodesy
KMS	National Survey and Cadastre of Denmark
KMS02	Danish Space Centre -2002 altimetry gravity anomaly data
KMS99	Danish Space Centre - 1999 Marine gravity field
Ksh/KSH/ksh	Korn Shell
KTH	Royal Institute of Technology
KTH-GEOLAB	KTH computer package for precise geoid model determination

LAGEOS	Laser Geodynamics Satellites
LHS	Left Hand Side
LINUX	Scientific computer programming language
LS	Least squares criterion/adjustment
LSC	Least Squares Collocation
LSMS	Least Squares Modification of Stokes method
MEE	Mean Earth Ellipsoid
MES	Mean Earth Sphere
mGal	Milligal
MLHSD	Ministry of Lands and Human Settlement Development - Tanzania
MS	Microsoft
MSE	Mean Square Error
MSL	Mean Sea Level
NASA	National Aeronautics and Space Administration (USA)
NGA	National Geospatial-Intelligence Agency of USA
NHD	National Height Datum
NIMA	National Imagery and Mapping Agency of USA
PDF	Gaussian Probability Density Function
POSIX	Portable Operating System Interface
RADS	Radar Altimeter Database System
RCR	Remove Compute Restore precise geoid method of Denmark
r-c-r	Remove-compute-restore technique
RD	Reciprocal Distance
RHS	Right Hand Side
RMS	Root Mean Square
RTE	Residual Terrain Effects
RTM	Residual Terrain Model
SErr	Standard error
SGG	Satellite Gradient Gradiometry
SH	Spherical Harmonics
SRTM	Shuttle Radar Topographic Mission
SST-hl	Satellite to Satellite Tracking in the high-low mode

SVD	Singular Value Decomposition
SWBD	Shorelines and Water Bodies Database
TE	Terrain Effect
TGDB	Tanzania Gravity DataBase
TNHD	Tanzania National Height Datum
TPDC	Tanzania Petroleum Development Corporation
TZG07	Tanzania Geoid Model 2007 by J.G. Olliver
TZG08	Tanzania Geoid Model 2008
UCLAS	University College of Lands and Architectural Studies
UDSM	University of Dar Es Salaam
UNB	University of New Brunswick, Canada
UNIX	A scientific computer programming language
USGS	USA Geological Survey
VCM	Variance Covariance Matrix
WGS84	World Geodetic Surface 1984
XV	Cross Validation/Validated
g_{L_λ}	Gravity long-wavelength component
g_{S_λ}	Gravity short-wavelength component
GGM^S	Pure satellite GGM
GGM^C	Combined/Composite GGM
M_N	Nyquist degree

Chapter One

INTRODUCTION

Geodesy is one of the oldest disciplines in the history of mankind. The early speculation and theorization about the shape of the Earth, ranged from rectangular by Anaximenes, the flat disc advocated by Homer to Pythagoras' spherical figure. The last idea was accepted also by Aristotle afterwards. Being mathematician, Pythagoras thought the most perfect figure was a sphere. It is now understood, that the shape of the Earth is best approximated by a triaxial ellipsoid, but due to its computational involvement, which do not warrant the slight increase in accuracy over a biaxial ellipsoid of revolution, the later is used as a mathematical approximation of the shape of the Earth. An ellipsoid of revolution is a figure realized by rotating an ellipse about its shorter axis, and the one describing the physical features of the Earth is referred to as reference ellipsoid.

Geodesy, a branch of earth sciences, is the scientific discipline that deals with the measurement and representation of shape and size of the Earth including its gravity field in a three-dimensional time varying space. The shape of the Earth to a large extent is dependent on the rotation of the Earth among Celestial bodies, also it is partly due to geological processes resisted by the Earth's gravity field. This applies to the solid surface, the liquid surface (dynamic sea surface topography) and the Earth's atmosphere. The Earth's equatorial bulge is an example of a result of such processes. For this reason, geodesists study also geodynamical phenomena, such as crustal motion, tides, and polar motion, and in this way they determine coordinate reference systems and datums at global, regional and local levels, using space and terrestrial data and techniques in a time varying space and a GEOID MODEL is one such product. Geoid model determination has been, and still is, one of the main objectives of geodesy.

1.1 Geoid Model

The Geoid is essentially the real shape of the Earth, without topographic and atmospheric masses. The Geoid is defined as the equipotential surface of the Earth's gravity field which coincides with the sea surface in the absence of disturbing factors like tsunamis, ocean currents, salinities, wind, etc., and it extends through the continents (Vaníček and Krakiwsky 1986). Though the geoid is much smoother than the actual earth surface, unlike the ellipsoid, it is still too complicated to serve as the computational surface on which to solve geometrical problems, but it is suitable as a vertical datum. Determination of a geoid model requires extensive gravitational measurements and computations.

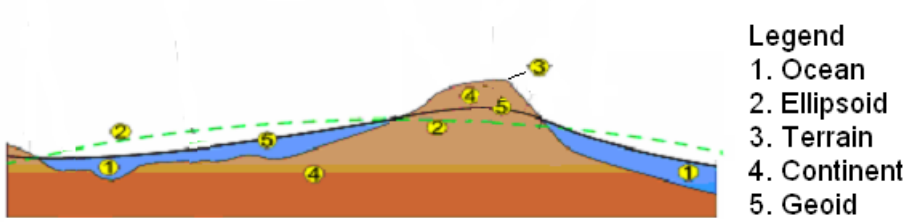

Figure 1-1: The Earth, Ellipsoid and Geoid

1.1.1 Uses of Geoid

Below is a list of various applications of the geoid:

a. Vertical datum for orthometric heights.
b. Determination of orthometric heights from ellipsoidal heights. Global Navigation Satellite Systems (GNSS) provide us with heights referring to geocentric ellipsoids; the ellipsoidal height is of little use for day-to-day requirements of height. Usually our need for height is in the form of orthometric or normal height, and to obtain these, geoid height is needed.
c. Understanding of ocean circulation patterns and dynamics
d. Description of the positions of satellites and ground stations in suitable reference frames. The fact that the geoid reflects gravity field irregularities means that, a better understanding of the geoid enables refinement of satellite orbits.
e. Oceanography, hydrographic surveying and maritime. The geoid is valuable for oceanographers, hydrographic surveyors and maritime industries in general as vessels navigate vast bodies of water. The knowledge of the geoid is essential to better model ocean currents and under sea mapping especially in soundings. Sea-going vessels can take advantage of the currents and characteristics of the ocean to plan faster and safer routes, which in turn will use less fuel (conservation) and cost less.
f. Knowledge of the geoid is important to model geodynamical phenomena (e.g. polar motion, Earth rotation, crustal deformation). Geoid is useful in interpretation of precursors to geo-hazards researches such as the study of post-glacial rebound, earthquakes, volcanoes, land slides, tsunamis etc. and mitigation.
g. Vertical and horizontal control networks definition, establishment, transformation and adjustment.
h. Vertical datum unification: 1) When direct land access is a problem: Datum transfer and unification is possible with good geoid model even when the land parcels can not directly be accessed by land. 2) When there is datum inconsistencies brought about say by differences in MSL/tide gauges; geoid and ellipsoidal heights (e.g. GPS heights on benchmarks) can minimize by far the problem.

The list above is not exhaustive by any means. Other uses in engineering and geosciences exist, especially in scientific and engineering research.

1.1.2 Previous Geoid Models in Tanzania

Geoid determination in Tanzania has a short history. With regards to literature review by the author, a dedicated gravimetric geoid model of Tanzania was achieved only recently (Olliver 2007); otherwise the existing gravimetric geoid models for Tanzania are part of regional or international gravimetric geoid model projects. Models worth emulation are

the African Geoid Project (AGP) geoid models AGP2003 and AGP2006 by Parker et al. (2007) and the geoid model by Olliver (2007). Parts of the geoid of Tanzania have been determined mostly for academic purposes, such as the MSc. thesis by R. Fursdon in 1984 from Nairobi University entitled "A geoid model section in East Africa", which determined a local astrogeodetic geoid model profile of about 970 km from south west to northern Tanzania, the PhD thesis from Oxford University by M.K. Gachari in 1997 with title "Determination of a Gravimetric Geoid model for the Eastern African Region", which covered mainly Kenya and Uganda. Gachari and Olliver (1998) determined "A high resolution gravimetric geoid model of the Eastern African Region", which included a small part of the northern Tanzania. The AGP2006 and Olliver (2007) geoid models, which cover fully the country, are described shortly below.

a. The African Geoid Project Geoid Model

The AGP was initially established as a project of the Committee for Developing Countries (CDC) of the International Association of Geodesy (IAG). In July, 2003, the IAG General Assembly in Sapporo Japan handed over the AGP task to Commission II (Gravity Field Commission) of the IAG. The project is manned by a small working group of African geodesists, who collaborate to obtain data and investigate appropriate models. The AGP goal is to have near continuous data coverage over the continent at station spacing of the order of 5 to 10 km. The data will then be used to interpolate gravity anomalies on regular grids of 5'x5' (about $10\,km \times 10\,km$) or smaller, from which a geoid model can be computed. Until now, gravity data coverage over Africa falls short of this expectation by far.

A preliminary geoid model of Africa, referred to as AGP2003, was computed by Merry et al. (2005), and the geoid of Tanzania is part of it.

A brief about AGP2003

Method: AGP2003 is computed through quasi-geoid height anomaly ζ and a correction, by the remove-compute-restore (RCR) technique, cf. Sect. 2.1 for elaboration. The correction is given as

$$\frac{\overline{\mathsf{g}} - \overline{\gamma}}{\overline{\gamma}} H \,, \tag{1.1}$$

where $\overline{\mathsf{g}}$ is the mean gravity along the plumb line between geoid and ground, and $\overline{\gamma}$ is the mean normal gravity along the normal plumb line between ellipsoid and telluroid. The quasi-geoid model is obtained as a combination of four components, namely: Long-wavelength ζ_L, short-wavelength ζ_S, the contribution from Molodensky G1 term ζ_{G1}, and inner zone contribution ζ_I. The long-wave component of the quasi-geoid model ζ_L is computed from the Global garvitational model (GGM) EGM96 to degree and order 360. The short-wavelength is obtained by 2D spherical convolution of terrestrial gravity anomaly, reduced of its long-wavelength part by EGM96, in Stokes function. The ζ_I part is obtained from a linear approximation of gravity anomaly in the innermost small circle

using reduced and thinned gravity anomaly grid spacing around the CP. During computation, ζ_I and ζ_S are computed together. The ζ_{G1} part is obtained from convolution of free-air anomalies using smaller grid anomaly ($1'$) obtained from larger-$5'$ grids with a kernel consisting of inverse distance to power three.

Data used consist of:

1. Combined EGM96 GGM to degree and order 360
2. $5'$ and $1'$ free-air gravity anomaly grids
3. $1'$ GLOBE DEM

The geoid model was computed in steps as follows:

- The long-wavelength component of the height anomalies (quasi-geoid model) was computed using the EGM96 gravitational model.
- The short-wavelength component was computed using the residual gravity anomaly in the 2D spherical convolution in Stokes integral.
- The terrain effect (Molodensky term G1) was computed using the $1'$-GLOBE digital elevation model (DEM) and $1'$-residual free-air gravity anomaly grid.

A revised AGP geoid model was computed in 2006 for the continent of Africa (Parker et al. 2007), and the model is named AGP2006. In this geoid model, special attention has been given to the refinement of the 2D spherical convolution, refinement of the contribution of Molodensky term G1 and the influence of changing the gravitational reference model from EGM96_360 to CG03C_120 and EGM2006. Thus the data used are:

- Terrestrial point and mean gravity anomalies from University of Cape Town in South Africa and Leeds in UK.
- KMS02-$2' \times 2'$ mean marine altimetry gravity anomaly grid from Denmark
- CHAMP-GRACE combined Global Gravitational Model CG03C (120)
- SRTM 30" DEM
- EGM2006.

The model has been tested using GPS/levelling data from South Africa and Algeria for the respective locations. For the 62 points in South Africa a RMS agreement of 18 cm was achieved, while for the 14 points in Algeria the RMS agreement was 27 cm. The best results were obtained using the low-order (less than degree 120) GGM CG03C as reference model. The high order model versions of CG03C and EGM96 produced less accurate results (ibid).

Comments on AGP2003 and AGP2006 determinations

Foremost, for the two AGP geoid models, there is no specific description of Tanzania or assessment of the quality of the geoid model in Tanzania. Moreover the conclusion in Merry et al. (2005 Sect. 4.4) on AGP2003 is that the model almost resembles EGM96 except in mountainous and in new gravity data areas. We believe, that the situation can further be improved using the Shuttle Radar Topographic Mission (SRTM) 30 arc seconds Digital Elevation Model (DEM) to enhance short-wavelength component, and either EGM96 or CG03C GGM to fill the data gaps, as advocated in Sect. 5.2. Therefore our comments on the determination of AGP2006 are listed below:

i. First order approximations and often planar as used in this paper, when coupled by unfavourable data situation (density, distribution and quality), definitely limits the achievable geoid accuracy to low orders. The mathematical models should be improved, so that we are left with improving data condition.
ii. The steps followed to create different data types, and the role of two combined GGMs is unclear or missing.
iii. The motive of having four components of quasi-geoid model is advantageous, when appropriate data types are used. For example, when combined GGM is used to compute long-wavelength component of quasi-geoid, care must be exercised to ensure that high frequencies of gravity have been filtered out.
iv. When gravity in low frequencies is needed, instead of using combined GGM CG03C to degree 120, a pure satellite GGM like GRACE03S truncated at appropriate degree could be used with less risk.
v. Molodensky's quasi-geoid model component ζ_{G1} is supposed to carter for short-wavelengths, thus the data used should have high frequencies. When $1'$ blocks gravity are created from $5'$ blocks, we are basically using the frequencies of $5'$ blocks, while the intention was to use high frequencies of $1'$.
vi. The data in use is referred to as "free-air gravity anomaly", but Molodensky's method for quasi-geoid determination; cf. Sect. 2.1 also Sjöberg (2005a), requires surface gravity anomaly, this needs clarification.

b. Geoid Model of Tanzania 2007 by J.G. Olliver; (TZG07)

According to a literature review by this author, and to the author's knowledge, the geoid model TZG07 by Olliver (2007) is the first dedicated, full coverage geoid model of Tanzania, whose boundaries are latitudes $12^{\circ}S$ to $1^{\circ}S$ and longitudes $29^{\circ}E$ to $40^{\circ}E$, with 5 arc minutes resolution. The model is referred to the Geodetic Reference System 1980 (GRS80).

Data used to compute TZG07 are:

- 43,402 point and mean terrestrial gravity anomalies
- 9,539 observations in the form of a combination of marine ship track (point) and $2'$ KMS02 mean altimetry data to form marine $5'$ mean gravity anomaly dataset
- A digital elevation model derived from 3-arc second Shuttle Radar Topography Mission (SRTM3)
- EIGEN-GRACE02S pure satellite GRACE gravitational model up to degree and order 120.

Method:
Residual remove-compute-restore (RCR) through Helmert's 2nd condensation and Stokes method using 1-D Fast Fourier Transform (FFT) in processing, similar to RCR method described in Sect. 2.1 with a few exceptions. The paper comments, that residual free-air gravity anomaly is created to be as small as possible in magnitude, and that Stokes integration errors are minimized. The residual gravity anomaly is obtained by removing the long-wavelength component from the terrestrial free-air gravity anomaly by a GGM, which is restored outside the integration. The main equation for geoid height N is

(Olliver 2007, Eq. 4):

$$N = N^{gm} + N^{res} + \delta N\,, \tag{1.2}$$

where N^{gm} is the GGM long-wavelength component, N^{res} is residual geoid height computed from residual gravity anomaly obtained by subtracting GGM gravity anomaly from free-air gravity anomaly within the Stokes integration boundary and δN is the truncation bias computed from the residual gravity anomaly outside the cap, (Olliver 2007 Eq. 8).

Comments on Olliver (2007) about determination of TZG07:

1. In Olliver (2007) integration distance is variable, i.e. utilizes all the residual data after leaving 2° margins outside the geoid model borders, this is likely to lead to variable geoid model quality due to truncation error.
2. Outside the data area, there is only low frequency EIGEN-GRACE02S (120). Truncation error could be reduced further by using combined GGM with all the possible frequencies instead of pure satellite EIGEN-GRACE02S (120).
3. Secondary indirect effect to gravity has been considered insignificant and thus left out without assessment of how much insignificant the correction is.
4. Simple free-air reduction has been used to take care of direct topographic effect and downward continuation. The data situation may not warrant cm-geoid model, and thus necessitate better reduction method especially for a region like Tanzania with rough and high elevations (Vaníček and Martinec 1994), (Ågren 2004a), (Sjöberg 1994a, 2000, 2001a, 2007 and many others on the treatment of masses outside the geoid bounding surface). Use of a better gravity reduction approach would allow improvement of geoid model quality, since the data is of variable quality (density, distribution and accuracy).
5. For the regional/local geoid model determination, ellipsoidal correction may be considered negligible and thus not effected, as it is in this paper, but this depends much on the approach followed, see Sjöberg (2003). The approach followed is not clear. In (ibid) it is commented, that use of gravity anomalies computed on ellipsoid (cf. Eq. 7) with spherical Stokes formula does not eliminate ellipsoidal correction, which in equatorial region can reach 1dm or more with un-modified Stokes formula and without data limitation.
6. Whether SRTM DEM has been used to enhance short-wavelength component where it lacks, is not evident, but its use to smooth free-air gravity anomaly prior to gridding is clear.
7. Although the direct atmospheric correction is accounted for, it is not shown where the atmospheric indirect effect is restored; the one provided reinstates topography only. Besides the model used is not clearly stated. If it is the International Association of Geodesy (IAG) model, it could lead to a serious bias, given that the method equates to the classical Stokes method (Sjöberg 1999).
8. The altimetry KMS02 gravity anomaly from Danish Space Center is a $2' \times 2'$ grid data that covers fully the marine area. The process of combining it with ship track point data, improves the short-wavelength content, but to mean the entire dataset into $5' \times 5'$ grid removes the high frequencies, and consequently the marine geoid model is

smoothed.

9. Since the KMS02 $2' \times 2'$ mean altimetry data fully covers the land and ocean areas, the process of removing the land part and then merging the land and marine gravity grids is not explained. If not done properly, very likely it affects the quality of data on both sides of the ocean/land demarcating boundary.

Results:

Quality of the computed geoid model

i. For quality of the N^{gm}, error degree variances are used to obtain it, (see Eqs. 15 and 16), but for the N^{res}, its accuracy is obtained by error propagation, whereby error estimates for the residual gravity are taken from Australia. The values could be extremely different due to the very different scenarios involved.
ii. Truncation bias is accounted for by pure GGM limited to degree and order 120 only, significant bias is likely to remain (cf. bulletin #2 above).

Quality control (external comparisons)

a) 15 Doppler satellite points observed on trigonometric heights were used. Trigonometric heighting in Tanzania commenced long before spirit levelling and thus, most likely, not referenced to any tide gauge. The accuracy of the Doppler is quoted as 1.5 metres in each axis at 90 % confidence level. The fit of TZG07 with the Doppler geoid height has a standard error (SErr) of 1.36 metre, and after 4-parameter fit it is 1.04 metre. This means that the difference of 1.36 m and 1.04 m accounts for systematic effects. The 1.04 m fit is a combination of residual errors from the three height types involved, i.e. trigonometric, Doppler and geoid heights. The assessment could be improved by comparing the differences of geoid heights.
b) Use of astrogeodetic information is more realistic, especially when differences of geoid heights are compared as it was done in this case. Thus the standard error of 47 cm reflects better the quality of TZG07.

Conclusion

We highly commend the efforts by J.G. Olliver to determine the first dedicated geoid model of Tanzania. Given the assessment carried above, we believe that there is still a room for further improvement especially in view of the new avenues cited in Sect. 1.3.

1.2 Geoid Determination Limitations in Tanzania

To conceive that Tanzania had not had its own geoid model until Olliver (2007) is not easy, although it is true. Small parts of a geoid model of Tanzania have been determined for academic uses or as part of regional determinations and occasionally a geoid model of Tanzania has been portrayed in global geoid determinations, e.g. African Geoid Project (AGP) which is still at preliminary stage, EGM96 and EGM2008 global geoid models. Below we try to outline some of the major factors, which could have been the impediments.

i) Data

- Terrestrial gravity: Is limited to areas where exploration has taken place, leaving big gaps elsewhere (cf. Figure 4-1). Moreover, the data is primarily not for geodetic uses, and has been collected over wide time span, leading to differing undocumented accuracies, mainly due to instrumentation and methodology. Often the exploration gravity data is classified until after production, and even then not easily accessible.
- Marine gravity: It is only recently that ship gravity surveys were conducted for gas and oil exploration offshore coast of Tanzania. As pointed out above, the data could not be accessed immediately thereafter.
- Digital Elevation Model: Hitherto there is no Digital Elevation Model (DEM) solely for the country or for the area of interest (AIO). Therefore, before the DEMs from international bodies were available, it was not possible to compute precise terrain effects or reductions, which require precise dense DEM, and even then, a commitment to validate the DEM is inevitable, since in the past some have proved to be very imprecise in the region (Merry 2003b, Christopher 2006).
- Heterogeneous geodetic data exist, which together could ease by far some of the lacking data requirements. Unfortunately, there has not been a purposely concerted effort, country-or regional-wise, to archive all the important data for geoid model determination in a suitable way. I believe this is a common problem to many African countries, thus the present AGP has a lot to do before it succeeds to collect all the available relevant data from organizations and individual researchers in the continent and elsewhere.
- Precise geoid model determination requires skilled geodesist, and Tanzania has shortage of these scientists.

ii) Geoid model use

Absence of dedication from the nation or region to observe and collect the right data to determine a geoid model of the country/region, could very much emanate from little awareness of the advantages of a geoid model to the country's economic prosperity, especially in a developing country. Construction engineering, navigation and mapping stand to benefit more, especially in this era of GNSS, when a precise geoid model is in place. Policy markers need to be enlightened to a level of appreciating the necessity of having a country's precise geoid model. Once they are aware of the benefits, it will be possible to solicit funds for training, research and development in the area of geodesy and essentially geoid model determination.

1.3 New Avenues

The demand and necessity for a geoid model of Tanzania is higher now than ever before. Fortunately, new avenues have opened up, which may see to a fairly accurate geoid model of Tanzania at the present. They can be grouped under:

- Data
- Methodology
- Infrastructure.

i) Data

Satellite Gravity data in the form of a GGM from dedicated satellite missions like CHAllenging Mini-satellite Payload (CHAMP), Gravity Recovery And Climate Experiment (GRACE) are readily and freely available. The Gravity field and steady state Ocean Circulation Explorer (GOCE) of European Space Agency (ESA) gravity mission has taken off recently (17th March 2009). The GOCE is expected to provide much higher gravity resolution than CHAMP and GRACE. Simulation studies carried out earlier provide that at degree and order 200 which corresponds to 100 km resolution, geoid model commission error is expected to be around 1 cm, (Mark et al. 2007). Unlike before, the above gravity missions are now capable of offering reliable long to medium wavelength gravity. Combined GGM can give even better resolution due to improved computational techniques, facilities and availability of other secondary data like high resolution DEM. Nevertheless, satellite gravimetric data is far from replacing terrestrial data. This implies that there is still uncertainty in areas which lack terrestrial data. Global evaluation of the present pure and combined GGMs has been carried out by the International Centre for Global Earth Models (ICGEM), using GPS/Levelling data from USA, Canada, Europe and Australia, Table 1-1 portrays this information.

Table 1-1: Global evaluation of CHAMP and GRACE GGM using GPS/Levelling data expressed as RMS of differences of mean [GPS/Level MINUS GGM geoid height]
Where the letters C and S at the end of GGM name stand for Combined and Pure Satellite respectively

Model	Nmax	USA 6169 points	Canada 1930 points	Europe 186 points	Australia 201 points
ITG-GRACE03	180	0.646 m	0.560 m	0.699 m	0.610 m
ITG-GRACE02S	170	0.638 m	0.513 m	0.638 m	0.499 m
EIGEN-GL04S1	150	0.642 m	0.579 m	0.703 m	0.473 m
EIGEN-GL04C	360	0.363 m	0.261 m	0.332 m	0.262 m
EIGEN-CG03C	360	0.367 m	0.311 m	0.397 m	0.277 m
GGM02C	200	0.491 m	0.381 m	0.492 m	0.390 m
GGM02S	160	0.986 m	1.120 m	1.282 m	1.362 m
EIGEN-CG01C	360	0.374 m	0.277 m	0.412 m	0.281 m
EIGEN-GRACE02S	150	0.750 m	0.644 m	0.851 m	0.547 m
EGM96	360	0.402 m	0.366 m	0.487 m	0.314 m
GGM01C	200	0.494 m	0.385 m	0.531 m	0.410 m
GGM01S	120	0.757 m	0.722 m	0.905 m	0.642 m
EIGEN-GRACE01S	140	0.776 m	0.708 m	0.946 m	0.560 m
EGM96S	70	1.121 m	1.128 m	1.779 m	1.505 m
EGM2008	2190	0.248 m	0.126 m	0.191 m	0.217 m

(http://icgem.gfz-potsdam.de/ICGEM/favicon.ico, 10.05.08)

We observe that the pure satellite models ITG-GRACE02S, EIGEN-GLO4S1 and ITG-GRACE03S have minimum differences of 0.499 m and maximum of 0.703 m. For the combined models, EIGEN-GL04C, EIGEN-CG03C, EIGEN-CG01C and EGM96C, all of degree and order 360, show better results in the order they appear with minimum difference of 0.261 m and maximum of 0.412 m. The new EGM2008 shows even better results, with a minimum of 0.126 m and maximum of 0.248 m. This is a great achievement at global scale. Proper utilization of a high resolution DEM like SRTM3 could further improve the geoid model, and if knowledge of lateral density variation is available, results would be much better, especially in the rough and high altitude terrain. Presence of SRTM3 not only enables computation of residual terrain effects (RTE), but

greatly improves prediction of gravity by remove-compute-restore (r-c-r) approach; this will be elaborated in Sect. 5.3.

ii) Methodology

Computation of a gravimetric geoid model is usually by use of Stokes method (Stokes 1849). The conditions and requirements of the original Stokes method were stringent, and for many years it has been not easy to fulfil them (Heiskanen and Moritz 1967 Ch.3 & Sect. 8-2). Over time, scientists have modified the method such that it is not only possible to meet considerably the requirements, but also to achieve better accuracies within much less time as appreciated, e.g. in Sjöberg and Featherstone (2004). For example

- The problem of having the geoid as the bounding surface without masses external to it is gradually been alleviated to almost a reality by development of mathematical models and computational techniques, e.g. Sjöberg (1991).
- Requirement for availability of gravity data all over the globe is now possible to a great extent due to the presence of Global Gravitational Models (GGMs), developed primarily from satellite geodetic data, which should be combined with short-wavelength terrestrial gravity data in the AOI.
- High resolution DTMs have made it possible to have quite small gravity anomaly grids with almost global coverage, this addresses the need to have continuous gravity data.
- Different modification of the original Stokes method exist, the preferred modifications use combination of terrestrial and satellite gravity data, for example the Remove-Compute-Restore (r-c-r) of Denmark, the Stokes-Helmert's of Canada (UNB) and the Royal Institute of Technology (KTH) "Least Squares Modification of Stokes method (LSMS) with additive corrections (AC)", hereafter referred to in short as "LSMS with AC". The modified methods have made tremendous achievement as compared to the classical Stokes approach. For example the LSMS with AC not only removes the requirement for global data coverage by involving a small computational cap, e.g. 3 degrees or less, but also:
    - reduces substantially the effect of the assumption made in the classical Stokes method e.g. there are no masses outside the geoid. It starts with approximate geoid model computed from unreduced surface gravity and then adds corrections for topographic and atmospheric masses, ellipsoidal correction to spherical earth and downward continuation to the geoid.
    - makes it easy to update and revise an old geoid model,
    - reduces truncation error outside the cap efficiently,
    - Handles all data errors sources in most optimal way.

iii) Infrastructure

Compared to the past, there are many positive changes emerging and paving way to ease local/regional geoid model determination. These are

- Sound forum for geodetic matters, e.g. organization of geodetic community through international bodies like International Association of Geodesy (IAG), International Union of Geophysics and Geodesy (IUGG), data archiving centres and databases, dedicated journals as forum for presentation of scientific research

findings and knowledge frontiers worldwide; easily accessible, reliable and efficient and often free.

- Internet; knowledge and data availability is colossal; dissemination and retrieval is amazing.
- Computational facilities: Data storage, specialized software and computing devices (e.g. computers) capabilities are also astounding.

1.4 Research Objective, Author's Investigation and Contribution

▪ Research Objective

In Section 1.1.1, many uses of geoid were given. The importance and need for a precise geoid model has become more important now than ever before, due to the great improvement in GNSS, which has the ability to provide three-dimensional positioning over the entire Earth at a tremendous speed and accuracy, i.e. horizontal and vertical positioning in terms of ellipsoidal height. Unfortunately, ellipsoidal height is just a geometrical quantity, which has not much direct use, but with geoid model in situ, it is possible to convert the ellipsoidal height to orthometric height, which has physical meaning, is widely used and is useful in almost all the day-to-day applications requiring height information. In the past, realization of orthometric heights was from spirit levelling, a process which is time consuming, tedious and expensive especially in mountainous and rough terrain, which is widely spread in Tanzania as explained in Sect. 4.5. The ability to obtain accurate orthometric heights from GNSS given its provision speed and cost effectiveness, will not only boost substantially economic growth of a country like Tanzania, and greatly increase project completion time, but will also enhance peace and harmony amongst her people and in the region. The main objective of this research is to convert ellipsoidal heights to orthometric ones by developing a precise gravimetric geoid model of Tanzania, which will enable the country to obtain accurate orthometric heights from GNSS and replace the snail slow spirit levelling process as far as possible.

▪ Author's Investigation

As explained above, so far (September 2008) it is only the Olliver (2007) geoid model (TZG07) which covers fully Tanzania and was determined solely for Tanzania. The AGP geoid models AGP2003 (Merry et al. 2005) and AGP2006 (Parker et al. 2007) are still provisional, though with a geoid model of Tanzania as integral part, their assessments in Tanzania is missing. From Sect. 1.1.2, we saw that quality and capability of AGP2006 in Tanzania are not known. Given the deficiencies identified in the determination of the geoid model coupled by data sparseness and rough terrain including high elevations, the quality is likely to be much worse in Tanzania than in the test areas, i.e. South Africa and Algeria. The EGM96 and EGM2008 global geoid models also cover Tanzania, but to my knowledge, there has not been a dedicated evaluation of their quality performance and suitability over the country. All the same, it is very likely, that their quality will be much worse than in the developed countries cited in Table 1-1. That is why our discussion about the existing geoid models of Tanzania in Sect. 1.1.2, we referred only to AGP2006 and TZG07 by Olliver (2007). As a matter of fact it is only the Olliver (2007) geoid

model we should have considered, since it is the only one which provides quality assessment for Tanzania. Again, from Sect. 1.1.2, amongst the approaches followed to assess the TZG07 it is only the comparison with astrogeodetic profile which can be relied upon to some extent; it gave a standard error of 47 cm. It is very possible, that in areas which lack data and/or in rougher and higher elevations, the accuracy will be much lower. In view of the above discussion, absence of quality performance of the EGM96, EGM2008 and AGP2006 geoid models in Tanzania render them useless. As for the TZG07 geoid model, its uses are very much limited unless another validation with a superior approach is conducted.

The quantity, quality and distribution of gravity data over the research area of interest (AOI) (cf. Sect. 4.4.3 for the extent of the AOI), for regional/local geoid model determination has great influence on the final quality of the geoid model determined from it. The capability of the KTH method of LSMS with AC to determine a precise gravimetric geoid model has been demonstrated by many scientists and researchers over time, such as Nsombo (1996), Nahavandchi (1998), Hunegnaw (2001), Ellmann (2004), Ågren (2004b), Kiamehr (2006a), Ågren, Kiamehr and Sjöberg (2006 a-b) and Ilias (2008). Therefore, with regards to the determination of a regional precise gravimetric geoid model by the KTH method, the only other important factor that can affect its quality is the data that goes into it. In this research, special investigation is dedicated to gravity data quantity, quality and distribution over the AOI. It is in the light of:

- The new avenues,
- The knowledge gained over years and especially during the PhD study at KTH, Division of Geodesy,
- Deficiencies noted in the determinations of AGP2006 and TZG07,

that the author has come to hypothesize, that in spite of the prevailing deficiencies in the terrestrial data for geoid determination in Tanzania, and indeed in the AOI, it is possible to compute a gravimetric geoid model of Tanzania of higher quality and accuracy than any of the existing geoid models.

Brief explanation is given on how to improve the data quality and quantity so as to achieve the main objective:

i) For the terrestrial data, only point gravity will be used since often, mean gravity data is not accompanied by information followed to obtain the mean, besides the process of averaging/meaning may remove important gravity frequencies.
ii) Cross validation and tailored statistical data analysis and cleaning will be used to remove all outliers prior to data processing.
iii) Special technique which utilizes absolute reference gravity to validate Global Gravitational Models (GGMs) will be developed and used in this research and furthermore compared to the accustomed GPS/levelling approach.
iv) Covariance function fit approach will be used to arrive at the optimal surface gravity grid density (grid spacing) to minimize discretization errors while trying to arrive at the smallest possible but realistic grid spacing.
v) Surface gravity data densification will follow specially designed remove compute restore (r-c-r) kind of approach so that data correlation is minimized statistically

and magnitude wise while ensuring, that patching empty grids has minimum effect on the quality of the rest of the existing observed data involved.

vi) All grids will be filled with appropriate quality data; no gap will be allowed in the data grids for the whole of AOI.

vii) Merging of land and marine gravity data is to follow a strict approach which will not compromise data quality on either side, also without creating discontinuities.

viii) Error degree variance models will be scrutinized and, if needed, improved to portray good qualities as possibly achievable.

If crustal density variation data had been acquired, further investigation would be conducted to check on the quality of the geoid model and if necessary how to improve it in the following areas:

- Mountainous and high elevation rugged terrain
- Tectonically active areas along the East Africa Rift Valley System (EARVS)

Depending on the distribution of GPS/levelling data, qualities of the computed geoid model in areas of sparse terrestrial data versus those of fairly high density may be conducted. (We are still trying to acquire more GPS/levelling data).

▪ Contribution

The new avenues given in Sect. 1.3, together with a specially designed data densification approach are taken on board to develop a new gravity database of Tanzania, which will promote not only this research but also other scientific researches now and in the future. The geoid model will not only benefit Tanzania economically, but also hasten its physical development especially in the fields of engineering, mapping and planning.

Description of Chapters

Chapter 1 is an introduction to geodesy and geoid uses, history of geoid determination in Tanzania, limitations to geoid determination and uses. The chapter continuous with new areas and opportunities in the world, which may lead to a better geoid model of Tanzania, and finishes with research objectives, author's investigation and contribution. Chapter 2 gives a short description of three frequently used methods for gravimetric geoid model determination with emphasis on those techniques which utilize combination of terrestrial and satellite Global garvitational model (GGM) data. Chapter 3 provides a detailed description of the nominated method for this research, the KTH method of Least Squares Modification of Stokes method with additive external corrections (LSMS with AC). Chapter 4 is dedicated to all data to be used. It starts with background to gravity data in Tanzania, reductions, error estimates, procurement and availability of all data needed. After this, data compilation, cleaning and validation is given. Chapter 5 is about all the preparations needed prior to computing a gravimetric regional geoid model by LSMS with AC. Thus chapter 5 deals mainly with hardware and software requirement, data formats, formation of the surface terrestrial gravity, GGMs and SRTM grid data at different densities and computation of important input parameters, including kernel modification. Chapter 6 computes the geoid model by the KTH method of LSMS with AC. First it computes it approximately by the LSMS then the AC and finally combines them to the gravimetric geoid model of Tanzania 2008 (TZG08). Chapter 7 evaluates and

assesses the accuracy of the computed TZG08 geoid model. Chapter 8 is about how best the computed geoid model can be utilized to convert GNSS (GPS) ellipsoidal heights to orthometric heights referred to the Tanzania National Height Datum (TNHD). Since the GPS/levelling data does not cover the country fully, it computes representative corrector surface (CS), followed by a discussion on the formation of hybrid geoid model as an alternative to vertical datum for conversion of ellipsoidal height to orthometric height. The CS is put to use by computing anew the height of Mt. Kilimanjaro, based on the TZG08 geoid model. Chapter 9 discusses the results, highlights on the study limitations, concludes the study and puts forward recommendations for further work. The thesis ends with a list of references.

Chapter Two

OVERVIEW OF PREFERRED GEOID MODEL DETERMINATION METHODS WITH EMPHASIS ON TERRESTRIAL AND GGM GRAVITY DATA

Determination of gravimetric geoid model is usually done by the famous Stokes formula. Since its inception in 1849, many variants to the original formula (cf. Eq. (3.1)) have emerged, often necessitated by the inability to meet precisely the assumptions and conditions on which the development of the formula was pegged upon (Heiskanen and Moritz 1967 Ch.3 & Sect. 8-2), but also due to emergent and/or search for situations which make it easier to practically attain the goal, i.e. the determination of a geoid model. The geoid height N from Stokes formula, Eq. (3.1), is obtained through Bruns' formula $\left(N = T/\gamma\right)$ in which T, the disturbing potential, is supposed to be harmonic on and outside the geoid as the bounding surface. The unknown T is obtained from gravity anomaly on the geoid as a solution to the third boundary value problem (BVP) of physical geodesy (cf. Heiskanen and Moritz 1967 p 86). For T to be harmonic on and outside the geoid, there should not be any masses outside the geoid (i.e. topography and atmosphere). Besides, gravity anomaly ought to be realized on the geoid and not on the Earth's surface, where it is observed. In the Stokesian geoid determination, the described procedure, which aims at meeting the BVP of Earth's potential theory on the geoid, is referred to as regularization of geoid, for more insight cf. Heiskanen and Moritz (1967 pp 288-89). In the modern approaches to geoid model determination, many variants to the classical regularization of geoid have emerged, one such alternative is referred to as remove-compute-restore (r-c-r). Usually the r-c-r closely adheres to the regularization procedure, with the exception that it uses residual gravity anomaly. Residual gravity anomaly is the observed gravity anomaly minus the GGM (usually pure satellite) gravity anomaly. Initially, the residual gravity anomaly could be reduced to geoid or given on the surface, this depends on which type of Stokes kernel is used and method of realizing geoid height followed, we will elaborate on this later. The one, which uses the original Stokes formula is known as the 'Standard Stokes formula'. Use of combination of terrestrial gravity and GGM data in modified Stokes formula (kernel or data or both) truncated to a spherical cap around the computation point, has become a usual practice and the contrary, i.e. use of pure terrestrial or pure GGM data fully or even truncated or in the original Stokes formula, is unusual practice nowadays.

Usually terrestrial, ship, aerial and to some extent altimetry gravity data, are rich in local details (short to medium wavelength), but are spatially limited and their long-wavelength

content is biased due to observational and datum errors among other factors. On the other hand, satellite data is smooth with broad features of the gravity spectrum, but medium to short wave components of gravity are either too weak or absent altogether. Therefore limitation of terrestrial data to a small cap around the point of interest is quite advantageous since it reduces the amount of erroneous long-wavelength component of the terrestrial gravity signal incorporation. Consequently, by removing the long-wavelength component from the terrestrial data, and combine it with a GGM in a suitable optimal way, results into much better data or procedure for gravimetric geoid model determination. Among the present time preferred methods, as expected, using combination of terrestrial and GGM data with modified Stokes formula are the:

1. Remove-Compute-Restore (RCR) method from the University of Copenhagen, Denmark.
2. Stokes-Helmert method developed at the University of New Brunswick (UNB), Canada.
3. Least Squares Modification of Stokes formula (LSMS) with or without Additive Corrections (AC) method developed at the Royal Institute of Technology (KTH), Division of Geodesy, KTH, Sweden.

We should point out, that often variations to the above methods, especially the first two, exist and even combination thereof. The first two basically follow the r-c-r approach, but the last one, when with additive corrections, does not follow the r-c-r procedure directly, but it is implied. This study is based on the last method i.e. the KTH LSMS with AC, the explanation for its nomination will be given at the end of this chapter. Therefore in this chapter, only brief descriptions of the first two will be given. The last is described extensively in the rest of the study, but more so theoretically in Ch. 3 and practically in Chs. 5 and 6.

2.1 Remove-Compute-Restore (RCR) Geoid Method

The intention is to describe the method of local and regional gravimetric geoid model determination developed in Denmark, jointly by the National Survey and Cadastre of Denmark (KMS), and the Geophysics Department of the Neils Bohr Institute of the University of Copenhagen; we will refer to the method as “RCR” to avoid repetition of the long statement. Two approaches of geoid model computation feature most in the RCR method, depending on how the terrain is handled during gravity data preparation prior to using it in the Stokes integral. In the course of data preparation, or computation of the geoid model, Least Squares Collocation (LSC) and or the Fast Fourier Transform (FFT) techniques may be deployed. Usage of LSC and FFT will not feature here explicitly, the reader is referred to the references like Forsberg (1984, 1998), Haagmans et al. (1993) and others to come in this section. The two approaches of RCR in handling topography for geoid model determination by Stokes integral, lead to two methods of realizing geoid model by RCR described as:

1) Quasi-geoid by Residual Terrain Model (RTM)
2) Helmert’s second condensation method and classical Stokes method.

Generally the philosophy of the Danish method is, remove from the observed gravity anomaly the long-wavelength reference field effect through a GGM, smooth the resulting residual gravity by converting it to Bouguer residual gravity anomaly to make the gravity

signal small and smooth so that it is more suitable for gridding. The removed effects of GGM and topography (Bouguer plate) are later on restored and that is why the methods are termed after RCR. Each of the two methods handles topography slightly different and hence the different approaches. The mathematical rigor of RCR does not match the improvement in geoid data in the developed Western countries cf. Omang and Forsberg (2000), therefore the practically achievable accuracy of the method should be re-examined critically in the light of a cm-geoid model.. A brief review of the two approaches is given below.

I. Quasi-geoid by RTM

Through RTM, Quasi-geoid height anomaly ζ is determined. To obtain the corresponding geoid height N, it requires a correction as given in Eq. (2.1). The foundation of this approach is the Molodensky et al. (1962) with further modifications by Moritz (1980a). By limiting the approximations to first order of the vertical gradient of the gravity anomaly $\partial\Delta g/\partial h$, the method is given as

$$N = \zeta + \frac{\Delta g_B h}{\gamma}, \tag{2.1}$$

where ζ is the height anomaly, Δg_B Bouguer gravity anomaly, γ normal gravity at the telluroid (i.e. at the normal height of the surface point P), h is ellipsoidal height of P. If the normal height of surface point P is H^N, then geometrically the relationship between geoid and quasi-geoid models is established through the orthometric and normal heights of point P as

$$H_P + N_P = H_P^N + \zeta_P \tag{2.2}$$

Basically this approach determines quasi-geoid model, which is converted to geoid model through Eq. (2.1), thus our main concern will be on the data input to RCR quasi-geoid model determination through RTM. The starting point is surface gravity anomaly data Δg, from which residual gravity anomaly Δg_{res}, is determined by doing the following to Δg:

1. Remove GGM gravity anomaly Δg^{gm} (long-wavelength)
2. Add terrain correction, t_c which is determined from topographic irregularity upon removal of planar Bouguer gravity anomaly Δg_B, (Dahl and Forsberg 1999).
3. Remove RTM gravity anomaly obtained from approximate formula.

RTM is obtained from terrain irregularities referred to a smooth reference surface, h_{ref} of the area in question. Therefore Δg_{res} is given as

$$\Delta g_{res} = \Delta g + t_c - \Delta g^{gm} - 2\pi\mu\left(h - h_{ref}\right), \tag{2.3}$$

where h and h_{ref} are ellipsoidal heights of actual and reference surface points respectively, $\mu = G\rho$ with G the gravitational constant and ρ the topographic density. The residual gravity anomalies are gridded and then the RTM anomalies are restored, effectively leaving gridded residual Faye surface gravity anomalies; residual since they lack the long-wavelengths of the GGM, thus the resulting surface residual Faye gravity anomalies are given by

$$\Delta g_{\text{Faye}}^{res} = \Delta g + t_c - \Delta g^{gm} \tag{2.4}$$

Using Moritz's method of surface height anomaly determination by analytical continuation; (Moritz 1980a Ch. 48), residual height anomaly, ζ_{res} is computed from $\Delta g_{\text{Faye}}^{res}$ as,

$$\zeta_{res} = \frac{R}{4\pi\gamma}\iint_{\sigma} S(\psi)\left[\Delta g_{\text{Faye}}^{res} + (h_P - h)\frac{\partial \Delta g}{\partial h}\right] d\sigma\,, \tag{2.5}$$

where $S(\psi)$ is the Stokes function, h_P is ellipsoidal height of surface point P and σ is the integration cap size. The $\partial \Delta g / \partial h$ is expressed by Heiskanen and Moritz (1967 Eq. 2-217) as

$$\frac{\partial \Delta g}{\partial h} \approx \frac{R^2}{2\pi}\iint_{\sigma} \frac{\Delta g - \Delta g_P}{l_{PQ}^3} d\sigma - \frac{2\Delta g}{R}\,, \tag{2.6}$$

where l_{PQ} is the slope distance between point P on the surface and point Q at the sphere of radius R below P, Δg_P is gravity anomaly at point P, the rest of symbols maintain the previous meanings. If gravity anomalies were given on the sphere the last term of Eq. (2.6) would be zero. Normally $\partial \Delta g / \partial h$ is not known in RCR, as a result Eq. (2.6) is approximated by

$$\frac{\partial \Delta g}{\partial h} \approx \frac{\mu R^2}{2\pi}\iint_{\sigma} \frac{h - h_P}{l_{PQ}^3} d\sigma \tag{2.7}$$

That is, in Eq. (2.6), the last term has been neglected, and the gravity anomaly has been approximated by a linear equation correlated to topography. Eventually, the form of Eq. (2.5) deployed in practice to compute ζ_{res} is

$$\zeta_{res} = \frac{R}{4\pi\gamma}\iint_{\sigma} S(\psi)\Delta g_{\text{Faye}}^{res} d\sigma - \frac{\pi\mu h^2}{\gamma}\,, \tag{2.8}$$

The long-wavelength component of the geoid model which was removed from the surface gravity anomaly is computed from the GGM gravity anomaly Δg^{gm} and restored to give the full wavelength height anomaly ζ as

$$\zeta = \zeta_{gm} + \zeta_{res} \tag{2.9}$$

Furthermore in Eq. (2.1) the Bouguer gravity anomaly Δg_B is planar approximated.

$$\Delta g_B = \Delta g - 2\mu\pi h \tag{2.10}$$

Gravsoft package; a suite of programs for gravity field modelling (Tscherning et al. 1992, 1994), is then used to execute the method. Therefore estimation of height anomaly at P, in RCR (Denmark) ζ^{RCR} is obtained as

$$\zeta^{RCR} = \zeta_{gm} + \zeta_{res} = \left[\frac{r}{2\gamma}\sum_{n=2}^{l}\frac{2}{n-1}\Delta g_n^{gm}\right] + \left[\frac{R}{4\pi\gamma}\iint_{\sigma} S(\psi)\Delta g_{Faye}^{res}\, d\sigma - \frac{\pi\mu h^2}{\gamma}\right], \tag{2.11}$$

where Δg_n^{gm} is the n^{th} spherical harmonics Laplacian of Δg^{gm}. By substituting ζ in Eq. (2.1) with ζ^{RCR} in Eq. (2.11) and taking into account Eq. (2.10), we obtain geoid height by RCR via residual terrain modelling (RTM), N_{rtm}^{RCR} as

$$N_{rtm}^{RCR} = \zeta^{RCR} + \frac{(\Delta g - 2\pi\mu H)H}{\gamma} \tag{2.12}$$

Truncation error outside the cap is taken care of by only the long-wavelength contribution which has global coverage i.e. by ζ_{gm}, but in non-optimized way. Combined topographic effect on quasi-geoid model though zero, other corrections like downward continuation effect exist (Ågren 2004b Eq. 27), these do not feature explicitly in the literatures consulted.

II. RCR Geoid Model by Helmert's 2nd Condensation and Stokes Method

This method like the previous one, computes geoid height as a sum of long-wavelength reference (GGM) and residual components of geoid model using similar approach as for the RTM Quasi-geoid model, but with two main exceptions, namely reduction of gravity data from the surface to the geoid by free-air reduction and requirement for global gravity data i.e. no limitation to a cap.

We start with free-air gravity anomaly Δg_F, this means topographic masses are condensed to the geoid model according to Helmert's second method and the surface gravity is downward continued to the geoid model through free air using simple linear

gravity gradient as a function of elevation. The following preparations are pre-requisite to the Δg_F before using it in the classical Stokes formula:

1. Smooth the Δg_F by converting it to the Bouguer gravity anomaly, approximated by planar Bouguer anomaly $-2\pi\mu h$
2. Reduce its magnitude by removing the long-wavelength component represented by GGM gravity anomaly Δg^{gm} on the mean Earth sphere
3. Add terrain correction, t_c which is determined from topographic irregularity upon removal of planar Bouguer gravity anomaly
4. Remove gravity indirect effect due to withdrawal of Helmert's topographic masses, given by $\delta\Delta g = (2\pi\mu / R)h^2$, R is mean Earth radius. (Omang and Forsberg 2000).
5. Grid the residual reduced gravity anomaly Δg_{res}^{red} given by

$$\Delta g_{res}^{red} = \Delta g_F + t_c - 2\pi\mu h - \Delta g^{gm} + \delta\Delta g \tag{2.13}$$

6. Restore the Bouguer plate anomaly removed to smooth the Δg_F in equally grid format, thus Δg_{res}^{red} of Eq. (2.13) becomes geoid reduced residual Faye gravity anomaly Δg_{res}^{Faye} (in grid format) given by

$$\Delta g_{res}^{Faye} = \Delta g_F + t_c + \delta\Delta g - \Delta g^{gm} \tag{2.14}$$

7. Use the Δg_{res}^{Faye} in classical Stokes formula to compute residual geoid height N_{res} as

$$N_{res} = \frac{R}{4\pi\gamma}\iint \Delta g_{res}^{Faye} S(\psi)\, d\sigma \tag{2.15}$$

8. Compute and restore the reference geoid height from the removed Δg^{gm} as

$$N_{ref}^{gm} = \frac{R}{2\gamma}\sum_{n=2}^{M}\frac{2}{n-1}\Delta g_n^{gm} \tag{2.16}$$

9. Restore the Helmert's condensed masses, this leads to first and secondary indirect effects to geoid height, $\delta N_{i,1}$ and $\delta N_{i,2}$ given by (ibid) as

$$\delta N_{i,1} = -\frac{\pi\mu}{\gamma}h^2 \quad \text{and} \quad \delta N_{i,2} = -\frac{\mu}{6\gamma}\iint \frac{h^3 - h_P^3}{(h - h_P)^3}dxdy\,, \tag{2.17}$$

where height of data point is h and that of computation point is h_P

10. Assemble Helmert's geoid height by RCR Danish method N_H^{RCR} from its components in Eqs. (2.15) to (2.17) as

$$N_H^{RCR} = N_{ref}^{gm} + N_{res} + \delta N_{i,1} + \delta N_{i,2} \tag{2.18}$$

That is

$$N_H^{RCR} = \left[\frac{R}{2\gamma} \sum_{n=2}^{M} \frac{2}{n-1} \Delta g_n^{gm} \right] + \left[\frac{R}{4\pi\gamma} \iint \Delta g_{res}^{Faye} S(\psi) d\sigma \right] + \left[-\frac{\pi\mu}{\gamma} h^2 - \frac{\mu}{6\gamma} \iint \frac{h^3 - h_P^3}{(h - h_P)^3} dx\, dy \right] \tag{2.19}$$

Approximations exercised in this approach, just like the previous one, limit the method, consequently some corrections are found unnecessary e.g. effect of atmospheric masses external to the geoid model and ellipsoidal corrections cf. Sect. 3.2. Inspired by the need for a cm-geoid model in Europe, and the comment in Omang and Forsberg (2000) that despite improved data quantity and quality geoid model computed by the RCR do not become better, Sjöberg (2005a), took the effort to analyze the limitations of the RCR geoid model determination methods, the following are excerpts from the paper.

A brief highlight of the limitations of RCR method

Cited problems with the RCR method

- The basic theory used is the first-order approximation of M.S. Molodensky's method for either quasi-geoid model or Helmert's geoid model determination, but this theory was developed for around $10\,cm$ geoid model. Improvements by Bjerhammar and Moritz for more accurate geoid model have not been implemented seriously in RCR with a cm-geoid model objective.
- Removal of long-wavelength from terrestrial gravity data and its restoration by a GGM could be done in a better way (ibid).
- The assumption that by working with smaller magnitude residual gravity anomaly, less accurate mathematical models can be used has no justification whatsoever (Sjöberg 2005a).

Recommendations

- Stokes kernel ought to be modified differently so that errors of terrestrial gravity, GGM and truncation in the light of the present demand for 1-cm geoid model are addressed.
- Topographic, atmospheric and ellipsoidal corrections must carefully be studied and applied in optimal way.

Specific areas of problem in the two approaches of RCR explained above.

a) Compared to M.S. Molodensky's method which was subsequently improved by Bjerhammar and Moritz in its first order approximation cf. Eq. (1) and (2) in Sjöberg (2005a), Eq. (2.11) has become even less accurate due to further approximations, for example

- The gravity anomaly gradient, $\partial\Delta g/\partial h$ expressed by Heiskanen and Moritz (1967 Eq. 2-217) has been approximated by a simpler linear gradient correlated to topography; it is doubtful whether it can meet the requirements of a cm geoid model.
- Heiskanen and Moritz (1967 Eq. 8-102) should be used for the conversion of quasi-geoid model to geoid model, see also (Sjöberg 1995).

b) The terrain correction t_c in Eq. (2.14) which impliedly takes care of direct effect and downward continuation of gravity from surface to geoid in Eq. (2.15) has been computed based on planar approximation with uniform crust density, this may not hold for mountainous areas, besides the assumption is not quite true (Sjöberg 1994b).

The magnitude of errors which stem out of RCR are explained in detail in Sjöberg (2005a) Sect. 2, see it for more details.

As for the Helmert's second condensation with classical Stokes method, the error is less serious but still significant at cm-level.

Other observations are

- While use of I-D FFT in Stokes integration does not cause approximation, but planar approximation introduces bias.
- Working with residual gravity anomaly does not reduce original data errors
- Working with small optimal spherical cap together with a GGM is advantageous versus otherwise.
- The methods suffer from GGM signal truncation to maximum degree M and limitation of Stokes integration to a small cap or rectangle σ_0. It is shown, that for cap size $\leq 10^\circ$, the truncation error is significant to both approaches, but more so with Helmert's when confined to a cap. For example for Helmert's approach, for a cap of 2°, truncation error is 3.2 cm. Evaluation of optimized Molodensky's method shows that truncation is insignificant for cap size as small as 2°.
- Handling of both terrestrial and GGM data errors should be re-approached. Given the present amount of gravity data in the World from many different sources, more realistic gravity data error models can be developed to address the problem of geoid truncation error in this and similar methods, see for example Sjöberg (1984b).

The practical approach of RCR is commended as the use of residual gravity in Stokes reduces the errors of integration.

2.2 Stokes-Helmert Method

(Tenser et al. 2003) "… Many methods for geoid model determination exist and are in use around the world. One of the most advantageous methods is the Stokes-Helmert approach developed at the University of New Brunswick (UNB). The main theoretical development of this method is attributed to Vaníček, along with the contribution of other authors, such as Martinec, Sjöberg, Kleusberg, Heck and Grafarend. The theoretical aspects of the UNB approach were published in more than fifty contributions …" Since

there has been many graduate geodesists from the UNB around the globe, there is not much doubt about the above quotation, especially in usage.

The UNB Stokes-Helmert method for precise regional gravimetric geoid model determination follows the r-c-r approach (Tenser et al. 2003) via a modified Stokes kernel (Vaníček and Kleusberg 1987, Vaníček and Sjöberg 1991) with the following visions:

- To reduce truncation errors based on Molodensky's theory (Molodensky et al. 1962).
- To separate reference and higher-degree gravity field and reformulation of Stokes BVP for the higher-degree reference spheroid (kernel modification) as described in Vaníček and Sjöberg (1991) and Vaníček and Featherstone (1998).

Assessment of how much the above visions have been successful, is left to the reader upon going through the available appropriate literature and cited references, since inhere, only an outline of the method will be given with appropriate reference(s) whenever possible. In 1884 Helmert recognized that the presence of Earth topographical and atmospheric masses external to geoid violate the basic Stokes assumption that disturbing potential must be harmonic outside the geoid, henceforth he formulated, that the earth's topography can be replaced by an infinitesimally thin layer of density equal to that of the product of topographic density and height. This layer could either be placed beneath the geoid model or right on the geoid model without violating the required assumption of harmonicity. The second option commonly known as Helmert's "second condensation method" together with the Stokes method are pursued in the UNB approach and hence the "Stokes-Helmert" method. The method is tailored in seven stages as follows:

1. Formulation of the fundamental formula of physical geodesy at the surface of the Earth in the real space.
2. Transformation of the gravity anomalies referred to the Earth's surface, from the real space into the no topography gravity space.
3. Solution to Dirichlet's inverse boundary value problem in the no topography gravity space by applying the Poisson integral equation, i.e. downward continuation of the surface gravity anomalies to the geoid model.
4. Transformation of the gravity anomalies referred to the geoid surface, from the no topography gravity space into the Helmert gravity space.
5. Reformulation of the geodetic boundary-value problem by decomposition of Helmert's gravity field into the low-frequency and high-frequency part of the gravity field.
6. Solution to the Stokes BVP for the high-frequency Helmert gravity field using the modified spheroidal Stokes' kernel and evaluation of the Helmert reference spheroid by GGM.
7. Transformation of the geoid from the Helmert gravity space back into the real Earth space.

The outline of the method will follow the above stages with the limitation that the issues of gravity data accuracy, distribution and crustal density requirement though very crucial and inevitable for precise accurate geoid model, are almost universal to all methods, and thus will not feature here explicitly.

Disturbing potential T at point P is computed from the Earth's gravity potential W and the normal potential of the reference ellipsoid U at the same point P from

$$T_P = W_P - U_P \tag{2.20}$$

Geoid is one of the many equipotential surfaces of the Earth's gravity potential with value W_g which very closely coincides with the open mean sea level. It is straight forward to determine U_g, therefore W_g will be known if T_g is known for all points on the geoid. As pointed out in the introduction, solution for T_g is obtained from gravity anomaly on the geoid as a solution to the third boundary value problem (BVP) with geoid as the boundary surface i.e. the Laplace's equation

$$\nabla^2 T = \Delta T = 0 \tag{2.21}$$

We have seen that

$$\mathrm{N} = \frac{T_g}{\gamma_0}, \tag{2.22}$$

where γ_0 is the normal gravity on the reference ellipsoid. To make T harmonic outside the Earth's surface, the observed gravity g is corrected of the atmospheric mass attraction effect above the observation point. From Heiskanen and Moritz (1967)

$$\mathsf{g} = \left| grad\ W \right| = \left| grad\ U + grad\ T \right| \tag{2.23}$$

Under the assumption that the correction for atmospheric mass attraction has removed fully the influence of the atmosphere in g, then the resulting disturbing potential T' from the gravity corrected of atmospheric effect on the Earth's surface, g', is harmonic on and above the Earth's surface given by

$$\Delta T'(r) = 0 \ \text{ for } r \text{ outside the Eath's surface} \tag{2.24}$$

Unfortunately this approach can not lead to geoid height since the Bruns' formula works only when the normal potential on the reference ellipsoid equals actual potential on the geoid model i.e. $U_o = W_g$. Thus we still need to reduce T and have it harmonic on and outside the geoid model and hence the need for Helmert's condensation layer on the geoid model.

Helmert's Model Space

Helmert's model space consists of the same mass distribution inside the geoid model, with added Helmert's condensation layer of the topography of areal density $\mu = \bar{\rho} H$,

where $\bar{\rho}$ is the mean density of the vertical column of height H above the geoid as the real Earth, moreover the model has no atmosphere. If the actual potential of the topographic masses is V^t, and that of the condensed masses on the geoid model is V^c, then residual potential δV is obtained as

$$\delta V = V^t - V^c \tag{2.25}$$

On the other hand, it is possible to divide the actual gravitational potential V into potential of the masses below geoid V^g, and that of the topography above it as

$$V = V^g + V^t . \tag{2.26}$$

From Eqs. (2.25) and (2.26) we get

$$V = \left(V^g + V^c\right) + \delta V$$

or (2.27)

$$V = V^H + \delta V,$$

where $V^H = V^g + V^c$ is Helmert's model potential, which is very close to the actual gravitational potential V, and is regarded to be harmonic on and outside the geoid since both V^g and V^c are. If Φ is the centrifugal potential, we can write for the actual Earth

$$W = V + \Phi = U + T , \tag{2.28}$$

similarly for the Helmert's model space we can write

$$W^H = V^H + \Phi = U + T^H \tag{2.29}$$

From Eqs. (2.27) to (2.29) we deduce that

$$\delta V = T - T^H \qquad \Rightarrow \qquad W = U + T^H + \delta V \tag{2.30}$$

Now we can express the Laplacian

$$\Delta T^H = 0 \qquad \text{outside Helmert's geoid} \tag{2.31}$$

To solve the Laplacian in Eq. (2.31) for T^H we need to have some boundary conditions satisfied on the geoid model, as we saw before, it is the third BVP (Eq. (2.32)), therefore in this case we need gravity anomaly defined on the geoid model, this is carried out in Vaníček and Martinec (1994 Eq. 15-30) which results into

$$\Delta g_g^H = -\left.\frac{\partial T^H}{\partial r}\right|_g - \frac{2}{R} T_g^H , \tag{2.32}$$

where

$$\Delta g_g^H = g_g^H - \gamma_0 \tag{2.33}$$

is Helmert's gravity anomaly, g_g^H is Helmert's gravity on the geoid and subscript g stands for geoid model. Eq. (2.32) represents spherical approximation of Helmert's fundamental gravimetric equation for radius R. The big question now is, how the observed surface gravity g, or even g' corrected of atmospheric effect on the surface, is transformed into g_g^H on the geoid model through topographic masses? The procedure is as follows, first the Helmert's gravity g_t^H on the surface is obtained from g' by further reducing it of the topographic masses effect i.e. the direct topographic effect, obtained by taking the gradient of right hand side (RHS) equation in Eq. (2.30), this results into

$$g_t^H = g' - \frac{\partial V}{\partial H} + \ldots , \tag{2.34}$$

contribution from the next term is regarded too small and thus negligible for 1-cm geoid model (ibid). Next the g_t^H is downward continued to the geoid model in Helmert's model space by developing the g_t^H into Taylor series, which is justified by regarding Helmert's potential W^H of Eq. (2.29) above the geoid, satisfies Poisson's equation with a constant RHS (i.e. $\Delta W^H = 2\omega^2$) and thus all the derivatives with respect to height H exist, hence we obtain Helmert's reduced gravity to geoid model g_g^H as

$$g_g^H = g_t^H + \left.\frac{\partial^2 W^H}{\partial H^2}\right|_g H + \left.\frac{\partial^3 W^H}{\partial H^3}\right|_g + \ldots , \tag{2.35}$$

where the second and above terms constitute the downward continuation (dwc) of the Helmert's surface gravity g_t^H to the geoid model i.e. to g_g^H. Upon substitution of Eq. (2.29), it becomes

$$g_g^H - g_t^H = \left[\frac{\partial^2 U}{\partial H^2} + \frac{\partial^2 T^H}{\partial H^2}\right]_g H + \frac{1}{2}\left[\frac{\partial^3 U}{\partial H^3} + \frac{\partial^3 T^H}{\partial H^3}\right]_g H^2 + \ldots , \tag{2.36}$$

Since contribution from $\left(\frac{\partial^3 U}{\partial H^3}\right)_g$ is only about -48.4×10^{-6} μGal/m^2, it means higher terms in Eq. (2.36) can comfortably be neglected. Differentiation of Eq. (2.36) is still tricky since it involves the sought parameter T^H. If it is opted to seek solution by

iteration of derivatives of T^H, the convergence may be very slow due to successive negative and positive oscillations of the Taylor terms and possibly will require additional higher order terms. It is possible to re-write Eq. (2.36) in terms of T^H only as

$$dwc_g^H = \left.\frac{\partial T^H}{\partial H}\right|_g - \left.\frac{\partial T^H}{\partial H}\right|_t , \tag{2.37}$$

which happens to represent the downward continuation of T^H from surface to geoid model. It is found out that a better way to solve Eq. (2.37) is by use of Poisson's integral equation (Heiskanen and Moritz 1967, Kellog 1929, Ellmann and Vaníček 2006 Eq. 25). There is no doubt, that the key to accurately solving Eq. (2.36) lies in having precise density distribution information and more so solution to the tricky Eq. (2.37). As has been cited in many geodetic literatures, also in Section 3.2, solution to Eq. (2.37) through Poisson's integral or inversion, is not a simple and straight forward matter and therefore herein also it posses a threat to the achievable accuracy of Δg_g^H on the geoid model.

The approach followed in Martinec et al. (1993) is worth noting since it improves upon the simple (classical) free-air anomaly Δg_g^F we are accustomed to get to the Helmert's Δg_g^H. Only a brief explanation and the results are presented. Upon combining the results after taking gradient, first of both sides of the RHS Eq. (2.30) and then last part of Eq. (2.27), we obtain for the surface point s

$$\left.\frac{\partial T^H}{\partial r}\right|_s = -g_s + \gamma_s + A_s^t - A_s^c , \tag{2.38}$$

where A_s^t and A_s^c, g_s and γ_s are the radial attraction of the topographical and condensed masses, the observed and normal gravity all at the surface point s respectively. Further the surface normal gravity γ_s is developed into

$$\begin{aligned} \gamma_s &\doteq \gamma_q + \left.\frac{\partial \gamma}{\partial r}\right|_q (N + H) + \ \ldots , \\ \gamma_s &\doteq \gamma_q - \frac{2}{R} T_g^H - \frac{2}{R} \delta V_g^t - F \end{aligned} \tag{2.39}$$

where

$$F = -\frac{\partial \gamma}{\partial r} H \tag{2.40}$$

is free-air gravity reduction, the subscripts $s, g \text{ and } q$ stand for surface, geoid and ellipsoid respectively. Also the left hand side of Eq. (2.38) is expanded into

$$\left.\frac{\partial T^H}{\partial r}\right|_s = \left.\frac{\partial T^H}{\partial r}\right|_g + \left.\frac{\partial}{\partial r}\left(\frac{\partial T^H}{\partial r}\right)\right|_g H + \ \ldots\ , \tag{2.41}$$

Substitution of Eqs. (2.39) and (2.41) into Eq. (2.38), and taking into account Eq. (2.32) gives

$$\Delta g_g^H = \Delta g_g^F - A_s^t + A_s^c + g_1 + \delta s \tag{2.42a}$$

where:

$\Delta g_g^F = g_s + F - \gamma_q$ is the usual linear free-air gravity anomaly

$\delta s \doteq \frac{2}{R}\delta V_g^t$ is the secondary indirect effect to the gravity (Heiskanen and Moritz 1967 Eq.3-51)

$g_1 = \left.\frac{\partial^2 T^H}{\partial r^2}\right|_g H$ is the downward continuation of the Hemert's anomalous gravitation from surface to geoid model

The reduced and downward continued Helmert's gravity anomaly of Eq. (2.42a) can be put in three parts as

$$\Delta g_g^H = \left(g_s\right)^1 + \left(\delta s - A_s^t + A_s^c\right)^2 + \left(g_1 + F\right)^3 + k\ , \tag{2.42b}$$

where the superscripts $1,2,3$ stand for the components of Eq. (2.42a) explained as: component 1 is the surface gravity free of atmospheric effect, component 2 is the direct topographic effect on the surface gravity, component 3 is the downward continuation (dwc) effect on the surface gravity to geoid model and $k = \left(-\gamma_q\right)$ can be treated as a constant for the given point of interest. Just as in the previous case, all of the components of Eq. (2.42) are computed to acceptable accuracies except for the contentious dwc effect component g_1, which requires inversion of Poisson's integral, and so is dwc_g^H of Eq. (2.37).

We have discussed two approaches on how to formulate and downward continue observed gravity in Helmert's model space to Helmert's geoid; Eqs. (2.36) and (2.42). In the recent past, the UNB has re-approached the formulation of the Stokes BVP via surface gravity anomaly and in fact mean surface gravity anomaly (Tenzer et al. 2003, Vaníček et al. 1999, Ellmann and Vaníček 2006) whereby, to solve the geodetic BVP in the Helmert's space, Helmert's mean $5' \times 5'$ gravity anomalies (Vaníček et al. 1999) are evaluated on the Earth's surface and downward continued to Helmert's geoid model by iterative inversion of Poisson integral. Since naturally, Helmert's gravity anomalies are smooth, the process is made even smoother by deployment of mean anomalies. The ill position usually encountered in Poisson's inversion, is completely alleviated in this case (Vaníček et al. 1996 p 32). Further to the previous standard treatment, it is shown that a

correction for quasi-geoid to geoid separation has to be considered, and the secondary indirect effect ought to be evaluated at the topography rather than at the geoid level. An approach is then proposed for determining the mean Helmert anomaly from gravity data observed on the Earth's surface, based on the complete Bouguer anomaly, which is believed to be fairly smooth and thus useful for interpolation, approximation and averaging. On the anticipation, that any error in realizing Helmert's gravity anomaly Δg_g^H on the Helmert's geoid model, is tolerable for 1-cm geoid model, then Eq. (2.32) is now harmonic, and known on and above the Helmert's geoid boundary surface, as the third BVP solution to the Helmert's Laplace's equation (2.31).

Geoid Height from Helmert's Model

The UNB method strives to get the real T from the Helmert's disturbing potential T_g^H, this is realized by restoration of the masses external to Helmert's geoid model (co-geoid) i.e.

$$T_g = T_g^H + V_g^t + V_g^a , \tag{2.43}$$

where V_g^t and V_g^a are Helmert's primary indirect effects due to topographic and atmospheric masses on the Helmert's potential respectively. V_g^t is given in Vaníček and Martinec (1994 Eq. (47)), V_g^a is about one order of magnitude smaller than V_g^t, it is hoped that it can be evaluated to a sufficient degree of accuracy from existing atmospheric models (ibid). Once the real disturbing potential T is known then geoid height N is obtained from Bruns' formula,

$$N = \frac{T_g}{\gamma_0} \tag{2.44}$$

We still have a question to answer, namely, how do we obtain T_g in Eq. (2.44) or even T_g^H in Eq. (2.43)? The answer is, that since we have Δg_g^H harmonic on the spherical Helmert's geoid model as the bounding surface, the relation in Eq. (2.32) can be solved as a solution for the Helmert's Laplacian in Eq. (2.31). Once Δg_g^H has the said properties, it can then be used in the Stokes integral (Heiskanen and Moritz 1967 p 93) to determine T_g^H from which we can obtain the desired geoid height N in the real space by Bruns' formula through Eq. (2.43) as in Eq. (2.45) and hence the answer to the question.

$$N = \frac{T_g}{\gamma_0} = \frac{T_g^H}{\gamma_0} + \frac{V_g^t}{\gamma_0} + \frac{V_g^a}{\gamma_0} = N^H + \frac{V_g^t}{\gamma_0} + \frac{V_g^a}{\gamma_0} \tag{2.45}$$

Very seldom the original Stokes integral requirements are met (Heiskanen and Moritz 1967 Ch.3 & Sect. 8-2). The practice is to use modified Stokes function, which can reap

the advantages of terrestrial and satellite data types (as explained briefly in the beginning of this chapter), in a suitable optimal manner and leave out as much as possible their short comings. That is why, a combination of terrestrial and satellite data (GGM) is desired, the UNB approach is not an exception. So as pointed out in the introduction, the Stokes kernel is modified to use data limited to a spherical cap and a combination of terrestrial and satellite (GGM) gravity data. The kernel is modified such that from the original Stokes function $S(\psi)$ a low frequency part (usually corresponding to the available relevant GGM spectral degree) is removed and the left out high frequency part $S^h(\psi)$ is used together with residual high frequency terrestrial gravity data, Δg^h (residual meaning terrestrial gravity anomaly less the GGM frequencies) in the Stokes formula to compute high frequency N_h^H, part of the Helmert's geoid height N^H, limited to a spherical cap Ω_0, therefore

$$S(\psi)=\sum_{n=2}^{\infty}\frac{2n+1}{n-1}P_n(\cos\psi)=\sum_{n=2}^{l}\frac{2n+1}{n-1}P_n(\cos\psi)+\sum_{n=l+1}^{\infty}\frac{2n+1}{n-1}P_n(\cos\psi)$$

and hence (2.46)

$$S^h(\psi)=S(\psi)-\sum_{n=2}^{l}\frac{2n+1}{n-1}P_n(\cos\psi)=\sum_{n=l+1}^{\infty}\frac{2n+1}{n-1}P_n(\cos\psi)$$

The residual high frequency gravity data Δg^h is obtained as

$$\Delta g^h=\Delta g^T-\Delta g_n^G \tag{2.47}$$

where Δg^T is Helmert's terrestrial gravity data equivalent to Δg_g^H explained earlier, and Δg_n^G is GGM gravity anomaly on the Helmert's geoid model. The low frequency Hemert's geoid height, which in the UNB approach is referred to as the reference geoid height N_{ref}^H, is computed from the GGM gravity anomaly given on the Helmert's geoid so that N^H is obtained as

$$N^H=N_{ref}^H+N_h^H+N_{bias}^H \qquad \text{i.e.}$$

$$N^H=c\sum_{n=2}^{l}\frac{2}{n-1}\Delta g_n^G+\frac{R}{4\pi\gamma_0}\iint_{\Omega_0}\sum_{n=l+1}^{\infty}\frac{2n+1}{n-1}P_n(\cos\psi)\Delta g^h d\Omega+N_{bias}^H \tag{2.48}$$

From Eq. (2.48), the truncation bias is from the rest of the zone outside the cap, it is computed from the high frequency gravity data and thus the kernel is modified further to $S_M^h(\psi),\ \psi\in(\psi_0,\pi)$ (Vaníček and Kleusberg 1987) so that

$$N_{bias}^H=\frac{R}{4\pi\gamma_0}\iint_{\Omega-\Omega_0}S_M^h(\psi,\psi_0)\Delta g^h d\Omega, \tag{2.49}$$

where

$$S_M^h(\psi,\psi_0) = S^h(\psi) - \sum_{n=0}^{l} \frac{2n+1}{2} t_n(\psi_0) P_n(\cos\psi), \tag{2.50}$$

with

$$\sum_{n=0}^{l} \frac{2n+1}{2} t_n(\psi_0) r_{n,s}(\psi_0) P_n(\cos\psi) = Q_s(\psi_0) - \sum_{n=2}^{l} \frac{2n+1}{n-1} r_{n,s}(\psi_0) \tag{2.51}$$

In the above equations, t_n, $r_{n,s}$ and Q_s are modification parameters, the so called Paul-coefficients and Molodensky's truncation coefficients respectively (ibid). The parameters t_n are obtained by minimizing in least squares way, the mean square of the spheroidal modified kernel in the far zone so that

$$\forall t_n \in \mathbb{R}, \left\{ \int_{\psi=\psi_0}^{\pi} \left[S_M^h(\psi,\psi_0) \right]^2 d\Omega \right\} \text{ is minimum} \tag{2.52}$$

Due to non availability of Δg^h in the outer (far) zone, $\Delta g_n^G \frac{\delta y}{\delta x}$ is used instead, hopefully from composite GGM.

To compute N_h^H within the cap around computation point (CP), N_h^H is further split into two parts, one for the effect at the CP so as to cub the singularity effect as $\psi_0 \to 0$ and the other for the rest of the cap, this is arrived at by adding and removing Δg^h at the CP so that we have two parts as

$$\begin{aligned} N_h^H &= N_{h(\odot)}^H + N_{h(\odot-\psi_0)}^H \\ &= \frac{R}{4\pi\gamma_0} \iint_{\Omega 0} S^h(\psi,\psi_0) \left\{ \Delta g^h(\Omega) + \left[\Delta g^h(\Omega') - \Delta g^h(\Omega) \right] \right\} d\Omega \end{aligned} \tag{2.53}$$

The second component i.e. for the rest of the cap except the CP is expressed by (Novak et al. 2001a) as Eq. (2.54) to which the contribution from the CP is zero

$$N_{h(\odot-\psi_0)}^H = \frac{R}{4\pi\gamma_0} \iint_{\Omega_\odot} S^h(\psi,\psi_0) \left[\Delta g^h(\Omega') - \Delta g^h(\Omega) \right] d\Omega, \tag{2.54}$$

and after a few manipulations (ibid) contribution from the CP, i.e. the first part, is

$$N_{h(\odot)}^H = -\frac{R\Delta g^h(\Omega)}{2\gamma_0} \tilde{Q}_0^l(\psi_0) \tag{2.55}$$

Ω and Ω' are the geographical coordinates of the CP and running point respectively, $\omega_\circ$ stands for the cap area without the CP and $\tilde{Q}_0^l(\psi_0)$ is the mean Molodensky coefficient in the cap.

From Eq. (2.48), N_{ref}^H is given by

$$N_{ref}^H = c\sum_{n=2}^{l}\frac{2}{n-1}\Delta g_n^G \tag{2.56}$$

Therefore we can now realize N^H of Eq. (2.48) from Eqs. (2.56), (2.55), (2.54), (2.49) and use it in Eq. (2.45) to obtain the actual geoid height N referred to the real space as

$$N = N^H + \frac{V_g^t}{\gamma_0} + \frac{V_g^a}{\gamma_0} = N^H + \delta N_I^t + \delta N_I^a \tag{2.57}$$

Besides N^H we need the last two terms which correspond to the effect of restoration of topographic and atmospheric masses external to the Helmert's geoid model i.e. the co-geoid model. They are termed primary indirect effect of topographic (δN_I^t) and atmospheric (δN_I^a) masses on the geoid height respectively. The expression for δN_I^t and δN_I^a are given explicitly in Tenzer et al. (2003 Sections 9.1 and 9.2)

Cited Short Comings of Stokes Helmert Gravimetric Geoid Method of UNB

1. Downward continuation from Helmert's atmosphere free-space to Helmert's geoid by Poisson's integral inversion suffers a number of problems which have been cited many times cf. Martinec (1998) Sjöberg (1998a, 2001a), Ågren (2004 a-b). The problem still prevails in the new approach to compute geoid by quasi-geoid and a correction, in which the grids are required to be not less than $5' \times 5'$, consequently the high frequency part of the signal is removed leading to smoothed unrealistic geoid model.
2. The UNB kernel modification approach is fine except, it disregards both the terrestrial and the GGM gravity data errors, because the kernel modification does not involve errors from data in any suitable optimum way. Moreover, in the absence of terrestrial data outside the cap, truncation bias could be improved by involving global statistical estimation of gravity instead of GGM only.

2.3 Nomination of LSMS with AC for TZG08 Geoid Model

Sections 2.1 and 2.2 ended with the problems besetting two of the more frequently used gravimetric geoid model determination methods, in view of attainment of 1-cm geoid, namely RCR (Denmark) and Stokes-Helmert's (UNB-Canada). The third method is the KTH LSMS with AC, this is described in Ch.3 separately because it is the method found

most suitable for the determination of Tanzania geoid model of 2008; TZG08. The LSMS with AC has been found to be the state of art for almost all scenarios encountered in regional and local geoid model determinations. To start with, the method has taken care of all the cited problems in the two other methods in Sects. 2.1 and 2.2. Besides, it has additional advantages, these can be evidenced in numerous practical and/or theoretical literatures, too many to mention all. For example, most of the Sjöberg LE publications cited in this thesis deal with either the development or/and improvement of the LSMS or/and AC, so the reader is referred to the references at the end. Others are like Fan (1989), Nsombo (1996), Nahavandchi (1998), Sjöberg and Nahavandchi (2000), Sjöberg and Hunegnaw (2000), Hunegnaw (2001), Ellmann (2003-4), Ellmann and Sjöberg (2004), Sjöberg and Featherstone (2004), Ågren (2004 a-b), Ågren and Sjöberg (2004), Kiamehr and Sjöberg (2005), Kiamehr (2006 a-b), Ågren , Kiamehr and Sjöberg (2006 a-b), Ilias (2008) and many others not mentioned here.

This section intends to enumerate some of the prominent features of the LSMS with AC.

1. LSMS is developed to combined in a suitable manner, terrestrial and GGM gravity data while accounting for all data errors and truncation bias in the most efficient and optimal way, cf. Sjöberg (1984 a-b, 1991).
2. The additive corrections (AC), account efficiently for all significant corrections to the approximate geoid model determined from surface gravity anomaly, without the need for gravity reductions, at the same time ensuring, that all the conditions for Stokesian geoid model are abided to closely, see (Heiskanen and Moritz 1967 Ch.3 & Sect. 8-2) for the conditions.
3. All formulas for both the LSMS and the AC are rigorously developed, proved and tested theoretically and practically for 1-cm geoid model or better as witnessed in the many relevant literatures in the references, please refer to them.
4. LSMS with AC requires dense gravity anomaly grid and small computation cap, both of these are advantageous for better geoid model in the sense, that dense gravity grid when obtained in the right way, it reflects reality and hence eventually the geoid model frequencies are preserved. As for the small cap in the modified Stokes integral, it lowers the chance of incorporating long-wavelength terrestrial gravity errors.
5. Separation of the geoid model computation into approximate geoid model and corrections, increases computational efficiency at the same time minimizes the chances of computational errors and assumptions, besides, debugging is improved.
6. With the computation of approximate geoid model and corrections separated, it is very ease to update an old geoid model, depending on what has changed for better, i.e. often it may not be necessary to do all afresh, since the geoid model is computed in parts, cf. Ch. 6.
7. The KTH-GEOLAB literature is quite detailed. In some of its many programs, computation time is included, so that after the first run, one can plan more accurately for the next time processing, especially for those programs which take longer time e.g. the one for the determination of gravity anomaly gradient.

It should be emphasized here, that the method has its limitations, such as:

- Determination of the least squares modification parameters, cf. Sect. 3.1, requires input of suitable terrestrial gravity anomaly error and GGM signal degree variances (σ_n^2 and c_n respectively) to infinity, cf. Eq. (3.19). This requirement is not met easily, it is estimated from error models, cf. Sect. 5.3.2
- While the requirement of dense surface gravity anomaly is good thing, but its realization can be very involving and often laborious, tedious and time consuming and sometimes difficult to achieve.

Conclusion: In view of the highlights on the limitations versus advantages of the three prominent methods, it is right and appropriate to use the KTH LSMS with AC to conduct the research of this study, i.e. determination of Tanzania new geoid model in spite of the big data gaps with varying density and poor distribution found in the AOI.

Chapter Three

LEAST SQUARES MODIFICATION OF STOKES METHOD WITH ADDITIVE CORRECTIONS

In the previous chapter we had a brief review of two prominent methods which utilize combination of terrestrial and satellite gravity data, and modified Stokes formula to determine gravimetric geoid model. In this chapter we describe in detail the Royal Institute of Technology of Sweden (KTH) method of gravimetric geoid model determination; the unbiased least squares modification of Stokes method (LSMS) with additive corrections (AC), since it is the method for this research i.e. to determine new gravimetric geoid model of Tanzania 2008 (TZG08). In addition to its qualities, some explained at the end of Ch.2, the method has proven to be the state of art and most viable option for precise gravimetric geoid model determination as it gradually evolved and verified in Fan (1989), Nsombo (1996), Nahavandchi (1998), Hunegnaw (2001), Ellmann (2004), Ågren (2004b), Kiamehr (2006a), Ågren, Kiamehr and Sjöberg (2006 a-b), Ilias (2008) and many others. Stokes method, which dates way back 1849, is still the basis for gravimetric geoid model determination. The urge for modification came from the stringent conditions posed by the original Stokes approach as pointed out in Sect. 1.3 (ii) and more explicitly expressed in Heiskanen and Moritz (1967 Ch.3 & Sect. 8-2). The idea of modifying Stokes method to reduce the impact of truncation of integration to a small cap around the computation point (CP) originated from M.S. Molodensky; (Molodensky et al. 1962), thereafter many methods developed which used heterogeneous gravity data to estimate geoid height. The methods modified Stokes kernel in different fashions for different aims. For example Wong and Gore (1969), Meissl (1971) including Molodensky et al. (1962) which endeavoured to minimize truncation error. Other initiatives like Sjöberg (1980), Wenzel (1981, 1982) modified the kernel by taking into account errors of terrestrial and GGM gravity data supposedly known in advance. Since 1984 KTH has worked and improved gradually on the optimization of geoid height errors emanating from deterministic as well as stochastic sources in a least squares approach; we cite such works as (Sjöberg 1984 a-b, 1991, 2003 a-b, 2005 a-b; Sjöberg and Featherstone 2004, Sjöberg and Hunegnaw 2000, Ågren and Sjöberg 2004 and Ågren, 2004b). The cited works either modified the kernel or discussed critically the LSMS. The LSMS and LSMS with AC are basically described in Sjöberg (1991 and 2003b), respectively.

3.1 The Least Squares Modification of Stokes Formula (LSMS)

The aim of LSMS is to reduce in a least squares sense, errors of geoid height springing from truncation, terrestrial gravity and GGM potential coefficients. The original Stokes formula for gravimetric geoid model is given by

$$N = \frac{R}{4\pi\gamma}\iint_{\sigma} S(\psi)\Delta g\, d\sigma\,, \tag{3.1}$$

where N is geoid height, R is mean radius of the Earth, ψ geocentric angle, γ normal gravity on the reference ellipsoid, Δg gravity anomaly on the geoid, $d\sigma$ infinitesimal surface element of integration over a unit sphere σ and $S(\psi)$ is Stokes function, which in closed form is given (Heiskanen and Moritz 1967 p 94) as

$$S(\psi) = \frac{1}{\sin(\psi/2)} - 6\sin\frac{\psi}{2} + 1 - 5\cos\psi - 3\cos\psi\ln\left(\sin\frac{\psi}{2} + \sin^2\frac{\psi}{2}\right) \tag{3.2}$$

and in spectral form (ibid p 97) as

$$S(\psi) = \sum_{n=2}^{\infty}\frac{2n+1}{n-1}P_n(\cos\psi)\,, \tag{3.3}$$

and P_n is Legendre polynomial

The fact is;

- Assumptions and conditions of original Stokes method are difficult to fulfil parse.
- Terrestrial gravity data is usually contaminated by long-wavelength systematic errors.
- Gravity data from dedicated satellite gravity missions like CHAMP and GRACE, which is of long-wavelength nature, has global coverage and small commission and omission errors (Ågren 2004b).
- There exist dense, fairly accurate global DEM models like SRTM and GLOBE.
- Global gravity anomaly signal and error degree variance models which have given reliable results exist; cf. Sect. 5.3.2 for details also Ågren (2004b Ch.2).

The above facts necessitated a kernel modification, which could optimize in a suitable manner, all deterministic and stochastic error sources, without compromising the basic assumptions and conditions set out by Stokes method. Thus the KTH LSMS method aims at a kernel which addresses and or acknowledges the following:

- Filter out the often erroneous long-wavelength component of gravity from terrestrial gravity data and substitute it with one from a GGM.
- Acknowledge the presence of terrestrial and GGM gravity data errors and account for them; this includes limitation of GGM to degree M.
- Minimize bias due to truncation of integration to a cap by making use of GGMs and global gravity anomaly error models.
- Minimum mean square error (MSE) of computed geoid height.

By taking some of the above facts into consideration, and that the observed terrestrial gravity anomaly $\Delta\hat{g}$ is limited to a cap of radius σ_0, with corresponding geocentric angle ψ_0, the GGM gravity anomaly Δg^S is known up to degree and order M, the modified Stokes method provides approximate geoid height $\tilde{N}$ as

$$\tilde{N} = \frac{c}{2\pi}\iint_{\sigma_0} S^M(\psi_0)\Delta\hat{g}\,d\sigma + c\sum_{n=2}^{M} s_n \Delta\hat{g}_n^S \,, \tag{3.4}$$

where $S^M(\psi)$ is the modified Stokes function and s_n are the modification parameters with the assumption that s_0 and s_1 are zero. $S^M(\psi)$ is expressed as

$$S^M(\psi) = S(\psi) - \sum_{n=2}^{M} \frac{2n+1}{2} s_n P_n(\cos\psi) \tag{3.5}$$

Stokes kernel modification differences often stem from variations in the modification parameters s_n. A true geoid height of Eq. (3.4) is given by

$$N = \frac{c}{2\pi}\iint_{\sigma} S^M(\psi)\Delta g\,d\sigma + c\sum_{n=2}^{M} s_n \Delta g_n^S \tag{3.6}$$

At the moment we have assumed in Eqs. (3.4) and (3.6), that there are no masses external to geoid model, and the Earth is spherical (these assumptions are lifted up in Sect. 3.2), with these reservations, error of Eq. (3.4) is

$$\delta N = \tilde{N} - N = \frac{c}{2\pi}\iint_{\sigma} S^M(\psi)\varepsilon^T d\sigma + c\sum_{n=2}^{M} s_n \varepsilon_n^S - \frac{c}{2\pi}\iint_{\sigma-\sigma_0} S^M(\psi)\Delta g\,d\sigma \,, \tag{3.7}$$

where ε^T and ε_n^S are errors of the terrestrial and nth GGM Laplace harmonic of gravity anomaly respectively. By assuming these errors are random with zero statistical expectation, i.e.

$$E\{\varepsilon^T\} = 0 \text{ and } E\{\varepsilon_n^S\} = 0 \qquad \textit{for all } n \,, \tag{3.8}$$

then

$$E\{\delta N\} = -\frac{c}{2\pi}\iint_{\sigma-\sigma_0} S^M(\psi)\Delta g\,d\sigma = -c\sum_{n=2}^{\infty} Q_n^M \Delta g_n\,d\sigma \tag{3.9}$$

The truncation coefficients Q_n^M are further expressed as

$$Q_n^M = Q_n - \sum_{k=2}^{M} \frac{2k+1}{2} s_k e_{nk} \,, \tag{3.10}$$

where the Molodensky's truncation coefficients Q_n are given by

$$Q_n = \int_{\psi_0}^{\pi} S(\psi) P_n(\cos\psi) \sin\psi d\psi \,, \tag{3.11}$$

and the Paul's coefficients, e_{nk} (Sjöberg 1984a) are expressed as

$$e_{nk} = \int_{\psi_0}^{\pi} P_n(\cos\psi) P_k(\cos\psi) \sin\psi \, d\psi \tag{3.12}$$

Thus from Eq. (3.9) we deduce that the estimator (3.4) is biased for all degrees from $n = 2$. We can now use Eq. (3.9) to take care of the bias due to truncation in Eq. (3.4), at the same time allowing for more parameters than the available degree of the GGM. First by modifying further the Stokes function to

$$S^L(\psi) = S(\psi) - \sum_{n=2}^{L} \frac{2n+1}{2} s_n P_n(\cos\psi), \quad L \geq M \tag{3.13}$$

and then take care of truncation bias. This way the estimator $\tilde{N}$ becomes,

$$\tilde{N} = \frac{c}{2\pi} \iint_{\sigma_0} S^L(\psi) \Delta\hat{g} d\sigma + c \sum_{n=2}^{M} \left(Q_n^L + s_n \right) \Delta\hat{g}_n^S \tag{3.14}$$

Comparison of Eqs. (3.6) and (3.14) leads to the geoid model error,

$$\delta N = \frac{c}{2\pi} \iint_{\sigma_0} S^L(\psi) \varepsilon^T d\sigma + c \sum_{n=2}^{M} \left(Q_n^L + s_n \right) \varepsilon_n^S - c \sum_{n=M+1}^{L} \left(Q_n^L + s_n \right) \Delta g_n - c \sum_{L+1}^{\infty} Q_n^L \Delta g_n \,, \tag{3.15}$$

and assuming that ε^T and ε_n^S are random with zero statistical expectation leads to

$$E\{\delta N\} = -c \sum_{n=M+1}^{L} \left(Q_n^L + s_n \right) \Delta g_n - c \sum_{L+1}^{\infty} Q_n^L \Delta g_n \tag{3.16}$$

Eq. (3.16) implies that the estimator $\tilde{N}$ is unbiased from degree 2 to M. The global mean square error (MSE) of the unbiased estimator (3.14) can be obtained from

$$\overline{\delta} N^2 = E\left\{ \frac{1}{4\pi} \iint_{\sigma} (\delta N)^2 d\sigma \right\} \tag{3.17}$$

Under the assumption, that error covariance function of Δg is homogeneous and isotropic (Sjöberg 1991) given by

$$C(\psi) = \sum_{n=2}^{\infty} \sigma_n^2 P_n(\cos\psi), \tag{3.18}$$

with σ_n^2 as the n^{th} gravity anomaly error degree variance. Furthermore it is assumed that the terrestrial and GGM gravity anomalies are uncorrelated. The last assumption has been implemented partially in this work by involving only a pure satellite GGM in the Stokes kernel modification by least squares approach and determination of approximate geoid model from GGM. On the other hand, the composite GGM is used in patching of empty surface gravity grids in Sect. 5.2. That way the assumption was not fully honoured in the patched grids. The MSE Eq. (3.17) is developed in Sjöberg (1985, 1986) and improved for the unbiased geoid model estimator in Sjöberg (1991) as:

$$\overline{\delta} N^2 = c^2 \sum_{n=2}^{\infty} \left\{ \left(\frac{2}{n-1} - Q_n^L - s_n^* \right)^2 \sigma_n^2 + \left(Q_n^L + s_n^* \right)^2 dc_n^* \right\}, \tag{3.19}$$

here

$$s_n^* = \begin{cases} s_n & \text{if } 2 \le n \le L \\ 0 & otherwise \end{cases} \quad \text{and} \quad dc_n^* = \begin{cases} dc_n & \text{if } 2 \le n \le L \\ c_n & n > L \end{cases}$$

where c_n is the GGM gravity anomaly signal degree variance, also known as the power spectrum component, which can be evaluated from

$$c_n = \frac{1}{4\pi} \iint_{\sigma} (\Delta g_n)^2 d\sigma \tag{3.20}$$

dc_n is the expected mean square error (noise) of GGM also known as error degree variance, usually obtainable from GGM potential coefficients variances $\sigma_{c_{nm}}^2$ and $\sigma_{s_{nm}}^2$ as

$$dc_n = E\left\{ \frac{1}{4\pi} \iint_{\sigma} \left(\varepsilon_n^S \right)^2 d\sigma \right\} = \left(\frac{GM}{a^2} \right)^2 (n-1)^2 \sum_{m=-n}^{n} \left(\sigma_{c_{nm}}^2 + \sigma_{s_{nm}}^2 \right), \tag{3.21}$$

Terrestrial anomaly error degree variance, σ_n^2 of $\hat{\Delta g}_n^T$ is obtained as

$$\sigma_n^2 = E\left\{ \frac{1}{4\pi} \iint_{\sigma} \left(\varepsilon_n^T \right)^2 d\sigma \right\}, \tag{3.22}$$

where ε_n^T is the error of $\hat{\Delta g}_n^T$

The minimum MSE of the unbiased estimator, i.e. $\bar{\delta} N^2 = \min$, is attained when Eq. (3.19) is differentiated with respect to parameters s_n i.e. $\partial\left(\bar{\delta}\mathrm{N}^2\right)/\partial s_n$ and then set to minimum by equating to zero. This results into a system of linear equations (Sjöberg 1991).

$$\sum_{r=2}^{L} a_{kr} s_r = h_k, \qquad k = 2,3, \ \ldots \ , \mathrm{L}, \tag{3.23a}$$

where a_{kr} and h_k are modification coefficients dependent on $Q_{n,}$ e_{nk}, c_n, dc_n and σ_n^2. The difference between many kernel modification methods comes from the way the modification parameters s_l, $l = 2,3, \ldots, L$ are realized, which are the solution to the system of linear equations in formula (3.23a). For the KTH LSMS, the solution is obtained through the least squares approach and this leads to Sjöberg (1991 p 371 Eqs. 3.6 a-c)

$$a_{kr} = d_k \delta_{kr} - \frac{2r+1}{2} d_k e_{kr} - \frac{2k+1}{2} d_k e_{kr} + \frac{2k+1}{2}\frac{2r+1}{2} \sum_{n=2}^{\infty} e_{nk} e_{nr} d_n \tag{3.23b}$$

and

$$h_k = \frac{2\sigma_k^2}{k-1} - Q_k d_k + \frac{2k+1}{2} \sum_{n=2}^{\infty} \left(Q_n e_{nk} d_n - \frac{2}{n-1} e_{nk} \sigma_n^2 \right), \tag{3.23c}$$

where

$$d_n = \sigma_n^2 dc_n^* \text{ , with } dc_n^* = \begin{cases} dc_n & \text{if } 2 \le n \le L \\ c_n & \text{if } n > L \end{cases} \text{ and } \delta_{kr} = \begin{cases} 1 & \text{if } k = r \\ 0 & \text{if } k \ne r \end{cases} \tag{3.23d}$$

The system of equations in (3.23a) involves inversion of the matrix $A = [a_{kr}]$, which becomes ill-conditioned with increasing size L thus quite involving. Investigations by Ellmann (2003) and Ågren (2004b) have shown that while not all regularization methods work well with the inversion, but singular value decomposition (SVD) technique is more effective and efficient, besides Ågren (2004b) concludes, that appropriately truncated SVD produces insignificant effect to the modification parameters of the LSMS.

The LS optimized solution s_n henceforth leads to the KTH LSMS when used in kernel modification, truncation coefficient, bias and MSE for geoid model determination.

The assumption that terrestrial and GGM gravity data are not correlated is usually not realistic. The effect of data correlation is further considered in the LSMS. Let the error degree covariance between ε_n^T and ε_n^S be Υ_n, by following the same approach as before, it is concluded in Sjöberg (1991) that the MSE of the geoid height ($m_{\bar{N}}^2$) using correlated data in the LSMS (unbiased) is given by

$$m_{\bar{N}}^2 = c^2 \left\{ \sum_{n=2}^{\infty} \left(\frac{2}{n-1} - Q_n \right)^2 \sigma_n^2 + \sum_{n=2}^{M} \left[Q_n^2 dc_n + 2 \left(\frac{2}{n-1} - Q_n \right) Q_n \Upsilon_n \right] + \sum_{n=M+1}^{\infty} Q_n^2 c_n - \sum_{k=2}^{L} s_k h_k \right\}$$

…. (3.24)

The KTH LSMS, which has been extended to take into account data correlation, has been tested extensively since 1991. It is anticipated, that the impact of uncertainties in the gravity anomaly signal and error degree variance models to the KTH method will gradually subside as more terrestrial and altimetry gravity data availability and distribution improve and when GGMs from more dedicated satellite gravity missions like GOCE come into play.

The assumption imposed onto Eqs. (3.4) and (3.6) for non existence of external masses to geoid model and zero ellipticity, are unrealistic, they will be lifted up in the next section as external corrections to the approximate geoid height of Eq. (3.14).

3.2 Additive Corrections to Approximate Geoid height

One is at liberty to use the KTH LSMS with reduced or unreduced gravity anomalies. Gravity anomaly reduction intends to correct the surface gravity anomaly (dg_surf) for the forbidden topographic and atmospheric masses external to the geoid also ellipsoidal correction to meet the spherical surface requirement in Stokes method. Consequently some kind of remove-compute-restore (r-c-r) approach is followed to compute gravimetric geoid model through classical or modified Stokes method when reduced anomalies are used (cf. Heiskanen and Moritz 1967 Sect. 8-2). Seldom classical approach is used to compute geoid model nowadays, but usually a GGM is used to obtain reduced residual gravity anomaly $\delta\Delta g$. Often the integration is limited to a spherical cap σ_0 of unit sphere σ around the computation point (CP), so some kind of modified Stokes function $S^N(\psi)$ is used instead of the usual Stokes function $S(\psi)$, the kernel modification could cater only for truncation bias e.g. Molodensky (1962) or deterministic and stochastic errors as in Sjöberg (1984b) depending on the modification parameters s_n in use, then geoid model is computed through r-c-r approach as explained in Ch 2. In this case a complete general model for the determination of geoid height, $\hat{N}$ at a point of interest using reduced residual gravity anomaly, $\delta\Delta g$ would be

$$\hat{N} = \frac{R}{4\pi\gamma_0} \iint_{\sigma_0} S^N(\psi) \delta\Delta g \, d\sigma + \delta N_I^t + \delta N_I^a + \delta N_e + N^{GGM}, \quad (3.25a)$$

(3.25a)

where

$$\delta\Delta g = \Delta g + \delta\Delta g_{dir}^t + \delta\Delta g_I + \delta\Delta g_{dir}^a + \delta\Delta g_{dwc} + \delta\Delta g_e - \Delta g^{GGM} \quad (3.25b)$$

and

$$N^{GGM} = \frac{R}{2\gamma_0}\sum_{n=2}^{M}\frac{2}{n-1}\Delta g_n^{GGM}, \quad \text{where} \quad \Delta g^{\mathrm{GGM}} = \sum_{n=2}^{M}\Delta g_n^{GGM} \tag{3.25c}$$

and

$$S^N(\psi) = S(\psi) - \sum_{n=2}^{N}\frac{2n+1}{2}s_n P_n(\cos\psi) \tag{3.25d}$$

R is mean Earth radius, γ_0 is normal gravity on the reference ellipsoid, $\delta\Delta g$ is reduced residual gravity anomaly which is the difference between surface gravity anomaly Δg; [corrected of topographic and atmospheric reductions $\delta\Delta g_{dir}^{t}$ and $\delta\Delta g_{dir}^{a}$ respectively and downward continued to sea level by $\delta\Delta g_{dwc}$, secondary indirect effect $\delta\Delta g_I$ and scaling effect due to ellipsoid to spherical gravity anomaly $\delta\Delta g_e$] and GGM gravity anomaly at the geoid model Δg^{GGM} cf. Sjöberg (1999, 2000, 2001b, 2003c) for details. δN_I^t is indirect topographic effect due to restoration of topographic masses, δN_I^a is indirect atmospheric effect due to restoration of atmospheric masses, δN_e is ellipsoidal effect which accounts for the mapping of a spherical geoid model onto ellipsoidal geoid model, Sjöberg (2003d, 2004c), N^{GGM} is the long-wavelength geoid height component due to GGM gravity anomaly on the geoid model. There is no doubt from the references and the general approach given in Eqs. (3.23)a-d, that reduction of surface gravity anomaly to sea level and computation of corrections to sufficient accuracies up to the realization of geoid height is quite involving and tricky undertaking (cf. Sjöberg and Ågren 2002). The above burden is expected to be reduced considerably when unreduced surface gravity anomalies (dg_surf) are used in the LSMS with additive corrections (AC) (Sjöberg 2003b). This task is carried out in Chapter 5 and 6, but before we get there let us describe the AC to LSMS first.

Geoid height from LSMS with Additive Corrections (AC)

The KTH LSMS with AC uses surface gravity anomaly, that is, unreduced gravity anomaly at the Earth's surface to compute the approximate geoid height, (i.e. the approximate separation between geoid model and reference ellipsoid). The surface gravity anomaly is used as if it were given on the bounding spherical geoid model surface. Corrections to the approximate geoid height to be added externally are developed to alleviate the unrealistic assumptions implied to the founding mathematical formula (Stokes) and the surrounding geometry also to realize a better physical geoid model, in this case $\hat{N}$ of Eq. (3.25a) is obtained in a different fashion (Sjöberg 2003b) as

$$\hat{N} = \tilde{N} + \delta N_{comb}^{t} + \delta N_{dwc} + \delta N_{comb}^{a} + \delta N_e \tag{3.26}$$

$\tilde{N}$ is the approximate geoid height of Eq.(3.14) as explained in Sect. 3.1. δN_{comb}^{t} is the combined direct and indirect topographical effect on the geoid height, δN_{dwc} is the effect on the geoid height due to analytically downward continued dg_surf to sea level, δN_{comb}^{a}

is the sum of direct and indirect atmospheric effect on the geoid height, and δN_e is the sum of the ellipsoidal corrections. Equation (3.26) is the main formula which will be deployed in this research to compute TZG08. Since much was explained about $\tilde{N}$ in Sect. 3.1, it remains to do so for the rest of the terms of Eq. (3.26).

Comment: Before we embark on the description of AC, we would like to explain, that our main concern in this section is specifically about AC to the KTH LSMS; a lot of development has been achieved over time at KTH with regards to gravimetric geoid model computation without gravity reduction.

Since the relevant literature is readily available and well documented in detail, we have not found a good reason for literature change hence the appropriate correction will be introduced alongside the relevant reference(s) followed by conclusion. Thus for clearer insight into this subject of AC the reader is urged to consult the cited references.

Total Topographical Effect on the Geoid model, δN^t_{tot}

Total topographic effect δN^t_{tot} is sum of combined topographic effect δN^t_{comb} and downward continuation effect δN_{dwc} at the geoid model, as a result we distinguish four components to δN^t_{tot} correction: they are direct, indirect; primary and secondary, and downward continuation; description of these effects is given in Heiskanen and Moritz (1967 pp 288-289). In Sjöberg (1994a, 2000) the direct topographic effect on the surface gravity anomaly includes secondary indirect effect on gravity, hence we only need to deal with three components to determine δN^t_{tot}.

a. Combined Topographical Effect on the Geoid Model δN^t_{comb}

First the direct and indirect topographic effects are determined separately, and then summed into the combined topographic effect δN^t_{comb}. The effect of downward continuation to geoid model δN_{dwc} is treated independently, and then the two are combined into δN^t_{tot}.

i. Direct Topographic Effect δN_{dir}

Using topographic mass above the geoid model with the surface CP as the centre, the direct effect to the potential, δV_{dir} due to withdrawal of topographic masses outside the geoid model is computed as

$$\delta V_{dir} = -\mu \iint_{\sigma} \int_{R}^{r_s} \frac{r^2 dr d\sigma}{l_p} + \mu R^2 \iint_{\sigma} \frac{H}{l_0} d\sigma \,, \tag{3.27}$$

where

$r_s = R + H;\ l_p = \left(r_p^2 + r^2 - 2r_p r\cos\psi\right)^{1/2},\ l_0 = \left(r_p^2 + R^2 - 2Rr_p\cos\psi\right)^{1/2};\ \mu = G\rho;$ r is the radial distance of the running point, r_p is radial distance of the CP, ρ is the topographic mass density *and* R, H, ψ, G remain as defined earlier.

Further application of δV_{dir} given in Eq. (3.27) in spherical approximation of the fundamental boundary equation gives the corresponding direct effect on the gravity anomaly at surface point P as

$$\delta\Delta g_{dir}\left(P\right) = -\frac{\partial\delta V_{dir}\left(P\right)}{\partial r_P} - 2\frac{\delta V_{dir}\left(P\right)}{\partial r_P} \tag{3.28}$$

Eq. (3.28) is developed in Sjöberg (2000) in power series into

$$\delta\Delta g_{dir} \doteq -\frac{2\pi}{R}\sum_{n=2}^{\infty}\frac{\left(n+2\right)\left(n-1\right)}{2n+1}\mu H_n^2,$$

where (3.29)

$$H_n^{\upsilon} = \frac{2n+1}{4\pi}\iint_{\sigma} H^{\nu} P_n\left(\cos\psi\right)d\sigma; \qquad \nu = 2,3,4,...$$

Often it suffices to evaluate Eq. (3.29) up to $\nu = 2$, but for rough and high elevation terrain, higher terms of ν may be necessary before the contributions from additional terms become insignificant. Replacing Δg_n^{GGM} of Eq. (3.25)c with $\delta\Delta g_{dir}$ in Eq. (3.29) we obtain the corresponding direct effect on the geoid height from degree 2 to infinity as

$$\delta N_{dir}\Big|_2^{\infty} \doteq -\frac{2\pi}{\gamma_0}\sum_{n=2}^{\infty}\frac{n+2}{2n+1}\mu H_n^2, \tag{3.30a}$$

Note that the lowest two degrees (0 & 1) of the direct effect are missing in Eq.(3.30a), the reason being, Stokes function is always non-responsive to the two degrees. In theory, a scheme like, total mass conservation (Martinec 1998) would lead to zero topographic effect from degree 0 & 1 but in practice they subsist sometimes to several centimetres, also atmosphere contributes zero degree harmonics of about a centimetre Sjöberg (2001b), the problem is tackled (ibid) for the zero degree effect as

$$\delta N_{dir,0} = -\frac{4\pi\mu}{\gamma_0}\left[H_0^2 + H_0^3\right] \tag{3.30b}$$

and for the first degree effect as

$$\delta N_{dir,1} = -\frac{4\pi\mu}{\gamma_0}\left[\frac{3}{2}H_1^2 + \frac{H_1^3}{R} + \frac{H_1^4}{4R^2}\right], \tag{3.30c}$$

where the terms $H^{\upsilon}_{0,1}$ are explained in the second line of Eq. (3.29). Eqs. (3.30) a-c are combined into more exact formulas which utilize positional surface radius $r_s = R + H$ without limitation to specific powers of elevation of CP (ibid) as

$$\begin{aligned}\delta N_{dir} &= \delta N_{dir,0} + \delta N_{dir,1} + \\ &-\frac{1}{R\gamma_0}\sum_{n=2}^{\infty}\iint_{\sigma}\mu\int_{R}^{r_s}\left(\frac{r}{R}\right)^n r^2 dr P_n\left(\cos\psi\right)d\sigma + \frac{R}{\gamma_0}\sum_{n=2}^{\infty}\iint_{\sigma}\mu H P_n\left(\cos\psi\right)d\sigma + \\ &-c\sum_{n=M+1}^{\infty}\left(Q_n^L + s_n^*\right)\left(\delta\Delta g_{dir}^*\right)_n\end{aligned} \tag{3.31}$$

ii. Indirect Topographic Effect, δN_I

The primary indirect effect or simply the indirect effect (δN_I) corresponds to the restoration of the reduced topographic masses and thus it is the negative of the direct effect at the same point. Hence

$$\delta N_I = -\frac{\left(\delta V_{dir}\right)}{\gamma_0}, \tag{3.32}$$

In Hemert's 2nd condensation, spherical approximation of $r = R$ gives

$$\delta N_I = \frac{1}{R\gamma_0}\sum_{n=0}^{\infty}\iint_{\sigma}\mu\left[\int_{R}^{r_s}\left(\frac{R}{r}\right)^{n+1} r^2 dr - R^2 H\right]P_n\left(\cos\psi\right)d\sigma \tag{3.33a}$$

(3.33a)

The 0 and 1 degree indirect effects are separated, thus

$$\delta N_{I,0} = -\frac{2\pi}{\gamma_0}\left(\mu H^2\right)_0 \tag{3.33b}$$

and

$$\delta N_{I,1} = 0 \tag{3.33c}$$

Combined topographical effect to the geoid model δN^t_{comb}

δN^t_{comb} is obtained by adding the corresponding direct and indirect effects for the same point on the geoid model

$$\delta N^t_{comb}\left(P\right) = \delta N_{dir}\left(P\right) + \delta N_I\left(P\right) \tag{3.34}$$

By combining separately the 0, 1 and (2 to ∞) direct and indirect terms at P we get

$$\delta N^t_{comb} = \delta N^t_{comb,0} + \delta N^t_{comb,1} + \delta N^t_{comb,}\Big|_2^\infty \tag{3.35}$$

The sum of Eqs. (3.30b) and (3.33b) is $\delta N^t_{comb,0}$, and that of Eqs. (3.30c) and (3.33c) gives $\delta N^t_{comb,1}$. $\delta N^t_{comb,}\Big|_2^\infty$ is obtained in the same manner from Eqs. (3.31) and (3.33a) upon exclusion of 0 and 1 degree components from each part so that

$$\delta N^t_{comb,0} = -\frac{2\pi}{\gamma_0}\left[\left(\mu H^2\right)_0 + \frac{2}{3R}\left(\mu H^3\right)_0\right], \tag{3.36a}$$

(3.36a)

$$\delta N^t_{comb,1} = \delta N_{dir,1} = -\frac{4\pi}{\gamma_0}\left[\frac{3}{2}\left(\mu H^2\right)_1 + \frac{\left(\mu H^3\right)_1}{R} + \frac{\left(\mu H^4\right)_1}{4R^2}\right] \tag{3.36b}$$

The rest of the topographic combined effect is given by

$$\begin{aligned}\delta N^t_{comb,}\Big|_2^\infty = {} & \frac{1}{R\gamma_0}\sum_{n=2}^{\infty}\iint_\sigma \mu\int_R^{r_s}\left[\left(\frac{R}{r}\right)^{n+1} - \left(\frac{r}{R}\right)^n\right] r^2 dr\, P_n(t)\, d\sigma + \\ & -c\sum_{n=M+1}^{\infty}\left(Q_n^L + s_n^*\right)\left(\delta\Delta g^*_{dir}\right)_n, \qquad \text{where: } t = \cos\psi\end{aligned} \tag{3.36c}$$

Numerical evaluation of Eqs. (3.36a-b) to terms of H^2 in Sjöberg (2001b) show that the contribution from $\delta N^t_{comb,0} \approx -5.1\ cm$ and from $\left|\delta N^t_{comb,1}\right| \le 10.3\ cm$. The last term in Eq. (3.36c) is the direct effect of bias due to limitation of integration to a cap σ_0 and GGM to degree M if disregarded, the formula can further be simplified by introducing a kernel $\mathrm{I}(R, r_s)$ such that

$$\delta N^t_{comb,}\Big|_2^\infty \doteq \frac{1}{\gamma_0}\sum_{n=2}^{\infty}\iint_\sigma \mu I(R, r_s) P_n(t)\, d\sigma \quad i.e. \quad \mathrm{I}(R, r_s) = \frac{1}{R}\int_R^{r_s}\left[\left(\frac{R}{r}\right)^{n+1} - \left(\frac{r}{R}\right)^n\right] r^2 dr \tag{3.37}$$

Upon integration of the above kernel we get

$$I(R, r_s) = \begin{cases} R^2 \ln\left(\dfrac{r_s}{R}\right) - \dfrac{\left(r_s^5/R^3\right) - R^3}{5} & if\ n = 2 \\ -R^2\,\dfrac{(1+H/R)^{-(n-2)} - 1}{n-2} + \dfrac{(1+H/R)^{n+3} - 1}{n+3} & if\ \mathrm{n}{>}2 \end{cases} \tag{3.38a}$$

Eq. (3.38a) is approximately given by

$$\mathrm{I}\left(R,r_s\right)\simeq-\left(2n+1\right)\left(\frac{H^2}{2}+\frac{H^3}{3R}\right) \tag{3.38b}$$

In the above formula, the 3rd power term contribution from the highest mountain, is in the tone of a centimetre. Combined topographic effect; Eq. (3.34) at the geoid is thus given by

$$\delta N^t_{comb}=-\frac{2\pi\mu}{\gamma_0}\left[\tilde{H}^2+\frac{2}{3R}\tilde{H}^3\right]+\frac{1}{\gamma_0}\sum_{n=2}^{\infty}\iint_{\sigma}\mu\left[I\left(R,r_s\right)+\left(2n+1\right)\left(\frac{H^2}{2}+\frac{H^3}{3R}\right)\right]P_n\left(t\right)d\sigma\,,$$

where …. (3.39)

$$\tilde{H}^{\nu}=H^{\nu}-H_0^{\upsilon}-H_1^{\upsilon}$$

and for $\nu=2,3$

$$H_n^{\upsilon}=\frac{2n+1}{4\pi}\iint_{\sigma}H^{\nu}P_n\left(\cos\psi\right)d\sigma$$

Eq. (3.39) includes all the frequencies of the direct and indirect effects to the geoid height. The assumption of constant crustal density, can be waived by moving the density to the inside of the integral, which would require to modify the kernel in Eq. (3.37) to

$$\mu\mathrm{I}\left(R,r_s\right)=\frac{1}{R}\int_R^{r_s}\mu\left[\left(\frac{R}{r}\right)^{n+1}-\left(\frac{r}{R}\right)^{n}\right]r^2dr \tag{3.40}$$

Furthermore, Sjöberg (2007) has shown that for laterally variable topographic density, the combined topographic effect on geoid height is proportional to terms of power two and three of topographic height H, and all higher order terms disappear. Thus practically for most applications, is suffices to compute δN^t_{comb} from

$$\delta N^t_{comb}=-\frac{2\pi\mu}{\gamma_0}H^2-\frac{4\pi\mu H^3}{3R} \tag{3.41}$$

This approach besides been independent of the reduction method, has reduced enormously the tedious computational involvement when compared to similar tasks (cf. Novak et al. 2001a).

b. Downward Continuation Effect δN_{dwc}

In the classical approach often direct and downward continuation (dwc) effects were combined into what is termed 'Terrain Effect, (TE)', under the assumption that surface gravity anomaly changes linearly with elevation; it is a crude assumption and approximation (Moritz 1980a p 415), which can lead to error of the tone of 0.5 m. This

kind of error can no longer be accommodated in this era of 1-cm geoid model. Therefore, the problem of dwc effect is treated separately. Practically, the downward continuation of surface gravity anomaly to sea level is an ill-posed problem. If the direct effect accounts fully for the topographic masses, the ill conditioning would not prevail. Unfortunately residual attraction is usually present, which makes it unstable, i.e. leading to attenuation effect (Ågren 2004a, Martinec 1998). Often inversion of Poisson's integral has been used to arrive at the solution, (Heiskanen and Moritz 1967 p 317), but one crucial problem with the inversion of Poisson's integral is that it is extremely laborious and time consuming and it is unclear whether the Jacobi iterations used in the process converge for dense grids needed in the combined approach (Ågren 2004b). Sjöberg (1998a) and (2001a) separates the two effects. Moreover, he came up with a method of solving dwc effect without inversion of Poisson's integral by direct derivation of integral formulas for dwc effect on the geoid height δN_{dwc}, and height anomaly, $\delta\zeta_{dwc}$. In addition, the solution was stabilized by optimized spectral smoothing, which minimizes the geoid model MSE. The final formula is a function of the gravity anomaly, height anomaly and topographic height. The same author continues with a solution that avoids the intermediate step of downward continuation of the gravity anomaly in (2003c), which originates from (Sjöberg 2001a), where it was underscored, that Stokes integration implies a process of smoothing of the gravity anomalies. By directly computing the effect on the geoid via Stokes formula, the task should more easily be solved. The solution is given in parts as truncated Taylor series, and spherical harmonics. The formulation has come out with a much more computer efficient practical solution than the previous endeavours, where spectral smoothing was used to stabilize the dwc effect on the geoid height in an optimum way. The process amounts to analytical downward continuation (A_{dwc}) of surface gravity anomaly through topographic masses. A_{dwc} in this context means a mathematical process that extends an operation valid on and above the Earth's surface to the inside of topographic masses. If it is a harmonic operation, then it leads to an error, which is termed here 'topographic bias'. Fortunately the bias is the negative of the combined topographic effect, δN^{t}_{comb}, (Sjöberg 1997, Ågren 2004a and Sjöberg 2007). Simple numerical tests have proven the method to be capable of meeting the demands for a 1-cm geoid model. The dwc effect on the geoid corresponding to the surface point say P is (Sjöberg 2003c)

$$\delta N^{P}_{dwc} = \kappa \iint_{\sigma} S(\psi)\left(\Delta g^{*}_{Q} - \Delta g_{Q}\right) d\sigma_{Q}, \tag{3.42}$$

where Δg^{*}_{Q} and Δg_{Q} are gravity anomalies analytically continued down to geoid model and at the Earth's surface respectively, $\kappa = R/4\pi\gamma_{0}$; R is the geocentric radius of geoid model, γ_{0} is the normal gravity on the reference ellipsoid along the normal through P, Q is running point, ψ is geocentric angle between P and Q, $S(\psi)$ and σ maintain the previous definitions. By removing the brackets in Eq. (3.42), we obtain (ibid)

$$\delta N^{P}_{dwc} = \tilde{\zeta}^{*}_{P} - N_{P}, \tag{3.43}$$

where $\tilde{\zeta}_P^*$ is the downward continued re-scaled height anomaly and N_P is the approximate geoid height computed from surface gravity anomalies. Thus δN_{dwc}^P has two components, which can be written as

$$\delta N_{dwc}^P = \delta N_{dwc,1}^P + \delta N_{dwc,2}^P \tag{3.44}$$

Although from Eq. (3.43) it is evident that both components have all the frequencies of the gravity spectrum, it is afterwards shown in (ibid) that $\delta N_{dwc,1}^P$ mainly contributes to the short-wavelengths whereas a good part of $\delta N_{dwc,2}^P$ constitutes the long-wavelengths. The two components are developed separately and are referred to as short and long-wavelength components.

The short-wavelength component $\delta N_{dwc,1}^P$ is developed under the following rules and/or understanding:

- Elevation of P is expressed as Taylor's series expansion to second power
- Bruns' formula for disturbing potential is applied to the normal height of P
- Vertical gradient of normal gravity at P is in spherical approximation
- Gravity anomaly gradient as given in Heiskanen and Moritz (1967 Eq. 2-217) is applied, consequently

$$\delta N_{dwc,1}^P \simeq \frac{H_P \Delta g_P}{\gamma} + \frac{\mathrm{H_P}}{r_P}\zeta_\mathrm{P} - \frac{H_P^2}{2\gamma_0}\left(\frac{\partial \Delta g}{\partial H}\right)_P - \frac{H_P^2 \Delta g_P}{\gamma_0 r_P} + \Delta\zeta_P, \tag{3.45a}$$

with

$$\left(\frac{\partial \Delta g}{\partial H}\right)_P \simeq \left(\frac{\partial \Delta g}{\partial r}\right)_P = \frac{1}{16\pi r_P}\iint_\sigma \frac{\Delta g_Q - \Delta g_P}{\sin^3\frac{\psi}{2}} d\sigma_Q - \frac{2\Delta g_P}{r_P} \tag{3.45b}$$

and

$$\Delta\zeta_P \simeq -2\frac{H_P^2}{r_P}\left(\frac{\zeta_P}{r_P} + \frac{\Delta g_P}{\gamma_0}\right) \tag{3.45c}$$

The second component $\delta N_{dwc,2}^P$ is obtained from Eq. (3.43) by subtracting from it Eq.(3.45a), which results into

$$\delta N_{dwc,2}^P = \frac{R}{r_P}\tilde{\zeta}_P - N_P \tag{3.46}$$

where $\tilde{\zeta}_P$ is given by $(\gamma/\gamma_0)\zeta_P$, with ζ_P, the height anomaly at P. Sjöberg (2003c) breaks $\delta N_{dwc,2}^P$ into two parts with the intention, that the first part $\delta N_{dwc,2.1}^P$ takes care of

the contribution from the innermost zone around the CP, and the second part $\delta N^P_{dwc,2.2}$ accounts for the far zone or the remainder, thus

$$\delta N^P_{dwc,2} = \delta N^P_{dwc,2.1} + \delta N^P_{dwc,2.2} \tag{3.47}$$

The first part is selected to be so close to the CP that it can be approximated by a plane surface, and its effect computed in a fashion similar to one in Heiskanen and Moritz (1967 pp 120-122). Thus we have

$$\delta N^P_{dwc,2.1} = \kappa \iint_{\sigma_0} S(\psi)\left(\Delta g_{P,Q} - \Delta g_Q\right) d\sigma_Q \tag{3.48}$$

and

$$\delta N^P_{dwc,2.2} = \kappa \iint_{\sigma-\sigma_0} S(\psi)\left(\Delta g_{P,Q} - \Delta g_Q\right) d\sigma_Q \tag{3.49}$$

Eqs. (3.48) and (3.49) consider only the up/down continuation effect from the running point Q to CP P. This means $\delta N^P_{dwc,1}$ contributes to the downward continuation from the CP P to the mean sea level. Advantage is taken of the Molodensky's truncation coefficients $Q_n(\psi_0)$ to express $\delta N^P_{dwc,2.2}$ so that Eq. (3.47) becomes

$$\delta N^P_{dwc,2} = \frac{\overline{\Delta H}_S}{\gamma}\left(\frac{\overline{\partial \Delta g}}{\partial r}\right)_P + c\sum_{n=2}^{n_{\max}} Q_n(\psi_0)\left[\left(\frac{R}{r_P}\right)^{n+2} \Delta g^P_{n,g} - \Delta g^P_{n,S}\right] \tag{3.50}$$

where $c = R/2\gamma_0$ and $\overline{\Delta H}_S$ is the mean height difference over the inner circle of radius s_0 around the CP computed as

$$\overline{\Delta H}_S = \frac{1}{2\pi}\int_0^{2\pi}\int_0^{s_0} \Delta H_{PQ}\, ds\, d\alpha; \quad \Delta H_{PQ} = H_P - H_Q, \text{ thus } \overline{\Delta H}_S = H_P s_0 - \frac{1}{2\pi}\int_0^{2\pi}\int_0^{s_0} H_Q\, ds\, d\alpha \tag{3.51}$$

and $\left(\partial\overline{\Delta g}/\partial r\right)_P$ is the average gravity anomaly gradient in the inner zone of radius s_0. $\Delta g^P_{n,g}$ and $\Delta g^P_{n,S}$ are the gravity anomaly Laplace harmonics at the geoid model and surface corresponding to the CP P respectively. As far as the approach by Sjöberg (2003c) is concerned, sum of Eqs. (3.45 a-c) and (3.50) provide us with the downward continuation correction (δN_{dwc}) to the approximate geoid height as required in Eq. (3.26) . Numerical tests based on typical data and elevations of 5 km and 8.8 km and s_0 1 km show, that dwc effect can be of the order of a few metres in the highest mountains. With regards to truncations in the Taylor's series and harmonic expansion to maximum degree 360, the error in the worst topographic cases is within 1.1 cm, to reduce the truncation error from far zone i.e. $\delta N^P_{dwc,2.2}$ it is suggested to use modified Stokes kernel, the author

has done so, refer (ibid). Ågren (2004b Sect. 5.4) has driven δN_{dwc} in the same philosophy as (Sjöberg 2003c), except he commences with least squares modified Stokes kernel of (Sjöberg 1991), and for the innermost grid with the CP, he uses bi-cubic spline interpolation, the end formulae differ slightly to (Sjöberg 2003c). The results will be quoted; for details refer to the reference.

$$\begin{aligned}\delta N_{dwc,1}^{L,P} &\simeq \frac{\Delta g_P}{\gamma} H_P + 3\frac{\zeta_P^0}{r_P} \mathrm{H_P} - \frac{1}{2\gamma}\left(\frac{\partial \Delta g}{\partial H}\right)_P H_P^2 \\ &\cong \frac{\Delta g_P}{\gamma} H_P + 3\frac{\tilde{N}}{r_P} \mathrm{H_P} - \frac{1}{2\gamma}\left(\frac{\partial \Delta g}{\partial H}\right)_P H_P^2\end{aligned} \tag{3.52}$$

Approximation of height anomaly with approximate geoid height has negligible effect to δN_{dwc} as tested by Ågren (2004b p 120)

$$\delta N_{dwc,1}^{L(far),P} = c\sum_{n=2}^{M}\left(s_n^* + Q_n^L\right)\left[\left(\frac{R}{r_P}\right)^{n+2} - 1\right]\Delta g_n^P \tag{3.53}$$

$$\delta N_{dwc,2}^{L,P} = \frac{c}{2\pi}\iint_{\sigma_0} S^L(\psi)\left(\left(\frac{\partial \Delta g}{\partial r}\right)_Q \left(H_P - H_Q\right)\right) d\sigma_Q \tag{3.54}$$

Eqs. (3.52) to (3.54) provide dwc effect according to least squares modified Stokes kernel. Numerical tests with modified kernels according to remove compute restore (RCR) both standard and non standard, and LSMS, show that truncation error of $\delta N_{dwc,2}^{L,P}$ is not negligible for RCR, but it is insignificant for LSMS kernel (Ågren 2004b). This goes along with the suggestion in Sjöberg (2003c), that the $\delta N_{dwc,2.2}^{P}$ could be improved by consideration of a modified kernel. Now it is possible to compute the total topographical effect on the geoid model, say, for point P, as summation of the combined topographic effect and the downward continuation effect for the same point. That is

$$\delta N_{tot}^{t}(P) = \delta N_{comb}^{t}(P) + \delta N_{dwc}(P) \tag{3.55}$$

c. Direct and Indirect Atmospheric Effects on the Geoid height δN_{comb}^{a}

Like topography, atmospheric masses are external to geoid model, and thus must be removed or reduced prior to application of Stokes formula, which requires the geoid to be a bounding surface. Until 1999 among the famous techniques to do so, is the one referred to as 'the IAG approach to the atmospheric geoid model correction in Stokes formula', Sjöberg (1999). This approach was challenged by (ibid) on the following grounds among others:

a. The IAG approach considers a spherical atmospheric layer above a spherical Earth through surface point, with no regard to topographic and atmospheric masses in

between the surface point and the geoid model. The effect of topography can not be negligible, moreover the density of atmosphere decreases as we move away from the sea.

b. The point of consideration of atmospheric mass is away from the bounding surface, this requires downward continuation of the direct effect to the geoid through topographic masses, but it is not implemented.
c. The IAG considers only the direct effect, that is, it does not consider the secondary indirect effect or restoration of the removed atmospheric masses; the primary indirect effect.
d. The most crucial problem is that it confines its consideration to a spherical cap around the CP with no regard to truncation effect. This means, that very small proportion of the atmosphere is considered, and hence a serious bias.

A new approach has been developing at the KTH since 1998, (Sjöberg 1998b, 1999, 2001b, 2006a, Sjöberg and Nahavandchi 1998). The new approach mainly addresses the shortcomings of the IAG model under the following foundations:

- The Earth surface is a sphere with spherical sea of radius R and variable topography of height H above it i.e. radial distance of the topography is $r_s = R + H$.
- The density of atmosphere ρ_a is laterally layered. If $\rho_a^* = G\rho_a$; with G the Earth gravitational constant then, $\rho_a^*(r) = \rho_{a,0}^*(R/r)^\nu$, where $\rho_{a,0}^*$ is atmospheric density at the geoid model, r is the geocentric radius of running point P' and ν is a positive constant number > 2.

Sjöberg (1999) found that the most serious problem of the IAG approach was truncation bias, which could lead up to 3 m error. If the integration is carried out all over the Earth it differs by a few millimetres to the new approach. The new approach computes the total atmospheric effect externally with zero and first degree effects included. Besides enabling improvement of previous erroneous geoid model, it is also easier, faster and computer efficient. The new approach total atmospheric effect to approximate geoid height, computed from modified Stokes formula, e.g. LSMS (Sjöberg 2001b) is given by

$$\delta N^a_{comb} = \frac{V_0^a}{\gamma_0} + \frac{V_1^a}{\gamma_0} - \frac{R\rho^*_{a,0}}{\gamma_0}\iint_\sigma S(\psi)\,H\,d\sigma + c\sum_{n=0}^{M}\left(Q_n^M + s_n^*\right)\delta\Delta g_n^a + c\sum_{n=M+1}^{\infty}\left(Q_n^M + s_n^*\right)\Delta g_n^a, \quad \ldots \quad (3.56)$$

where, $V_0^a = \dfrac{-4\pi\rho^*_{a,0}R^2}{(\nu-2)(\nu-3)}$ and $V_1^a = 0$;

$\Delta g_n^a = 4\pi\rho^*_{a,0}\dfrac{n+2}{2n+1}H_n$, for $n > 0$; $\delta\Delta g_n^a = 4\pi\rho^*_{a,0}H_n$, for $n > 0$ and

$H_n(P) = \sum_{m=-n}^{n} H_{mn}Y_{nm}(Q)$

is the harmonic representation of the surface topographic height at point P. $\rho^*_{a,0} \approx 1.23\times10^{-3}\,g/cm^3$ is density of the air at the geoid and ν is a constant estimated in Sjöberg (2001b) to be about 850

The total or combined atmospheric zero degree effect is within 1 cm and there are no first degree effects. Eq. (3.56) indicates that the δN^{a}_{comb} is mainly dependent on the atmospheric density $\rho^{*}_{a,0}$ and topographic height H/H_n, in the endeavour for 1-cm geoid model, Sjöberg (2006a) searched for an improved atmospheric model by considering an ellipsoidal layering and improved atmospheric density model rather than spherical layering considered in the previous attempts. The outcome of the study shows, that the total atmospheric effect varies between -1.2 cm and 1.9 cm from equator to poles respectively for ellipsoidal approximation. For spherical approximation, which is the normal practice, the range is from 0.3 cm to 4.0 cm at equator and poles respectively. The total atmospheric effect to geoid height of the ellipsoidal layering approach δN^{ae}_{t}, which is much a function of atmospheric mass layering and ellipsoidal parallel (zonal harmonics) is given by

$$\delta N^{ae}_{t} = -\frac{1}{\gamma}\iint_{\sigma}\int_{b}^{\infty}\frac{M^{a}(\nu)}{\nu^{2}+E^{2}}\,d\nu + \frac{GM^{a}R}{b^{2}\gamma}ce^{2}Y_{2,0}(\theta,\lambda)_{P}, \tag{3.57}$$

where a and b are semi major and minor axes of the ellipsoid respectively. M^{a} is atmospheric mass whose volume depends on the atmospheric layer (ν) under consideration, $E = ae$; e the first eccentricity of the ellipsoid, $c = 2/\left(3\sqrt{5}\right)$, $Y_{2,0}(\theta,\lambda)_{P}$ is fully normalized zonal harmonic at the surface point $P(\theta,\lambda)$ i.e. $(\theta,\lambda)_{P}$, $\mathrm{d}\nu$ is elemental volume of integration; G, γ, σ and R retain the same meanings as before. Eq. (3.57) is approximately given for geoid model point P of co-latitude θ as

$$\delta N^{ae}_{t} \doteq -1.2 + 3.1\cos^{2}\theta \text{ in cm} \tag{3.58}$$

Spherical approximation in Eq. (3.57), modifies δN^{ae}_{t} to δN^{a}_{t}, approximately given by

$$\delta N^{a}_{t} \doteq \left(3.7\cos^{2}\theta + 0.3\right) \text{ in cm} \tag{3.59}$$

Note, that there is no truncation consideration in the last model, since the whole atmosphere is always involved in the development of the atmospheric effect to geoid height at point P on the surface of ellipsoidal.

d. Ellipsoidal Correction δN_{e}

In the struggle for 1-cm geoid model, ellipsoidal correction is likely to be significant. We realize that observations needed in geoid model determination are carried out on and/or above the Earth. The Earth is approximated better by a Mean Earth Ellipsoid (MEE) rather than a Mean Earth Sphere (MES). Stokes formula is founded on a (bounding) sphere, and the resulting geoid model closely coincides with spherical mean sea level, but

a better geoid model (which was expressed in the introduction as the physical geoid model) is the one which closely follows ellipsoidal mean sea level. In view of the above, we identify the following operations to obtain the physical (ellipsoidal) geoid model,

- Transformation of observed gravity anomaly from MEE to MES to make it compatible with the requirements of the Stokes formula, which is founded on a spherical bounding surface.
- Conversion of the disturbing potential (T) from MES to MEE.

The above operations are carried out at different levels in the Sjöberg (2003d, 2003e, 2004a, 2004c) also in Ellmann and Sjöberg (2004). We start with an introduction to the subject matter, and to keep pace with the current study, a presentation of the findings of the ellipsoidal correction based on modified Stokes formula will follow. Details are found in the quoted references. The assumption is that there are no topographic or atmospheric masses external to the MEE or MES and the observed gravity anomaly has been downward continued to the MEE. The observed gravity anomaly on the MEE must either be up/down ward continued to the MES, and transformed to spherical gravity anomaly, before it can be used in the Stokes integral due to the requirement of spherical bounding surface in Stokes formula. Therefore, ellipsoidal correction to the gravity anomaly from ellipsoid to a sphere is required. Eq. (3.1) is the original Stokes formula for correct geoid height; it is rewritten here with changed symbolisms and meanings to ease comprehension:

$$N^0 = \frac{R}{4\pi\gamma}\iint_{\sigma} S(\psi)\Delta g^0 d\sigma\,, \tag{3.60}$$

where N^0 is spherical geoid height and Δg^0 is gravity anomaly on MES. On the MEE, divergence of the direction of observed gravity (plumb line of ellipsoidal Earth) from radial direction of spherical Earth, is of the order of first eccentricity of the Earth/MEE to power two (e^2), thus, the observed gravity anomaly Δg on the ellipsoidal Earth, is different to Δg^0 required in Stokes formula. Sjöberg (2003d) shows, that Δg^0 on a sphere of radius R, is obtained from Δg as follows:

$$\Delta g^0_{r=R} = \Delta g + \delta g^0\,, \tag{3.61}$$

where

$$\delta g^0 = \delta g^1 + (R - r_e)\left(\frac{\partial \Delta g^0}{\partial r}\right)_{r=R} \quad \text{and} \quad \delta g^1 = e^2\left(2 - 3\cos^2\theta - \sin\theta\cos\theta\frac{\partial T}{a\partial\theta}\right) \tag{3.62}$$

With $r_e = r_e(\theta)$, the radius of the ellipsoid is obtained as, $r_e = a\sqrt{1 - e^2\cos^2\theta}$, where θ is the geocentric co-latitude, a is semi major axis of the MEE, R is the radius of the MES, T is disturbing potential and r is geocentric radius vector. Take note of the continuation of the gravity anomaly and disturbing potential from MEE to MES by the

gradients $\left[\frac{\partial \Delta g^0}{\partial r}, \frac{\partial T}{\partial \theta}\right]$ in δg^0 and δg^1 respectively. Upon correcting Δg by δg^0, and inserting into Eq. (3.60), we obtain the geoid model as a bounding MES which closely coincides with mean spherical sea level as,

$$N^0 = \frac{R}{4\pi\gamma}\iint_\sigma S(\psi)\left(\Delta g + \delta g^0\right) d\sigma \tag{3.63}$$

To obtain correct geoid height which closely coincides with the actual mean sea level of the Earth, we have to account for the departure of the MES from the MEE. Using Bruns' formula, its gradient and the separation between the MES and MEE $\left(r_e - R\right)$, the last correction is

$$\delta N_{e1} = \frac{r_e - R}{\gamma}\left(\frac{\partial T}{\partial r}\right)_{r=R} \tag{3.64}$$

Correct geoid height N is thus given by

$$N = N^0 + \delta N_{e1} = \frac{R}{4\pi\gamma}\iint_\sigma S(\psi)\left(\Delta g + \delta g^0\right) d\sigma + \frac{r_e - R}{\gamma}\left(\frac{\partial T}{\partial r}\right)_{r=R} \tag{3.65}$$

Under the assumption we had before that Δg has been corrected for direct and indirect effects of topographic and atmospheric masses, and moreover it had been downward continued to the bounding MEE, we can deduce the ellipsoidal correction δN_e from Eqs. (3.60) and (3.65) to be

$$\delta N_e = \frac{R}{4\pi\gamma}\iint_\sigma S(\psi)\,\delta g^0 d\sigma + \frac{r_e - R}{\gamma}\left(\frac{\partial T}{\partial r}\right)_{r=R} \tag{3.66}$$

In case in the previous formula, $R \neq a$, we should substitute R for a and introduce a scale factor k so that the correct ellipsoidal correction is

$$\delta N_e = kN^0 + \frac{R}{4\pi\gamma}\iint_\sigma S(\psi)\,\delta g^0 d\sigma + \frac{r_e - a}{\gamma}\left(\frac{\partial T}{\partial r}\right)_{r=a} \tag{3.67a}$$

with

$$\delta g^0 = \delta g^1 + \left(a - r_e\right)\left(\frac{\partial \Delta g^0}{\partial r}\right)_{r=a} \qquad \text{and} \qquad k = \frac{a - R}{R} \tag{3.67b}$$

Using some of developments in Sjöberg (2003d) Eq. (3.67b), we can express δN_e in spherical harmonics as

$$\delta N_e = kN^0 + \frac{\delta T_0 + \delta T_1 + \delta T'}{\gamma} = kN^0 + \frac{\delta T_0 + \delta T_1}{\gamma} + \frac{a}{\gamma}\sum_{n=2}^{\infty}\left(\frac{\delta G_n^0}{n-1} + \frac{\delta T_n}{a}\right), \tag{3.68}$$

where $\left(\delta g^0 = \delta G^0\right)_n$ when $R = a$, furthermore, δT_n and $\left(\delta T' = \delta T_e\right)_n$ are developed in ibid (Eqs. 19b, 20b and 22c) respectively, into spherical harmonics, and when substituted into the RHS of Eq. (3.68), we obtain ellipsoidal correction δN_e in spherical harmonics. Note, that δT_n are the differences of the disturbing potential at the bounding MES and MEE, with δg_n^0 as the nth Laplace harmonic of δg^0, (Eq. (3.62)). The δT_i, $i = 0,1$ are added separately because Stokes function is silent to zero and first- degree terms.

For the modified Stokes formula, which is usually limited to a spherical cap about the CP and often involves terrestrial and GGM gravity data, the situation is different. For the modified Stokes method, it is advocated to compute $\Delta\hat{g}_n^S$ on the MEE instead of MES before they are used in the Stokes formula. The difference is insignificant due to the fact that the cap is usually small e.g. in the LSMS, in addition the separation $\left(r_e - R\right)$ is also small, if R is selected to be the mean of r_e in the area of interest (AOI). As cap radius $\sigma_0 \to 0$ in the modified Stokes formula, the geoid height N^M becomes

$$N^M = \frac{T_{r=R}}{\gamma}, \tag{3.69}$$

and the ellipsoidal correction within elemental cap is given without significant loss by

$$\delta N_e = \frac{T_{r=r_e} - T_{r=R}}{\gamma} \approx \frac{r_e - R}{\gamma}\left(\frac{\partial T}{\partial r}\right)_{r=R} \tag{3.70}$$

On the other hand, Eq. (3.68) can be written more rigorously for the modified Stokes formula, Eq. (3.14), as

$$\delta N_e^M = \frac{\delta T_0 + \delta T_1}{\gamma} + \frac{R}{4\pi\gamma}\iint_{\sigma_0} S^M(\psi)\left(k\Delta g + \frac{a}{R}\delta g_e\right)d\sigma, \tag{3.71}$$

where $\delta g_e = \left(\delta G^0 + \delta g\right) = \sum_{n=2}^{\infty}\frac{n-1}{a}\left(\delta T_e\right)_n$ is given in ibid (Eq. 36).

Therefore, Eq. (3.71) provides us with ellipsoidal correction for the modified Stokes kernel limited to a spherical cap σ_0. When developed in spherical harmonics, it becomes (Sjöberg 2004c)

$$\delta N_e^M = \frac{\delta T_0 + \delta T_1}{\gamma} + \frac{R}{2\gamma}\sum_{n=2}^{\infty}\left(\frac{2}{n-1} - Q_n^M - s_n\right)\left(k\Delta g_n + \frac{a}{R}\left(\delta g_e\right)_n\right) \tag{3.72}$$

The assumption in deriving the formula for δN_e for the modified Stokes formula, which utilizes GGM gravity anomalies ($\Delta\hat{g}_n^S$), has been that the $\Delta\hat{g}_n^S$ are computed for MEE of semi major axis a, and surface radius r_e, even though they are utilized in spherical Stokes formula defined on the MES of radius R (obtained as explained earlier) using

$$\Delta\hat{g}_n^S = \frac{GM}{aR}(n-1)\left(\frac{a}{r_e}\right)^{n-1}\sum_{m=-n}^{n} C_{nm}Y_{nm} \ , \tag{3.73}$$

where C_{nm} and Y_{nm} are the Laplace's GGM coefficients and disturbing potential of degree and order n and m respectively. In case the above assumption is not observed, and instead the $\Delta\hat{g}_n^S$ are computed on the MES directly, an error of magnitude equal to Eq. (3.74) will prevail.

$$\frac{r_e - R}{\gamma}\left(\frac{\partial T}{\partial r}\right)_{r=R} \doteq \left(k - e^2\frac{\cos^2\theta}{2}\right)\left(\frac{a\Delta g}{\gamma} + 2N^0\right) \tag{3.74}$$

Chapter Four

DATA: GRAVITY, HEIGHT AND CRUSTAL DENSITY

The ultimate goal is to determine as accurately as possible the geoid model of Tanzania, referenced to the official Geodetic Reference System GRS80, (Moritz 1980b, Hofmann-Wellenhof and Moritz 2005 pp 84-85). The main data input into gravimetric geoid model determination is gravity. Geoid model can be determined from the following original sources:

- Terrestrial gravity.
- Air-borne gravity.
- Satellite gravity including altimetry data.
- Satellite Gradiometry.
- Astro-geodetic deflection of the vertical.
- Ship borne gravity (on the surface or at sea bottom).
- GNSS/levelling.
- Combination of the above.

Experience has shown that geoid model determined from one source of gravity data suffers a number of drawbacks; hence, current procedure is to combine different data sources, which will lead to sound long, medium as well as short frequencies of gravity data and often use such data in a manner consistent with one of modified Stokes formula, (Sjöberg 2005b). Usually terrestrial, ship and aerial data and to some extent satellite altimetry data, are rich in local details (short to medium wavelength), but are spatially limited, and the long-wavelength is biased due to observational and datum errors. On the other hand, satellite data is smooth with broad features of the gravity spectrum, but details of gravity (short-wave components of gravity spectrum) are absent. Determination of geoid model demands that there are no masses external to the geoid; therefore information of topographic mass density is important for reduction of data and sometimes other quantities from the surface of the Earth to the geoid/mean sea level. Gravity data coverage and distribution in some areas and especially in developing countries, is sparse and unevenly distributed, also, free-air gravity anomaly is highly correlated with elevation. Therefore computation of gravity irregularities due to terrain undulation (i.e. terrain effect) requires detail information of topography, usually in the form of dense digital terrain elevation. Removal of terrain effect (TE) from the observed gravity, smoothes the latter, and that way becomes more amenable to prediction. Hence, besides gravity, other types of data for geoid model determination are:

- Digital Elevation Model (DEM).
- Lateral crustal density variation.

Amongst the data for geoid model determination, the following data have not been observed in Tanzania. If available, they are from secondary source(s), often data archiving centres for international community and dedicated mission databases:

- Satellite gravity.
- Satellite Altimetry marine gravity data.
- DEM.

If aerial gravity survey has ever been conducted in Tanzania, we did not succeed to get the data or such information. Even then, almost all available gravity data sets were not observed for geodetic purposes, but they were mainly collected for exploration of hydrocarbons and precious elements; shore and off-shore. Next we take a closer look on the individual gravity data types, namely:

- Terrestrial gravity anomalies.
- Marine gravity anomalies.
- Satellite gravity anomalies.
- Height and
- Crustal density.

All the necessary achievable data will be gathered and sieved, so that we remain with only the best possible without compromising too much the quantity and quality beyond necessity. Lastly we reduce the data to address the main objective. For example when we discuss gravity data in this undertaking, it means surface gravity anomalies, and later when we get down to the method of geoid model computation, i.e. the LSMS with AC (Sjöberg 2003a) in Ch. 6, it will imply a dense, even grid of surface gravity anomalies or DEM, which may not necessarily be of the same grid spacing as the surface gravity anomaly.

4.1 Terrestrial Gravity Data

4.1.1 Introduction

Gravity observation in Tanzania started in the 1890's and reference was to different local datums prior to arrival of the Potsdam datum in early 1950's. To unify gravity information, gravity data should be referred to a standard international datum and heights to mean sea level (MSL)/geoid. Gravity data collected after 1971, i.e. after the declaration of the International Gravity Standardization Network 1971 (IGSN71), was invariably standardized to Potsdam and IGSN71. Reduction of observed gravity for gravity anomaly or other geodetic products, which involve normal gravity, is referred to one of the following reference ellipsoids: International 1924, GRS1967 or GRS1980, and computation of normal gravity (γ) used the respective International Gravity Formula (IGF) i.e. IGF1930, IGF1967 and IGF1980, respectively. In Tanzania, a majority of the reductions used either IGF1930 or IGF1967. Since Potsdam datum existed during the period of International 1924 and most of the GRS1967, vast of the gravity data in Tanzania has been standardized to Potsdam datum. Very few data reductions have used GRS80 even when it was observed after 1980. Two versions of the IGF1967 are found in Tanzania, referred to as GRS1967a and GRS1967b; they differ by 0.04 to 0.86 mGal across the country, (Parker and Marobhe 1991).

Tanzania has a network of 7 interconnected IGSN71 base stations, which are integral part of the IGSN71 world wide network. Unfortunately, only few gravity surveys are referenced to IGSN71, since majority of the surveys were conducted prior to inception of

IGSN71. Most are tied to a network of 40 base stations established across the country between 1958 and 1961 as part of the Eastern and Central Africa Gravity Network (ECAGN), (ibid), which is referenced to the Potsdam datum. Prior to ECAGN, there had been other base stations, e.g. Bullard Pendulum station in Dar es Salaam, to which many gravity surveys were tied. This was established in 1934. Its value was first revised by W. Horsfield and E.C. Bullard (Sir) in 1936 and again in 1954 by OSTROM (Office de la Recherche Scientifique et Technique Outre-mer, 1952-54) following establishment of many more base stations across Africa. Finally, the station was tied to ECAGN in 1962. Record of ECAGN (Potsdam) and IGSN71 base station values is well documented, including previous values and other local base stations (ibid).

Gravity Data: Observation and Distribution in Tanzania.

Gravity coverage in many places of Tanzania is sparse. Most of the gravity data has been observed for mineral prospecting, and big gaps are found in game reserves and national parks and areas which so far have no indication of having hydrocarbon products or valuable minerals.

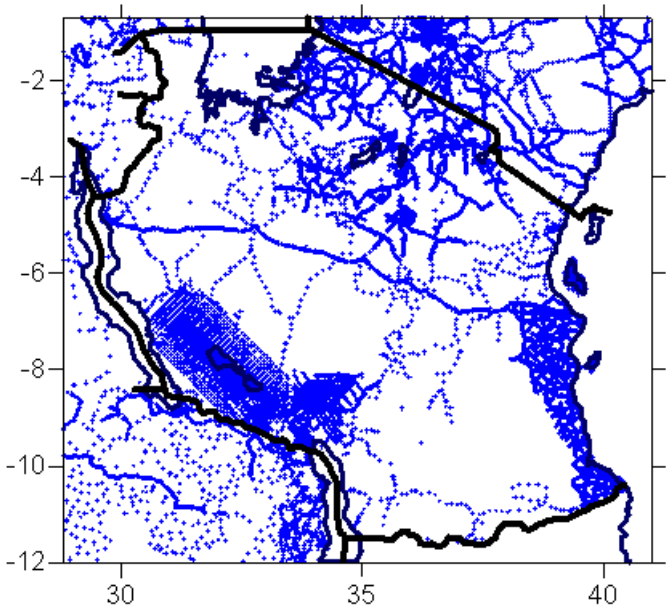

Figure 4-1: Terrestrial land point gravity locations in Tanzania

Denser concentrations are found where deposits/minerals have been found in abundance, for example coastal strip ~ 200 km south of Dar Es Salaam, south-west, north and north-west Tanzania as reflected in Figure 4-1.

Despite existence of different gravity datums, some local, several unified gravity data bases are found in the country, which together contain most of the gravity data. First serious compilation was produced in 1968, which was tied to Potsdam datum, but later on in 1978 the database was tied to IGSN71. To convert from ECAGN to IGSN71 i.e. Potsdam to IGSN71, in this region we can use the formula provided by BGI:

$$g_{IGSN71} = g_{ECAGN} - 13.706 - 0.00036(g_{ECAGN} - 977500) \qquad (4.1)$$

Analysis carried out by Parker and Marobhe (1991) in 1990, came out with a slight variation to the BGI formula given in Eq. (4.2)

$$g_{IGSN71} = g_{ECAGN} - 13.69 - 0.00039\left(g_{ECAGN} - 977500\right) \quad (4.2)$$

Conversion from ECAGN to IGSN71 followed the first Eq. (4.1), the difference is about 0.01mGal, (ibid).

In our research most of the terrestrial gravity data will be point products, i.e. observed point gravity and gravity anomalies. Abundant mean gravity anomalies have been obtained from different sources, but they do not provide enough information of the procedures followed to get the mean values. Besides they are more or less at the same locations as the point gravity data, hence mean gravity data will not be used in this research. The majority of the point gravity data is from Ardhi University (ARU). Gravity Data base (ARUDB), archived by the department of Geomatics. The next big source is Bureau Gravimetric International (BGI). The ARUDB has been compiled from different sources in Tanzania, which include to list but the main: Tanzania Petroleum Development Corporation (TPDC), Geology Department of the University of Dar Es Salaam, Eastern, Central and Southern Africa Mineral Prospecting Centre (ECSAMPC) and the Ministry of Minerals Tanzania.

In some instances, the point gravity anomalies have been reduced to mean sea level (MSL) using free-air gravity gradient of 0.3086H mGal/metre, where H is the orthometric height of the gravity anomaly point. The normal gravity is computed from the IGF1967. In this research, surface gravity anomalies will be used; these will be computed from observed point gravity data or recomputed from the reduced point gravity anomalies. Our intention is to work on the GRS80, thus the surface gravity anomalies will be referred to GRS80 reference ellipsoid.

4.1.2 Gravity Reduction to Geoid: GRS67, GRS80

Small amount of the point and mean gravity anomalies received from different sources had been reduced to mean sea level (MSL) using free-air gravity gradient 0.3086H mGal/metre, with normal gravity computed on the GRS67. In this research, surface gravity anomalies are used. These are computed from point gravity data or recomputed from sea level reduced gravity anomalies. Unlike classical gravity anomaly, which is a function of normal gravity on the reference ellipsoid, surface gravity anomaly is computed from normal gravity given on the telluroid; a surface separated from the actual terrain by the height anomaly (ζ). The height anomaly is a distance along the normal to the reference ellipsoid through the point of interest on the terrain to telluroid, (Featherstone and Kirby 1998). The intention is to work on the GRS80, thus the surface gravity anomalies will be referred to GRS80.

To compute normal gravity γ on ellipsoid to a desired accuracy, we use the following formulas given in Heiskanen and Moritz (1967 p 77) by substituting the defining parameters of the ellipsoid in question.

$$\gamma = \gamma_e(1 + f_2 \sin^2\varphi + f_4 \sin^4\varphi) \tag{4.3a}$$

where

$$f_2 = -f + \tfrac{5}{2}m + \tfrac{1}{2}f^2 - \tfrac{26}{7}fm + \tfrac{15}{4}m^2, \tag{4.3b}$$

$$f_4 = -\tfrac{1}{2}f^2 + \tfrac{5}{2}fm, \tag{4.3c}$$

$$f = \frac{a-b}{a} \quad and \quad m = \frac{\omega^2 a}{\gamma_e} \tag{4.3d}$$

Here

γ_e ... equatorial normal gravity

a ... semi major axis of the ellipsoid

b ... semi minor axis of the ellipsoid

ω ... angular velocity of the earth

φ ... latitude of the point

Simplifications have been conducted for different accuracy levels. By substituting parameters of the GRS80 in the above equations, we obtain the equation for normal gravity on the GRS80 as:

$$\gamma_{GRS80} = \gamma_e(1 + 0.0052790414\sin^2\varphi + 0.0000232718\sin^4\varphi + 0.0000001262\sin^6\varphi + 0.0000000007\sin^8\varphi)\ \text{mGal} \tag{4.4}$$

Further substitution of γ_e gives normal gravity on GRS80 for the given geodetic latitude φ as

$$\gamma_{GRS80} = 97832.67715(1 + 0.0052790414\sin^2\varphi + 0.0000232718\sin^4\varphi + 0.0000001262\sin^6\varphi + 0.0000000007\sin^8\varphi)\ mGal, \tag{4.5}$$

which has a fractional error of 1 to 10^{-10}, corresponding to 10^{-4} mGal, this formula should be used for precise conversions instead of the approximate formula (4.6) if quality of the data warrants:

$$\gamma_{1980} = 978032.7(1 + 0.0053024\sin^2\varphi - 0.0000058\sin^2 2\varphi)\ mGal \tag{4.6}$$

To get surface point gravity g^{obs} corresponding to the free-air point gravity anomaly reduced to the MSL (the geoid) Δg_o, the same formula used is reversed
Thus from

$$\Delta g_o = g^{obs} + 0.3086H - \gamma_{1967} \tag{4.7}$$

We get the observed gravity as

$$g^{obs} = \Delta g_o - 0.3086H + \gamma_{1967} \tag{4.8}$$

Here H is orthometric height and γ_{1967} is normal gravity on the GRS67 computed from

$$\gamma_{1967} = 978031.84558(1 + 0.005278895\sin^2\varphi + 0.000023462\sin^4\varphi)\ mGal\,, \tag{4.9}$$

which introduces an error of 0.0004 mGal, but for less precise work we can use

$$\gamma_{1967} = 978031.8(1 + 0.0053024\sin^2\varphi - 0.0000059\sin^2 2\varphi)\ mGal \tag{4.10}$$

Formula (4.10) has an error of 0.1 mGal. Elevation H should be obtained from the gravity data file and here we should be careful to ensure we use the same formula used to compute γ_{1967}. Since the intention is to work on the GRS80, to convert from GRS67 to GRS80, the following formula is used to convert normal gravity on the ellipsoids

$$\gamma_{GRS80} - \gamma_{GRS67} = \left(0.8316 + 0.0782\sin^2\varphi - 0.0007\sin^4\varphi\right) mGals \tag{4.11}$$

For further reading refer to (Moritz 1980b). Upon having all the obtainable surface point gravity data, the next step is to compute surface gravity anomalies referenced to GRS80.

4.1.3 Surface Gravity Anomaly Referenced to GRS80

Figure 4-2 is used to provide better understanding of surface gravity anomaly.

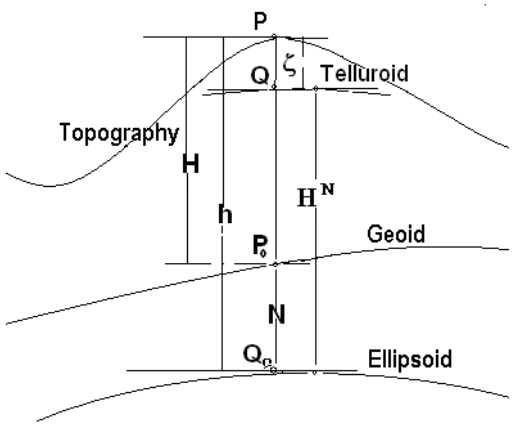

Figure 4-2: Geometry of surface gravity anomaly

Surface gravity anomaly at terrain point P Δg_P, is given by

$$\Delta g_P = g_P - \gamma_Q \tag{4.12}$$

Explanation of symbols in the
Figure 4-2 and Eq. (4.12): g_P is observed gravity on the surface point P, γ_Q is normal gravity on the telluroid point Q along the normal to ellipsoid through P, h is ellipsoidal height of P, H is orthometric height of P i.e. from geoid/MSL, ζ is height anomaly of P and H^N is normal Height of P

Realization of Surface Gravity Anomaly Δg_P

To obtain Δg_P, γ_Q on the telluroid is needed, which in turn requires normal height of P, i.e. ellipsoidal height of Q on the telluroid h_Q. That can be determined from

$$h_Q = h_P - \zeta_P = H_P + N_P - \zeta_P \tag{4.13}$$

Often we have orthometric height of surface point P, thus the above is re-written as

$$h_Q = H_P + (N_P - \zeta_P) \tag{4.14}$$

N_P is geoid height at P. This means, if $(N_P - \zeta_P)$ or generally $(N - \zeta)$ is known at P, then h_Q is obtainable. Either ζ or $(N - \zeta)$ can be obtained in a number of ways; unfortunately all require surface gravity anomaly input, that is the sought information. For example $\tilde{N} \simeq \zeta$, where $\tilde{N}$ is the approximate geoid height. It can be obtained from the least squares modified Stokes method/kernel (LSMS) in combination with a GGM as in Eq. (3.4)

$$\tilde{N} = \frac{c}{2\pi} \iint_{\sigma_0} S^M(\psi_0) \Delta \hat{g}^T d\sigma + c \sum_{n=2}^{M} s_n \Delta \hat{g}_n^S \tag{4.15}$$

In the above equation, $\Delta \hat{g}^T$ is terrestrial surface gravity anomaly, which takes us back to square zero since the sought Δg_P is needed to compute $\tilde{N} \simeq \zeta$. Alternatively $(N - \zeta)$ can be determined approximately from Heiskanen and Moritz, (1967 pp 327-328), first

$$N - \zeta = \frac{\bar{g} - \bar{\gamma}}{\bar{\gamma}} H, \tag{4.16}$$

Eq. (4.16) is developed in Sjöberg (1994b) to higher orders, which take into account roughness of terrain and topography as

$$(N-\zeta)=\frac{\Delta g_B}{\bar{\gamma}_P}H_P-\frac{H_P^2}{2\bar{\gamma}_P}\left(\frac{\partial\Delta g_{FA}}{\partial H}\right)_P-0\left(H_P^3\right), \tag{4.17}$$

with

$$\Delta g_B=\Delta g_{FA}-2\pi\mu H_P, \tag{4.18}$$

where Δg_{FA} is free air gravity anomaly, H is orthometric height and $\bar{\gamma}_P$ is mean of normal gravity at the reference ellipsoid and the telluroid. For the purpose of getting approximate normal height of CP, we have opted to use the traditional first term only i.e.

$$(N-\zeta)\doteq\frac{\Delta g_B}{\gamma_0}H_P \tag{4.19}$$

The fact, that magnitude of $(N-\zeta)$ is often less than a metre, the error associated with the approximate formula is thus within tolerance. For example for elevation 3,797m, $(N-\zeta)$ is around -35cm (Hofmann-Wellenhof and Moritz 2005 p 384). For the 40,350 land point gravity observations in the AOI, statistics of the elevation and geoid to quasi-geoid separation $(N-\zeta)$ are given in Table 4-1.

Table 4-1: Variation of $(N-\zeta)$ in the AOI with 40,350 gravity stations

	H (m)	$N-\zeta$ (m)
Min	0	-0.82
Max	4,305	0.08
Mean	1,078	-0.18
SErr	624	0.13
RMS	1,245	0.22

Since H is part of the data for all the gravity stations, and $(N-\zeta)$ is obtainable for all the gravity stations according to Eq. (4.19), we need to know normal gravity γ_Q on the telluroid before we proceed to compute the surface gravity anomaly according to Eq. (4.12); this is done as follows

$$\gamma_Q=\gamma_0\left[1-\tfrac{2}{a}\left(1+f+m-2f\sin^2\varphi\right)h_Q+\frac{3}{a^2}h_Q^2\right] \tag{4.20}$$

For the GRS80, γ_0 on its surface is continued upward to telluroid point Q to get γ_Q according to the following equation from (Moritz 1980)

$$\gamma_Q=\left[\gamma_0-\left(0.3087691-0.0004398\sin^2\varphi\right)h_Q+7.2125\times10^{-8}h_Q^2\right]mGal \tag{4.21}$$

In Eq. (4.14) if we regard, that accuracy of h_Q depends only on $(N_P - \zeta_P)$, then its effect on γ_Q for the maximum elevation in the AOI (5,895 m), is approximately given by

$$\delta_{\gamma_Q} \simeq -\left(0.3087691 - 0.0004398\sin^2\varphi\right)\delta_{N-\zeta} + 2(7.2125\times10^{-8})\delta_{N-\zeta}\ mGal \qquad (4.22)$$

Contribution of φ is very negligible and thus the effect of $(N_P - \zeta_P)$ on γ_Q for about 10 % error of 1 m, i.e. 0.1 m, is about -0.03 mGal, which is insignificant. Henceforth, surface gravity anomaly Δg_P is computed from equation (4.12)

$$\Delta g_P = g_P - \gamma_Q \qquad (4.23)$$

Computation of surface gravity anomaly is continued in the preparations for geoid model computation in Section 5.2; meanwhile we continue with improvements to Tanzania gravity database (TGDB) for geoid model computation in terms of quantity, quality and error estimates in the next sections.

4.1.4 Qualification and Improvement of Tanzania Gravity Database

There are four big contributors to the Tanzania gravity database (TGDB) products,

1. Within the country, the data are mainly from:
   - Ardhi University gravity database manned by the department of geomatics (ARUDB).
   - Geology department of the University of Dar Es Salaam.
   - Tanzania Petroleum Development Corporation (TPDC); a parastatal organization within the Ministry of Energy and Water Development.
   - Eastern, Central and Southern Africa Mineral Prospecting Centre (ECSAMPC).
   - Ministry of Lands and Human Settlement Development (MLHSD).
2. Bureau Gravimetrique International (BGI), whose objectives are to collect, compile and store on a worldwide basis, all existing gravity measurements and pertinent information about the gravity field of the Earth, into a computerized database, then redistribute on request to a large variety of users for scientific purposes. Data and Products include, gravimeter observations, mainly location - three coordinates, gravity value, corrections, anomalies, mean or point free-air gravity values, gravity maps, reference station descriptions and publications dealing with the Earth's gravity.
3. Global Exploration Technology (GETECH). Offers services to the international oil and mining exploration industry, also to the rest of the world for scientific purposes, but not the original raw data. Address: Kitson House, Elmete Hall, Leeds LS8 2LJ, U.K. Email:info@getech.com and homepage is at: http://www.getech.com/index.html
4. African Gravity Project (AGP). AGP was initially established as a project of the Committee for Developing Countries of the IAG, but was handed over to Commission II; (Gravity Field Commission) of the IAG during the General Assembly of the IAG in Sapporo Japan, in July 2003. The project is managed by a small working group of African geodesists chaired by Professor Charles L. Merry of the University of Cape Town, South Africa. The group collaborates to obtain data from

all over the world and investigates appropriate models for the determination of unified geoid model of Africa.

Of the data obtained from the four sources, we observe the following:

- Only TGDB and BGI provided some of their data as point gravity products.
- There is substantial data overlap amongst the sources as witnessed in Figure 4-3 to Figure 4-7.
- Most data records do not have information on the accuracy of the products; the column for accuracy/standard error is often filled with '9999', meaning there is no information or it is absent altogether.
- Some data were highly corrupted, and we suspect the data formats were mixed up to the extent that sometimes we could not infer any meaningful information out of it.
- There were many multiple observations, sometimes replication or the data were located within a radius of less than 100 m, with the same gravity value, but different accuracies (if present). In other instances, some had specified accuracy. What we did was to compute the mean of the data clustered within the radius of 100 m and the minimum standard error was picked to be the accuracy of the mean; this was exercised only on point gravity products.
- In some files vital information is missing, rendering the whole record useless. For example, of the 29,899 land point gravity data records from BGI, 2,100 had no height and gravity information, of which 2007 had no gravity value.

For the point and mean gravity data obtained, their location maps are presented in Figure 4-3 to Figure 4-8 for visual perception and differentiation. A summary of combined point gravity data quantity is then given in Figure 4-9. A brief discussion on the merging and cleaning for outliers (point data only) and multiple observation removal will follow, then cross validation for errors and statistical testing, culminating with new cleaned and refined land point gravity database for the determination of Tanzania Gravimetric Geoid model 2008, hereinafter referred to as TZG08. Take note, that the data locations displayed below show both good and bad data locations. This kind of information is vital, since in a way it reflects the quality of the mean grid data. Point gravity data was obtained only from BGI and TGDB. For all the maps presented below, boundary limits are latitudes $15^{\circ}S$ to $4^{\circ}N$ and longitudes $26^{\circ}E$ to $44^{\circ}E$, but the AOI borders are slightly different, they are latitudes $15^{\circ}S$ to $4^{\circ}N$ and longitudes $26^{\circ}E$ to $46^{\circ}E$. The decision for the AOI was reached a bit too early before the extent of gravity data was known clearly. Fortunately the marine gravity covers as far as latitude $45^{\circ}E$. The intention is to compute the geoid model bounded by latitudes $12^{\circ}S$ *to* $1^{\circ}N$ and longitudes $29^{\circ}E$ *to* $41^{\circ}E$ using 3° cap cf. Sect. 4.4.3 for more details of limits of different data types.

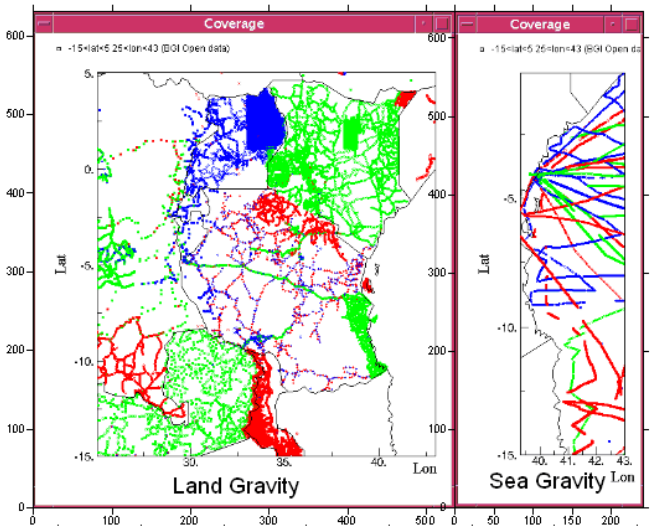

Figure 4-3: BGI locations of point gravity products. Most of the data is used in the research after filtering and validation.

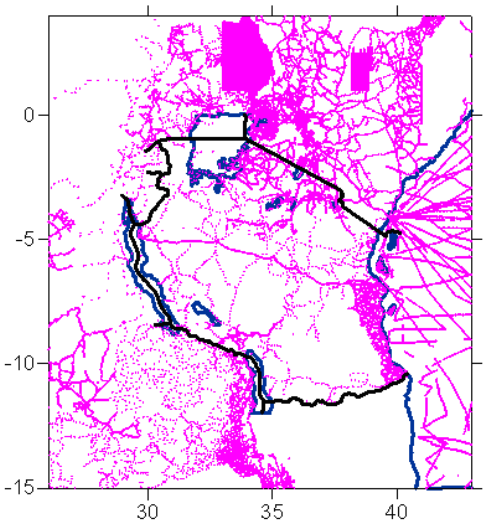

Figure 4-4: AGP $5' \times 5'$ mean Marine KMS99 data locations. The data has not been used

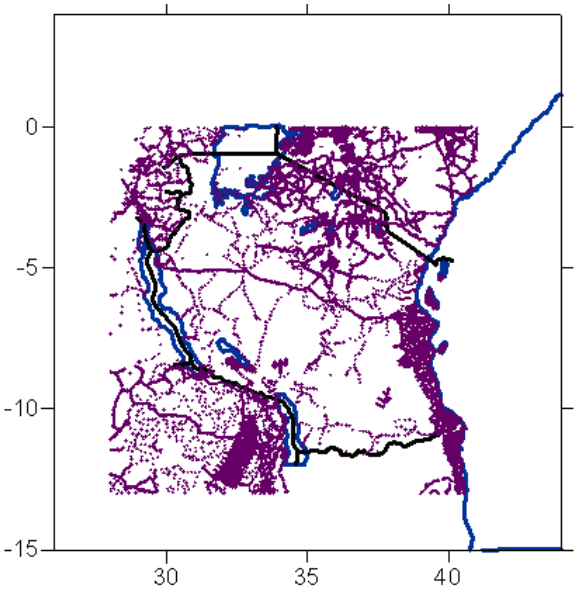

Figure 4-5: GETECH data locations which produced the $5' \times 5'$ grid data obtained from the organization; since the apriori information is absent the data has not been used.

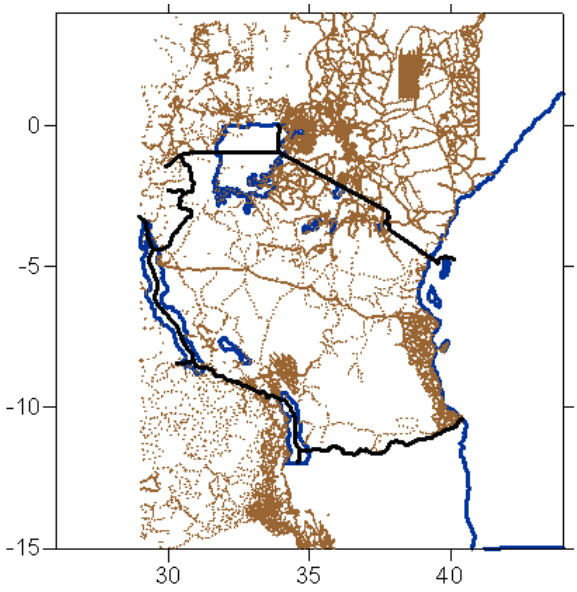

Figure 4-6 : Point gravity from the ARUDB plus other sources listed in Sect. 4.1.4-1. but not wholly from the Geology department of the University of Dar es Salaam.

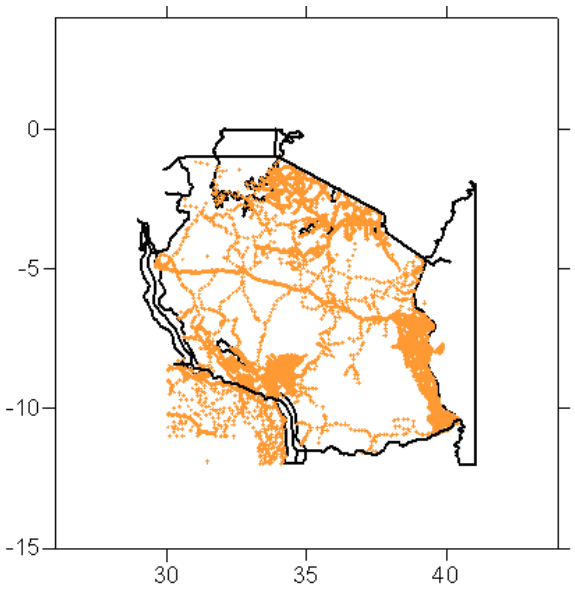

Figure 4-7: Point gravity from the Geology department of the University of Dar es Salaam. Most but not all of the data is also part of ARUDB. Some data have been acquired recently from joint researches with some USA Universities.

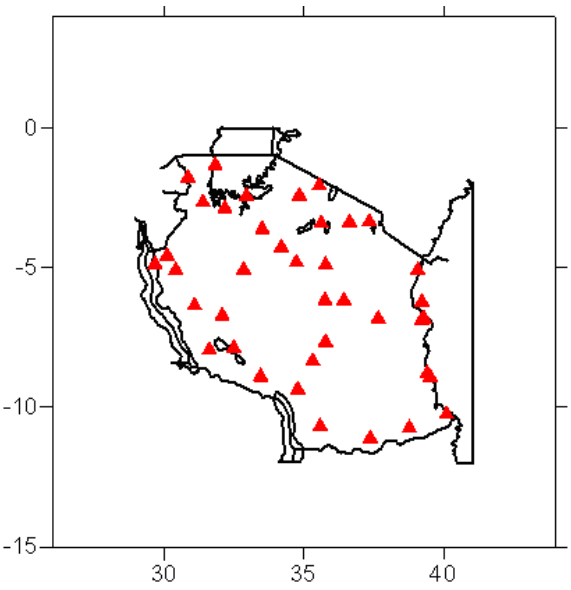

Figure 4-8: Absolute gravity reference stations from BGI and TGDB, the data is also used to validate the GGMs and densifying land gravity $1' \times 1'$ grid data.

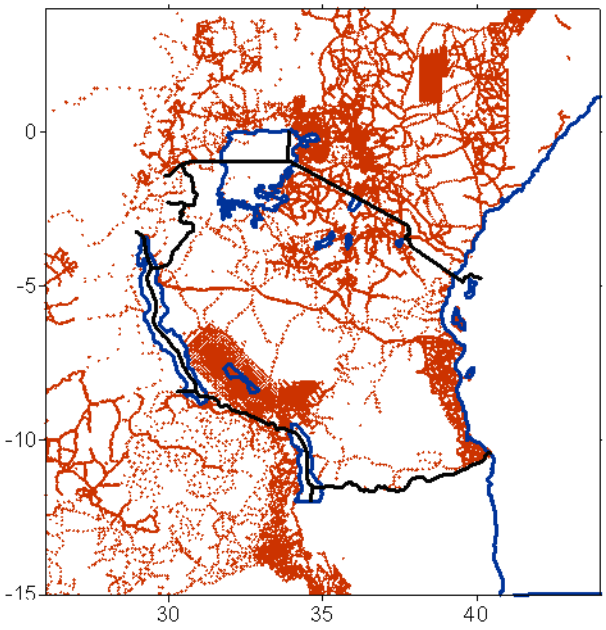

Figure 4-9: 40,350 land point gravity data obtained from the rest of the listed sources after removing all the data missing necessary information and merging multiple observations; the data is yet to be cross validated and tested.

4.1.5 Cross Validation of Land Point Surface Gravity Anomaly Dataset

Using Eq. (4.12), surface gravity anomalies will be computed in Sect. 5.3, but before we embark on geoid model computation, we need to ensure that the data is free of gross and systematic errors as much as possible. To begin with, visual inspection is carried out to check for such things as consistency of coordinate system and units, presence of necessary record components like coordinates (latitude & longitude), height, gravity and preferably accuracy, thus each of the data column was sorted in ascending and descending order in MS-excel to eliminate any dubious record and obvious outliers. Often you find non numeric characters in numeric data columns, which can be very frustrating in the subsequent processes. The method of cross-validation; (henceforth referred to in short as XV) with Kriging technique (Golden 2002), has been selected as the approach to clean the gravity data due to its enormous advantages over many others. Generally, XV is considered a very appropriate method of assessing the quality of a gridding method, or to compare the relative qualities of two or more gridding methods but also to assess the spatial variation in data sampling when the sample size is not small. XV process can be explained as follows: Given known values at N observation locations in the original data set, XV assesses the relative quality of the N data by removing one observation at a time from the data set, and use the remaining data in the neighbourhood and the specified algorithm in this matter Kriging, to predict a value at the removed observation location. Thereafter, the first observation is put back into the data set and the second observation is removed from the data set, using the remaining data (including the first observation), and the specified algorithm, a value is predicted at the second observation location. The second observation is put back into the data set and the process is continued in this fashion all the way through up to and including observation N. This process generates N interpolation errors or differences. By comparing predicted values with observations, various statistics computed for the differences can be used as a quantitative objective measure of spatial variation of the data set. Thus, XV involves four steps:

1. Selection of suitable gridding method.
2. For each observation location, predict a value using the neighbouring data, but not the observation itself, using natural behaviour of the data type (anisotropy).
3. Compute the difference of observed and predicted value.
4. Use the differences to assess the quality of the data from suitable statistical approaches, where difference is given as

$$\text{difference} = \text{predicted value} - \text{observed value} \tag{4.24}$$

Eq. (4.24) is a function of among other factors, the quality of the predicting technique and the known value at the location. For a reputable technique like Kriging, see for example Golden (2002) and Kiamehr (2005), we anticipate minimal prediction error, thus gross error in the observation will definitely show up when the differences/errors are assessed for natural behaviour like the normal distribution. Therefore in this XV process we plot the frequency distribution of the differences at intervals of 5 mGal after sorting the differences to get their range. Prior to XV, the gravity data was made amenable to prediction by removing the erratic residual terrain effect (RTE), which corresponds to short-wavelength of gravity (g_{S_λ}) and long-wavelength of the gravity (g_{L_λ}). RTE was

computed from dense CGIAR SRTM DEM (cf. Sect. 5.1 for more details) and the g_{L_λ} from ITG-GRACE03S GGM evaluated up to degree and order 120. In this way we remained with residual point surface gravity anomaly (dg_surf.res) to validate. Table 4-2 gives the statistics of the gravity data file prior to cross validation.

Table 4-2: Statistics of gravity data files before XV and cleaning in units of mGal.

Gravity File	Population	Min	Max	Mean	SErr	RMS
dg_surf	40,350	-202.718	319.546	-12.987	50.750	52.384
RTE (CGIAR)	40,350	-249.171	268.380	-10.541	28.240	30.143
GRACE03S_120	40,350	-40.960	52.849	4.878	20.060	20.644
dg_surf.res	40,350	-158.580	345.294	-7.347	37.077	37.797

The number of known observations prior to XV is 40,350 i.e. data of file dg_surf.res. Out of the 40,350 dg_surf.res, 56 records could not meet the set XV conditions, and thus their XV results were not output. Frequency distribution of the residuals/differences at intervals of 5 mGal are plotted in Figure 4-10

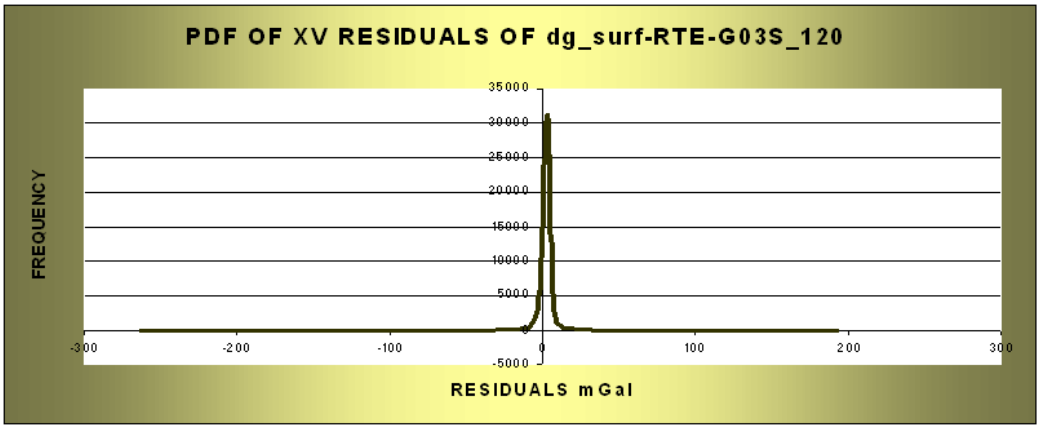

Figure 4-10: Frequency distribution of residuals from XV of dg_surf.res

The curve is almost normal, i.e. Gaussian Probability Density Function (PDF). Although the PDF is not normalized, we observe, that the mean and most of the population is very close to zero. This information is further witnessed in Table 4-3, which displays the statistics of the PDF curve in Figure 4-10. The remainder of the gravity data file without the points which could not be XV amounting to 40,294 gravity records, is further subjected to statistical data analysis and testing using the XV residuals/differences.

Table 4-3: Statistics of the XV residuals i.e. of differences (predicted- observed) of dg_surf.res and estimation of dg_surf.res by Kriging. Unit is mGal

Gravity File	Population	Min	Max	Mean	SErr	RMS
Residuals=Est - Obs	40,294	-261.090	189.551	0.008	6.784	6.784
Est. dg_surf.res	40,294	-158.600	372.414	-7.320	36.601	37.325

Est= Estimated, Obs = Observation, dg_surf.res as explained before Statistical Data Testing

The total area under the Gaussian PDF curve is unity. To work with confidence level according to Gaussian PDF, the population distribution from the mean μ with respect to the spread i.e. square root of the variance, σ is according to the following relations, which give the probability of the confidence interval (Mikhail and Gracie 1981)

$$\begin{aligned} P(-\sigma \le x-\mu \le +\sigma) &\doteq 68.3\ \% \\ P(-1.96\sigma \le x-\mu \le +1.96\sigma) &\doteq 95.0\ \% \\ P(-2\sigma \le x-\mu \le +2\sigma) &\doteq 95.4\ \% \\ P(-2.575\sigma \le x-\mu \le +2.575\sigma) &\doteq 99.0\ \% \\ P(-3\sigma \le x-\mu \le +3\sigma) &\doteq 99.7\ \% \\ P(-\infty \le x-\mu \le +\infty) &\doteq 100.0\ \% \end{aligned} \qquad (4.25)$$

From Table 4-3 $\mu = 0.008\ mGal$ and $\sigma = 6.784\ mGal$. In geodesy it is often common to work between $(95 \to 99)\,\%$ confidence levels, and under these conditions, the confidence intervals for the cross-validated residuals are computed according to Eq. (4.25) yielding the results in Table 4-4.

Table 4-4: Data rejection with respect to XV residual PDF confidence levels

Confidence Interval (CI)	Residual Range (mGal)	Total Data Rejected, %	Retained Data
$\mu \pm 1.96\sigma$, 95 %	-13.289 to 13.305	1,179; ~2.9 %	39,171
$\mu \pm 2.575\sigma$, 99 %	-17.462 to 17.478	673; ~1.7 %	39,677

We settled at 99 % confidence level, and consequently the original land point gravity data rejects 673 out of 40,350 data points and retains 39,677 gravity stations all over the AOI. Table 4-5 provides the quality of the gravity file after statistical data rejection at 95 % and 99 % confidence levels.

Table 4-5: Statistics of gravity data files after statistical data testing at 95 % and 99 % CL in mGal.

Gravity File	CL	Count	Min	Max	Mean	SErr	RMS
dg_surf	95 %	39,171	-202.718	319.546	-13.203	50.451	52.149
	99 %	39,677	-202.718	319.546	-13.147	50.525	52.206
RTE (CGIAR)	95 %	39,171	-242.657	268.380	-10.287	26.867	28.769
	99 %	39,677	-242.657	268.380	-10.327	27.126	29.025
dg_G03S_120	95 %	39,171	-40.404	52.849	5.054	20.166	20.789
	99 %	39,677	-40.404	52.849	5.010	20.118	20.732
dg_surf.res	95 %	39,171	-158.578	330.193	-7.970	35.477	36.361
	99 %	39,677	-158.578	330.193	-7.831	35.785	36.631

dg_G03S_120 = Gravity anomaly of [ITG GRACE03S to degree & order 120] at point gravity locations, CL = Confidence Level, CI = Confidence Interval

Table 4-6 compares the statistics of the point surface gravity anomaly file in GRS80 in its original form (i.e. with outliers) and after effecting XV and statistical testing at 99 % confidence level.

Table 4-6: Statistics of original and outlier free point surface gravity anomaly (dg_surf) at 99 % confidence level (CL) in mGal

File CL	Count	Min	Max	Mean	SErr	RMS
Original; 100 %	40,350	-202.718	319.546	-12.987	50.750	52.384
Clean; Tested at 99 %	39,677	-202.718	319.546	-13.147	50.525	52.206

The null hypothesis is that the residuals have a normal distribution with mean μ and variance σ^2; we now test the sample mean ($\overline{x}$) and variance (s^2) to see if they really belong to normal distribution $N(\mu, \sigma^2)$, which we have assumed all along, i.e.

$$E\{\overline{x}\} = \mu \;\; and \;\; E = \{s^2\} = \sigma^2, \tag{4.26}$$

where $E\{\ \}$ is statistical expectation of the statistic within the brackets. Then it will suffice to test if the sample mean $\overline{x}$ and variance s^2 are within the confidence interval of the population mean μ and variance σ^2 from which the sample is drawn. Using Table 4-3 we hypothesis is as follows:

$$\text{Null hypothesis } H_0: \; \mu = 0.008 \; mGal \tag{4.27}$$

Let the residuals be represented by $x_i, i = 1, 2, ..., n$ with estimated statistics $\overline{x}$ and s. Then the standardized sample mean $\overline{x}$ has a T-distribution given by

$$\frac{\overline{x} - \mu}{s/\sqrt{n}} \xrightarrow{d} t(n-1), \tag{4.28}$$

with $(n-1)$ degrees of freedom, where $\xrightarrow{d}$ means left hand side (LHS) is distributed according to right hand side (RHS). At 99 % probability level, it implies that the interval of μ should be

$$\overline{x} - t_{0.99}^{(n-1)} \frac{s}{\sqrt{n}} \le \mu \le \overline{x} + t_{0.99}^{(n-1)} \frac{s}{\sqrt{n}} \tag{4.29}$$

From statistical tables and Table 4-3 we have $t_{0.99}^{(n-1)} = 2.326$, $\overline{x} = 0.008$ mGal, $\sqrt{n} = 200.734$ and $s = 6.784$ mGal and then the interval becomes

$$-0.071 \le \mu \le 0.087 \tag{4.30}$$

Eq. (4.30) implies acceptance of the null hypothesis of Eq. (4.27). In the same fashion we test the sample variance s^2 to see if it is a true estimate of the population variance σ^2. Only this time the distribution is chi-square (χ^2), whereby

$$\frac{(n-1)s^2}{\sigma^2} \xrightarrow{d} \chi^2(n-1) \tag{4.31}$$

Thus examination of σ^2 is given by probability (P)

$$\mathrm{P}\left(\chi^2_{P1} \le \frac{(n-1)s^2}{\sigma^2} \le \chi^2_{P2} \right) = 0.99 \tag{4.32}$$

which leads to confidence interval given by:

$$\frac{(n-1)s^2}{\chi^2_{P1}} \le \sigma^2 \le \frac{(n-1)s^2}{\chi^2_{P2}}, \tag{4.33}$$

where $P_1 = \frac{1-\alpha}{2} = \frac{1-0.99}{2} = 0.005$ and $P_2 = \frac{1+\alpha}{2} = \frac{1+0.99}{2} = 0.995$, and (4.34)

α is the statistic confidence interval level i.e. testing probability, here it is 99 %

Unfortunately most of the printed statistical tables do not give χ^2 values when the degrees of freedom ($df = n-1$) are >120. It was possible to get values for large df at http://www.fourmilab.ch/rpkp/experiments/analysis/chiCalc.html; February, 2008. Thus $\chi^2_{0.005}(40,342) = 41{,}028.982$ and $\chi^2_{0.995}(40,242) = 39{,}566.529$ together with Table 4-3 we get from Eq. (4.33)

$$45.202 \le \sigma^2 \le 46.873 \;\Rightarrow\; 6.723 \le \sigma \le 6.846 \tag{4.35}$$

Since the sample standard error $s = 6.784$, the null hypothesis is accepted in Eq. (4.35), and therefore we conclude that the sample is drawn from the parent normally distributed population $N(\mu, \sigma^2)$ assumed apriori. That is to say, the differences of the sample statistics ($\bar{x}$ and s^2) from population statistics (μ and σ^2), respectively, are not significant at 1 % probability risk level. Figure 4-11 displays 39,677 point gravity values of the new TGDB in the AOI, which is clean of most of the errors, and cross-validated and statistically tested at 99 % confidence level ready for subsequent geoid model computation processes.

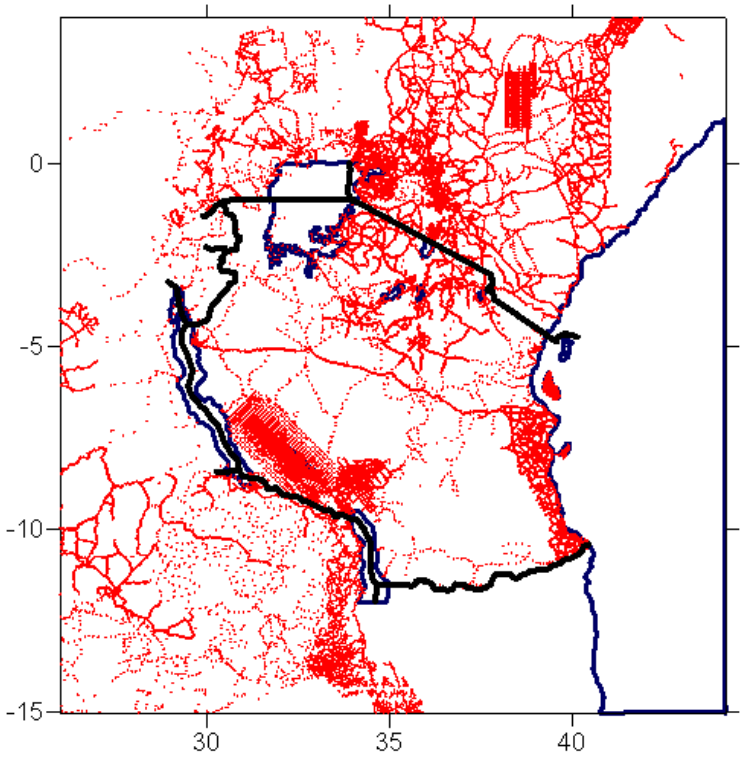

Figure 4-11: 39,677 land surface point gravity anomaly free of outliers at 99 % confidence level for the computation of TZG08

4.1.6 Error Sources, Estimates and Propagation

In many observations there were no error estimates. Fortunately, in the two main sources of point gravity data from BGI and TGDB, most of the gravity records have a remark on the instruments used to obtain the horizontal coordinates and height of the gravity station, and very rarely about the accuracy estimates. They can be summarized as follows:

1. Gravity observations: It is believed that gravity observations were cleaned of all major systematic influences like drift, tare, water and land tidal etc. Geodetic gravimeters were used in data collection. Notwithstanding manufacturer's accuracy description of the gravimeters, repeated observations onto gravity control stations, gave a maximum difference of less than 1 mGal.

2. Elevations: Methods used range from trigonometric heighting, tacheometry, barometric, spirit levelling to water levelling in some lake areas. We take that none of the methods could have an error exceeding 1 m.

3. Horizontal positioning: Methods used are optical (theodolite), Doppler satellite, inertia surveying, GPS - single point positioning and occasionally differential. Also extraction from maps. The smallest map scale mentioned is 1:250,000. Of the aforementioned methods, the worst error could come from extraction from maps. Here two processes are involved; identification of the observation station on the map and once done, extraction of the coordinates. For the smallest map, we take the

station could be identified within a circle of 1 cm radius on the map. Then one could read the coordinates without problem to 2 mm resolution. Thus major error comes from identification of the location. 1 cm on 1:250,000 map corresponds to 2500 m on the ground which is equivalent to about (2500/30) arc seconds. Thus the error in latitude is $\pm 1.5'$. The error due to horizontal positioning mainly affects determination of normal gravity when computing gravity anomaly, and gravity gradient, but not the actual gravity observation.

Moreover, from Parker and Marobhe (1991), TGDB overall accuracy of gravity is quoted without further explanation as given in Table 4-7

Table 4-7: Quoted land gravity observation errors in TGDB

Error type	Mean	Maximum
Elevation error, e_H	1 m	-
Horizontal error, e_{xy}	10 m	-
Overall gravity, e_g	1.5 mGal	4.2 mGal

Unfortunately the above quotation is not supported by the methodologies used to get the data; we find e.g. the overall maximum gravity error to be too high, unless it refers to gravity anomaly. The same observation applies for the BGI file. Fortunately the BGI file has most of the information on positioning and instrumentation in the field, thus it is opted to go by the conclusion from analysis of the methodology and instrumentation verified before cf. Table 4-8.

Table 4-8: Quoted observation errors in BGI gravity file

Error type	Maximum
Elevation error, e_H	5 m
Horizontal error, e_{xy}	20 m
Gravity, e_g	1 mGal
Free-air anomaly, $e_{\Delta gFA}$	9 mGal
Bouguer anomaly, $e_{\Delta gbg}$	7 mGal

Occasionally density is quoted in the TGDB, the quoted figures are 1.6g/cc, 2.67g/cc and "mean=2.32g/cc", and in the BGI file there are two quotations of 2.67g/cc and 2.74g/cc and also "mean= 2.69g/cc". Unfortunately this has been given in very few gravity stations and not areal, i.e. for points and not area. Table 4-9 provides error estimates based on quantification from methodology and instrumentation, they are to be used for the assessment of accuracy of computed quantities in case explicit accuracy information is not given.

Table 4-9: Error estimates to be used to compute other quantities

Quantity	Error Estimate
Gravity	$\sigma_g = \pm 1.5\ mGal$
Elevation	$\sigma_H = \pm 5\ m$
Latitude	$\sigma_\varphi = \pm 1.5'$

Accuracy Estimates for Computed Quantities
From Eqs. (4.3a) and (4.10), accuracy of normal gravity on the reference ellipsoid γ_0 as a function of position φ (extracted from maps) is computed from

$$\sigma_{\gamma_0}^2 = \left(\frac{d\gamma_0}{d\varphi}\right)^2 \sigma_\varphi^2 \tag{4.36a}$$

or $$\sigma_{\gamma_0} = \pm\gamma_e \left(f_2 \sin 2\varphi + 2 f_4 \sin 4\varphi \right) \sigma_\varphi\ mGal \tag{4.36b}$$

For the GRS67

$$\gamma_e = 978031.8\ mGal,\quad f_2 = 5.3024\times10^{-3},\ f_4 = 5.9\times10^{-6}, \tag{4.36c}$$

and from Table 4-9, $\sigma_\varphi = 4.36332\times10^{-4}\ rad$, this enables determination of $\sigma_{\gamma_{GRS\,67}}$

Observed gravity is recomputed from reduced free-air gravity anomaly by

$$g^{obs} = \Delta g_o - 0.3086H + \gamma_{0,1967}, \tag{4.37}$$

and therefore

$$\sigma_{g^{obs}}^2 = \sigma_{\Delta g_o}^2 + (0.3086)^2 \sigma_H^2 + \sigma_{\gamma_{0,1967}}^2 \tag{4.38}$$

Under the assumption that the same elevation H and normal gravity γ are used, the only additional error sources would be from mathematical modelling, which has insignificant error. Therefore, the accuracy of g^{obs} should basically be that of the observed gravity and therefore obtained from Table 4-9 unless explicitly given.

In both the BGI and TGDB, gravity was referred to IGSN71, and gravity anomalies were computed with respect to GRS67, but we are to work with GRS80, therefore to obtain the accuracy of gravity anomaly on GRS80, Eq. (4.11) should be used. Consequently we get

$$\sigma_{\gamma_{GRS\,80}}^2 = \sigma_{\gamma_{GRS\,67}}^2 + \sin^2 2\varphi (a^2 + 4b^2 \sin^4 \varphi)\sigma_\varphi^2 \tag{4.39}$$

Using Eq. (4.11) , Eqs. (4.36a) to (4.36c) and Table 4-9, $a = 0.8316$,

$\sigma_\varphi = \pm 1.5' = 4.36332 \times 10^{-4}\ rad$ *and* $b = 0.0007$, and therefore $\sigma_{\gamma_{GRS80}}$ in Eq. (4.39) can be determined.

Now we can consider accuracy of surface gravity anomaly

The variance of the surface gravity anomaly cf. Eq. (4.12), is generally given by

$$\sigma^2_{\Delta g_P} = \sigma^2_{g_P} + \sigma^2_{\gamma_Q} - 2\sigma_{g\gamma}, \tag{4.40}$$

where $\sigma_{g\gamma}$ is the correlation between g_P and γ_Q. $\sigma_{g\gamma}$ is taken to be zero because the observed gravity g_P and the normal gravity γ_Q at the corresponding point on the telluroid Q have no common parameters which relate them, see Eq. (4.42). While $\sigma^2_{g_P}$ is obtained from Table 4-9, to compute $\sigma_{\Delta g_P}$ we further need to obtain σ_{γ_Q}. This is obtained from upward continuation of normal gravity on the surface of ellipsoid to Q on the telluroid as given in Eq. (4.20) or in (Wellenhof and Moritz 2005) and simplified for GRS80 by (Moritz 1980b) as given by Eq. (4.21)

$$\gamma_Q = \left[\gamma_0 - \left(0.3087691 - 0.0004398\sin^2\varphi\right)h_Q + 7.2125\times10^{-8}h_Q^2\right] mGal \tag{4.41}$$

Accuracy of γ_Q depends on γ_o, φ and h_Q. That is

$$\gamma_Q = f(\gamma_o, \varphi, h_Q) \tag{4.42}$$

We therefore observe, that

- Accuracy of $\sigma_{\gamma_{GRS80}}$ is obtained from Eq. (4.39)
- Accuracy of φ is given by Table 4-9 i.e. $\sigma_\varphi = 4.36332\times10^{-4} rad$.
- Accuracy of h_Q should be obtained from Eq. (4.14) i.e.

$$h_Q = H^N = H + (N - \zeta) \tag{4.43}$$

But we saw, that magnitude of $(N - \zeta)$ is mostly less than a metre (1 m), and therefore, the accuracy of Eq. (4.43) is basically that of orthometric height H_P which is given in Table 4-9. Hence from Eq. (4.41) we get

$$\sigma^2_{\gamma_Q} = \sigma^2_{\gamma_o} + \left(a^2 + 4c^2h_Q^2\right)\sigma^2_{h_Q} + b^2\left(h_Q \sin 2\varphi\, \sigma_\varphi + \sin^2\varphi\sigma_{h_Q}\right)^2, \tag{4.44}$$

where

$$a = 0.308\,76\,91;\quad b = 0.000\,43\,98;\quad c = 7.2125\times10^{-8};$$
$$\sigma_{h_Q} = \pm 5\ m;\quad \sigma_\varphi = 4.36332\times10^{-4} rad$$

With regards to Eq. (4.40), accuracy of surface point gravity anomaly can now be computed from Eq. (4.44) and Table 4-9 taking into consideration the remark after Eq. (4.40), henceforth for subsequent processes of realization of TZG08, Table 4-10 gives the statistics of the accuracy of the clean new TGDB.

Table 4-10: Statistics of accuracy of land point surface gravity anomaly referred to GRS80 in mGal

Population	Mean	Min	Max	SErr	RMS
39,677	2.209	2.153	2.433	0.061	2.210

The gravity density is about 1-gravity point per 75 square kilometres in land area.

4.2 Marine Gravity Data

Tanzania is surrounded by a number of water bodies. Foremost it is the United Republic of Tanganyika (the mainland) and Zanzibar (isles of Unguja & Pemba). Mafia is also a big isle, but it is part of Tanganyika. Moreover Tanzania is found between three great lakes of the world, Victoria, Tanganyika and Nyasa. Without overlooking the entire Eastern boundary of Tanganyika is Indian Ocean; Figure 4-12

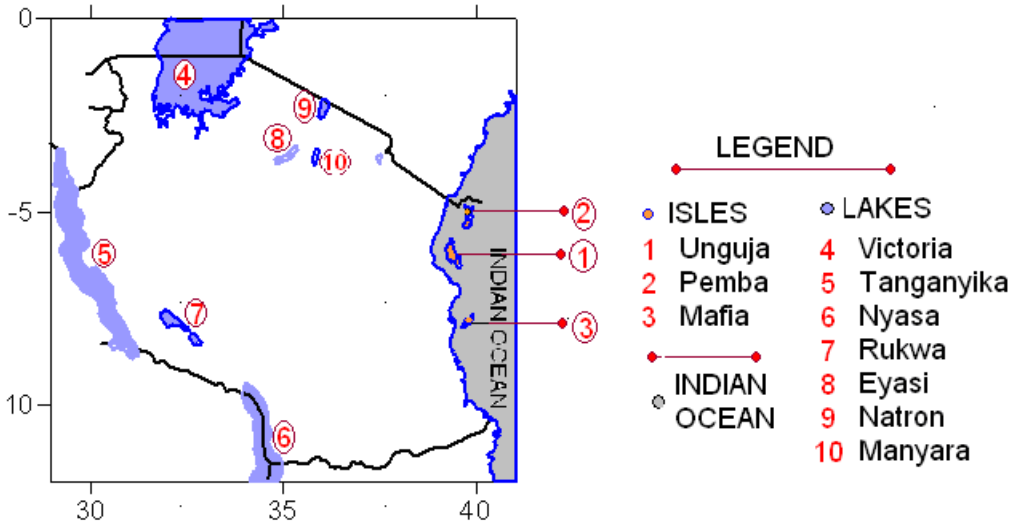

Figure 4-12: Tanzania and water bodies

Marine gravity data incorporates terrestrial ship borne (sea surface and or sea bottom), and satellite altimetry. We did not succeed to obtain any of the marine data from sources in Tanzania. But mean altimetry and point ship track sea gravity data have been obtained from different sources outside Tanzania as outlined below.

i) The Bureau Gravimetrique International (BGI).

7,843 ship track point gravity were given to this research by the BGI as seen in Figure 4-13; each data record includes geographical coordinates (latitude and longitude), elevation, gravity, free-air and simple bouguer gravity anomalies also metadata for the

file. The metadata consist of the background to the observations and positioning; both horizontal and vertical.

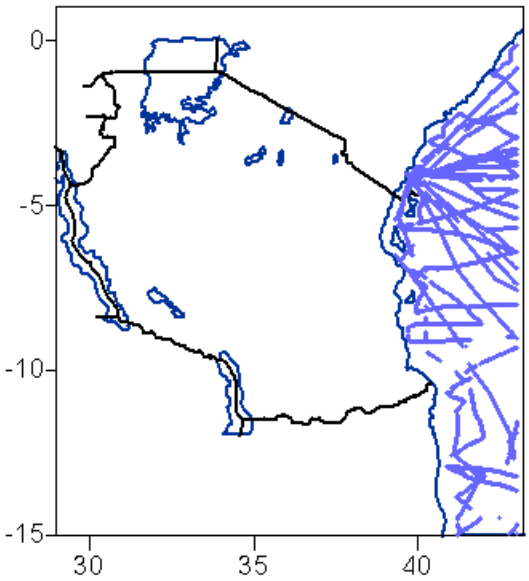

Figure 4-13: Sea point gravity (ship tracks) from BGI, unit mGal

ii) The Sea Altimetry Data.
We received KMS02 2' x 2' grid gravity anomaly data from the Danish National Centre for Space-related activities, i.e. the Danish National Space Centre (DNSC) of the Technical University of Denmark (DTU) covering the AOI as explained further below. KMS02 "Global marine free-air gravity field" is computed from ERS-1 and GEOSAT satellite altimetry. The KMS02 2' x 2' surface gravity anomaly grid data is an upgrade of the previous KMS99 marine gravity field. In this model all new data and corrections of that time were applied. They included:

- The ERS and GEOSAT Geodetic Missions data DEOS – RADS.
- The ERS2 ERM (repeat 60-63) including ground track drift corrections by GYRO.
- The ERS ERM data (repeat 1-85) from the NASA Pathfinder project to ensure complete coverage.

The GOT00.2 tide model was used; further reference is found at http://www.spacecenter.dk/data/global-bathymetry-model-1/ERS-1Marine Gravity Anomalies.gif/view

The data format is that of Gravsoft package grid data, (Tscherning et al. 1994) i.e. grid data for the AOI contains a header describing the area and resolution of the grid data given by minimum and maximum latitude and longitude respectively, then grid spacings in latitude and in longitude followed by marine gravity anomalies. The KMS gravity field is available through the KMS anonymous file transfer protocal site at: ftp.kms.dk cd pub/GRAVITY/KMS02, (Andersen and Knudsen 2003).

iii) Other Sources:
The African Geoid Project supplied us with 5' x 5' grid marine gravity anomalies for almost the whole of the AOI. But during XV, the data did not qualify; most probably it is due to the smoothing effect of the big grid size compared to the KMS02, this will be explained further afterwards. The research will use $1' \times 1'$ grid surface gravity data. Combination of $2' \times 2'$ KMS02 grid data (refer to Table 4-11) and BGI 7,843 point surface gravity anomalies, justifies gridding from $2' \times 2'$ to $1' \times 1'$. Usually it is not expected to densify from less dense to denser grid, e.g. from $2' \times 2'$ to$1' \times 1'$, but distribution and density of ship track gravity data to be added, cf. Figure 4-13, justifies this densification as seen in Figure 4-14, and besides, we have to incorporate the richness of ship gravity data for better quality results. The BGI data is referred to GRS67 and the KMS02 to WGS84. The BGI gravity anomalies will be converted to GRS80 but due to small difference between WGS84 and the GRS80 ellipsoids (Hofmann-Wellenhof and Moritz 2005 p 90), it is not necessary to transform the KSM02 data to GRS80.

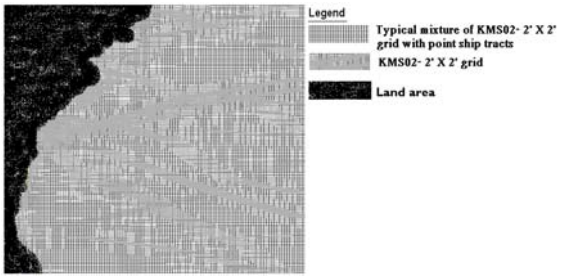

Figure 4-14: Formation of $1' \times 1'$ marine gravity from $2' \times 2'$ grid and ship tracks, unit mGal

4.2.1 Point and Mean Sea Gravity Anomaly

Sea Point Free Air Gravity Anomalies

Although the BGI metadata shows that the elevations of the gravity records refer to the ocean surface, it does not explain where the gravity was observed, and the code supplied is annotated "No information". This is further supported by the fact that in some records, the supplied gravity anomalies can be computed accurately from the record data, but there are other instances when it is not possible. The BGI records explain clearly that the free-air gravity anomalies have been reduced to the geoid model. Given this ambiguous situation, we opted to work solely with the supplied free-air point gravity anomaly on the ocean surface after transformation from GRS67 to GRS80 according to Eq. (4.11) i.e.

$$\Delta g_{GRS80} = \left[\Delta g_{GRS67} + \left(0.8316 + 0.0782 \sin^2 \varphi - 0.0007 \sin^4 \varphi\right) \right] mGals\,, \qquad (4.45)$$

where

Δg … Refers to 'Free Air Surface Gravity Anomaly'

Marine KMS02 $2' \times 2'$ Grid Free-Air Gravity Anomaly

The supplied grid data covers fully the AOI. Since the data is from altimetry, its quality in the land areas is usually not to the standard needed. Therefore from foregoing information, we are confronted with two major issues;

- To limit the grids to marine areas only. From Figure 4-15 the boundary of about 20° long from north to south is meandering i.e. not straight.
- To merge the grid and point data i.e. KMS02 and BGI data, respectively, and re-grid to $1' \times 1'$
-

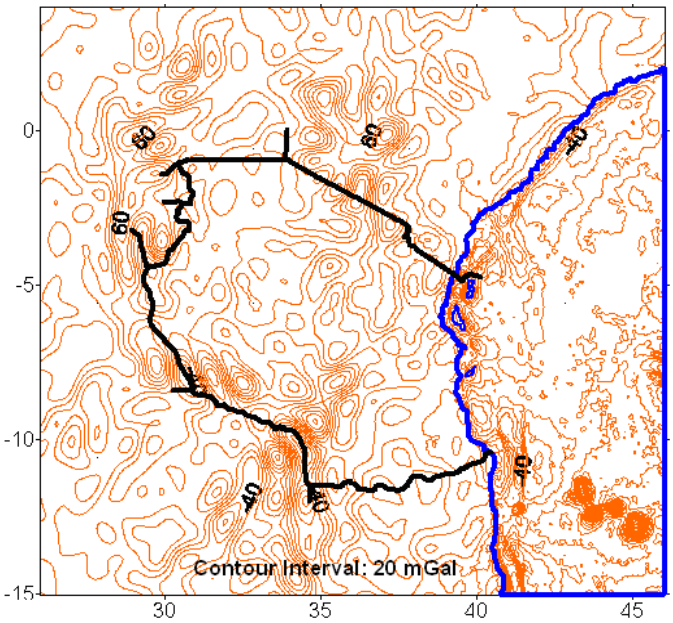

Figure 4-15: KMS02 contour grids covering the entire AOI in mGal

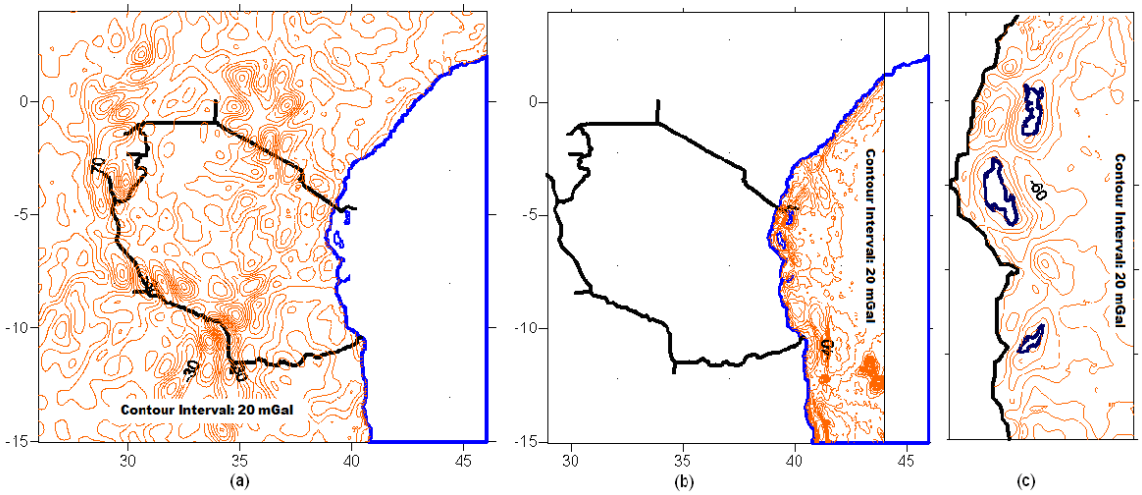

Figure 4-16: KMS02 contour grids in mGal are limited to marine ocean area only
(a) Grids confined to mainland (but redundant data)
(b) Grids in ocean area and limited to longitude $44^{\circ} E$
(c) Marine contours do not cross Isles

We start with limiting KMS02 to ocean area only i.e. with the Indian Ocean coast and the three isles as border to the $2' \times 2'$ grids within the AOI (cf. Figure 4-16). First we digitize the four borders separately and store them in boundary line data format. Then we extract the grids from the entire KMS02 data by blanking the area inside or outside the blanking

boundaries accordingly. This is the reason why the four boundaries had to be stored separately. The order of extraction needs logical approach for successful end result.

Merging KMS02 Limited to Ocean Area with Ship Surface Gravity

After transformation of ship surface gravity anomalies from GRS67 to GRS80, compatibility of the point and grid anomalies was sought by predicting ship anomalies, first from KMS02 $2' \times 2'$, and then from AGP/GETECH $5' \times 5'$ grid anomalies. The agreement of ship data with KMS02 $2' \times 2'$ is much better than with AGP/GETECH $5' \times 5'$ as seen from the statistics of the differences in Table 4-11. In addition, the table portrays statistics of the participating three anomaly data sets. The wider gap between the statistics of the two grid data is most probably due to the difference in grid spacing. Furhermore, given the decision to use $1' \times 1'$ grids, the AGP/GETECH $5' \times 5'$ data is rendered unsuitable for this research. We started by blanking land altimetry data so that it does not mix up and compromise the entire gravity data quality in the subsequent processes of merging sea and land gravity data. First the sea grid data is converted to list data, which refers to the grid nodes prior to merging the sea KMS02 and ship tracks. Formation of $1' \times 1'$ marine gravity grids from the resultant ocean data does not follow exactly the same procedure as in the land, described in Sect. 5.3, because

- Usually marine gravity anomalies are smoother than their land counterpart and therefore prediction is more reliable even without using r-c-r approach.
- The KMS02 $2' \times 2'$ data, which is medium to long-wavelength gravity, is present.
- The ship gravity more or less covers the entire ocean area of interest (cf. Figure 4-13 and Figure 4-14), therefore inhere, we do not have sparse areas parse, besides we need to use the short-wavelength rich ship gravity to fill in the missing frequencies in the KMS02 $2' \times 2'$ altimetry gravity.

Table 4-11: Statistics of marine point grid gravity and differences of altimetry with ship gravity at ship track locations. (Unit is mGal)

	dgS_fa (Ship)	Est_AGP02	Est_KMS02	Diff_AGP02	Diff_KMS02
SeaG_Stn	7,843	7,843	7,843	7,843	7,843
Sum	-225324.08	-220826.52	-201863.45	2037.65	-16925.42
Min	-141.93	-110.76	-135.54	-141.09	-61.42
Max	87.84	54.61	80.01	88.68	65.47
Mean	-28.73	-28.16	-25.74	0.26	-2.16
SErr	**32.74**	**25.40**	**31.05**	**18.92**	**10.40**

dgS_fa (Ship)=sea free-air gravity anomaly from ship, Est = Estimated value from, Diff = Known ship data minus estimate from grid data, SeaG_Stn=sea gravity stations

We observe from Table 4-11, that after predicting the AGP02 and KMS02 marine grid data at the ship track gravity positions, the best agreement (minimum difference) is obtained from the KMS02; the two will be combined to densify to $1' \times 1'$ ocean grid.

4.2.2 Gridding and Cross Validation of Marine Gravity

The blanked KMS02 $2' \times 2'$ marine data was converted to list data (i.e. record at the grid node is regarded as one data), giving a total of 51,935 records. Ship gravity data (7,843

records) were added and sorted to ensure the data is mixed up spatially. Statistics of the three data sets, i.e. the original files and the combined, are shown in Table 4-12.

Table 4-12: Statistics of marine surface gravity data in mGal

	KMS02	BGI_ship	KMS02+BGI
No. Records	51,935	7,843	59,778
Sum	-1353466.74	-218788.87	-1572255.61
Min	-139.72	-141.09	-141.09
Max	270.79	88.68	270.79
Mean	-26.06	-27.90	-26.30
SErr	29.60	32.74	30.04

The Kriging method is used to form $1' \times 1'$ grids from the KMS02+BGI data. The appearance after merging is seen in Figure 4-17. Close visual inspection of the resultant $1' \times 1'$ grids given as contours and surface in Figure 4-17, tickles something could be wrong with the ship data (Figure 4-13). Visibly on Figure 4-17, there is some resemblance to some of the ship tracks, which appear as break lines and trenches in Figure 4-17.

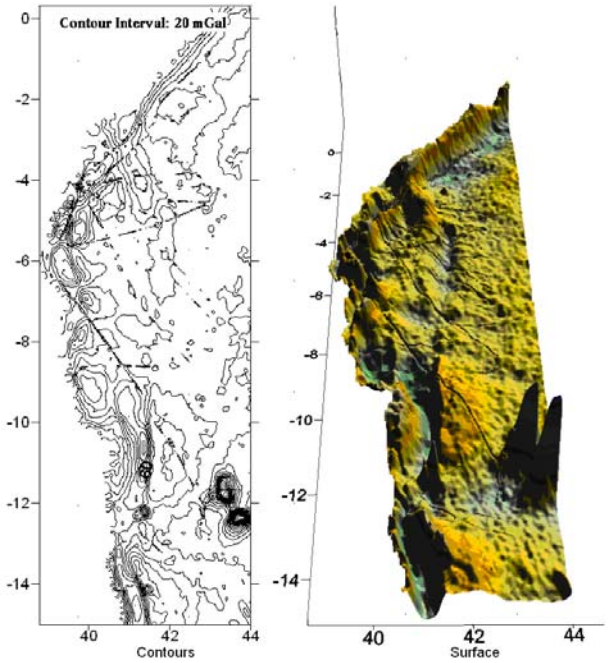

Figure 4-17: $1' \times 1'$ Marine gravity data prior to validation

This necessitated validation. The validation procedure explained before is adopted and the frequency curve for the residuals/differences is computed and used to validate the data. Figure 4-18 is the resultant frequency curve.

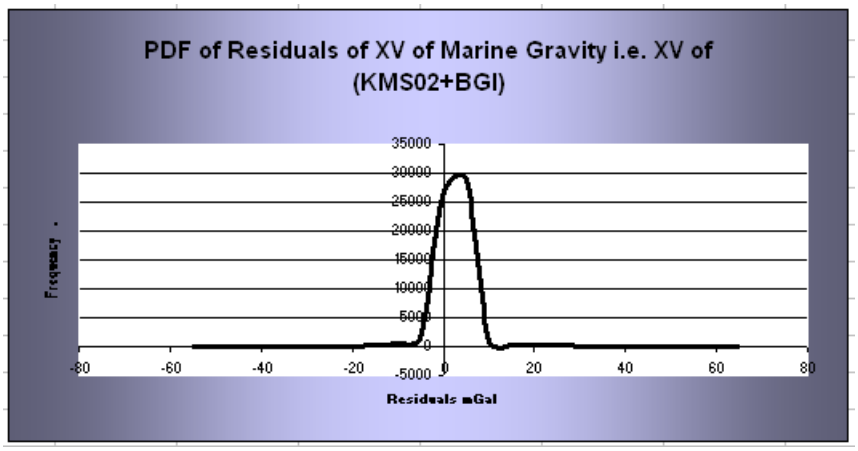

Figure 4-18: Frequency distribution of residuals from XV of marine gravity data

Table 4-13: Quality of estimation and properties of the frequency curve in Figure 4-18 i.e. of the XV residuals in mGal

Description	Estimated dg_surf.res	XV Residuals
Amount	59,773	59,773
Mean	-26.325	-0.025
Min	-140.280	-55.006
Max	268.212	63.811
SErr	29.918	4.120
RMS	39.851	4.120

During cross validation, 10 stations were duplicates, so only 5 were retained, otherwise all stations were cross-validated, which amount to 59,773 records. Some properties of the curve in Figure 4-18 are shown as the XV residual column in Table 4-13. From Figure 4-18 and Table 4-13, we can deduce the curve to be quite close to Gaussian distribution. So as in the previous case, we reject the data at 1 % significance level. From Eq. (4.25) and Table 4-13, confidence interval for the accepted data at 99 % is $\mu \pm 2.575\sigma$ whose range is from [-10.635 to +10.585] mGal. Upon rejection at 1 % risk level, 57,723 marine data are retained. The quality of the 99 % confidence level of the residuals and marine gravity data left are given in Table 4-14 and Table 4-15, respectively.

Table 4-14: XV residuals after 99 % CL statistical testing in mGal

Size	Mean	Min	Max	SErr	RMS
57,723	-0.087	-10.637	10.574	1.859	1.861

The density is about 1 gravity station in 8 square kilimetres in the ocean

The data was again gridded using Kriging method explained earlier. Results from $1' \times 1'$ final marine data are displayed in Figure 4-19.

It is the time we check our sample if it belongs to the assumed normal distribution $N(\mu, \sigma^2)$. The previous procedure of testing will be followed, and therefore attention should be to Eqs. (4.26) to (4.35) except here we use data from Table 4-13, i.e.

$\bar{x} = -0.025\,mGal$, $s = 4.120\,mGal$ and $n = 59,773$. First we test the population mean μ and our null hypothesis is:

$$H_0:\ \mu = -0.025\,mGal$$

Using Eq. (4.29) and the data above, we obtain

$$-0.064 \le \mu \le 0.014 \tag{4.47}$$

Next we test σ^2 using sample variance s^2 by postulating

$$H_0:\ \sigma^2 = (4.120)^2\,[mGal]^2 \tag{4.48}$$

We use information from Eqs. (4.33) and (4.34), Table 4-13 and χ_P^2 web calculator; so $\chi^2_{0.005}(59,773) = 60,666.3735$ and $\chi^2_{0.995}(59,773) = 58,885.1366$ together with the above equations and data we get

$$16.7274 \le \sigma^2 \le 17.2334 \ \Rightarrow\ 4.090 \le \sigma \le 4.151 \tag{4.49}$$

Eq. (4.49) ascertains Eq. (4.48) and thus together with Eq. (4.47) the sample has been drawn from the postulated normally distributed population at 99 % confidence level.

Although at 1 % significance level, is only about 3.4 % of the data is discarded, when Figure 4-17 and Figure 4-19 are compared, the improvement presents more confidence, besides, the results seem more reliable. Statistics of the cross validated and statistically tested and cleaned marine data are compared to the original unclean data in Table 4-15.

Table 4-15: Quality of marine data: before and after cross validation and statistical testing at 99 % CL, unit = mGal.

	Before KMS02+BGI	After XV_(KMS02+BGI)
No. Records	59773	57723
Min	-26.300	-25.848
Max	-141.093	-141.093
Mean	270.790	270.790
SErr	30.037	30.076
RMS	39.925	39.657

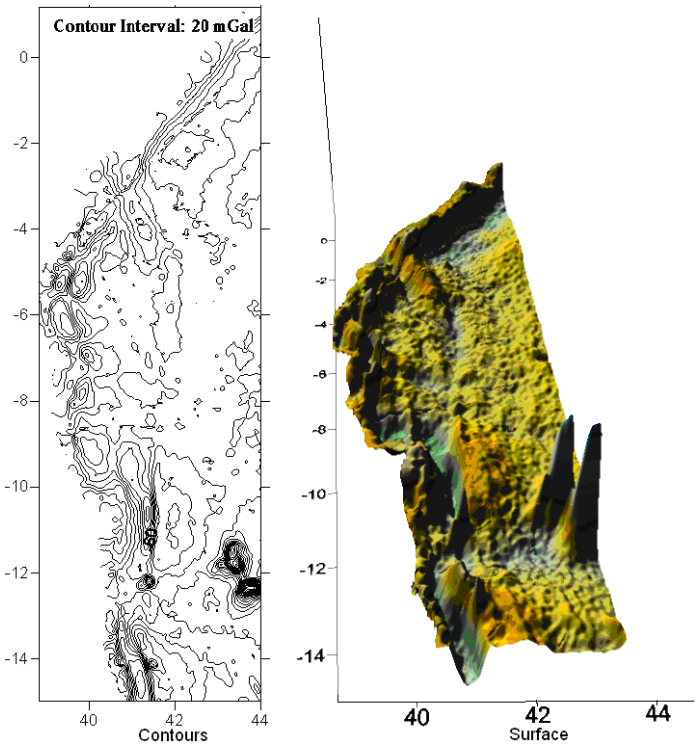

Figure 4-19: $1' \times 1'$ marine gravity after XV and testing of residuals at 99 % confidence level

Although the data was limited to marine area before XV, process of gridding re-introduced a few contours into land areas. So boundary blanking was repeated to confine the grids and consequently contours to Indian Ocean area only, this way the effect to data quality from either side of the blanking boundaries is minimized. The process is shown in Figure 4-20.

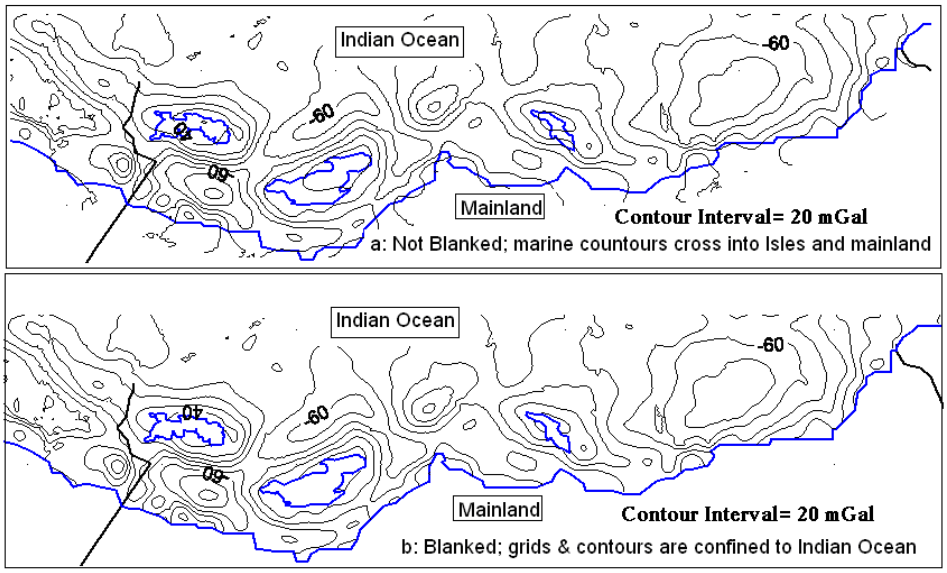

NB: Maps in Figure 4-20 are rotated through 270° *clockwise angle*

Figure 4-20: Grids and contours are confined to Indian ocean, they do not cross to land.

Finally the marine gravity data for TZG08 is displayed in Figure 4-21, it will be merged with similarly cleaned land gravity data for subsequent TZG08 processes in Section 5.3.

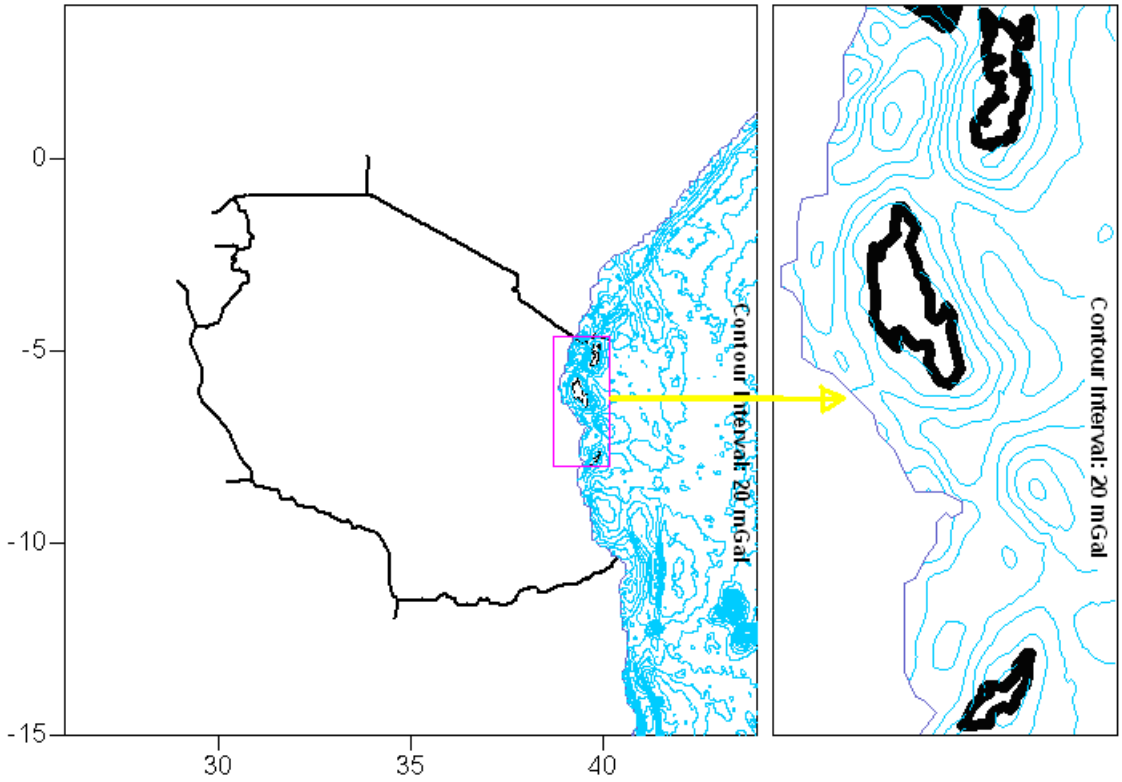

Figure 4-21: $1' \times 1'$ marine gravity in the AOI for TZG08 in mGal

4.3 Global Gravitational Models (GGM)

Introduction

Geoid model determination requires most of frequencies of the gravity field spectrum. Ground data is rich of high to medium frequencies, but the low frequencies are often contaminated and in entirety poorly positioned. On the other hand, satellite gravity data is well positioned globally, with the broad features of the geoid model, but the converse is true compared to ground data; the high frequency is practically absent (Ågren and Sjöberg 2004). Satellite gravimetry commenced with the launch of Sputnik in 1957, and since then a lot of effort has been directed towards the determination of the Earth's external gravity field from satellites. Recently we have realized extra commitment to map the external Earth's gravity field more accurately, and consequently, since the year 2000 the world perceived two operational satellite missions dedicated primarily to the recovery of gravity field of the Earth to higher degree and order. It commenced with CHAMP (CHAllenging Minisatellite Payload), which was launched on 15th July 2000. CHAMP is a small German satellite mission managed by GeoForschungsZentrum (GFZ) Potsdam. Its objectives are: Earth Gravity Field Recovery, Earth Magnetic Field Recovery, Electric Field Investigations, Atmospheric Limb Sounding and Ionosphere Sounding for geo-

scientific and atmospheric research and applications, for further CHAMP information cf. http://www.gfz-potsdam.de/pb1/op/champ/more/newsletter_CHAMP_016.html, 19.01.08
Then came GRACE (Gravity Recovery And Climate Experiment). The mission began its geo-scientific space operation on 17th March, 2002. GRACE is a joint project of the American Space Agency NASA, the German Aerospace Centre (DLR), the Centre for Space Research (CSR) and the GFZ. The science data from GRACE mission is used to estimate global models for the mean and time variable Earth gravity field approximately every 30 days, with the following specific objectives:

- Mapping of static and temporal variations of Earth's gravity field.
- Atmospheric Limb Sounding.
- Ionosphere Sounding.
- Temperature distribution and global atmospheric water vapour content.

For further information on GRACE mission, consult the GRACE home page on www. In addition to the two operational dedicated gravity field missions; CHAMP and GRACE, a third mission even more dedicated to gravity field determination is soon on the way from Living Planet Programme of the European Space Agency (ESA). The mission is Gravity field and steady-state Ocean Circulation Explorer (GOCE). With GOCE utilizing Satellite Gradient Gradiometry (SGG) in combination with Satellite to Satellite Tracking in the high-low mode (SST-hl), a major step forward is expected. GOCE mission will provide an accurate and detailed global model of the Earth's gravity field and geoid model, with the following specific objectives:

- To determine the gravity-field anomalies with an accuracy of 1 mGal (where 1 mGal = 10^{-5} m/s^2).
- To determine the geoid model with an accuracy of 1-2 cm.
- To achieve the above at a spatial resolution better than 100 km.

(http://www.esa.int/esaLP/LPgoce.html; 19.01.2008)

The gravity missions are providing broad features of the global external gravity field in the form of Global Gravitational Model (GGM). A GGM is usually a set of spherical harmonics (SH) coefficients of the Earth's gravity potential of external type i.e. external to Mean Earth Sphere (MES) as a bounding surface. The MES is not necessarily constant for different GGMs. Thus a GGM is introduced by header information which usually consists of the model name (with information about whether it is a pure satellite or composite GGM), product of the mass of the Earth and Newton's gravitational constant GM. Also radius of the MES used, maximum SH-degree and tide system used. Then the GGM is given in columns, often 8, the first, a key column and the last a remark column are redundant information. The six important columns constitute: degree n and order m of the GGM, its two potential coefficients C_{nm} and S_{nm} and their respective standard errors $\sigma_{C_{nm}}$ and $\sigma_{S_{nm}}$. For conversion of a GGM to gravity anomaly cf. Sect. 5.3.1. The GGMs are readily and freely available to the global scientific community. Gravity data from the new dedicated satellite gravity missions specifically CHAMP and GRACE, are continuously been improved and issued within short time spans at the same time reducing both the omission and commission errors, (Ågren 2004b). Sometimes the GGMs incorporate data from other satellite missions like LAGEOS, ERS, GEOSAT, all these are termed pure satellite GGM, but when in addition, a pure GGM involves terrestrial gravity data, the GGM is named invariably combined or composite. Until now there are

many GGMs pure as well as combined. GRACE GGMs pure or combined are the most recent, and they are dedicated to avoid as much as possible the deficiencies cited in the previous GGMs. This study requires a pure and a combined GGM for the determination of TZG08 geoid model. Pure GGM will be used in the KTH LSMS, and combined GGM to improve deficiencies in the terrestrial and marine gravity data for determination of the most accurate possible geoid model of Tanzania. Thus, this research intends to take full advantage of the present achievements in the satellite gravimetry. To start with, sufficient set of most recent pure and combined GRACE GGMs, alone or in combination with others will be investigated for the pair which better fits/suits the AOI. In addition, EGM96 combined GGM has proved to be suitable for many regional/local geoid model determinations in the near past, thus it will be added and if possible and time allows, EGM2008. The list of the selected GGMs is briefly introduced in the next section.

4.3.1 Global Gravitational Models Selected for Investigation of Suitable Pair

1. ITG-GRACE03S: New Satellite-only pure GGM complete to degree and order 180; released in 2006.
2. EIGEN-GL04S1: Satellite-only pure GGM, complete to degree and order 150 from GRACE and Lageos data, released May 24, 2006.
3. ITG-GRACE02S: Pure GRACE Satellite-only GGM complete to degree and order 170; released in 2006.
4. EIGEN-GL04C: Combined GGM, complete to degree and order 360 from GRACE, Lageos and surface gravity data, released in March 31, 2006.
5. EIGEN-CG03C: Combined GGM, complete to degree and order 360 from CHAMP, GRACE, altimetry and surface gravity data, released on May 12, 2005.
6. GGM02C: Combined GGM, complete to degree and order 200, released in 2004.
7. EIGEN-GRACE02S: GRACE satellite-only GGM, complete to degree and order 150 released on February 13, 2004 to the GRACE Science Team and August 9, 2004 to the public.
8. EGM96: Combined GGM jointly of NASA GSFC and NIMA (USA) complete to degree and order 360 released in 1998.

For more GGMs consult the International Centre for Global Earth Models (ICGEM) at http://icgem.gfz- potsdam.de/ICGEM/ICGEM.html.

4.3.2 Global Evaluation of GGMs

ICGEM conducted spectral evaluation of some GGMs by comparing them to the new EIGEN-GL04C, cf. Figure 4-22 and Figure 4-23. Besides spectral evaluation, ICGEM also conducted global evaluation of the mean of differences between GPS levelling and quasi-geoid heights of the GGMs, some given in Sect. 4.3.1. The RMS of each difference is given in Table 4-16. The GPS levelling data is from USA, Canada, Europe and Australia. From the objectives of the dedicated satellite gravity missions, and the exiasting Global Gravitational Models (GGMs), it is the intention of this research to search for the most suitable GGMs for the research AOI, cf. Sect. 4.4.3, preferably involving GRACE gravity data. The so obtained models will be the source of gravity long-wavelength component, (required in the LSMS with AC and surface gravity

smoothing) and composite model for the fill-in of data voids. Often global evaluation of GGMs provides only indication and not conclusion on the suitable GGM for local or regional geoid model determination, (Kiamehr 2006a). Figure 4-22 is an extract from the ICGEM global spectral evaluation of GGMs. Our decision on the suitable maximum degree to use reliably the pure GGMs selected in the preceding section, will mainly be based on the global ICGEM spectral evaluation performance graphs in Figure 4-22, and also on the recommendation from the respective GGM documentations or similar research about the GGM. Our decision on the selection of GGMs in Sect. 4.3.1 above, which will take part in the nomination of suitable GGM pair for TZG08 geoid model determination, has very much been influenced by the RMS results of ICGEM GPS/Leveling evaluation in Table 4-16.

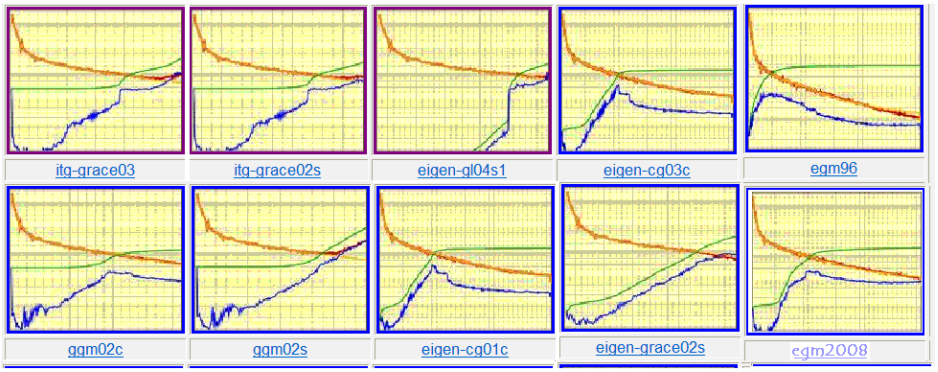

Figure 4-22: Spectral evaluation of pure and combined Global Gravitational Models

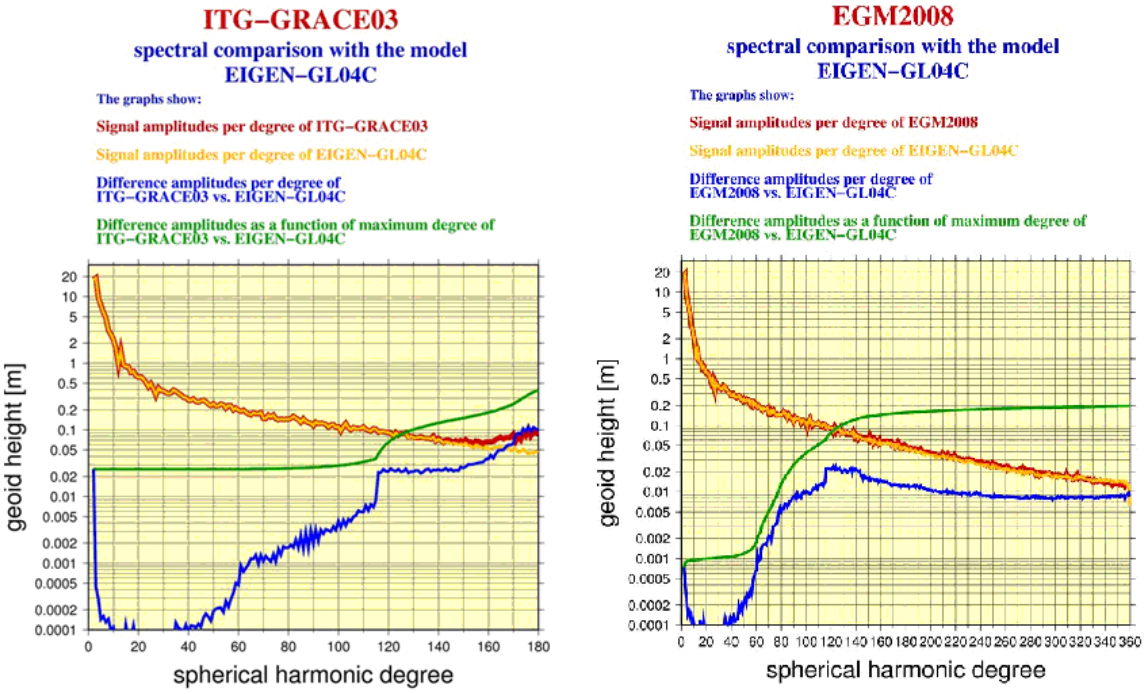

Figure 4-23: Spectral evaluation of pure and combined Global Gravitational Models, two typical views of any of the Figure 4-22 graphs.

Table 4-16: RMS of differences of mean [GPS/Level MINUS GGM geoid height (m)],
C = Combined, S = Pure Satellite model
(http://icgem.gfz-potsdam.de/ICGEM/evaluation/evaluation.html, 10.05.08)

MODEL/AREA No. of Points	Nmax	USA 6169	CANADA 1930	EUROPE 186	AUSTRALIA 201
ITG-GRACE03	180	0.633 m	0.557 m	0.687 m	0.604 m
EIGEN-GL04S1	150	0.630 m	0.576 m	0.689 m	0.465 m
ITG-GRACE02S	**170**	**0.623 m**	**0.511 m**	**0.629 m**	**0.490 m**
GGM02S	160	0.977 m	1.116 m	1.274 m	1.357 m
GGM01S	120	0.748 m	0.719 m	0.895 m	0.636 m
EIGEN-GRACE01S	140	0.765 m	0.705 m	0.934 m	0.554 m
EIGEN-GRACE02S	150	0.739 m	0.643 m	0.840 m	0.539 m
EIGEN-GL04C	**360**	**0.339 m**	**0.253 m**	**0.335 m**	**0.245 m**
EIGEN-CG03C	360	0.346 m	0.306 m	0.392 m	0.260 m
GGM02C	200	0.473 m	0.378 m	0.487 m	0.377 m
EIGEN-CG01C	360	0.351 m	0.271 m	0.408 m	0.264 m
GGM01C	200	0.477 m	0.381 m	0.525 m	0.398 m
EGM96	360	0.402 m	0.366 m	0.487 m	0.314 m

***** The most suitable pure and combined GGM with respect to global evaluation

Further evaluation of Mayer et al. (2006) on the ITG-GRACE02S GGM (Note ITG-GRACE02S and EIGEN-GRACE02S are different GGMs) concluded, that the model was more accurate than any other satellite only model of the time. Decision on the more appropriate degree of a pure satellite GGM is arrived at when the three graphs for a given GGM in Figure 4-23 are much closer i.e. minimum departure between signal amplitude per degree of GGM, difference of amplitudes of GGM with the reference EIGEN-GL04C, and difference of amplitudes at maximum degrees of GGM and EIGEN-GL04C. Based on this and the RMS figures of Table 4-16, also recommendations of Mayer et al. (2006), pure models are globally ranked as follows:

Satellite only Models (Pure):

- ITG-GRACE02S retains true spectral power at degree and order 110.
- EIGEN GL04S1 retains true spectral power at degree and order 110.
- ITG GRACE 03S retains true spectral power at degree and order 120.

Combined Models

Only the RMS of the differences in Table 4-16 have been used to nominate the three best combined GGM. By involving high frequencies of terrestrial and sometimes altimetry gravity, the combined GGM has the ability to retain its power to its maximum degree. Hence the selected combined GGMs in global terms are:

- EIGEN GL04C retains its spectral power at maximum degree & order 360.
- EIGEN CG03C retains its spectral power at maximum degree & order 360.
- EGM96 retains its spectral power at maximum degree & order 360.

Further Clarifications on the Model Names:

- EIGEN (**E**uropean **I**mproved **G**ravity **E**arth models using **N**ew techniques) implies the model is from the International Centre for Global Earth Models (ICGEM), whereas
- ITG means the model is from the **I**nstitute for **T**heoretical **G**eodesy, University of Bonn Germany.

- G stands for GRACE, C for CHAMP, L for Lageos and S and C at the end for Satellite-only and Combined/Composite model, when the last C or S misses, then further clarification should be sought.

4.3.3 Regional Evaluation of GGMs

Kiamehr (2006a) has cautioned and verified that global evaluation of GGMs should not be used directly to decide on the most suitable GGMs for a certain regional/local geoid model determination, but rather as performance indicator. The reason is that such performance evaluations sometimes tend to be too optimistic and global statistics are not necessarily true representatives of a region. Until now regional GGM evaluation is achieved through the following procedure(s):

a) Existing geoid model and GGM geoid heights are compared in absolute and relative sense at designated corresponding locations; often one is taken to be the reference. Analogous to this is the spectral analysis above, where EIGEN-GL04C is the reference.
b) GGM geoid heights are evaluated against GPS ellipsoidal height minus spirit levelling orthometric height at specified locations, generally referred to as GPS/Levelling.

Comments and recommendations on the appropriate approach to obtaining suitable GGMs, pure as well as combined for the determination of geoid model of Tanzania.

- Use of evaluation approach a) above is discouraged, first, of the three geoid models which cover Tanzania i.e. the EGM96, the AGP2006 and Olliver 2007, EGM96 is among the models which are to be tested, so we can not use it to test itself or the others since that will be very subjective. Second, the AGP2006 used CG03C up to degree and order 120, but it arrived at this decision after the tests which were conducted in South Africa and Algeria only, and this is more or less the same as using global model evaluation explained earlier. Third, the Olliver_2007 geoid model received most of the data from the AGP. Moreover, use of trigonometric and Doppler satellite heights to validate geoid model seems to be inappropriate, to geoid model validation given their accuracy and methodology.
- Use of evaluation approach b) is acceptable, but the available data for this purpose is found only on the eastern part of the country. Though GPS observations on Fundamental Benchmarks (FBM) and Intermediate Benchmarks (IBM) were carried out by this research in 2007 and 2008, it suffered a number of drawbacks, some of which are: i) The proposed and implemented Tanzania levelling network is almost as depicted in Figure 4-24. That is, it has not changed significantly for the better since early 1970s. Besides, maintenance and storage of the network pertinent data is poor. Consequently, enormous time, effort and money were spent to retrieve some data (location sketches and reduced orthometric heights) of FBMs and IBMs and afterwards relocation of the same in the field, which depended solely on the sketches drawn drawn over 40 years back. Often it was not easy to get the data, and many times it did not pay back. ii) Quite a number of FBMs were never used since their erection 40 years back. As a result, many have been destroyed by human activities, covered up by silt deposition over time or

moved by erosion. iii) Sometimes the marker would be found in situ, but not its data and vice versa, which rendered all the other data pertaining to it useless for this research.

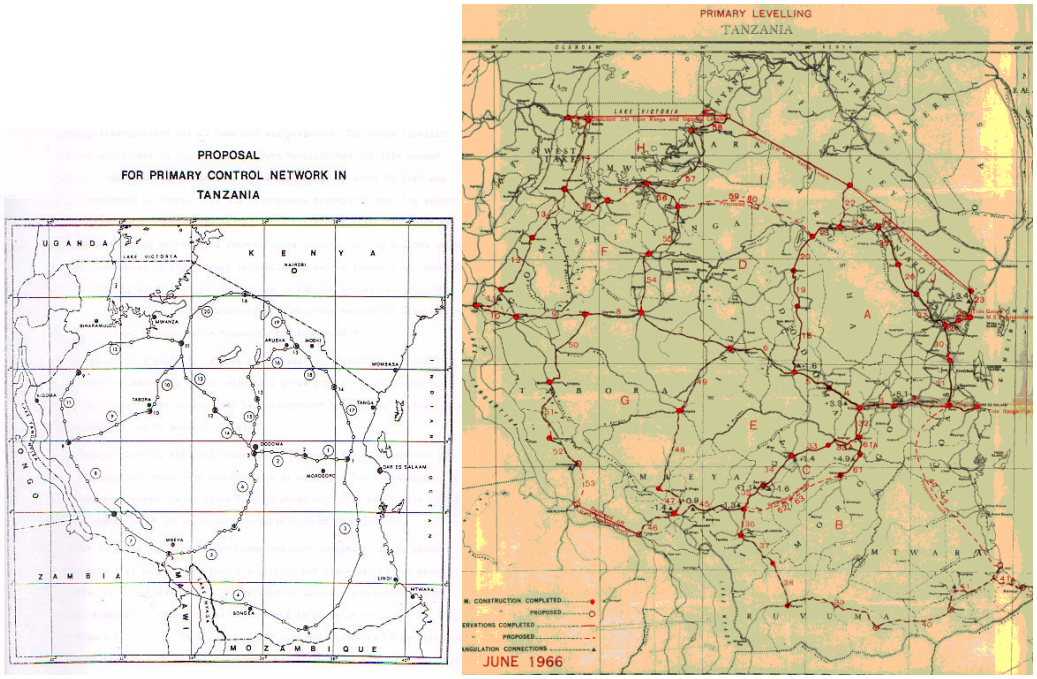

Figure 4-24: Tanzania primary levelling network

Figure 4-25 portrays locations of FBM/IBM on which GPS heighting was carried out by this research from February to March, 2007 in Tanzania. Absence of GPS observations on FBM/IBM in the western part of the country is mainly due to inability to retrieve the necessary records of the benchmarks from the Ministry of Lands and its departments, specifically for the western area and to a few locations, heavy rains which commenced prior to finishing the GPS heighting on FBM/IBM fieldwork in 2007 and made mobility almost impossible.

In this year (2008), we managed to obtain some more of the missing data for FBM/IBM (12 in number), mostly for the western part of the country, from the Ministry of Lands, Human Settlement and Development (MLHSD). In August-September, 2008 GPS observation on the FBM/IBM was conducted. Due to absence of reliable ITRF reference stations in the region, we decided to tie the GPS observations to the International GNSS Stations (IGS) close to the AOI. Therefore, GPS observations on FBM/IBM lasted between (2-3) consecutive days per station. The IGS stations used are Malindi, Seychelles, Ascension Islands, Haartebeesthoek, Sutherlands and UCLAS. The intention was to use Bernesse software, which is capable of processing long baselines. The expert in this software at the Division of Geodesy – KTH had to leave for long time assignment in Ethiopia. Given the time constraint, the data has not been processed and therefore not helpful to this study at the moment.

It is thus felt that use of the available GPS/orthometric height data as seen in Figure 4-25 to evaluate GGMs, will not lead to impartial results. It was at this juncture that use of absolute reference gravity to validate the GGMs was conceived. There are 57 absolute gravity reference stations in Tanzania, well placed as depicted in Figure 4-26, but one in Moshi is missing height record. Advantage will be made of the high resolution three arc second (3s, ~90m) Shuttle Radar Topography Mission (SRTM) Digital Elevation Model (DEM) to smooth the terrestrial data, also pure satellite GGM as explained further in Section 4.4.

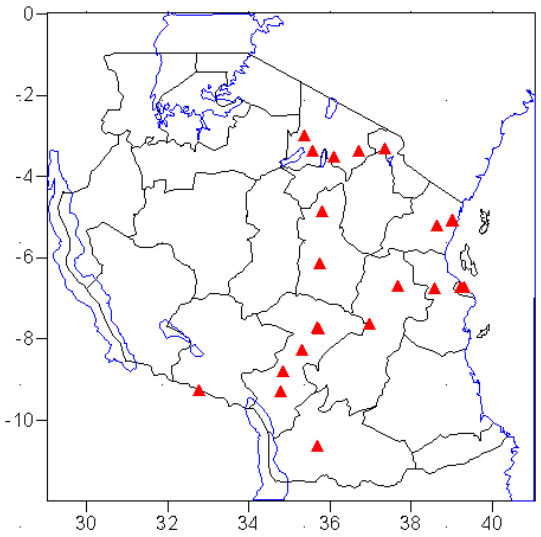

Figure 4-25: GPS/Levelling stations in Tanzania

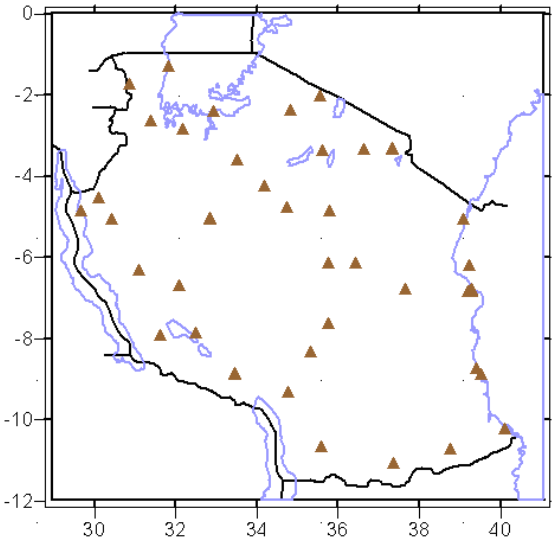

Figure 4-26: Absolute reference gravity sites in Tanzania

First surface gravity anomaly referred to GRS80 is computed from the absolute gravity as elaborated in Section 4.1.3. Then it is relieved of the short wave component due to surface topographic masses, which is computed at the locations of absolute gravity from the dense SRTM DEM as described in Sect. 5.3.2. The remaining part of the absolute gravity anomaly is much smoother and closer to long-wavelength GGM gravity anomalies though not parse. With regards to this approach, suitable GGM is the one which fits better or deviates less from the reduced surface gravity anomaly (absolute). First the gravity anomalies are computed for all the participating GGMs at the locations of the absolute gravity. Further, to the combined GGMs, but not the pure GGMs, we subtract the same short wave length component due to topographic masses subtracted from the reference absolute gravity (RTE), so that we get reduced combined GGM (GGM^C-RTE) gravity anomaly. The pure and the reduced combined GGMs are plotted in one graph. First with both the un-reduced and reduced reference absolute gravity anomaly, cf. Figure 4-27a, and then without the un-reduced reference absolute gravity anomaly, cf. Figure 4-27b. For better and clearer vision, alternatively each model is plotted with the reduced absolute surface gravity anomaly, but only a few examples are displayed, two for each of the combined and the pure satellite gravity anomalies in Figure 4-28 (i –iv).

Although the disparity of fit amongst the GGMs is very evident, still it is not easy to come to a reasonable conclusion on the suitable GGM based on the visual inspection of the fitness of fit to the reduced absolute gravity. A resort is taken to use the reduced absolute gravity anomaly as reference by deducting it from each of the GGMs gravity anomaly at the corresponding station; this portrays a better comparison as witnessed in Figure 4-29. Plotted in Figure 4-29 are the differences of gravity anomalies at the 56 absolute gravity stations in mGal. It can be observed, that at average, the GGM with smallest deviations is CG03C and the one with highest mean deviations is the GL04S at its maximum degree 150.

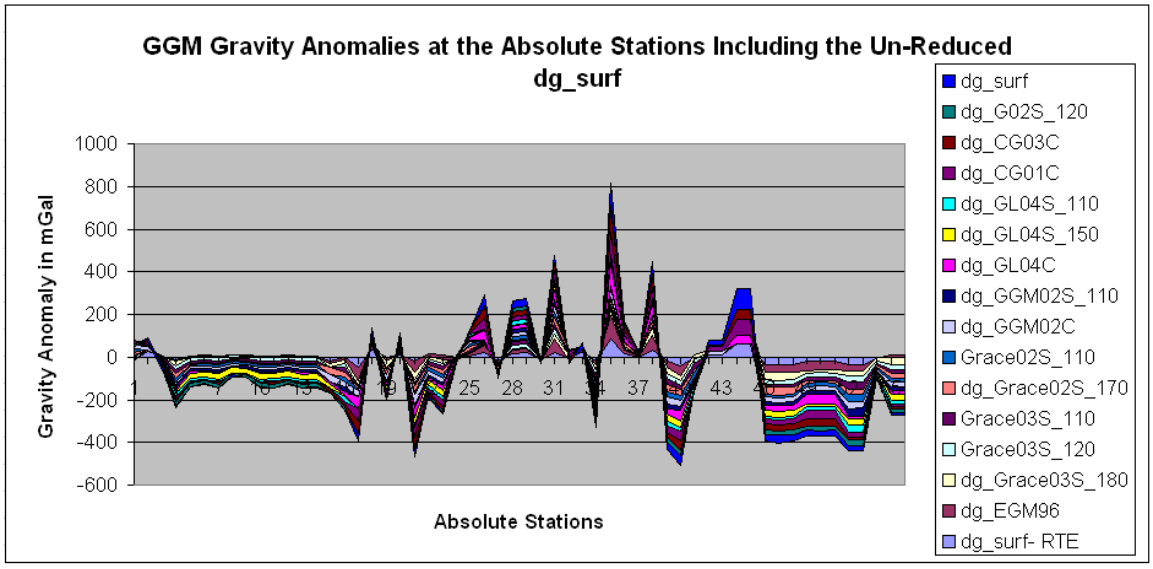

(a) Unreduced i.e. surface absolute gravity anomaly with all frequencies, plotted with the reduced and the rest of the GGMs

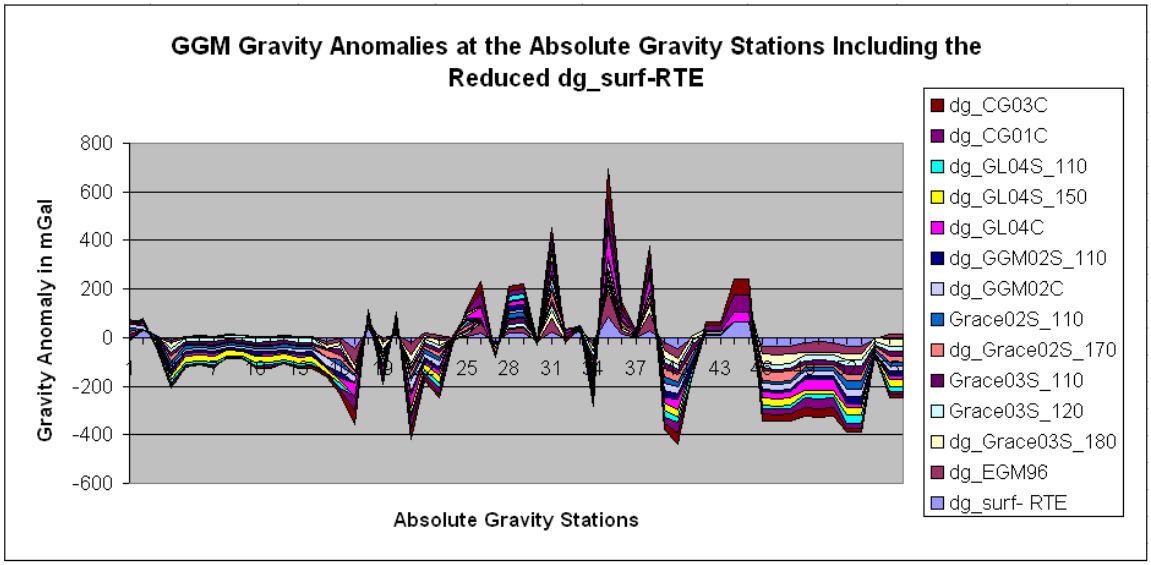

(b) Reduced i.e. surface absolute gravity anomaly less RTE (dg_surf - RTE), plotted with the rest of the GGMs gravity anomalies; for the GGM^C, RTE has been removed.

Figure 4-27: Fitting of GGMs and absolute gravity anomalies

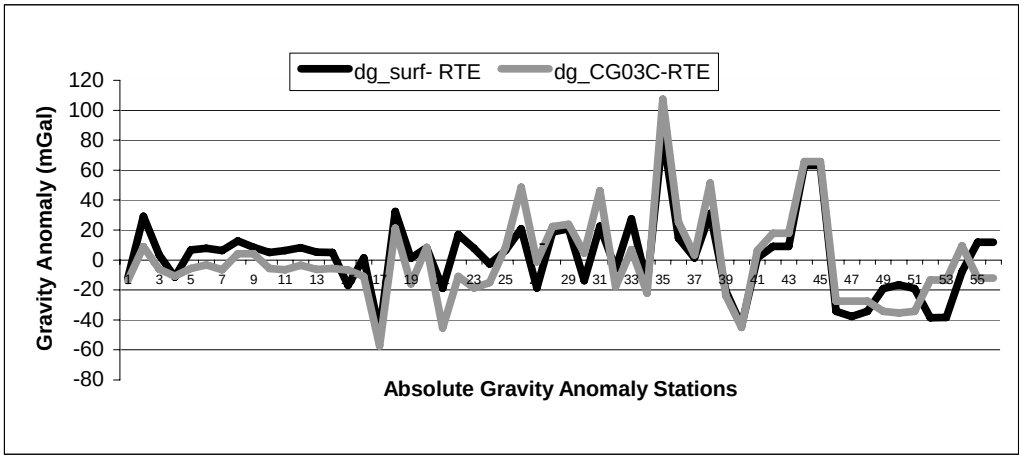

(i)

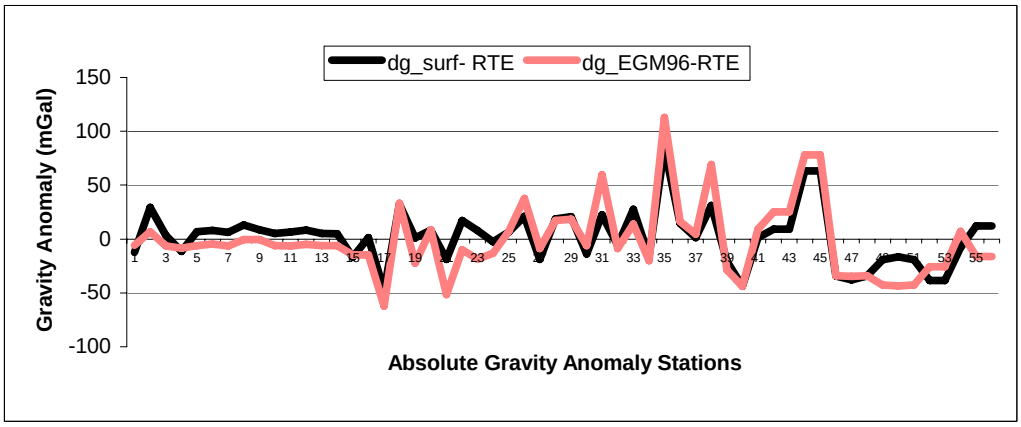

(ii)

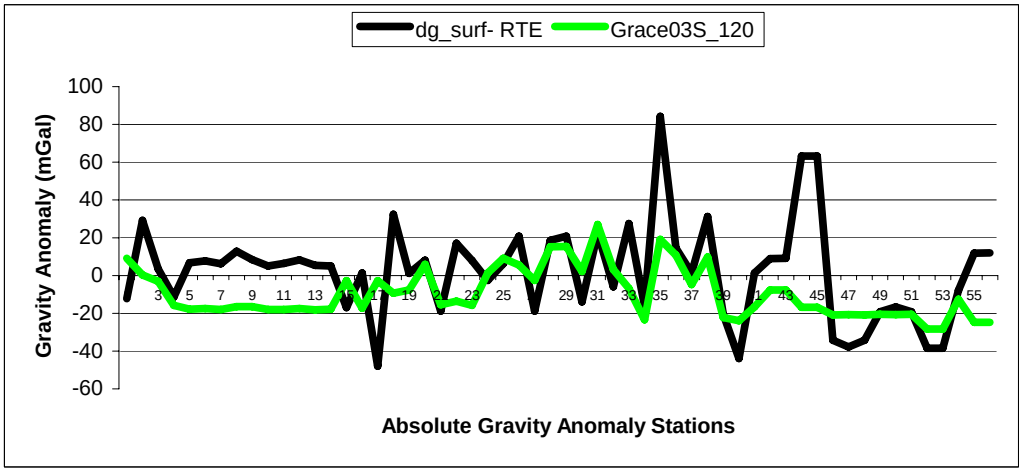

(iii)

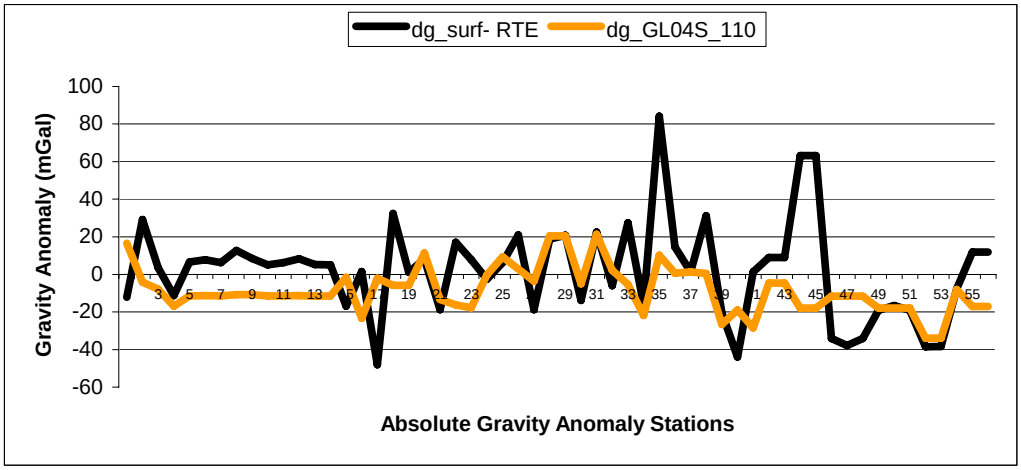

(iv)

Figure 4-28 (i – iv): Alternatively, each of pure dg_GGM and combined dg_GGM-RTE is plotted with the dg_surf-RTE. Although the difference of fit amongst the GGMs is very evident, still it is not easy to come to a reasonable conclusion on the suitable GGM based on the visual inspection of the fitness of fit between the graphs.

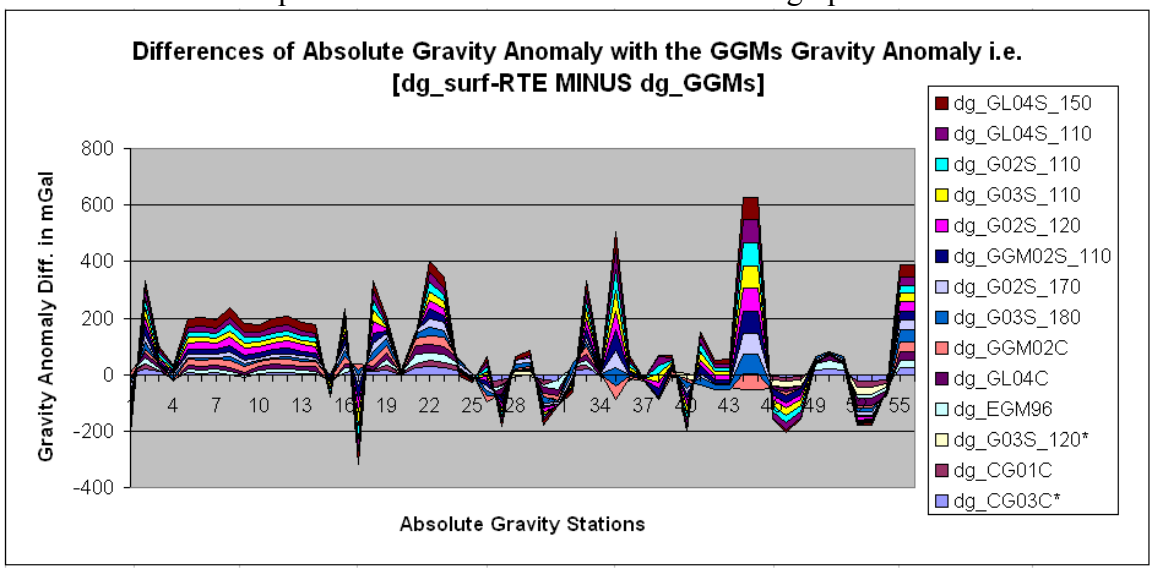

Figure 4-29: Deviations: (Absolute gravity-RTE MINUS GGMs) gravity anomalies plotted together. For combined GGMs, RTE has been removed to make it more compatible for comparison.

4.3.4 GGM Selection

To counter check the ranking of GGMs in Figure 4-29 based on GGMs deviations from the reduced absolute gravity anomaly, a decision is taken to compute statistics of the spread of the differences of the GGMs. Summary of statistics of the differences of all the GGMs is given in Table 4-17. By sorting the standard errors and RMS rows in Table 4-17, we can deduce the followings:

a) For the pure GGMs, G03S_120 i.e. ITG-GRACE03S_120 has the smalleststandard error of all, i.e. 13.19 mGal. Its RMS is the 3rd of all the participating GGMs, and the

1st of the pure satellite GGMs, i.e. 16.19 mGal, eventhough the pure satellite GGM maximum degrees are also involved. Therefore, G03S_120 i.e. ITG-GRACE03S_120 fits the absolute gravity better than any other participating pure GGM in the AOI.

b) For the combined GGMs, CG03C_360 or EIGEN-CG03C has the smallest RMS of all i.e. 14.89 mGal and the 2nd smalleststandard error i.e. 14.82 mGal, but the first when compared to the other combined GGMs. Thus with regards to combined models, CG03C_360 or EIGEN-CG03C has better fit to the observed absolute reference gravity in the research area (Tanzania) than any other participating combined GGM.

Looking back on the global evaluation, we observe that for the pure GGMs, ITG-GRACE03S_120 was ranked the 3rd and for the combined GGMs, EIGEN-CG03C was the 2nd. So if we had gone by the global evaluation, none of the two GGMs would have been chosen for the determination of TZG08 geoid model. Therefore based on the results in Table 4-17, Figure 4-29 and the above observations, a verdict on the selection of the best pure and combined GGMs can be reached.

Table 4-17: Statistics of differences of surface gravity anomaly of absolute gravity minus GGMs after removal of RTE from observed and combined GGMs in mGal.

GGM	CG03C	CG01C	G03S	EGM96	GL04C	GGM02C	G03S	G02S	GGM02S	G02S	G03S	G02S	GL04S	GL04S
Eval_Deg	_360*	_360	_120*	_360	_360	_200	_180	_170	_110	_120	_110	_110	_110	_150
No. Stns	56	56	56	56	56	56	56	56	56	56	56	56	56	56
Rank SErr	2	3	1	4	5	6	7	8	11	9	12	13	14	10
Rank RMS	1	2	3	4	5	6	7	8	9	10	11	12	13	14
Min	-27.86	-30.64	-28.36	-37.84	-30.60	-27.05	-29.91	-33.83	-46.66	-45.53	-46.07	-46.14	-45.94	-47.98
Max	28.11	34.77	26.94	32.78	30.06	57.19	66.67	73.08	80.75	79.94	80.75	80.99	81.05	78.65
Mean	2.48	3.00	-9.56	3.48	4.25	9.68	9.25	9.28	10.06	11.64	10.15	10.18	10.35	13.90
SErr	**14.82**	15.66	**13.19**	16.19	16.83	18.40	20.59	20.62	24.09	23.55	24.28	24.36	24.41	23.76
RMS	**14.89**	15.81	**16.19**	16.41	17.22	20.64	22.41	22.44	25.91	26.08	26.11	26.20	26.32	27.35

* means pure/combined GGM with the best fit to the absolute gravity.

Satellite Only Model (Pure)

The newest GRACE satellite only model **ITG-GRACE03S** has clearly come out the best followed by far by its predecessor, ITG-GRACE02S, both evaluated to degree and order 120 as deduced from the spectral evaluation in Figure 4-23.

Combined Model

Based on the absolute gravity evaluation summarized in Table 4-17, CG03C has the best statistical fit. On the other hand, four combined GGMs namely CG03C, CG01C, EGM96 and GL04C are very close to one another, but CG03C is an updated version of CG01C, thus we remain with three combined models. Closer inspection of Table 4-17, shows that with regards to fit, the differences among the remaining three GGMs, i.e. CG03C, EGM96 and GL04C are small. Contrary to the expectation, the newest GRACE combined model GL04C, which is actually an improvement of CG03C in a way as

explained in Mayer-Guerr (2006), and the one used by the ICGEM as reference for spectral evaluation of others in Figure 4-23, has not proved exclusively to be the best in this region. It will be of interest to check on the numerical performance of the three GGMs in the region, i.e. CG03C, GL04C and EGM96.

Therefore the GGMs which have proved to be the most suitable in this research AOI are:

- ✓ **ITG-GRACE03S** satellite only GGM up to degree and order 120
- ✓ **EIGEN-CG03C** combined GGM up to degree and order 360

The following is a brief description of the two qualified GGMs

ITG-GRACE03S is a GRACE mission pure satellite only GGM, computed up to degree and order 180 from data collected from September 2002 to April 2007, i.e. 57 months/4.75 years. The model is derived from accumulated normal equations without applying any a priori information or regularization, using short arc integration method as described in Mayer-Guerr (2006) also in Mayer-Guerr et al. (2007). The model uses ITG-Grace02S static gravity field and zero permanent tide.

EIGEN-CG03C is a combination of data from GRACE first 376 days with a few omissions, CHAMP 860 days plus altimetry and gravimetric surface data. This model is an upgrade of EIGEN-CG01C (Reigber et al. 2004), which was based on the same CHAMP and surface data. EIGEN-CG03C is complete to degree/order 360 with wavelengths of 110 km resolution in geoid model and gravity anomaly fields. A special band-limited combination technique was applied to preserve the high accuracy from the satellite data in the lower frequency band of the GGM and to ensure a smooth transition to the higher frequencies from altimetry and surface data. The overall accuracy of the full model is estimated to be 30 cm and 8 mGal in geoid model and anomaly respectively; refer to http://www.gfz-potsdam.de/pb1/op/grace/results/grav/g004_eigen-cg03c.html (February, 2008) and (Förste et al. 2005).

4.4 Height Data

Height information is indispensable ingredient in geoid model computation. In the preceding sections height data necessity revealed in different scenarios, for example, orthometric height for gravity stations and reduction to geoid/MSL, ellipsoidal/normal height for upward continuation of normal gravity from reference ellipsoid and computation of surface gravity anomaly, digital elevation models (DEM) for computation of residual terrain effect (RTE) which is used in smoothing and densification of gravity also in gravity anomaly gradient. Our intention is to use SRTM3 i.e. 3 arc second SRTM DEM in this research. This is from the fact, that qualities of the model exceeds any other in existence global wise, as cited in many scientific publications like Ellmann (2004), Ågren (2004b), Kiamehr (2006a), Parker et al. (2007) and also due to non availability of any other DEM covering fully the AOI with better resolution and accuracy.

4.4.1 SRTM, Digital Elevation Model (DEM)

SRTM is an international project, a joint endeavour of the National Aeronautics and Space Administration (NASA), the National Geospatial-Intelligence Agency (NGA) of USA government, and the German and Italian Space Agencies. On February 11, 2000, the Shuttle Radar Topography Mission (SRTM) payload onboard Space Shuttle Endeavour was launched into space. To acquire topographic (elevation) data, the SRTM payload was outfitted with two radar antennas. One located in the shuttle's payload bay, and the other on the end of a 60-metre (200-feet) mast that extended from the payload once the Shuttle was in space. With its radars sweeping most of the Earth's surfaces, during its ten days of operation, the Shuttle Radar Topography Mission collected topographic data over nearly 80 percent of Earth's land surfaces, creating the first-ever most complete near-global high-resolution database of the Earth's topography, further reference is found at: http://www2.jpl.nasa.gov/srtm/index.html. SRTM data is available at the USA Geological Survey's (USGS) EROS Data Centre for download via File Transfer Protocol (ftp); thus ftp to: ftp://e0srp01u.ecs.nasa.gov. Data are also available through the USGS seamless server at http://seamless.usgs.gov/. Several new web sites have posted SRTM data in different formats than available at the USGS ftp site or the Seamless Server and some have improved it for deficiencies like data voids and spikes, for example one may want to check the Global Land Cover Facility at (http://glcf.umiacs.umd.edu/data/srtm/index.shtml) or the CGIAR Consortium for Spatial Information (http://srtm.csi.cgiar.org/) and Jonathan de Ferranti site http://www.viwfind erpanoramas.org/dem3.html#images. Although the USGS SRTM data is available in two resolutions of 1″ and 3″, the 1-arc second data is available only for the USA government and its allies. In this research, the 3″-SRTM (SRTM3) will be downloaded from the CGIAR site given above; it is in $5^{\circ} \times 5^{\circ}$ tiles.

4.4.2 SRTM3 DEM, Global Evaluation and Analysis

The SRTM produced the most complete, high resolution global DEM. The project used dual radar antennas to acquire interferometeric radar data, processed to 1 arc-sec resolution digital topographic data. One of the primary goals of the mission was to produce a data set that was globally consistent with quantified errors. To achieve this goal, an extensive global ground campaign was conducted by NGA and NASA to collect ground truth data that would allow for the global validation of SRTM data set. The result of global continents validation at 90 % confidence level is given in Table 4-18, (Hoffmann and Walter 2006).

Table 4-18: NASA/NGA SRTM ground truth validation using mainly photogrammetric and or cartographic methods in metre

Continent	Absolute Position Error	Absolute Height Error	Relative Height Error
Africa	11.9	5.6	9.8
Australia	7.2	6	4.7
Eurasia	8.8	6.2	8.7
Islands	9	8	6.2
North America	12.6	9	7
South America	9	6.2	5.5

In relation with the archived SRTM data, several studies have been conducted by the scientific community. Several types of data have been used as basis for comparison, ranging from ground-truth to digital elevation models (DEMs) derived from different space-borne sources. The ground truth methods mainly use photogrammetric and cartographic methods e.g. (Ludwiga and Schneiderb 2006) also kinematic GPS. The most extensive global ground-truth effort was made in collecting a globally distributed set of ground check points using kinematic GPS transects. A typical transect spanned a substantial part of a continent, thus allowing for the characterization of errors at all lengths scales. The number of kinematic GPS check points ranged from 64,000 to 400,000. Table 4-19 shows the error in unit of metre.

Table 4-19: SRTM global validation using kinematic GPS differences, unit m.

Continent	Abs. Pos. RMS	Rel. Pos. RMS	Rel. Height RMS	Long_λ Height
Africa	7.2	3.4	5.9	1.9
Australia	4.4	3.6	2.8	3.6
Eurasia	5.3	3.8	5.3	1.6
Islands	5.5	4.9	3.8	2.2
N-America	7.6	5.5	4.2	2.4
S-America	5.5	3.8	3.3	3.0

Abs. is Absolute, Pos. is Position, Rel. is Relative and Long_λ is Long-wavelength RMS

Other approaches with global or near global coverage include use of completely independent height measurements derived from satellite altimeter echoes, primarily gathered by ERS-1. These heights are obtained using a rule-based expert system which identifies each echo as 1 of 11 different characteristic shapes, and selects the optimal re-tracking algorithm to obtain the best range to surface. Accprding to Berry et al. (2006), the result of this comparison, which includes over 54 million altimeter derived heights, show fairly good agreement with the SRTM data, with global statistics for mean difference of 3 m and a standard error of 16 m. Quantitative validation results are given for each continent and are summarized in Table 4-20, (Berry et al. 2006).

Table 4-20: ERS-1 echo validation of SRTM using land expert system

	Mean Difference (m)	SErr. of Difference (m)
Africa	1.86	15.62
Australia	1.09	11.49
Eurasia	2.54	16.09
North America	3.15	15.18
South America	12.22	18.51
Global	3.60	16.16

Accuracy of SRTM data depends much on the ground/cloud cover and morphology, this is revealed in the Geoscience Laser Altimeter System (GLAS) on the Ice, Cloud, and land Elevation Satellite (ICESat) which provides a globally-distributed data set, well suited for evaluating the vertical accuracy of SRTM DEM, with emphasis on different obstruction to radar signal. The horizontal error (2.4 ± 7.3 m) and vertical error (0.04 ± 0.13 m) per degree of incidence angle for the ICESat data used are small compared to those for

SRTM. Using GLAS echo waveforms they document differences between the SRTM C-band phase centre and the highest, centroid, and lowest elevations within ICESat laser footprints in the western United States. In areas of low relief and sparse tree cover, the mean and standard error of elevation differences between the ICESat centroid and SRTM are -0.60 ± 3.46 m. The differences are -5.61 ± 15.68 m in high relief, sparse tree cover areas, and -3.53 ± 8.04 m in flat areas with dense tree cover. The largest differences occur in rugged, densely-vegetated regions, (Claudia and David 2005).

Quantities like MSL reduced gravity anomalies, residual terrain effect (RTE) also geoid model and quasigeoid heights which are a function of a DEM have errors of the DEM propagated to them in the process of derivation. Moreover, in the KTH method of geoid model by LSMS and additive corrections, DEM errors are carried forward to final geoid model during topographic and downward continuation (dwc) corrections computation as emphasized in (Kiamehr and Sjöberg 2005). Usually the small scale global validation do not go down to details i.e. access local/ regional areas thoroughly, thus for minimum effects of DEM errors on local and regional geoid model e.g. TZG08, DEMs which cover thoroughly the AOI ought to be validated and cleaned of any gross and systematic errors in advance of subsequent processes. DEMs which cover AOI include GLOBE and SRTM. Literature review has shown that Global Land One-kilometre Base Elevation (GLOBE) is by far inferior to SRTM in this region, (Merry 2003a) logically this should be so because GLOBE is a 30 arc second whereas SRTM3 is a 3 arc second DEM. Kiamehr and Sjöberg (2005) portrays the risk of dependence on global evaluation exclusively; the article demonstrates that in Iran using GPS/levelling network data absolute vertical accuracy of SRTM is 6.5 m, which is comparable to the photogrammetric high-resolution DEM of the area, based on the same, they also found very large differences between GLOBE and SRTM models on the range of -750 m to 550 m. Summarizing the foregoing, we come to a conclusion that suitable DEM to be used in this research ought to be SRTM3 i.e. SRTM 3 arc seconds ~ 90m resolution.

4.4.3 USGS SRTM3, Area of Interest and Grid Densities

Area Of Interest (AOI)

AOI is slightly different in two incidences. Note that latitude is given by φ and longitude by λ

- For DEM, AOI is the area bounded by $-15^\circ \le \varphi \le 4^\circ \quad and \quad 26^\circ \le \lambda \le 46^\circ$
- For gravity, AOI extends between $-15^\circ \le \varphi \le 4^\circ \quad and \quad 26^\circ \le \lambda \le 44^\circ$ and

$-12^\circ \le \varphi \le 1^\circ \quad and \quad 29^\circ \le \lambda \le 41^\circ$ are the extents of Tanzania Geoid model 2008 (TZG08) to be computed.

Grid Densities

SRTM3 management problems such as storage, merging and computer processing time, forced breakdown of SRTM3 to bigger grids, consequently four resolutions of SRTM DEM are in use in this research, namely

i) 15 arc second DEM abbreviated to SRTM15s
ii) 30 arc second DEM abbreviated to SRTM30s

iii) 3 arc minute DEM abbreviated to SRTM3m
iv) 6 arc minute DEM abbreviated to SRTM6m

SRTM15s is considered as the dense DEM/grid and SRTM30s and SRTM3m as coarse DEM/grid. SRTM6m is further smoothed to a continuous mean elevation surface of the AOI and referred to as SRTMref meaning reference SRTM surface of the AOI; this finds use in the computation of RTE.

4.4.4 CGIAR SRTM3

The first release of Shuttle Radar Topography Mission (SRTM) data was provided in 1-degree digital elevation model (DEM) tiles from the USGS ftp server (ftp://e0srp01u.ecs.nasa.gov/srtm/) in 2003. Later on "finished" SRTM DEM was released, the product was supposed to have no voids and spikes and clearly marked water body surface boundaries. Unfortunately this was not the case with the original SRTM3 data purchased and downloaded from (ftp://e0srp01u.ecs.nasa.gov/srtm/version2/SRTM3/). The data was stored followed by processes of decoding, conversion to ASCII format, merging 3″ SRTM $1^{\circ} \times 1^{\circ}$ DEM tiles to cover the AOI and then re-grid to densities/resolutions of interest as explained above. When the data surfaces were plotted, the DEM was found to have too many voids and spikes. In the cause of seeking for solution to the cited USGS SRTM3 DEM problems, we came across the web site of the Consultative Group for International Agricultural Research (CGIAR) of the Consortium for Spatial Information (CGIAR-CSI), which offers post-processed USGS SRTM3 DEM data for the globe. The original SRTM data is subjected to a number of processing steps to provide seamless and complete elevation surfaces for the globe without regions of no-data. Voids and spikes were more frequent over water bodies (lakes and rivers), and in areas with insufficient textural detail in the original radar images. A total of 3,436,585 voids accounting for 796,217 km2 were cited. Existence of no-data regions causes significant problems in using SRTM DEMs especially when continuous surfaces are inevitable. The CGIAR-CSI applies a hole-filling algorithm to provide continuous void free surface. The resultant seamless dataset is then clipped along coastlines using the Shorelines and Water Bodies Database (SWBD). This dataset is very detailed along shorelines, and contains all small islands. The data is given in a geographic latitude and longitude with the WGS84 and EGM96 geoid model as horizontal and vertical datum respectively. For further details consult the web page of CGIAR-CSI at http://srtm.csi.cgiar.org/SRTMdataProcessingMethodology.asp, October 2007. In Section 4.4.1 it was pointed out that the Jonathan de Ferranti site at http://www.viewfinderpanoramas.org/dem3.html#images also archives improved USGS SRTM3 DEM. His method is void filling with photogrammetric and/or cartographic data; this way the quality of the filled voids is likely to be better than the CGIAR-CSI interpolation scheme, but only very few data void tiles have been filled. For the AOI, only six (6) $1^{\circ} x 1^{\circ}$ tiles are available hence the data was of no much use. The DEM adopted for the research is thus from the CGIAR-CSI database at http://srtm.csi.cgiar.org. Further details of use of CGIAR-CSI DEM in this research are found in Section 5.1

4.5 Other Height Data

4.5.1 GPS and Spirit levelling

GPS ellipsoidal height and orthometric elevation on benchmarks i.e. heights referred to MSL/Geoid find important use in geoid model performance evaluation, (Kiamehr 2006a, Fotopoulos 2003). One of the most preferred and independent assessment of gravimetric geoid model is by use of geoid height obtained from co-located GPS and spirit levelling heights, in this research this kind of data has been observed and will be used to validate TZG08; refer to Sect. 4.3.3 on regional evaluation of GGM bullet 2 and Figure 4-25 for clarification on the data and visualization of relative locations and Sect. 7.2 for the actual evaluation.

4.5.2 Trigonometric Heights

Though photogrammetric heighting is supposed to be referenced to sprit levelling, quite a number of heights from trig points sneak into the process. This happens since most of trig points are located on hill tops and small mountains with trigonometric heights, the heights are easily and clearly identifiable during photo control process. If trig height network has been referred to MSL/geoid and say reciprocal trig heighting was exercised, then its shift from spirit levelling should be small, that being the case, then

- Products from photogrammetric mapping like relief maps and contours could be used to assess quality of a product like SRTM DEM
- Benchmark and trig heights could be used to cross validate other heights e.g. SRTM DEM, but also to model a corrective surface. For Tanzania, this needs more investigation into the intrinsic and compatibility of the two networks i.e. primary levelling and trigonometric heighting before deploying them into such a development.

4.5.3 Normal Heights

As given in section 4.1.3, computation of surface gravity anomalies for the KTH method of LSMS with AC or in general using modern methods of geoid model computation, requires height on the telluroid i.e. normal height of the corresponding surface point. The height system in use in the AOI is Orthometric Height System, as a result normal height data is not readily available, that is the reason we had to go through the lengthy process outlined in Sect. 4.1.3 to determine normal heights for all the land gravity station points in this research.

4.6 Upper Crustal Density Variation

Geological exploration has been conducted extensively; almost every part of Tanzania has been covered. During prospecting, seismic surveys are conducted in many places; offshore and inshore. One would expect, among the by-products of such undertakings is density of the crust, which varies from one location to another. Nevertheless, our efforts to get data of crustal density variations from local and international bodies have not produced any meaningful results. One reason for not been able to obtain density model data or map is possibly due to the demand for this kind of data is low. Otherwise it is likely, that the need for topographic density variation has become important recently. If one succeeds to obtain geological map of rocks and soil types found in the AOI, i.e.

Tanzania, Kenya, Uganda, DR-Congo, Rwanda, Burundi, Zambia, Malawi, Msumbiji, Somalia and Ethiopia, then with a certain level of GIS (Geographical Information Systems) and density of different rocks and soils, it will be possible to compile an approximate upper crust density model. There are many areas with extremely rough topography in the AOI, probably not found elsewhere on the globe. The high frequency elevation is caused by among other factors, the presence of the two arms of the East African Rift Valley System (EARVS), with striking highly variant rims. Within and in the vicinity of the EARVS, we find many conspicuous features hardly seen elsewhere like:

- Ngorongoro crater; one of the official wonders of the World.
- Lake Tanganyika; the 2nd deepest and 7th largest lake in the World.
- Lake Victoria; 3rd largest lake in the World.
- Lake Nyasa; 4th deepest and 10th largest lake.
- Mt. Kilimanjaro, the highest mountain in Africa also volcanic, stands 5,895m above MSL and the highest stand alone volcanic doom in the world.
- Mt. Oldonyo Engai; active volcano.

Many others, like Usambara folding mountain ranges, a number of salt lakes like Eyasi, Natron, Magadi, and hot and sulfur springs in Manyara and many other places. More realistic density data is needed mostly in high altitude and high frequency elevation areas to enable more realistic computation of geoid model, (Kuhn 2003, Sjöberg 2004b, and Kiamehr 2006b). The KTH geoid model method of LSMS with additive corrections reduces the impact of non availability of actual terrain crust density variation from place to place, since the corrections are often small in magnitude, (Sjöberg 2003b). But corrections are significant in mountainous, high lands and erratic terrains, e.g., EARVS rim. Once the topographic density model is available, it should be used in reduction of additive corrections to geoid instead of the blanket density of $2.67\ g/cm^3$ (Sjöberg 2004b, Kiamehr 2006b).

Chapter Five

PREPARATIONS FOR GEOID MODEL DETERMINATION BY KTH METHOD

This chapter is a prerequisite for Chapter 6, where data and other inputs to the KTH method for precise gravimetric geoid model determination using LSMS with AC described in Chapter 3 for gravimetric geoid model of Tanzania 2008 (TZG08) is carried out.

5.1 DEM

In Sect. 4.4.3 we came to the conclusion, that the most viable Digital Elevation Model to be used in this research is the USGS SRTM3 reprocessed by the CGIAR-CSI which takes care of voids and spikes and other outliers in the USGS SRTM3 in a special way. Ideally the denser the DEM the better it approximates the actual terrain, but when the research area (AOI) is as big as $19^{\circ} \times 18^{\circ}$, management and processing of 3 arc second DEM is not an easy task. Therefore, we opted to merge the 3 arc second CGIAR-CSI SRTM DEM (SRTM3) to SRTM15s, SRTM30s, SRTM3m and SRTM6m as explained in Sect. 4.4.3.

5.1.1 DEM Formats, Programs and Programming Languages in Use.

The KTH soft package for precise gravimetric geoid model determination by LSMS with AC is known as KTH-GEOLAB. Most of its programs are written in FORTRAN computing language, and can be run under Disk Operating System (DOS) or UNIX. The processing is made even friendlier when run in UNIX in Microsoft Windows (MS) under special adaptation using CYGWIN. Cygwin stands for CYGnus solutions for Microsoft WINdows. Cygwin began development in 1995 at Cygnus Solutions (now part of Red Hat Software). Cygwin is emulation layer for Windows providing environment like a LINUX/UNIX, with substantial Portable Operating System Interface (POSIX) system call functionality, and a collection of tools, which provide a Linux/Unix look and feel. With Cygwin installed in a computer running MS Windows, users have access to many standard UNIX utilities. They can be used from one of the provided shells such as ksh (Korn Shell), bash (Born Again Shell), csh (C+ Shell) or from the Windows Command Prompt (DOS). If you are new to the world of UNIX, you may find it difficult to understand at first, so we recommend you use the many available internet resources to become acquainted with UNIX basics, search for "UNIX basics" or "UNIX tutorial". To install a basic Cygwin environment, download and install “cygwin setup.exe” program which is freely available from web archives under Cygwin, for more literature either search the internet for cygwin or refer to Harold (2003). In this research, most of the KTH-GEOLAB FORTRAN programs and others are run in a PC operating MS Windows under Cygwin using csh. A shell is a command language interpreter. Csh is a new

command language interpreter for UNIX systems. It incorporates good features of other shells like bash, ksh etc. and a history mechanism which makes writing C-shell programs (csh scripts) flexible and exciting. Most of the features unique to csh are designed more for interactive UNIX user. The primary purpose of csh is to translate command lines typed at a terminal into system actions; simple csh script can replace a huge terminal input and save a lot of time and mistakes. Csh is very useful program for interacting with UNIX system, which is emulated in MS-Windows by Cygwin (William 1998). Besides the KTH-GEOLAB, there are two more soft packages which have been used extensively in this work: a) Surfer 8, a contouring and 3D surface mapping for scientists and engineers from the Golden (2002). b) Gravsoft from the University of Copenhagen, Denmark, (Tscherning et al. 1994). Others include Microsoft Office 2003 especially the MS- Word, MS- Excel and MS-Paint, MathType 5.2, Adobe Acrobat 7.0 Professional, a David Gil executable code "DG terrainlister" which has been used to decode all the SRTM3 to readable text format and awk from GNU or simply GAWK/gawk/awk; GNU stands for Gnu's Not Unix. GAWK is the name for the complete Unix-compatible programming software, which is basically a pattern scanning and processing language.

Many programs of the KTH-GEOLAB have been written in FORTRAN77. Thus FORTRAN77 compiler or newer like 90 and 95 can compile, debug and run this package, very seldom with minor alteration if at all. Input data types for the package have been organized more or less like the Gravsoft package (ibid). For insight to data formats refer to Kiamehr and Sjöberg (2006) and also Forsberg (2003 Ch. 5). The data formats are mainly for:

- Spherical harmonic coefficients.
- Grid data (text format).
- Grid data (binary).
- Point data.

Usually a file which falls in the above bullets will end with an extension *.dat, *.gri, *.bin, and *.dat respectively (using *.txt for *.dat also works, but it is less informative, besides more cumbersome for subsequent processes), where * stands for the file name. Eventually all the source data directly or indirectly will end up determining surface gravity anomaly, either terrestrial or GGM gravity anomaly (dg_GGM). The data format accepted by the KTH LSMS with AC must be in grid format i.e. of the form *.gri. Surfer 8 package accepts point data in text, MS-excel, or surfer format (*.dat) also binary (*.bin), which must be organized in minimum of three columns (X, Y, Z), often for subsequent processing to grid format, (Golden 2002 Ch. 2 and 3). The grid data is in a format similar to Gravsoft but with different heading type and reversed start and end points. The different densities of the SRTM DEM of this study are in both Gravsoft (*.gri) and Surfer 8 (*.grd) formats. Conversion of GGMs in spherical harmonics to $1' \times 1'$ surface dg_GGM.gri and dg_GGM.grd is carried out in Section 5.3 while terrestrial point surface gravity anomaly conversion to similar formats is done in Section 5.2. Figure 5-1 portrays contour plots of SRTM3m & SRTM15s and surfaces of SRTM3m & SRTM30s (Surface of 15s failed to plot). Smoothed surface of SRTM6m (SRTMref) is given in Figure 5-3. Observe that the roughest topography is found along the two arms of the EARVS, which unite close to Lake Nyasa. For SRTM3m, topography is smoother (averaged) and thus less detailed, whereas for the SRTM30s the situation is

much more detailed and thus closer to reality. It would have appeared even more detailed if we had been able to plot SRTM15s.

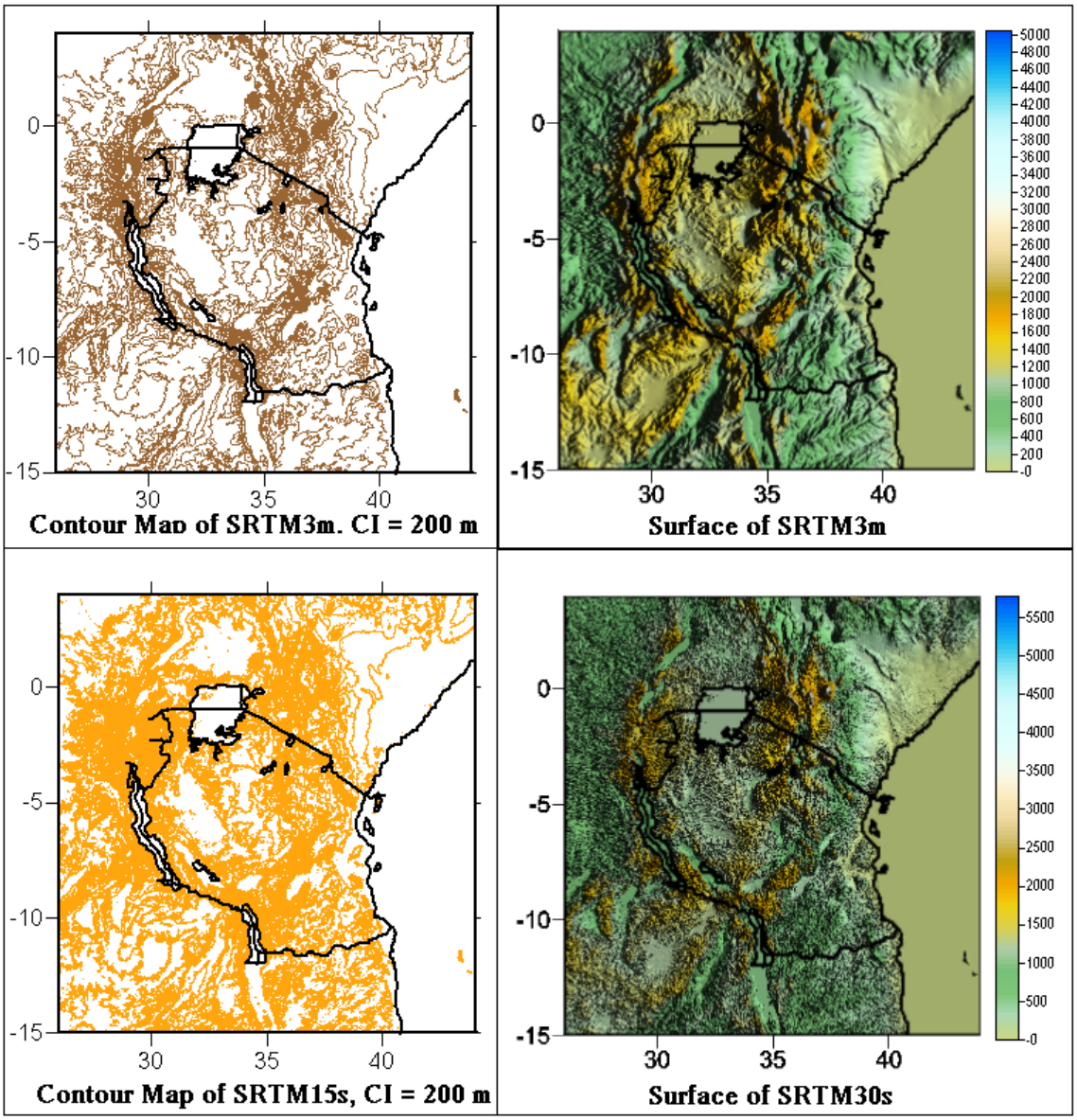

Figure 5-1: Contour and surface maps of dense and coarse SRTM DEMs, unit is m.

5.2 Surface Gravity Densification by Smoothing and Patching

Recall from Sect. 4.2 that the sea surface gravity anomaly was XV, cleaned, statistically tested, densified and gridded to the requirement of this research, namely $1' \times 1'$ surface gravity anomaly. Therefore, the sea gravity is ready for merging with equivalent land gravity. Since the land gravity surface data was XV, cleaned and statistically tested in Sect. 4.1, our main next concern is to densify and grid it to $1' \times 1'$ land surface gravity anomaly. Our approach to densification of land point surface gravity anomaly (dgL_surf) is different to that of sea surface gravity anomaly (dgS_surf) in Section 4.2. The approach

to the densification of dgL_surf is among the main concern of this research; this will be explained in the next sections.

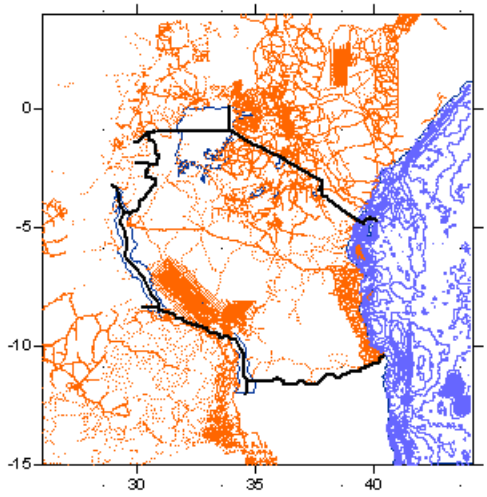

Figure 5-2: Clean gravity data for TZG08; points in the land and contours in the sea, CI=20 mGal

5.2.1 Surface Gravity Anomaly

Surface gravity data is necessary ingredient in the determination of precise regional gravimetric geoid model, and so the same applies to the KTH approach. Our reference is to the dgL_surf developed in Section 4.1. A clean set of 39,677 dgL_surf data records were retained after rejection of dubious at 1 % significance level. In this research, geoid model is computed from dense surface gravity anomaly grid data of $1' \times 1'$ using KTH approach. Unfortunately as explained in Section 1.2 (i), and further witnessed in Figure 4-11, the terrestrial gravity data is very sparse in a number of locations in the AOI. The KTH approach for precise geoid model needs fairly dense grid of surface gravity anomaly to take care of the roughness of the topography. Surface gravity anomaly and surface point gravity anomaly will be shortened to "surface gravity" or "dg_surf". To meet this requirement in developing countries is not easy given the sparseness of the observed gravity data. Thus high degree of care must be exercised to come out with realistic dense grid of surface gravity. Surface gravity is highly correlated with elevation, similarly spatial elevation changes are very erratic and thus not easy to model mathematically. Consequently, direct gridding of sparse surface gravity with the intension of densifying to small grid spacing must be done with great care, otherwise it could result into unrealistic representation. Appropriate gridding method should result into more or less the same amount of data approximately in the same spatial locations to preserve as far as possible, the original gravity data frequencies. The question is, if this is achieved, how do we fill in the missing grids? The most precise answer is to observe the rest of the terrestrial gravity data, but due to too many constraints, the most optimum and viable alternative at present is explained below.

5.2.2 Residual Terrain Effect (RTE), Smoothing and Gridding

Prior to gridding, the surface gravity data is made more amenable to prediction, foremost by reducing the roughness of the surface gravity which is highly correlated with erratic topographic elevation. The surface gravity is freed from the rough component of gravity i.e. the short-wavelength of gravity g_{S_λ} due to topography. The g_{S_λ} is computed about a much smoother mean surface of topography of the AIO by performing prism integration. To obtain the mean reference integration surface to which the RTE are computed from, 6 arc minute mean grids are determined from SRTM3 DEM for the whole of the AOI. Further this mean surface is smoothed by specifying a moving average of grids; the resultant surface is given in Figure 5-3.

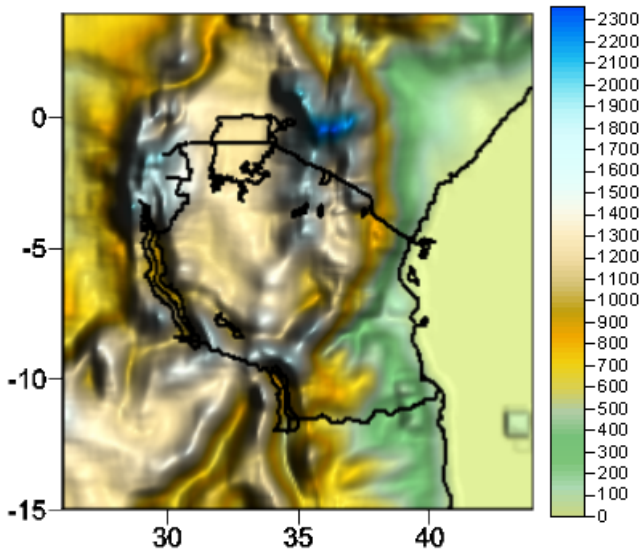

Figure 5-3: Smoothed $0.1^\circ \times 0.1^\circ$ mean surface over the AOI for RTE computation, unit m

During integration, the topography is approximated by a combination of dense and less dense (coarse) DEM with a base on the mean surface of the topography. The denser the better the approximation of the topography, whose effect is pronounced as we approach the computation point (CP). Both the dense and coarse grids are used to a limited radius from the CP, dense grid in the inner zone and coarse grid in the outer zone with a common boundary. Ideally the integration ought to involve all the masses around the Earth i.e. from $-\pi \; to \; \pi$, but due to the inverse proportionality to the square of the distance apart, it is not necessary to go all the way, the contribution from farther masses decays fast, (Heiskanen and Moritz 1967 Ch. 1). Moreover, in here the aim is to smooth the gravity for a better prediction, besides what is removed will be restored and hence the "remove-compute-restore; r-c-r " type of approach being used in this densification of surface gravity. Numerical experiment carried out by this research has shown that use of dense and coarse DEM of $15'' \; and \; 3'$ i.e. in the inner and outer zones to radii of 16.2 km and 81 km respectively suffices, but we have opted to use $15'' \; and \; 30''$ instead. Variations of up to 3° were tested but they did not lead to any appreciable difference, instead the

computation time increased significantly especially when the dense grid radius was increased. The g_{S_λ} component is referred to as "Residual Terrain effect" (RTE). On removing the RTE, the remainder is smoother than the original file but still uneven and sparse with big magnitudes. Gridding or prediction with smaller numbers is better so as to keep minimum amplification of prediction and discretisation errors; this is achieved by further removing the long-wavelength component g_{L_λ} from the surface gravity data. The g_{L_λ} is obtained from pure satellite GGM which corresponds to the correct signal power of the gravity field in the AOI. As recommended in Section 4.3,4, g_{L_λ} should be computed from ITG-GRACE03S up to degree and order 120. The residual surface gravity anomaly (dg_surf.res) is now smaller in magnitude, smoother, mainly with medium wavelength of surface gravity and hence much more suitable for prediction. Figure 5-4 and Figure 5-5 portray different surfaces of RTE and dg_G03S_120 respectively, whereas Table 5-1 gives the statistics of different gravity components involved in the smoothing and densification of dg_surf.

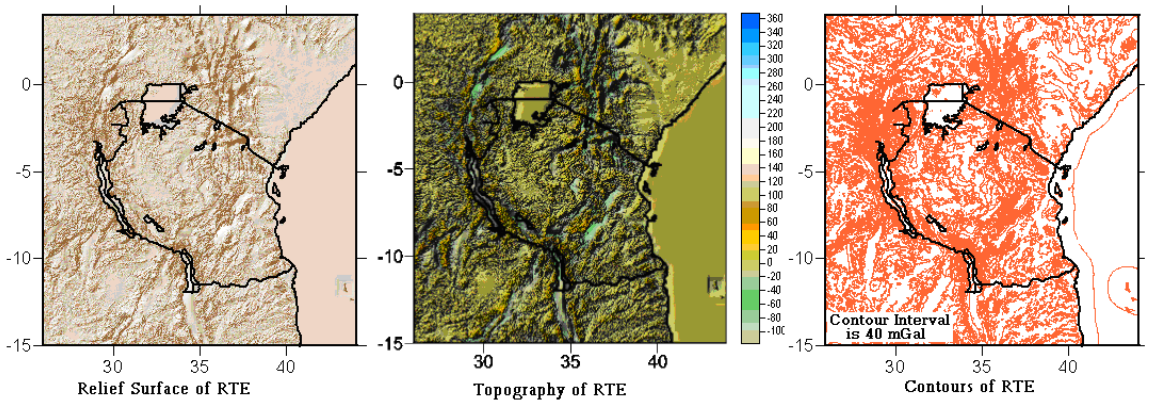

Figure 5-4: Relief, topography and contour maps of the RTE for the AOI

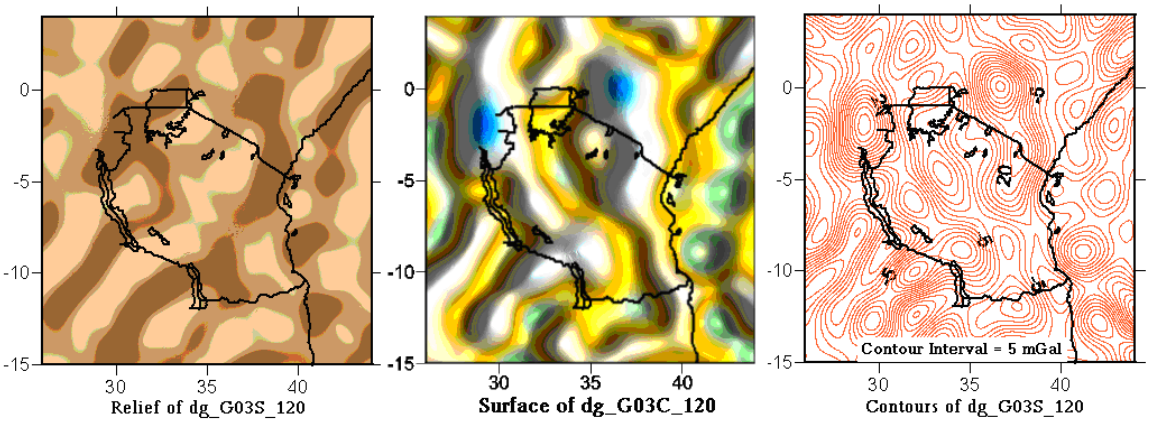

Figure 5-5: Relief, topography and contour maps of the dg_G03S_120 for the AOI

Table 5-1: Statistics of different components involved in the smoothing of surface gravity for the available gravity stations over the AOI in mGal

	dg_surf	RTE	dg_G03S_120	dg_surf-RTE	dg_surf.res
Count	39,677	39,677	39,677	39,677	39,677
Sum	-521635.4	-409733.4	198791.2	-111901.9	-310693.1
Min	-202.718	-242.657	-40.404	-157.452	-158.578
Max	319.546	268.380	52.849	331.213	330.193
Mean	-13.147	-10.327	5.010	-2.820	-7.831
SErr	50.525	27.127	20.118	39.291	35.785
RMS	52.206	29.025	20.732	39.391	36.631

dg_surf.res = dg_surf-RTE-dg_G03S_120

To conform to realistic gridding while keeping discretisation errors at minimum, average data spacing is searched for by averaging the horizontal distance amongst datasets point locations in the AOI. The outcome is approximately one arc minute. Closeness of the gridded data to the original locations of the point data is clarified in Figure 5-6, where the left part is the clean point dg_surf and the right part is the $1' \times 1'$ gridded dg_surf. Kriging method has been used to grid the dg_surf.res data under the following conditions:

- search radius 47 arc seconds.
- 8 sectors involving as much as 750 data within the radius.

This way about 150 % $1' \times 1'$ grid area around the computation point (CP) is involved, leading to overlap of about 50 % from the adjacent grids. This causes correlation amongst the adjacent grids; but then this is almost unavoidable amongst gridding methods, otherwise some data would not take part in the gridding process, (Golden 2002). As expected, a lot of grids are empty. The grid nodes where data exists and the original point data locations are very close to one another, besides in more or less the same locations; indeed it is not ease to see the difference without a closer look.

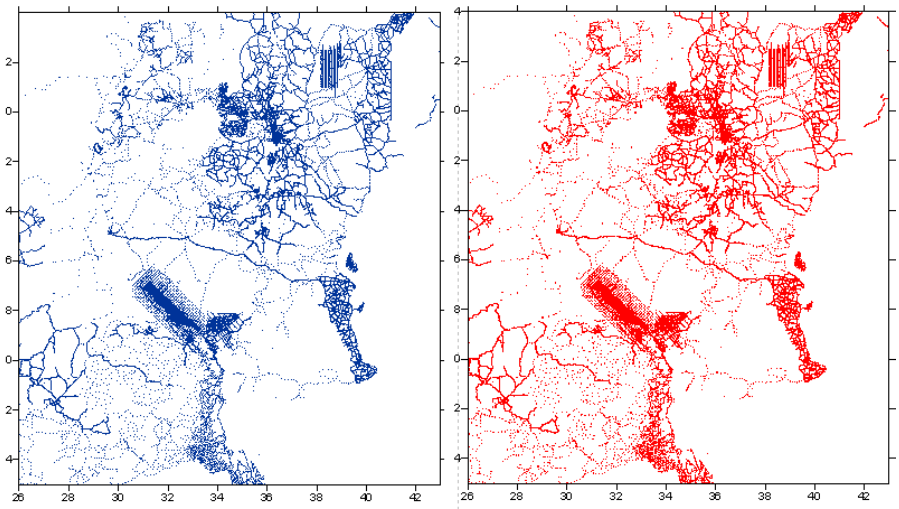

Figure 5-6: Point and gridded residuals surface gravity anomaly (dg_surf.res)

Figure 5-7 shows the above two maps overlaid when either is alternatively on top. The difference of locations is very minute which indicates small gridding error.

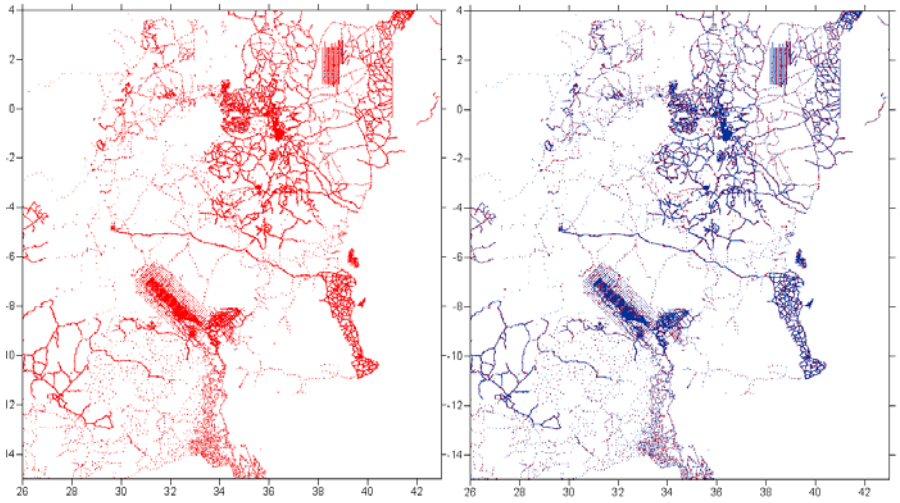

Figure 5-7: Overlay of the maps in Figure 5-6 when either is on top.

Although the grid spacing is small $1' \times 1'$ but due to too many empty grids, the contours of the gridded dg_surf.res are sketchy that is discontinuous in many places as evidenced in Figure 5-8 below

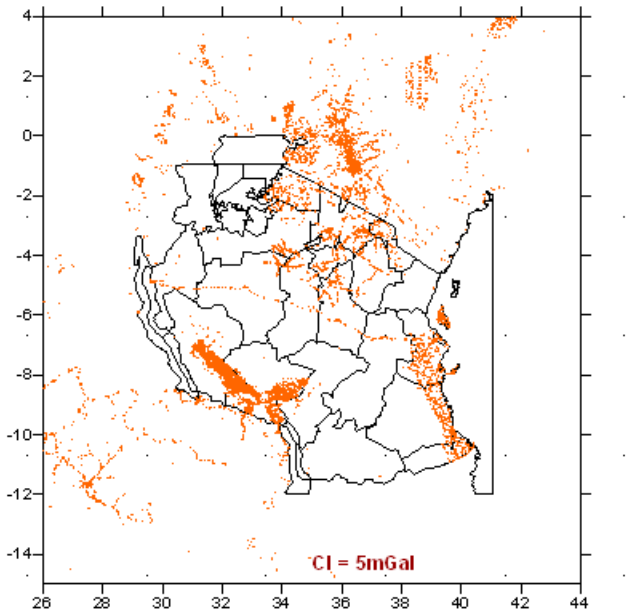

Figure 5-8: Contour map of residual surface gravity anomaly prior to densification

5.2.3 Patching From Selected GGMs

The result of processes in Section 5.2.2 is a $1' \times 1'$ grid of dg_surf.res which has a lot of empty grids which lead to a sketch discontinuous contour map evidenced in Figure 5-8.

Evaluation of pure and combined GGMs given in Section 4.3 has helped to select the most suitable pair of pure and combined GGMs of the present time (May 2008) for the research area. A pair of pure and combined GGMs is needed to fill in (patch) the missing surface gravity grids; description on how to go about the patching is as follows.

Often combined GGM incorporates pure satellite, altimetry and terrestrial gravity data (which sometimes includes aerial gravity), this way it can retain power at higher frequencies than the corresponding pure satellite GGM. All the combined GGMs involved in the selection of the most suitable for the AOI in Table 4-17, had 360 as the maximum degree except GGM02C. GGM02C maximum degree is 200. If we remove from a suitable combined GGM (GGM^C) of the AOI, g_{S_λ} and g_{L_λ}, which can be computed from RTE and obtained from the selected pure GGM (GGM^S) respectively as fore explained, we remain with the rest of the surface gravity frequencies of the GGM^C, i.e. dg_surf_GGM^C.res. The dg_surf_GGM^C.res should be much closer to the corresponding dg_surf.res. The computed/resultant surface residuals from GGM^C will be shortened to $dg\_surf.res^c$. The $dg\_surf.res^c$ unlike the dg_surf.res, covers fully the $1'\times1'$ grids in the whole of the AOI. The possibility that the terrestrial gravity data used in the development of GGM^C was point surface gravity covering fully the AOI, is almost zero. In addition the $dg\_surf.res^c$ is limited to the maximu degree of the GGM^C, consequently dg_surf.res has more qualities, and in addition, is richer of the surface gravity frequencies than the $dg\_surf.res^c$.

Patching for the empty grids in the AOI will be as follows: Two grid files, dg_surf.res (G1) and $dg\_surf.res^c$ (G2) with exactly the same grid specifications and limits will be loaded to an algorithm which scans the corresponding G1and G2 grid nodes sequentially. First it evaluates the G1 grid node whether it has data or empty. If it has, it continuous with the sequential scanning until it finds an empty grid node, when it does, it fetches the corresponding grid node data from G2 and replaces the empty grid node of G1 with the G2 data. This process continues until all the empty $1'\times1'$ grid nodes of G1 have been filled with the corresponding G2 grid node data from $dg\_surf.res^c$. Finally equally gridded $1'\times1'$ RTE and dg_GGM^S are restored to the patched $1'\times1'$ dg_surf.res grid file to result into densified surface gravity. This is our approach to the densification of dg_surf, which ensures that all the grids are filled in with fairly quality data with minimum effect to the original terrestrial gravity data quality. From Sect. 4.3.4 our GGM^S is ITG-GRACE 03S to degree and order 120 (or G03S_120) and the GGM^C is EIGEN-CGO3C to degree and order 360 (CGO3C). From Table 4-17, the next quality pair is EIGEN-GL04S to degree and order 110 (GL04S_110) and EGM96 (combined) to degree and order 360, if we take into account the following facts:

- ITG-GRACE03S is a succession of ITG-GRACE02S.
- EIGEN-GL04C is succession to EIGEN-CG03C, GGM02C and GGM01C; notwithstanding EIGEN-CG03C in the AOI proved to be more suitable than the newer EIGEN-GL04C.

Therefore if for comparison purpose we opt to test another different but suitable pair it should be GL04S_110 and EGM96; refer to Table 4-17. We would like to come to this decision of the second pair in a more suitable approach. To start with, in this endeavour, we have the following $1' \times 1'$ surface gravity anomaly GGMs grid files (dg_GGM) as candidates:

- dg_G03S_120 Pure satellite GGM
- dg_GL04S_110 Pure satellite GGM
- dg_CG03C Combined GGM
- dg_EGM96 Combined GGM
- dg_GL04C Combined GGM

Whose statistics are given in Table 5-3

First we remove the RTE (g_{S_λ}) in grid format (RTE.gri) from all the three GGM^C, then from each of the resulting three files, we remove at a time one of the two newest GRACE pure satellite gravity anomaly file (g_{L_λ}), this will result into six grid computed residual GGM files i.e. $dg\_surf.res^c$ explained earlier. Further we compute the difference between the dg_surf.res and $dg\_surf.res^c$ at all the locations with clean point gravity data i.e. at 39,677 locations. The one which agrees better to dg_surf.res should have the smallest deviation, and thus the best one to patch up the empty grids. This second validation of the GGM^C, which involves the whole of the AOI, and as a result much more data points, is expected to cement our earlier selection of the GGM-pair which was based on 56 absolute reference gravity stations, moreover in Tanzania only. But now, it is the whole of the research area (AOI), refer to Sect. 4.3.2. Result of the above description is summarized in Table 5-2.

Table 5-2: Statistics for the selection of most suitable pair of pure and combined GGMs for patching empty grids of surface gravity in the AOI in mGal.

Quality of $dg\_surf.res^c$ in $1' \times 1'$ grid format using two pure GGMs						
$dg\_GGM.res^c$	dg_CG03C - RTE - G03S.gri I	dg_EGM96 - RTE - G03S.gri II	dg_GL04C - RTE - G03S.gri III	dg_CG03C -RTE - GL04S.gri IV	dg_EGM96 -RTE - _GL04S.gri V	dg_GL04C -RTE - _GL04S.gri VI
Counter	39,677	39,677	39,677	39,677	39,677	39,677
Mean	3.412	2.987	2.769	3.066	2.641	2.423
Min	-259.212	-248.763	-257.449	-260.990	-250.541	-259.227
Max	125.999	139.877	131.015	129.441	143.319	134.457
SErr	29.866	29.917	29.297	30.192	30.420	29.759
RMS	30.059	30.066	29.427	30.347	30.534	29.857
Diff_dg.res = "Difference of dg_surf.res with one of I, II, III … VI" where "I, II, III … VI" refers to the corresponding $dg\_surf.res^c$ in the second row above						
$dg(.res - .res^c)$ Counter	Diff_ dg.res-I 39,677	Diff_ dg.res-II 39,677	Diff_ dg.res-III 39,677	Diff_ dg.res-IV 39,677	Diff_ dg.res-V 39,677	Diff_ dg.res-VI 39,677
Rank: SErr & RMS	1	2	4	3	5	6
Mean	-11.243	-10.818	-10.897	-10.600	-10.472	-10.254
Min	-145.507	-137.930	-142.666	-144.161	-135.488	-141.719

Max	314.360	314.975	323.311	316.252	323.926	325.202
SErr	34.678	34.707	34.844	34.999	35.026	35.273
RMS	36.454	36.353	36.507	36.568	36.557	36.732

Table 5-3: Statistics of the GGM gravity anomaly and the RTE grid files participating in the selection of the best two possible pairs to densify the sketch dg_surf.res grid in mGal.

dg_GGM File	dg_G03S _120.gri	dg_GL04S _110.gri	dg_ CG03C.gri	dg_ EGM96.gri	dg_ GL04C.gri	dg_ RTE.gri
Mean	-9.145	-9.074	-9.241	-9.287	-9.178	-0.564
Min	-53.430	-49.550	-122.180	-124.710	-121.400	-117.970
Max	53.470	54.580	158.020	144.780	155.820	368.416
SErr	17.854	16.906	28.048	28.219	28.178	16.936
RMS	20.060	19.188	29.531	29.708	29.635	16.946

From the standard errors and RMS of the differences of dg_surf.res (i.e. observed) and $dg\_surf.res^c$ (computed from combined GGMs) in the last two rows of Table 5-2, we observe that the pair, which fits best the observed gravity in the whole of the AOI maintains to be the same pair qualified by the 56 absolute reference gravity in Sect. 4.3.4 i.e. ITG-GRACE03S & EIGEN-CG03C. Moreover, the same hierarchy is followed, that is the second best pair is ITG-GRACE03S & EGM96. The 3rd pair still utilizes ITG-GRACE03S & EIGEN-GL04C. Performance of the newest GRACE models in the AOI namely EIGEN-GL04S & EIGEN-GL04C is the worst of the six pairs. Therefore, once again, our conclusion is that the pair which will patch the empty grids of the surface gravity in the research area and other processes of TZG08 determination by the KTH method of LSMS with AC is **ITG-GRACE03S_120 & EIGEN-CG03C**. In case of cross checking, given the explanation in the bullets above, **EIGEN-GL04S_110 & EGM96** should be deployed.

5.2.4 Densification, Restoration of RTE and Pure GGM and Re_Gridding of Land and Marine Grid Surface Gravity

Our method of densification was explained at the beginning of the previous section. Now that we have a qualified pair of pure and combined GGM, we proceed to patch the dg_surf.res and thus densify it using $dg\_surf.res^c$ from ITG-GRACE03S & EIGEN-CG03C and then restore the removed gravity frequencies namely RTE (g_{S_λ}) and dg_G03S_120 (g_{L_λ}) as explained in the preceding section. In patching, the two sets of paired GGMs proposed above were used. Figure 5-9 is a result of using the qualified pair i.e. ITG-GRACE03S & EIGEN-CG03C.

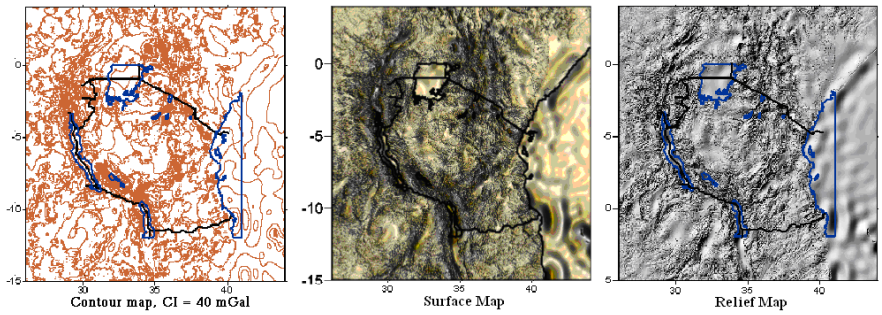

Figure 5-9: Patched surface land gravity grid prior to restoration of short and long-wavelengths, also before blanking the sea area.

Pictorially the outcome from the two sets look very similar (second pair not shown here), but if you overlay the contours, the dissimilarity is quite clear; refer to Figure 5-10. Quality of the two sets is given in Table 5-4.

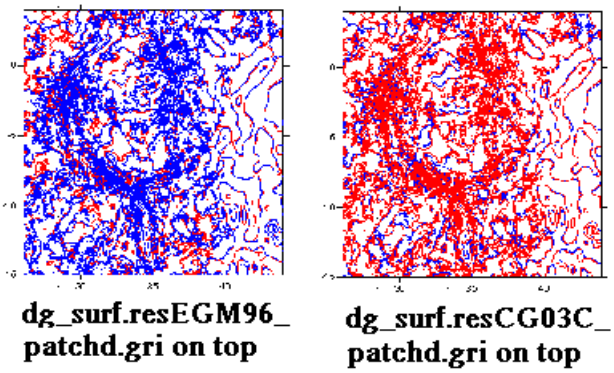

Figure 5-10: Overlay of the filled surface gravity residuals by EGM96 and EIGEN-CG03C either on top, using ITG-GRACE03S and RTE

Table 5-4: Statistics of the patching and patched residuals of the two best pairs of GGMs in mGal

	File	Mean	Min	Max	SErr
EGM96 + G03S	dg_EGM96-RTE- G03S.gri	0.42	-322.47	142.45	23.98
	dg_surf-RTE- G03S.gri	-1.8	-158.58	330.19	30.78
	dg_surf.resEGM96_patchd.gri	0.25	-322.47	330.19	24.05
CG03C + G03S	dg_CG03C-RTE-G03S.gri	0.47	-331.98	146.78	23.45
	dg_surf-RTE-G03S.gri	-1.8	-158.58	330.19	30.78
	dg_surf.resCG03C_patchd.gri	0.30	-331.98	330.19	23.55

5.2.5 Quality Control and Accuracy Assessment

You will recall that we minimized discretisation error when gridding dg_surf.res i.e. dg_surf-RTE-G03S_120 by having a small search circle of 47 arc seconds radius around the grid nodes of $1' \times 1'$ in the AOI. The dg_GGM were directly computed to $1' \times 1'$ i.e.

dg_GGM grids and not out of average. Our concern is on the residuals from GGM^C i.e. $dg\_surf.res^c$, it is improbable that sparseness of the gravity data that exist in the AOI is very different to the one that existed during the determination of GGM^C, furthermore the chance is, that much wider search area was used to compute the mean gravity anomalies for GGM^C. To minimize the effect of discretisation error originating from GGM^C in the (dg_surf.resCG03C_patchd.gri and dg_surf.resEGM96_patchd.gri) patched surface gravity residuals, the following procedure will be adopted in creating the ultimate patched residuals for surface gravity data for TZG08. To maintain proximity natural continuity of surface gravity, the $1' \times 1'$ patched surface gravity residuals will be re-gridded to the same format of $1' \times 1'$ but using a bit wider search circle of 5 arc minutes around the $1' \times 1'$ grid nodes using a method which takes into account natural trends, but at the same time with increasing weight as we approach the grid node i.e. computation point (CP). On the edge of the 5 arc minute circle, the weight is almost zero, and almost 1 at the CP. Two techniques qualify for this, namely, Kriging and inverse distance to a power (ID2P). Numerical computation reveals that their results are very much the same. Other techniques like, natural neighbour, moving average and modified Shepard's method were tested but their smoothing effect are too high with statistics of the outcome very different from the original data set. Therefore the option is to use ID2P since it takes less time. The resulting residuals are termed $dg\_surf.rec^{C2}$.

To ensure that the quality of the dg_surf.res is not lowered, the procedure explained in Sect. 5.2.3 will be adopted. In this case $dg\_surf.res^c$ is replaced by the newly determined $dg\_surf.rec^{C2}$ to form stage two patched residuals i.e. dg_surf.resCG03C_patchd_v2.gri and dg_surf.resEGM96_patchd v2.gri. Thus, unlike patches from $dg\_surf.res^c$, whose data was solely from GGM^C, $dg\_surf.rec^{C2}$ patches combine qualities of both the dg_surf.res (observed) and $dg\_surf.res^c$, i.e. qualities of GGM^C. After re-patching up all the empty grids of dg_surf.res with patches from $dg\_surf.rec^{C2}$, then RTE.gri and G03S_120.gri are restored. This way, two densified land surface gravity anomaly grid files are formed via EIGEN-CG03C and EGM96 GGMs. Below we compare the qualities of stage I (prior to re-gridding the patched residuals) and stage II of the two densified $1' \times 1'$ surface gravity anomaly grid data sets in Table 5-5 and Table 5-6 respectively.

Table 5-5 : Statistical comparison of the two resultant $1' \times 1'$ grid land surface gravity anomaly files; note that they cover the entire AOI, meaning the quality in the ocean is not to standard, (Stage I). (Unit is mGal)

	File	Mean	Min	Max	SErr	RMS
CG03C + G03S	dg_surf.resCG03C_patchd.gri	0.30	-331.98	330.19	23.55	23.56
	RTE+dg_G03S_120.gri	-9.71	-93.18	393.92	24.73	26.56
	dg_surfCG03C_patchd.gri	**-9.41**	**-179.25**	**379.09**	**28.62**	**30.13**
EGM 96 + G03S	dg_surf.resEGM96_patchd.gri	0.25	-322.47	330.19	24.05	24.05
	RTE+dg_G03S_120.gri	-9.71	-93.18	393.92	24.73	26.56
	dg_surfEGM96_patchd.gri	**-9.46**	**-179.25**	**379.09**	**28.79**	**30.30**

Table 5-6 : Quality of the final (Stage II) densified $1' \times 1'$ grid surface gravity anomaly data sets based on CG03C and EGM96 combined GGM in mGal

	File	Mean	Min	Max	SErr	RMS
CG03C + G03S	dg_surf.resCG03C_patchd_v2.gri	0.30	-331.98	330.19	23.55	23.55
	RTE+dg_G03S_120.gri	-9.71	-93.18	393.92	24.72	26.56
	dg_surf_CG03C_v2.gri	**-9.41**	**-179.25**	**379.09**	**28.62**	**30.13**
EGM 96 + G03S	dg_surf.resEGM96_patchd_v2.gri	0.25	-322.47	330.19	24.05	24.05
	RTE+dg_G03S_120.gri	-9.71	-93.18	393.92	24.72	26.56
	dg_surf_EGM96_v2.gri	**-9.46**	**-179.25**	**379.09**	**28.78**	**30.30**

Note: dg_surf.resCG03C_patchd_v2.gri and dg_surf.resEGM96_patchd_v2.gri are the $dg\_surf.rec^{C2}$ quoted in the literature.

It is of interest to note that despite the increased homogeneity arrived at by involving wider search circle in stage II surface data patches, statistics of stage I and II remain practically the same to two decimal places of milligal.

Furthermore the two $1' \times 1'$ densified surface gravity anomaly grid files i.e. dg_surf_CG03C_v2.gri and dg_surf_EGM96_v2.gri to be referred to as dg_surf and dg_surf2 respectively henceforth, are compared spatially through the contours in Figure 5-11. In spite of the small differences in statistics portrayed in Table 5-6 between dg_surf and dg_surf2, spatially the difference is clearer in Figure 5-11.

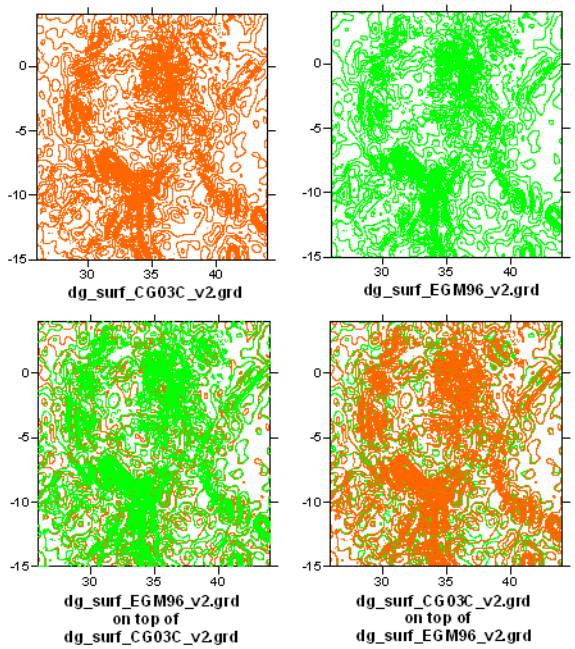

Figure 5-11 : Comparison of densified surface gravity anomaly using combined GGMs; EGM96 and EIGEN-CG03C via RTE and ITG-GRACE03S

To ensure that quality of sea gravity is not compromised by the land gravity data at the stage of combining the land and the sea grid gravity data, we have to confine the land data to land areas as we did for the sea gravity; refer to Sect. 4.2.2. This is achieved by

blanking the sea grids along the coastal line and isles' boundaries as evidenced Figure 5-12

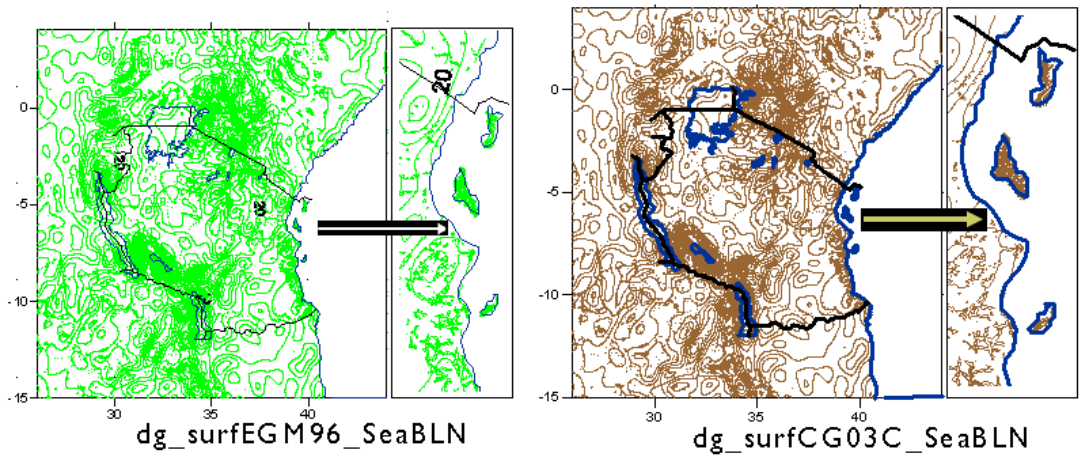

Figure 5-12 : Confinement of densified surface gravity grid data to land areas only

After blanking the ocean grids, accuracy of the remaining land grid data for the two surface gravity files is given in Table 5-7.

Table 5-7: Quality of the land surface gravity $1' \times 1'$ grid data i.e. after blanking the sea gravity grids in mGal.

Grid File	No. Nodes	Sum	Min	Max	Mean	SErr
dg_surfEGM96_BLN	1,043,299	-4,734,952.82	-179.25	379.09	-4.54	**28.35**
dg_surfCG03C_BLN	1,026,277	-4,682,442.67	-179.25	379.09	-4.56	**27.97**

Now each of the land and sea surface gravity in grid format is confined to its proper location as shown in Figure 5-13, but merging creates break lines, along the blanking boundaries.

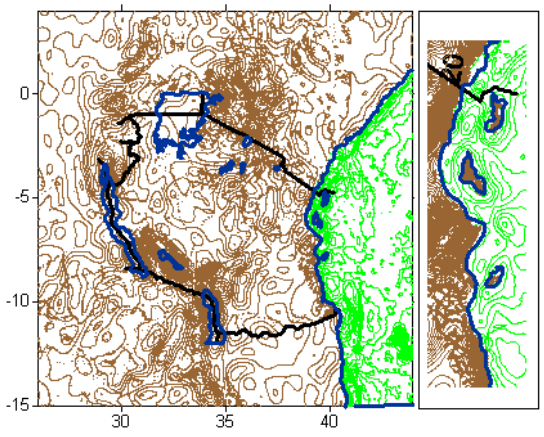

Figure 5-13 : Densified surface gravity anomaly for TZG08

To overcome the problem of break-lines, which are visualized as discontinuities, we mosaic the two grid files using nearest neighbour technique. The method is the most appropriate since it assigns the value of the nearest point to each grid node when the data are already evenly spaced or with a few data mis-aligned, leading to a smooth continuity

from the land to the sea and vice versa. Table 5-8 presents the final quality of the combined dg_surf2 and dg_surf in the AOI and Figure 5-14 shows the contour maps of dg_surf2 and dg_surf. Figure 5-15 portrays the surfaces of dg_surf only, i.e. the qualified surface gravity anomaly for the TZG08 determination.

Table 5-8: Quality of the final surface gravity anomaly data in the whole of AOI ready for the determination of Tanzania geoid model 2008 (TZG08) in mGal.

Grid File	Mean	Min	Max	SErr	RMS
dg_surf_EGM96_L+S.gri ⇒ dg_surf2	-8.29	-179.25	379.09	29.80	30.94
dg_surf_CG03C_L+S.gri ⇒ dg_surf	**-8.18**	**-179.25**	**379.09**	**29.38**	**30.50**

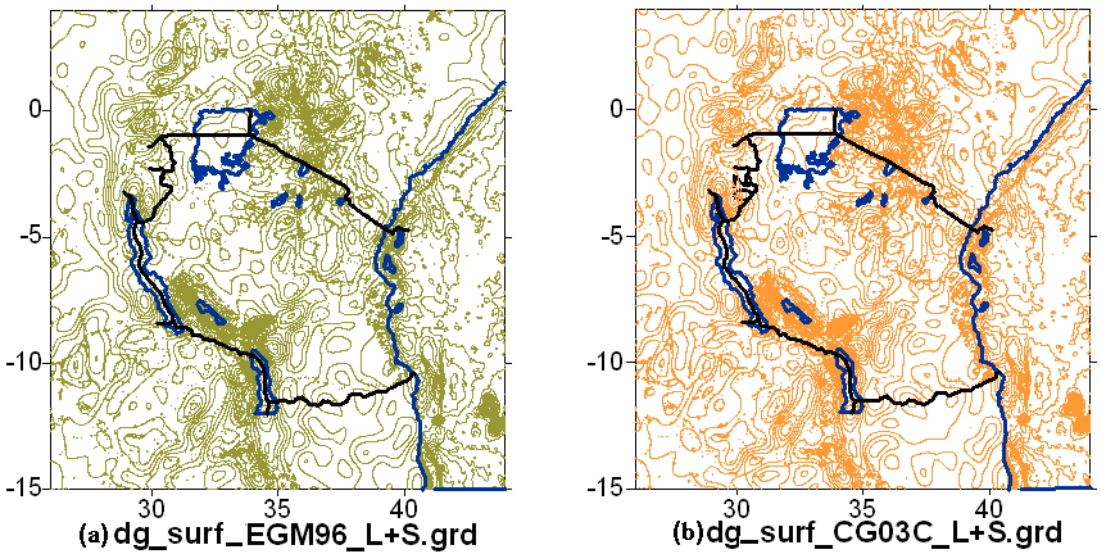

Figure 5-14: Contour maps of gridded ($1' \times 1'$), clean and densified surface gravity anomaly ready for the determination of Tanzania geoid model 2008.
(a) Densification based on EGM96 combined GGM
(b) Densification based on GRACE EIGEN-CG03C combined GGM

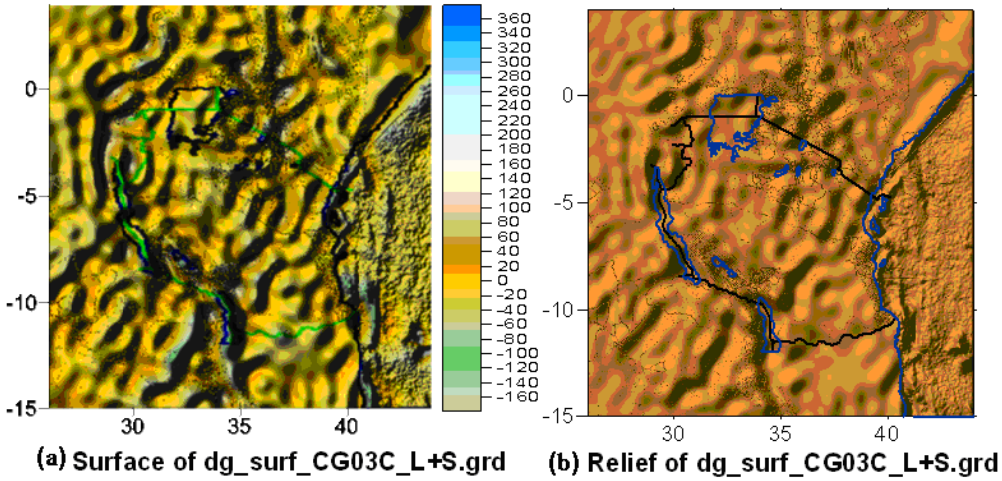

Figure 5-15: (a) and (b) represent surface and relief maps of the qualified surface gravity anomaly based on the GRACE EIGEN-CG03C combined GGM, unit mGal

5.3 Global Gravitational Model Conversion, Signal and Error Degree Variances and LSMS Parameters Determination

This section tackles conversion of GGM potential coefficients to disturbing potential (T), and then to GGM gravity anomaly Δg^S. It also selects appropriate signal and error degree variance models, which are prerequisite to the computation of modification parameters of the unbiased LSMS (Sjöberg 1991), for the determination of approximate gravimetric geoid height using the KTH-GEOLAB (Kiamehr and Sjöberg 2006). The spectral form of the unbiased LSMS of Eq. (3.14) after incorporating kernel modification and data errors can be written as:

$$\tilde{N} = c\sum_{n=2}^{\infty}\left(\frac{2}{n-1} - Q_n^L - s_n^*\right)\left(\Delta g_n^T + \varepsilon_n^T\right) + c\sum_{n=2}^{M}\left(Q_n^L + s_n\right)\left(\Delta g_n^S + \varepsilon_n^S\right), \tag{5.1}$$

where:

$\tilde{N}$	….	The approximate geoid height
c	….	$(R/2\gamma)$: R is mean Earth radius and γ is normal gravity on ellipsoid
T	….	Stands for terrestrial and S …. For Global Gravitational Model (GGM)
n	….	Evaluation spectral degree; M …. Maximum degree of the GGM
L	….	Modification upper degree
Δg_n^T	….	Laplace harmonic of terrestrial gravity anomaly, Δg^T
Δg_n^S	….	Laplace harmonic of GGM gravity anomaly, Δg^S
$\varepsilon_n^T, \varepsilon_n^S$	….	The nth spectral degree errors of the Laplace harmonics of terrestrial and GGM gravity anomaly respectively
Q_n^L	….	Truncation coefficients
s_n^*	….	Modification parameters

The truncation coefficients are further expressed as

$$Q_n^L = Q_n - \sum_{k=0}^{L}\frac{2k+1}{2}s_k e_{nk}, \tag{5.2}$$

where the Molodensky's truncation coefficients Q_n are given by

$$Q_n = \int_{\psi_0}^{\pi} S(\psi)P_n(\cos\psi)\sin\psi\, d\psi, \tag{5.3}$$

for the spherical cap σ_0 around the point of interest of geocentric angle ψ_0. The modification parameters are expressed as

$$s_n^* = \begin{cases} s_n & \text{if } 2 \le n \le L, \\ 0 & otherwise \end{cases} \tag{5.4}$$

where s_n are arbitrary coefficients, e_{nk} are referred to as the Paul (1973) coefficients; like Q_n they are function of ψ_0 as shown in Eq. (5.5)

$$e_{nk} = \frac{2k+1}{2} \int_{\psi_0}^{\pi} P_n(\cos\psi) P_k(\cos\psi) \sin\psi \, d\psi, \tag{5.5}$$

where $P_n(\cos\psi)$ is the Legendre polynomial of degree n and ψ is the geocentric angle between the computation point and the running point of integration, (Hofmann-Wellenhof and Moritz 2005 pp 16-27 and 105-108). The terrestrial $\left(\Delta g^T\right)$ and the GGM $\left(\Delta g^S\right)$ gravity anomalies are given by the following relations for the n[th] degree;

$$\Delta g_n^T = \frac{2n+1}{4\pi} \iint_{\sigma_0} \Delta g^T \, P_n(\cos\psi) d\sigma, \tag{5.6}$$

and

$$\Delta g^S = \sum_{n=0}^{\infty} \Delta g_n^S; \quad \Delta g_n^S = \frac{(GM)^s}{a^2} \left(\frac{a}{r}\right)^{n+2} (n-1) \sum_{m=-n}^{n} C_{nm} Y_{nm}, \tag{5.7}$$

where:

$d\sigma$	….	Infinitesimal surface integration element of unit sphere (σ)
a	….	Equatorial radius of the Global Gravitational Model (GGM)
r	….	Radial distance on the respective geocentric ellipsoid of the GGM
n, m	….	Degree and order of the spherical harmonic (SH) expansion
$(GM)^s$	….	GGM Adopted Earth_Mass Newton gravitational constant
C_{nm}	….	Fully normalized spherical harmonic coefficients of disturbing potential (T)
Y_{nm}	….	Fully normalized surface SHs T

5.3.1 Conversion of GGM Potential V to T and Δg^S

In Heiskanen and Moritz (1967), the gravity potential W, at a point $(x, y, z)/(r, \varphi, \lambda)$ is given as the sum of gravitational potential, (V), and the potential of centrifugal (Φ), i.e.

$$W = W(x, y, z) = W(r, \varphi, \lambda) = V(r, \varphi, \lambda) + \Phi(r, \varphi, \lambda)$$

or simply

$$W = V + \Phi \tag{5.8}$$

so that

$$W = G\iint_{\sigma} \frac{\rho d\sigma}{l} + \frac{1}{2}\omega^2\left(x^2 + y^2\right)$$

Laplacian of Eq. (5.8) leads to

$$\Delta W = \begin{cases} -4\pi k\rho + 2\omega^2 & \textit{Generally} \\ 2\omega^2 & \textit{Outside the attracting masses} \end{cases} \tag{5.9}$$

where k, ρ and ω are gravitational constant, density and angular velocity respectively. By the definition of reference ellipsoid, Laplacian of its gravity potential (i.e. normal potential, U) is given by

$$\Delta U = 2\omega^2 \tag{5.10}$$

At a given point outside the attracting masses,

$$W = U + T\,, \tag{5.11}$$

where T is termed disturbing potential. From Eqs. (5.9) to (5.11), we deduce that

$$\Delta T = 0 \tag{5.12}$$

i.e. T is harmonic outside the attracting masses ($\sim$ Earth). From Heiskanen and Moritz (1967 p 85), Bruns' formula relates T, N and γ by

$$N = \frac{T}{\gamma} \tag{5.13}$$

The fact is, reference ellipsoid approximates the Earth better than a sphere, but it deviates from a sphere in the order of flattening $f \doteq 3\times10^{-3}$ (ibid p 87), this coupled by the fact that T is harmonic, enables us to express T in spherical harmonics to facilitate determination of gravity anomaly from GGM (Δg^S). The error of the order of $3\times10^{-3}N$ to geoid height is minimized when the additive corrections (AC) are added to the approximate geoid height $\tilde{N}$ from LSMS. In SHs, T at point (r, φ, λ) on or outside the bounding surface is expressed as

$$T = \sum_{n=0}^{\infty} \left(\frac{a}{r} \right)^{n+1} T_n(\varphi, \lambda), \tag{5.14}$$

where $T_n(\varphi,\lambda)$ is the Laplace's surface harmonic of degree n of $T(\varphi,\lambda)$, a equals equatorial radius of the mean Earth, the rest are as defined earlier. Making use of Fundamental Gravimetric boundary Equation (FGE), (ibid p 89), gravity anomaly (Δg^S) at surface point of radial distance r is obtained from T as follows

$$\Delta g^S = \frac{1}{r} \sum_{n=0}^{\infty} (n-1) \left(\frac{a}{r} \right)^{n+1} T_n(\varphi, \lambda) \tag{5.15}$$

Due to the factor $(n-1)$ in Eq. (5.15), harmonics of T usually statrt at degree 2, since in Δg, degrees 0 and 1 will vanish, thus in KTH-GEOLAB, GGM should be scaled down to degree $n \geq 2$. From Eq. (5.8), we observe, that the part most crucial to handle is the gravitational potential V since Φ is analytical, it is easily removed from the W and thus GGM provides us with the Earth's gravitational potential V, in SHs it is represented as

$$V(r,\varphi,\lambda) = \frac{(GM)^s}{r} \left[1 + \sum_{n=2}^{n_{\max}} \left(\frac{a^s}{r} \right)^n \sum_{m=-n}^{n} P_{nm}(\sin\varphi) \left(c'_{nm} \cos m\lambda + s'_{nm} \sin m\lambda \right) \right], \tag{5.16}$$

where

$(GM)^s$	....	GGM adopted Gravitational-Earth Mass constant
a^s	....	GGM equatorial radius of the earth
r	....	Radial distance at point of interest
c'_{nm}, s'_{nm}	....	Fully normalized SHs coefficients of degree *n* and order *m*
$P_{nm}(\sin\varphi)$	....	Associated Legendre function of degree *n* and order *m*
(r,φ,λ)	....	Spherical coordinates

Normal potential of reference ellipsoid U in SHs is given by

$$U(r,\varphi,\lambda) = \frac{GM''}{r} \left[1 + \sum_{n=2}^{n_{\max}} \left(\frac{a}{r} \right)^n \sum_{m=-n}^{n} P_{nm}(\sin\varphi'') \left(c''_{nm} \cos m\lambda + s''_{nm} \sin m\lambda \right) \right], \tag{5.17}$$

where:

GM''	....	Gravitational-Ellipsoid Mass constant
a	....	Semi major axis of the reference ellipsoid
r	....	Radial distance at point of interest
c''_{nm}, s''_{nm}	....	Fully normalized SHs coefficients of degree *n* and order *m*
$P_{nm}(\sin\varphi)$	....	Associated Legendred function of degree *n* and order *m*
(r,φ,λ)	....	coordinates

The GGM gravitational potential Eq. (5.16) is scaled to address the reference ellipsoid of interest, here GRS80, also the potential coefficients. Adhering to the definition of reference ellipsoid, $M = M''$ then disturbing potential is obtained as the difference,

$$T = V - U = \frac{GM}{a}\sum_{n=2}^{n_{\max}}\left(\frac{a}{r}\right)^{n+1}\sum_{m=-n}^{n}\left(C_{nm}\cos m\lambda + S_{nm}\sin m\lambda\right)P_{nm}\left(\sin\varphi\right), \qquad (5.18)$$

where C_{nm} and S_{nm} are the differences between the fully normalized scaled geo and ellipsoidal potential (normal) coefficients. By disregarding harmonics of degree 0 and 1 and setting upper limit of the frequency domain to degree $n_{\max}$ in Eq. (5.14) and Eq. (5.15), and further equating Eq. (5.14) to Eq. (5.18) we get

$$T_n = \frac{GM}{a}\sum_{m=-n}^{n}\left(C_{nm}\cos m\lambda + S_{nm}\sin m\lambda\right)P_{nm}\left(\sin\varphi\right) \qquad (5.19)$$

Substitution of Eq. (5.19) into Eq. (5.15) under the stated limitations, gives GGM gravity anomaly at point (r,φ,λ) as

$$\Delta g^S(r,\varphi,\lambda) = \frac{GM}{a^2}\sum_{n=2}^{n_{\max}}(n-1)\left(\frac{a}{r}\right)^{n+2}\sum_{m=-n}^{n}\left(C_{nm}\cos m\lambda + S_{nm}\sin m\lambda\right)P_{nm}\left(\sin\varphi\right) \qquad (5.20)$$

Usually a GGM provides header information followed by annotation to different data columns. Typical header from NASA, GSFC and NIMA (EGM96) and GRACE Mission are shown below.

Table 5-9: Typical header information of a GGM, example of EGM96 and ITG-GRACE03S

Description Product	NASA, GSFC and NIMA (EGM96) Gravity field	GRACE MISSION Gravity field
GGM GM^S constant a n_max Errors Norm Tide_system	EGM96 3.986004415e+14 6.3781363e+06 360 Formal	ITG-Grace03 3.986004415e+14 6.3781366e+06 180 Formal fully_normalized zero_tide
url	ftp://cddis.gsfc.nasa.gov	http://www.geod.uni-bonn.de/itg-grace03.html

The data columns are often comprised of degree and order (n,m), SHs coefficients c'_{nm}, s'_{nm} followed by accuracy of the coefficients by degree and order of the GGM σ_{Cnm}, σ_{Snm}. It is common for the GGM to start at degree and order "0". The adopted GM

constant [$(GM)^s$] and radius [a^s] for a given GGM, are often different for different GGMs and sometimes different to Earth GM factor and equatorial radius of reference ellipsoid of interest, for example for GRS80, the equatorial radius is 6378137 m and GM is 3.98600.5e+14, (Moritz 1980b) and for WGS84, the equatorial radius is 6378137 m and GM is 3.986004418e+14. Given this situation, it becomes necessary to scale the $(GM)^s$ and a^s to address the reference ellipsoid in use also the potential coefficients.

Therefore, beware, that a GGM needs preparation prior to processing, so take note that:

- Different GGM sites/archives have different formats of presenting a GGM, thus the first step is to ensure, that the GGM format is converted to meet your needs, in this case the KTH-GEOLAB format, refer to (Kiamehr and Sjöberg 2006) for detail description of the format.
- Since $(GM)^s$ and GM are often different, also the radii, geometrical scaling is inevitable with regards to the reference ellipsoid to which the geoid model is to be referred to eventually, in this research, the GRS80.
- Ensure that the text editor you are using is capable of opening the entire model, for example MS-Excel is limited to 65,536 rows by 256 columns.
- Often there is redundant information which may not be visible in your current view window, so sorting by columns prior to processing, while ensuring the software and hardware are capable of handling the sorting is a necessary stage. This removes what could be termed outliers in a GGM for gravity anomaly production.

5.3.2 Signal and Error Degree Variances for LSMS Method

The KTH LSMS method aims at obtaining optimal geoid height by minimizing in a least squares way all sources of errors. The errors emanate from surface terrestrial and GGM gravity anomaly data, assumed to be contaminated by random errors only, limitation of terrestrial data to a cap around the computation point, and the GGM resolution limited to say maximum degree M. To realize the goal, geoid height $\tilde{N}$ in Eq. (5.1) is minimized through the expected global mean square (MSE) error by seeking for the least error variance solution to the MSE expression in Eq.(5.21), which is detailed in Sect. 3.1. Unfortunately the solution requires knowledge of gravity anomaly error degree variances, of both terrestrial and GGM gravity data, not only limited to GGM maximum degree M but to infinity, (Sjöberg 1984a-b, 1986, 1991, 2003a-b, 2005b, Sjöberg and Hunegnaw 2000). For comprehension, a few important formulae are re-quoted inhere. For Eq. (5.1), the MSE is given by Eq. (3.19) for uncorrelated data as

$$m_{\tilde{N}}^2 = c^2 \sum_{n=2}^{\infty} \left\{ \left(\frac{2}{n-1} - Q_n^L - s_n^* \right)^2 \sigma_n^2 + \left(Q_n^L + s_n^* \right)^2 dc_n^* \right\}, \tag{5.21a}$$

where

$$s_n^* = \begin{cases} s_n & \text{if } 2 \le n \le L \\ 0 & otherwise \end{cases} \quad \text{and} \quad dc_n^* = \begin{cases} dc_n & \text{if } 2 \le n \le L \\ c_n & n > L \end{cases} \tag{5.21b}$$

where

$c = R/2\gamma$, σ_n^2 is the error degree variance of the terrestrial gravity anomaly, c_n is GGM gravity anomaly (signal) degree variance or power spectrum component and dc_n is error (noise) degree variance of the GGM gravity anomaly. For adaptation or more explicit expression, some of the terms in Eq. (5.21) are given below

$$\sigma_n^2 = E\left\{\frac{1}{4\pi}\iint_\sigma \left(\varepsilon_n^T\right)^2 d\sigma\right\} = \frac{1}{4\pi}\iint_\sigma \left\{\left(\varepsilon_n^T\right)^2\right\} d\sigma, \tag{5.22}$$

where $\{\ \}$ is statistical expectation, ε_n^T is the n[th] Laplace global terrestrial gravity anomaly error, c_n is GGM gravity anomaly signal degree variance, given as

$$c_n = \frac{1}{4\pi}\iint_\sigma \Delta g_n^2 d\sigma = \gamma^2 (n-1)^2 \sum_{m=0}^{n}\left(C_{nm}^2 + S_{nm}^2\right),\ \gamma = \frac{GM}{a^2}, \tag{5.23}$$

where Δg_n is the n[th] Laplace gravity anomaly in spectral form

$$dc_n = E\left\{\frac{1}{4\pi}\iint_\sigma \left(\varepsilon_n^{GGM}\right)^2 d\sigma\right\} = \gamma^2 (n-1)^2 \sum_{m=0}^{n}\left(\sigma_{c_{nm}}^2 + \sigma_{s_{nm}}^2\right), \tag{5.24}$$

where ε_n^{GGM} is the n[th] degree GGM gravity anomaly Laplace error

s_n are LS-modification parameters, cf. Sect. 3.1 and it is the way they are determined that leads to least error variance solution to the MSE and thence optimally estimated $\tilde{N}$. According to Eq. (5.21), summation involve σ_n^2 and c_n to infinity and the dc_n is confined to the kernel modification degree L. Given the numerical investigation and broad coverage conducted in Ågren (2004b Ch. 2), on three prominent degree variance models for their performance with GOCE (GGM) ultra high degree, we can conclude that the appropriate model to account for the GGM signal degree variances (c_n) for the degrees above the GGM maximum degree, is the Tscherning and Rapp 1974 Model as explained in Moritz (1980a). The GGM error degree variance dc_n, which is limited to the maximum degree of the GGM utilized, can be obtained from the GGM itself according to Eq. (5.24). For estimation of terrestrial gravity anomaly error degree variance σ_n^2 some assumptions about the global covariance function $C(\psi)$ of global gravity anomaly function and its properties have to be adopted as explained in Moritz (1980a Sect. 22). The assumptions concern, the error variance $C(0)$ usually denoted by C_0, i.e. the variance of $C(\psi)$, which characterizes the local behaviour of the covariance function. Correlation length $\psi/2$ defined as spherical distance for which $C(\psi/2) = C_0/2$.

Horizontal gradient variance G_0, which is related to vertical gradient variance by been $G_0/2$, demonstrates curvature behaviour of the function at $\psi = 0$. This problem was also investigated in Ågren (2004 Sect. 2.4.2) based on uncorrelated data (white noise) using band limited white noise error model and correlated (white and coloured noise) using reciprocal distance model with synthetic GOCE ultra high frequency data.

The band limited white noise model for uncorrelated data with constant degree-order variances is put forward (ibid) as

$$\sigma^2_{nm,\Delta g} = \frac{\sigma^2_{n,\Delta g}}{(2n+1)}, \tag{5.25}$$

up to Nyquist degree $n = M_N$; M_N is defined as $\pi/\Delta\phi$, where $\Delta\phi$ is the block size of the gravity anomaly grid in question, the number of potential coefficients between degree 2 and M_N is given by $(M_N+1)^2 - 4$ and the degree variances by

$$\sigma^2_{n,\Delta g} = \frac{\sigma^2}{(M_N+1)^2 - 4}(2n+1) \ , \tag{5.26}$$

where $\sigma^2 = C(0)$. Numerical tests up to M_N = 3600 were good, (ibid). The band limited white noise (BLWN) error model constructed for the AOI is given in Figure 5-16-A. The model portrays little power in the lower frequencies but gradually improves up to Nyquist degree M_N.

To be able to show presence of systematic errors (long-wavelength error, g_{L_λ}), a model with more power in the lower degrees is needed, such a model is the reciprocal distance covariance function of Moritz (1980a), which is also adapted with slight modification in Sjöberg (1986) for correlated data. The model has often been used to map terrestrial gravity anomaly errors in the application of LSMS method with reliable results by other researchers like Fan (1989), Nahavandchi (1998), Hunegnaw (2001), Ellmann (2004) and Kiamehr (2006a). The degree variances for degree two and above for the reciprocal distance covariance model are expressed by

$$\sigma^2_{n,\Delta g} = c(1-\mu)\mu^n, \quad 0 < \mu < 1, \tag{5.27}$$

where c and μ are constants, the $C(\psi)$ is given in closed form as

$$C(\psi) = c\left[\frac{1-\mu}{1-2\mu\cos\psi+\mu^2} - (1-\mu) - (1-\mu)\mu\cos\psi\right] \tag{5.28}$$

The covariance model in Eqs. (5.27) and (5.28) is the Sjöberg (1986) model, which differs from Moritz (1980a) by exclusion of degree zero and one terms. For the determination of parameters of this model, refer to quoted references. One drawback found with the model is that it has unrealistic small variances at higher degree (Ågren 2004), which implies unrealistic modelling of terrestrial data errors in the higher frequencies of the spectrum as witnessed in Figure 5-16-B. The problem can be alleviated by taking advantages of both models, so that they address at least the following requirements:

- preserve some of the white character of the noise, at the same time keeping the power below the Nyquist degree (M_N).
- yield degree-order standard errors that are realistic in higher frequencies and be able to model the situation even when the terrestrial data is contaminated by systematic errors, which ought to decrease with increasing degree (g_{L_λ} errors).

A model capable of modelling errors in all frequencies of the gravity data is needed; this is obtained by a simple combination of the two models as shown in Figure 5-16-C as curve "sig2n_dg_blwn+rd". The combined model has the same power as the reciprocal distance model for the lower part of the spectrum and more or less the same as the uncorrelated band limited white noise model in the high part of the spectrum up to the Nyquist degree (M_N). After the degree M_N, the degree variance drop down almost to zero as would be expected, and this combined error model is the one selected for the determination of modification parameters of the LSMS, but with its arguments determined from the AOI. Table 4-10 establishes mean, minimum and maximum accuracies of the surface gravity anomaly, with reference to GRS80 to be adopted in the absence of more realistic information. Therefore, in the combined error model, we have taken the maximum standard error $\sigma = 2.5$ mGal as standard error for both the reciprocal distance and band limited white noise error models prior to combining them. The surface anomaly grid interval in this research is one arc minute ($1'$), since M_N is defined as $\pi / \Delta\phi$, where $\Delta\phi$ is the block size then M_N is obtained as 10,800. To minimize correlation, only the satellite GGM is used, the selected pure satellite model (Sect. 4.3.4 and 5.2.3) for this research is ITG-GRACE03S up to degree 120, hence this model up to maximum degree 120 is used to determine signal and error degree variances for the determination of modification and truncation parameters.

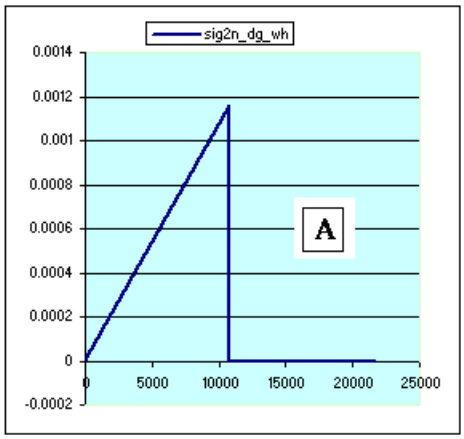

Graph of BLWN

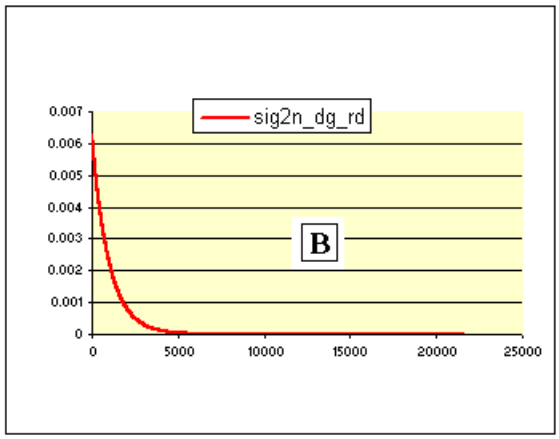

Graph of RD

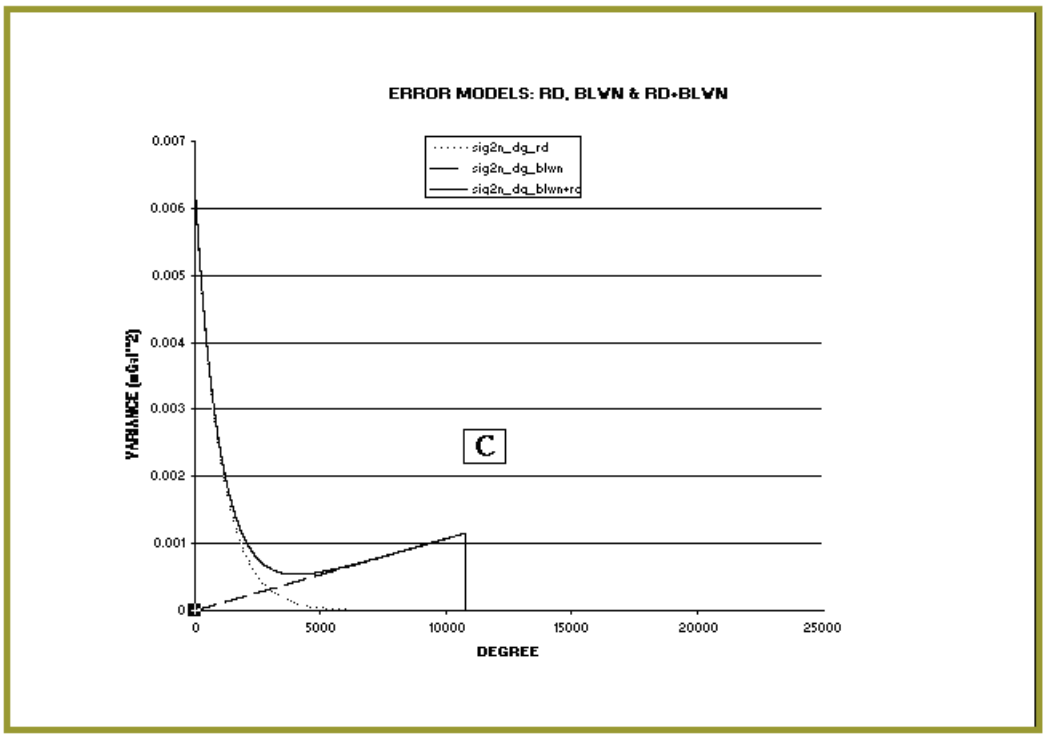

BLWN=Band Limited White Noise, RD=Reciprocal Distance

Figure 5-16: Selection of signal and error degree variance model. The continuous curve in part C is the combined error model BLWN_RD

5.3.3 Computation of Unbiased LSMS Parameters

Given the descriptions for error models in Section 5.3.2, GGM noise degree variance dc_n is computed from Eq. (5.24) i.e. using GGM itself. The GGM signal degree variance c_n and terrestrial data noise degree variance σ_n^2 are computed by the combined and the Tscherning and Rapp (1974) error models explained in Sect. 5.3.2. Since geoid model has more power in the lower degrees, when band limited white noise (BLWN) error model is

used alone to compute modification parameters, we obtain unrealistic low geoid model MSE. If we use reciprocal distance error model (RD) itself the results look more realistic, but as seen from Figure 5-16-B, the model has unrealistic small values in the higher frequencies. The results upon using combined error model are not very different from those of the RD model, but given the circumstance in Figure 5-16-C, it represents the actual situation better than the other two. Therefore the LS-modification parameters are computed using the combined error model - BLWN_RD, and they are displayed in Figure 5-17 as continuous curve. Numerical tests using parameters of the AOI and the selected satellite only GGM for the three error models are portrayed in Table 5-10.

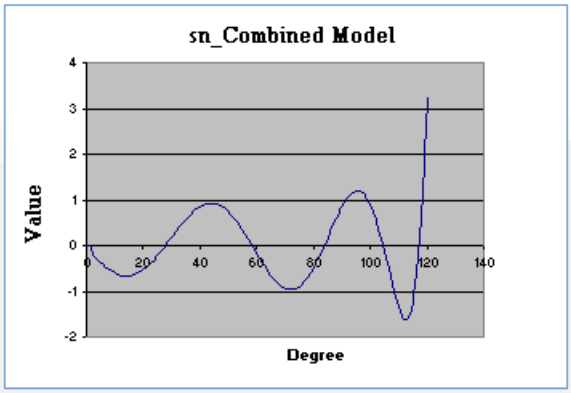

Figure 5-17: Modification parameters s_n of LSMS according to the combine (BLWN_RD) error degree variance model

Table 5-10: Geoid height RMS (mm) computed from three error models BLWN, RD and combined BLWN_RD, for signal and error degree variances for the selection of suitable modification parameters of the unbiased LSMS. See Sect. 5.3.2.

Model	**Band Limited White Noise (BLWN)**				**Reciprocal Distance (RD)**				**Combined (BLWN_RD)**			
Source → **Degree ↓**	Total	Ground	GGM	Trunc.	Total	Ground	GGM	Trunc.	Total	Ground	GGM	Trunc.
All	**5.06**	5.04	0.14	0.41	**49.29**	47.82	5.51	10.61	**49.21**	47.92	1.93	19.3
2-M	2.14	2.14	0.14	0.00	28.11	27.56	5.5	0.00	27.4	27.38	1.13	0.00
(M+1)-L	0.00	0.00	-	0.00	0.00	0.00	-	0.00	0.00	0.00	-	0.00
(L+1)-∞	4.58	4.56	-	0.41	40.49	39.08	-	10.61	40.88	39.33	-	11.13

For the AOI: Given SErr, $\sigma = 2.5\ mGal$ and $M_N = 10{,}800$

Chapter Six

COMPUTATION OF TANZANIA GRAVIMETRIC GEOID MODEL, TZG08

Computation of the New Geoid model of Tanzania 2008 – (TZG08) is by the KTH method of LSMS with AC as described in the previous chapters.

6.1 Approximate Geoid height $\tilde{N}$

We explained in Sect. 3.1, that the geoid height computation by the LSMS with AC has two main contributions: first part A, which is computed from the modified part of the formula, i.e. LSMS, and part B from the additive corrections (AC). When the two parts are put together, they provide us with the sought geoid model. Determination of part A is also divided into two components, one is computed from the qualified GGM gravity anomaly data defined on the MEE, as recommended in Sect. 3.2 (d) and the other from terrestrial surface gravity anomaly, that is long and short-wavelengths components of the geoid model respectively. Computation of AC will follow the approaches described in Sect. 3.2 (a-d).

6.1.1 N - Approximate from GGM ITG_GRACE03S_120

Reference is made to Eq. (3.14), where we use the second term on the right hand side (RHS) of the equation to determine the long-wavelength component of the geoid model $\tilde{N}_L^A$ as

$$\tilde{N}_L^A = c\sum_{n=2}^{M}\left(Q_n^L + s_n^*\right)\Delta\hat{g}_n^S \tag{6.1}$$

ITG_GRACE03S was qualified in Sect. 4.3.4 as the best pure satellite GGM of the present time for the AOI. To avoid data correlation, pure satellite GGM is used as entailed in Sect. 3.1. Outcome of computation of $\tilde{N}_L^A$ is portrayed in Figure 6-1 plotted from $1'\times 1'$ geoid height resolution grid, with the following statistics in unit of metre: mean -18.051, minimum -34.347, maximum -6.372 and standard error 6.052.

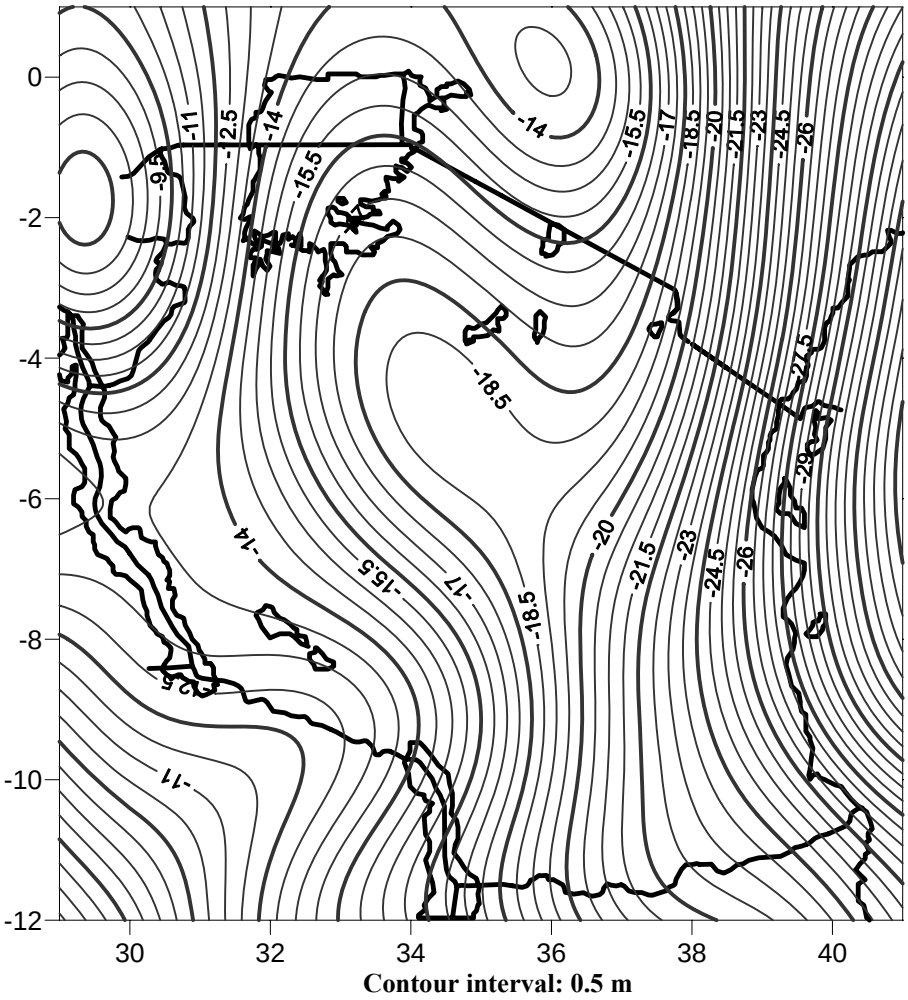

Figure 6-1: Approximate geoid model from pure satellite ITG-GRACE03S_120

6.1.2 N - Approximate from Terrestrial Surface Gravity

Reference is made to Eqs. (3.14)/Eq. (5.1). The first term on the left hand side (RHS) of Eq. (5.1) is used to compute the approximate short-wavelength component of the geoid model $\tilde{N}_S^B$ as

$$\tilde{N}_S^B = c\sum_{n=2}^{\infty}\left(\frac{2}{n-1} - Q_n^L - s_n^*\right)\Delta\hat{g}_n^T \tag{6.2}$$

The surface gravity anomaly used is the $1'\times 1'$ gridded point gravity data of the AOI, patched by EIGEN-CG03C, via RTE and ITG_GRACE03S, and merged with equivalent marine file as detailed in Sect. 5.2. $\tilde{N}_S^B$ is computed at $1'\times 1'$ resolution, and is displayed in Figure 6-2 as geoid height contour map of interval 0.5 m with the following statistics in metre: mean 0.151, minimum -3.732, maximum 3.691 and standard error 0.977.

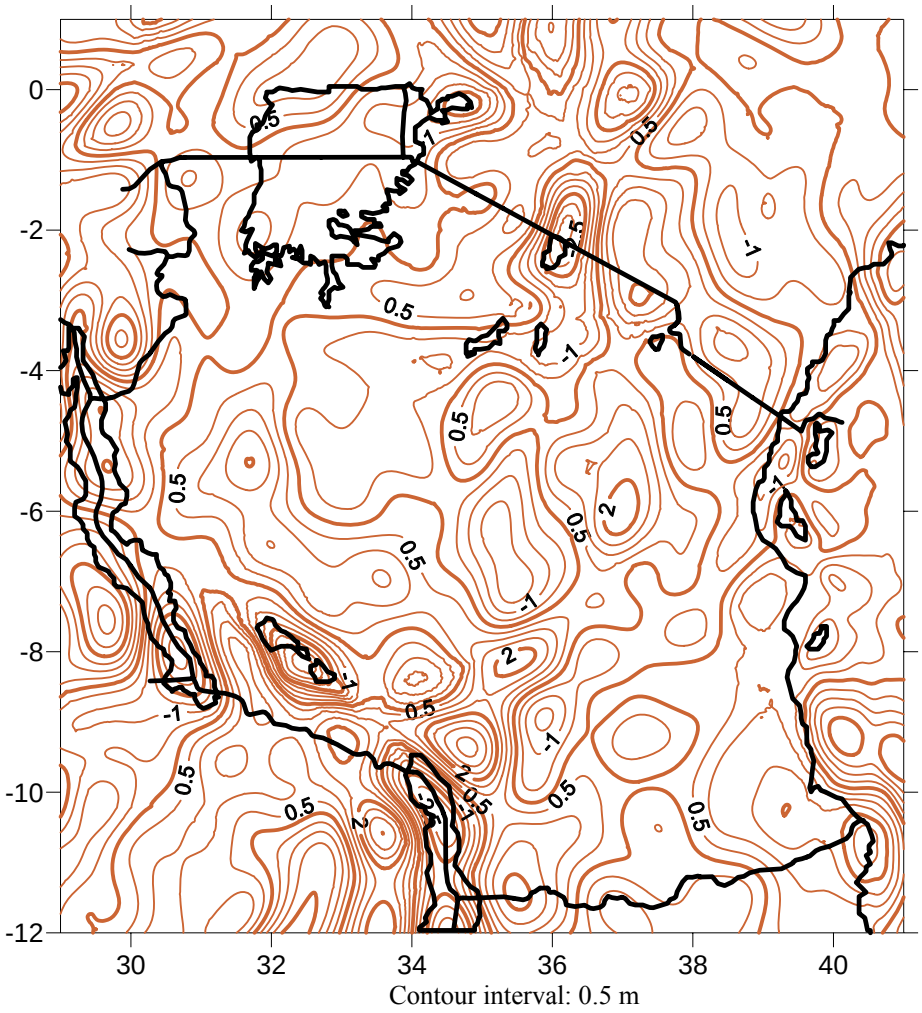

Figure 6-2: Short-wavelength geoid model component from $1' \times 1'$ surface gravity anomaly

Approximate Geoid Model by the KTH LSMS without Additive Corrections $\tilde{N}$

The approximate short and long wave components of the geoid model, i.e. $\tilde{N}_L^A$ and $\tilde{N}_S^B$ as computed above, are merged to form the approximate geoid height $\tilde{N}$ described in Sect. 3.1 and expressed by Eqs. (3.14)/Eq. (5.1). The statistics of $\tilde{N}$ in metre are: ean -17.900 m, minimum -34.122, maximum -5.803, standard error 6.114 and RMS 18.915. $\tilde{N}$ is presented in Figure 6-3 as geoid height contour map at 0.5 m contour interval. One can see that this map is much more detailed than the pure long-wavelength geoid model map of Figure 6-1.

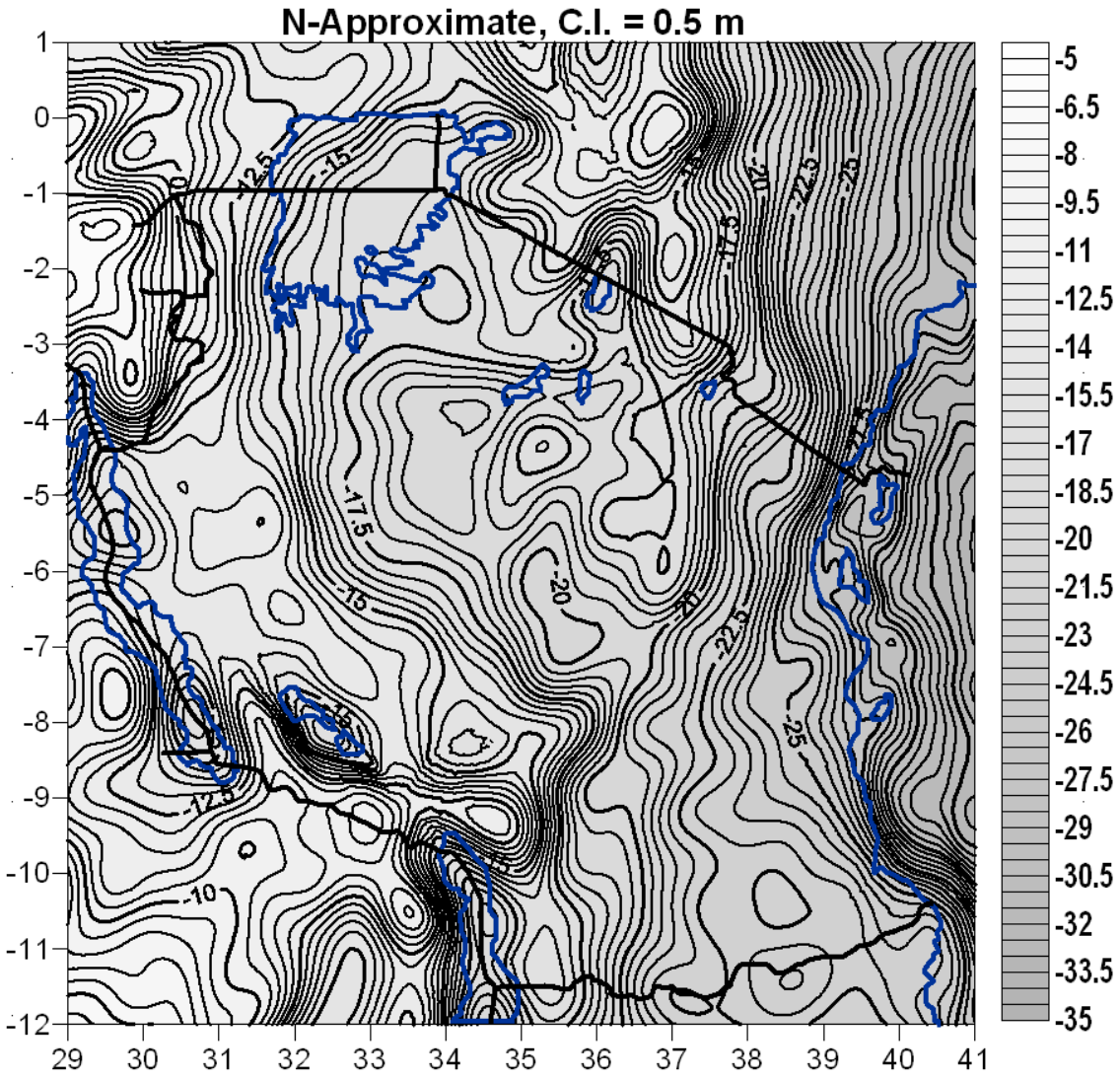

Figure 6-3: Approximate Tanzania geoid model in metre without additive corrections

6.2 Additive Corrections (AC) to $\tilde{N}$

The theory of this part is given in Sect. 3.2. The corrections are:

i. Combined topographical effects on the Geoid model, δN^{t}_{comb} which is obtained by adding corresponding direct and indirect effect for the same point at the geoid model

$$\delta N^{t}_{comb}(P) = \delta N_{dir}(P) + \delta N_{I}(P) \tag{6.3}$$

ii. Downward continuation effect δN^{P}_{dwc}. In Sect. 3.2 (b) it was decided, that δN^{P}_{dwc} should be separated into two parts so that

$$\delta N^{P}_{dwc} = \delta N^{P}_{dwc,1} + \delta N^{P}_{dwc,2} \tag{6.4}$$

Sum of combined topographic effects and downward continuation effect for the same point on the geoid model is termed total topographic correction δN^t_{tot}, i.e.

$$\delta N^t_{tot}(P) = \delta N^t_{comb}(P) + \delta N_{dwc}(P) \tag{6.5}$$

iii. Direct and indirect atmospheric effects δN^a_{comb}

iv. Ellipsoidal Correction δN_e

6.2.1 Combined Topographic Correction δN^t_{comb}

Since the DEM in use is the dense SRTM, and thus fairly good representative of the topography in the AOI, practical computation of Eq. (3.39) is carried out using (Sjöberg 2007) given below as

$$\delta N^t_{comb} = -\frac{2\pi\mu}{\gamma_0} H^2 - \frac{4\pi\mu H^3}{3R}, \tag{6.6}$$

where H is topographic height of the point in question, R is the mean radius of the Earth and the rest of the symbols retain their previous meanings. The statistics of the results in metre are: Mean -0.144; Min -3.657; Max 0.000; SErr 0.142 and RMS 0.202. Pictorially the effect is represented in a map of contour interval 0.1 m and its surface in Figure 6-4.

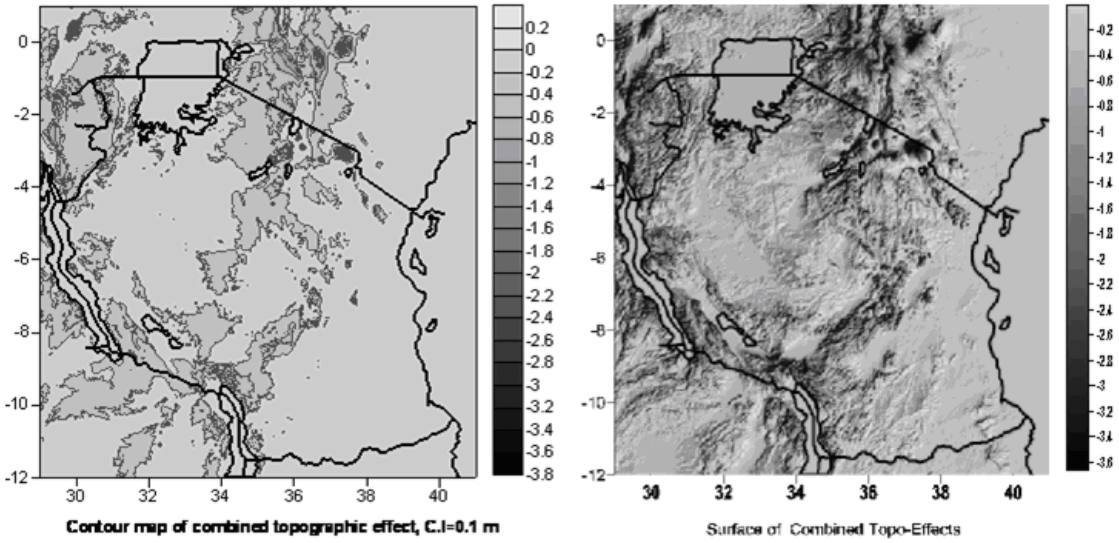

Figure 6-4: Combined topographic corrections in contour and surface form

6.2.2 Downward Continuation Correction δN^P_{dwc}

Further to having δN^P_{dwc} in two parts, $\delta N^P_{dwc,2}$ is separated into two constituents. Hence δN^P_{dwc} is computed in three stages as explained in Sect. 3.2 (b), thus

$$\delta N^P_{dwc} = \delta N^P_{dwc,1} + \delta N^P_{dwc,2.1} + \delta N^P_{dwc,2.2} \tag{6.7}$$

Although from Eq. (3.43) it appears that, both components have all the frequencies of the gravity spectrum, but the fact is, $\delta N^P_{dwc,1}$ contributes mainly to the short-wavelengths, whereas a good part of $\delta N^P_{dwc,2}$ constitutes long-wavelengths, except in the vicinity of the CP where $\delta N^P_{dwc,2.1}$ is mainly of short-wavelength character, cf. Sect 3.2. Thus, $\delta N^P_{dwc,1}$ and $\delta N^P_{dwc,2.1}$ are referred to as short-wavelength component and $\delta N^P_{dwc,2}$ as long-wavelength part. In addition to the previous preparation conducted, e.g. determination of LSMS modification parameters and Molodensky's truncation coefficients, a grid file of gravity anomaly gradients is required also; this is computed according to Eq. (3.45b). Gravity anomaly gradient effect is tested for two different computation distances, $\psi_0 = 1^\circ$ and $\psi_0 = 3^\circ$ to assess its spatial variation, since the effect is expected to decay fast with increasing computational distance (CD). Statistics of each of δN^P_{dwc} and its three components are displayed in Table 6-1

Table 6-1: Statistics of the downward continuation effect (DWC) on geoid height from its three components as explained in Sect. 3.2 (b) and its variation with gravity anomaly gradient computation distance (CD) $\psi_0 = 1^\circ$ and $\psi_0 = 3^\circ$ in metre

	DWC for CD $\psi_0 = 1^\circ$				DWC for CD $\psi_0 = 3^\circ$			
	$\delta N^P_{dwc,1}$	$\delta N^P_{dwc,2.1}$	$\delta N^P_{dwc,2.2}$	δN^P_{dwc}	$\delta N^P_{dwc,1}$	$\delta N^P_{dwc,2.1}$	$\delta N^P_{dwc,2.2}$	δN^P_{dwc}
Mean	-0.002	-0.006	0.005	**-0.002**	-0.002	-0.007	0.005	**-0.003**
Min	-0.591	-0.098	-0.133	**-0.661**	-0.590	-0.133	-0.133	**-0.662**
Max	3.593	0.069	0.048	**3.497**	3.614	0.074	0.048	**3.514**
SErr	0.044	0.007	0.018	**0.038**	0.045	0.008	0.018	**0.039**
RMS	0.044	0.009	0.019	**0.039**	0.045	0.011	0.019	**0.039**

We observe from Table 6-1, that in spite of tripled computational distance of the gravity anomaly gradient, its effect on the downward continuation correction on the geoid height is insignificant, but the increased computational time is enormous. Therefore it is concluded, that computational distance of ψ_0 equal to 1° is quite adequate for gravity anomaly gradient. Figure 6-5 shows surfaces of the three components of DWC correction and Figure 6-6 is the contour and surface of the total downward continuation effect on the geoid height.

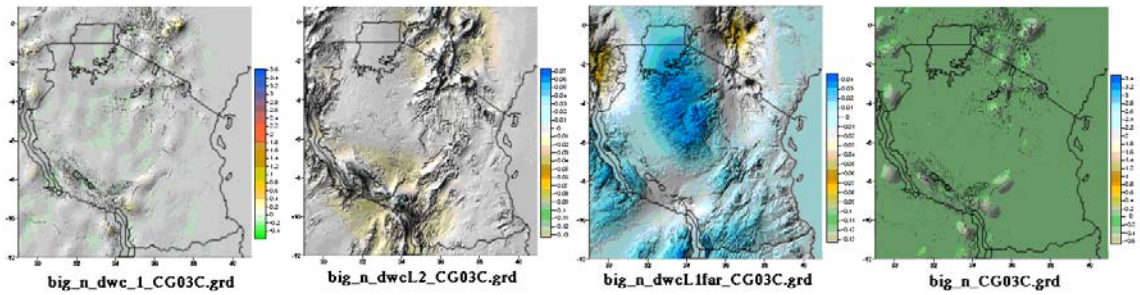

Figure 6-5: δN^{P}_{dwc} and its components is shown pictorially from left to right above as follows: $\delta N^{P}_{dwc,1}$, $\delta N^{P}_{dwc,2.1}$, $\delta N^{P}_{dwc,2.2}$ and δN^{P}_{dwc} in metre. δN^{P}_{dwc} is given in bigger scale in Figure 6-6 below

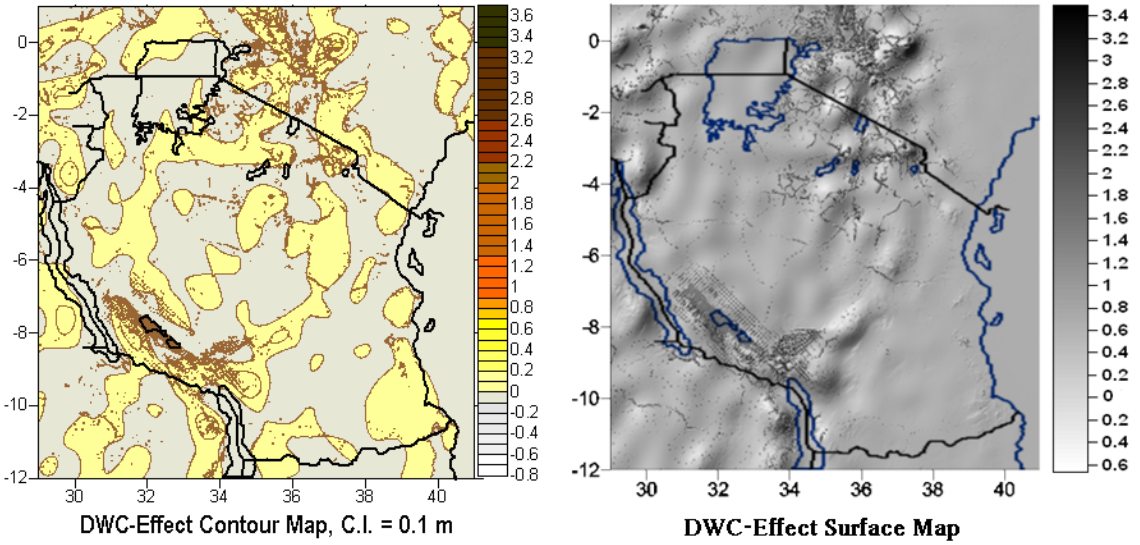

Figure 6-6: Downward continuation effect on the geoid height in contour and surface map in metre.

Total Topographical Effect δN^{t}_{tot}

When combined topographical and the downward continuation effects are put together according to Eq.(3.55), we get δN^{t}_{tot}, which has the following statistics in metre in the AOI: Mean -0.146; Min -3.513; Max 1.177, SErr 0.132 and RMS 0.196. The δN^{t}_{tot} is given as contour and relief maps in Figure 6-7. The location where the maximum absolute effect occurs is around Mt. Kilimanjaro, and this part is enlarged and displayed in the middle of Figure 6-7.

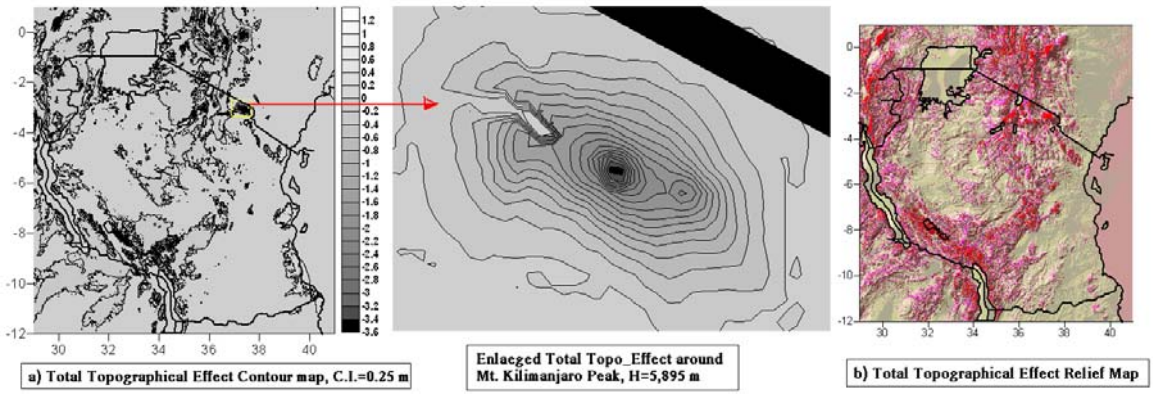

Figure 6-7: Total topographic effect, δN^{t}_{tot} in contour and relief maps with enlarged filled in contours around Mt. Kilimanjaro (5,895 m). Observe the black colour at the middle, signifying that δN^{t}_{tot} is ~ -3.5 m

6.2.3 Combined Atmospheric Correction, δN^{a}_{comb}

In Sect. 3.2 we arrived at Eq. (3.56) as the model for atmospheric effects. Numerical tests carried out show, that around the equator, the effect is at centimetre level. Thus for δN^{a}_{comb} correction, we use Sjöberg and Nahavandchi (2000) model given as

$$\delta N^{a}_{comb}(P) = -\frac{2\pi R\rho_0}{\gamma}\sum_{n=2}^{M}\left(\frac{2}{n-1} - Q^{L}_{n} - s_n\right)H_n(P) - \frac{2\pi R\rho_0}{\gamma}\sum_{n=M+1}^{\infty}\left(\frac{2}{n-1} - \frac{n+2}{2n+1}Q^{L}_{n}\right)H_n(P), \quad \ldots (6.8)$$

where ρ_0 is atmospheric density at sea level, $H_n(P)$ is the n^{th} spherical harmonic of global topographic height at surface point P. The rest of the symbols maintain the previous meanings. Result of numerical computation using Eq. (6.8) over the AOI has the following statistics in mm: Mean 1.2; Min -4.5; Max 4.3; SErr 1.1 and RMS 1.7.

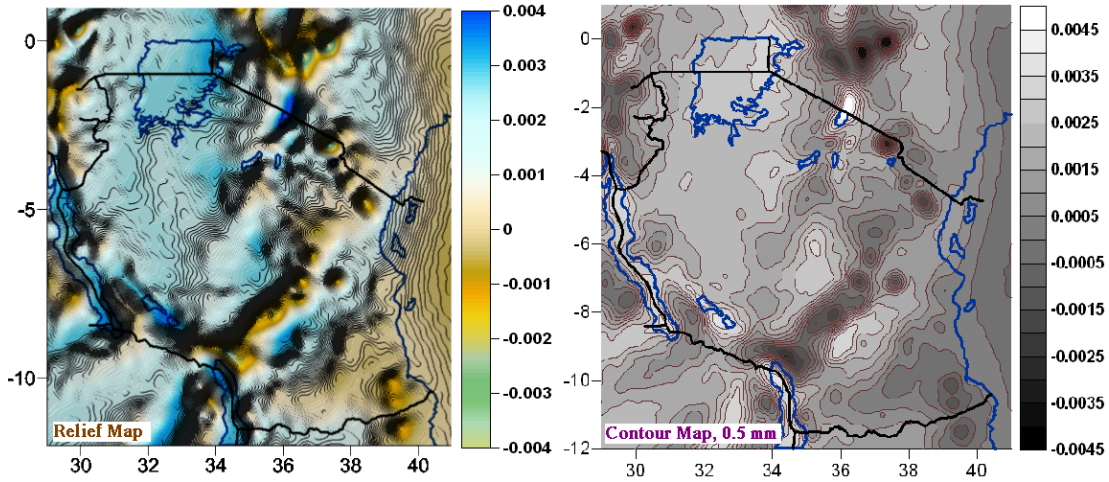

Figure 6-8: Total atmospheric correction in metre

6.2.4 Ellipsoidal Correction δN_e

Ellipsoidal correction to geoid height as additive correction to approximate geoid model by LSMS is explained in Sect. 3.2 (d) and is computed according to Eq. (3.72). The results have the following statistics in mm: Mean 0.5, Min 0.1, Max 1.2, SErr 0.2 and RMS 0.6, showing that the corrections are insignificant, mainly because the GGM gravity anomaly was computed on the MEE instead of MES as recommended in Sjöberg (2004c). Besides for all computations, radius of the MES has been selected so as to coincide with the GRS80 at a point close to middle of AOI which will lead to minimum departure at its edges and consequently minimum δN_e corrections. The results are portrayed Figure 6-9

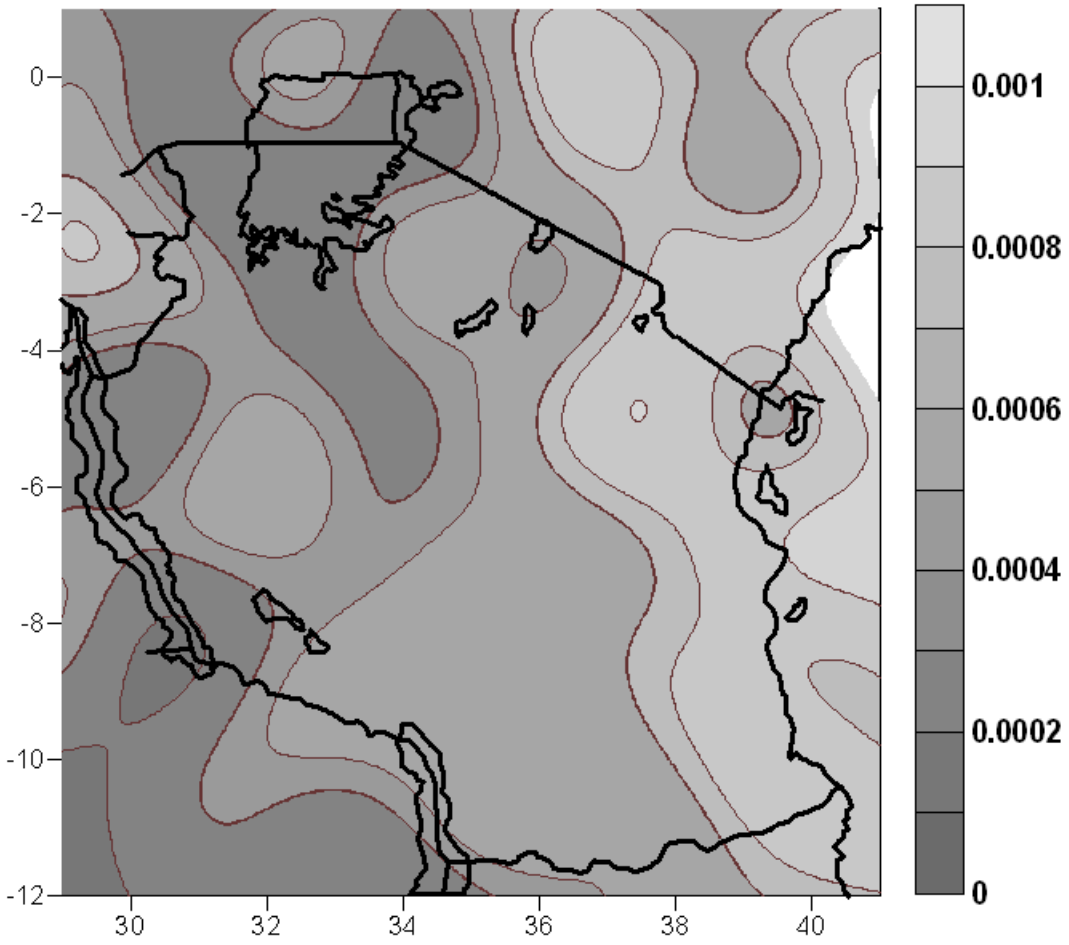

Figure 6-9: Ellipsoidal correction in metre.

Additive Correction AC

The additive correction to the approximate geoid model $\tilde{N}$ is obtained out of its separate components as

$$AC(P) = \left\{ \delta N^{t}_{tot}(P) + \delta N^{a}_{comb}(P) + \delta N_{e}(P) \right\} \tag{6.9}$$

The computed AC has the following statistics in metre: Mean -0.144, Min -3.516, Max 1.174, SErr 0.132 and RMS 0.195 and is displayed in Figure 6-10

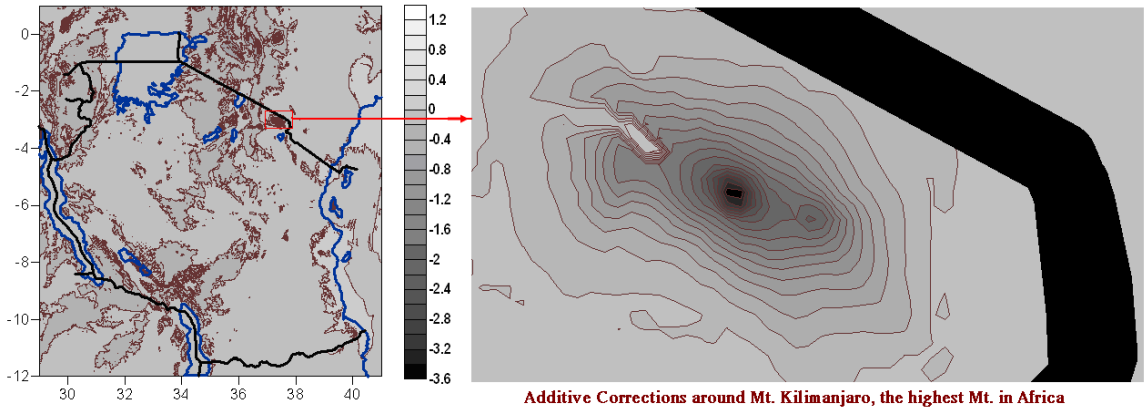

Figure 6-10: Total additive corrections for TZG08 in metre, with enlarged situation around Mt. Kilimanjaro.

6.3 Tanzania Geoid model -TZG08: Geoid height $\hat{N}$

Tanzania geoid model 2008, TZG08, has been computed as described in chapter 3, using LSMS with AC. In Sect. 6.1 the approximate geoid model of Tanzania ($\tilde{N}$) was computed from terrestrial surface point gravity anomalies and pure GGM ITG-GRACE03S to degree and order 120. Densification of terrestrial surface point gravity anomaly based on specially designed remove-compute-restore (r-c-r) approach, using combined GGM EIGEN-CG03C to degree and order 360 was carried out in Sect. 5.2. Each of the additive corrections (AC) described in Sect. 3.2 was computed in Sect. 6.2 separately and at the end put together.

At this juncture, TZG08 can be assembled as a sum of the approximate geoid model, $\tilde{N}$ computed in Sect. 6.1 and the additive corrections (AC) computed in Sect. 6.2, i.e. TZG08 geoid model ($\hat{N}$) is formed as

$$\hat{N}(P) = \tilde{N}(P) + AC(P) \tag{6.10}$$

Statistics of Tanzania geoid model TZG08 ($\hat{N}$) in unit of metre are: Mean -18.044, Min -34.122, Max -6.115, SErr 6.031 and RMS 19.025. The geoid model is portrayed in Figure 6-12 as surface and contour maps, respectively.

Overview of Determination of Geoid Model of Tanzania (2008), TZG08

The TZG08 geoid model of Tanzania is referred to GRS80 and has been computed by the KTH LSMS with AC, a precise geoid model determination method cf. Ch. 3. Among the qualities of LSMS with AC is, that it avoids gravity reduction. The geographical boundaries are latitude $29^{\circ}E$ *to* $41^{\circ}E$ and longitude $1^{\circ}N$ *to* $12^{\circ}S$ with grid resolution of

$1' \times 1'$. All the land gravity data was standardized to IGSN71 and referred to GRS80. The data used to compute the geoid model comprise of the following data sets:

1. After cross validation (XV) and statistical testing at 99 % confidence level of 40,350 data points, 39,722 clean point land surface gravity anomaly were retained.
2. For marine area, we commenced with 7,843 ship track points and 51,935 - $2' \times 2'$ KMS02 mean surface gravity anomalies, they were combined, XV and statistically tested at 99 % confidence level, as a result 57,723 marine data were retained. Thus in total 97,445 clean terrestrial gravity points in land and sea were used to determine $1' \times 1'$ surface gravity anomaly grid for determination of short-wavelength part of TZG08 geoid model.
3. CHAMP and GRACE GGM EIGEN-CGO03C combined GGM to degree and order 360 qualified to patch the voids in the AOI (cf. Sects.4.3 and 7.2) using specially designed r-c-r approach (cf. Sect. 5.2).
4. GRACE GGM ITG-GRACE03S pure satellite GGM to degree and order 120 qualified to determine modification and truncation parameters by LSMS method also to compute the un-correlated long-wavelength component of the TZG08 geoid model; cf. Sects. 4.3.4, 3.1, 5.3, 6.1.1 and 7.2.
5. SRTM $3''$,$15''$, $30''$,$1'$ and $6'$ were used at different stages, which include, densification for spline – interpolation in the innermost part around the computation point (CP), computation of residual terrain effects (RTE) - the short-wavelength part of gravity signal, gravity anomaly gradient for additive corrections and reference mean surface for RTE determination.
6. Constant upper topographic density of $2.67 g.cm^{-3}$; better density model could not be obtained.
7. Absolute reference gravity and GPS/Levelling data were used for evaluation and qualification of GGMs and the computed geoid model; cf. Sects. 4.3 and 7.2.

Normal height was determined for all the land gravity stations to compute point surface gravity anomaly; see Sect. 4.1.3. Extra care was exercised during merging of land and marine gravity to avoid compromising data quality on either part; cf. Sect. 5.2.5.

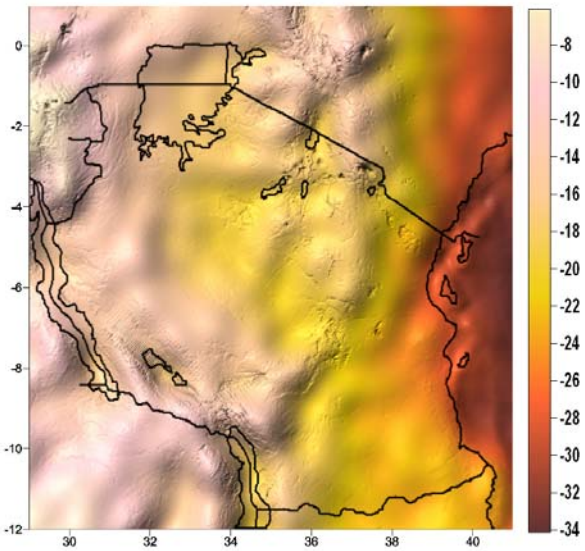

Figure 6-11: Surface map of Tanzania geoid model, TZG08. Unit is metre.

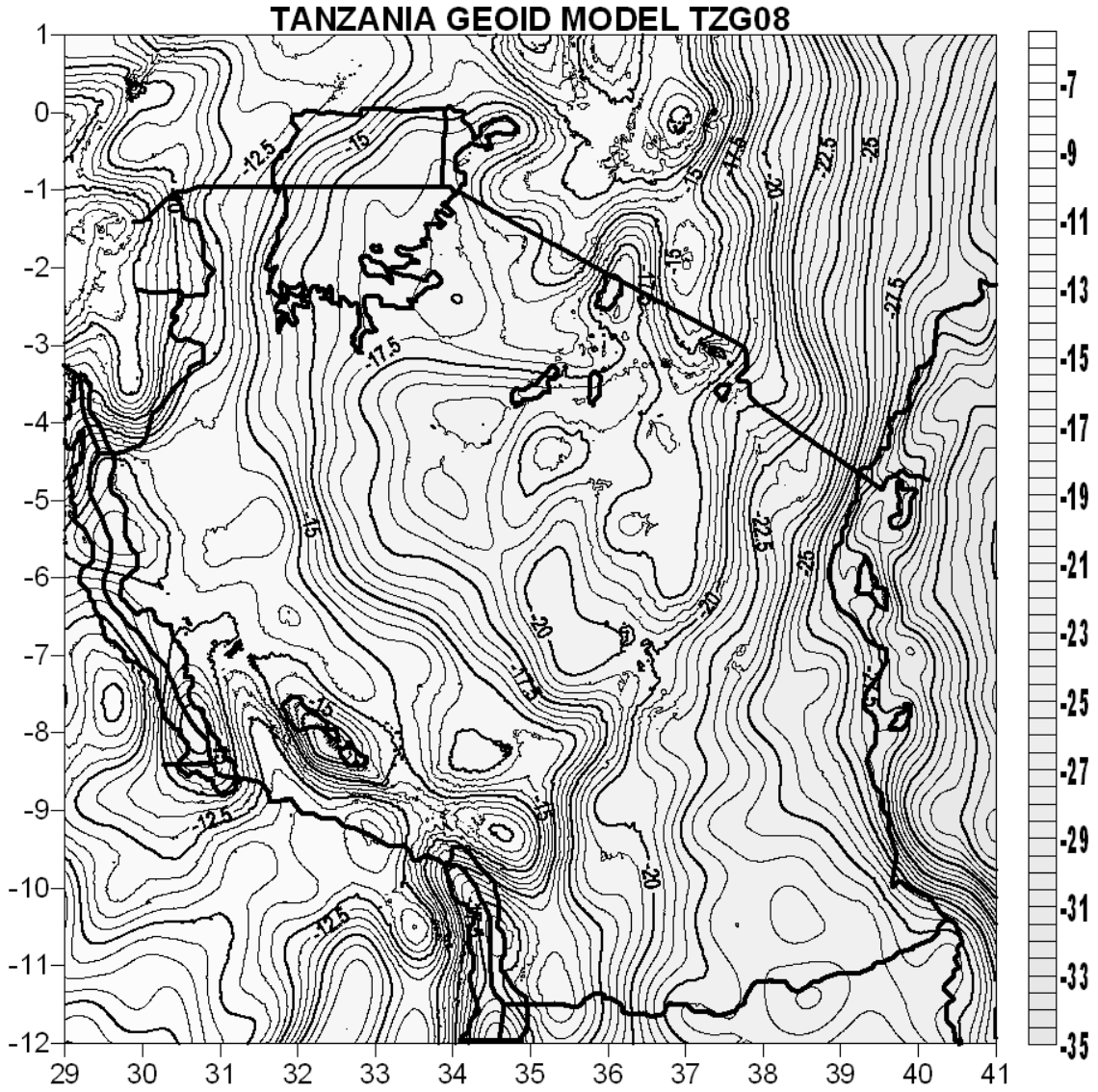

Figure 6-12: Contour map of geoid model of Tanzania 2008 –TZG08 geoid model. Contour interval is 0.5 m

An evaluation of TZG08 geoid model is carried out in the next chapter.

Chapter Seven

EVALUATION OF TANZANIA GEOID MODEL, TZG08

An overview of the existing geoid models of Tanzania was given in the introductory chapter Sect. 1.1.2, and summarized in Sect. 1.4. It was concluded that only one geoid model correctly represents the geoid of Tanzania, even though crudely evaluated, it is the Olliver (2007) model TZG07, with relative standard error based on the astrogeodetic profile conducted in 1984 of ~ 47 cm. Though the EGM96 and EGM2008 geoid models exist for Tanzania as for the rest of the world, their specific evaluation for Tanzania has not been conducted, but only global statistics are available; cf. Table 4-16, and as we saw in Sect. 4.3.3, it is very doubtful to bank on the global estimates. Since the models are available, it is one of the intentions of this chapter to analyze them in the Tanzanian context along with the newly determined TZG08 geoid model. We would do the same for AGP2006 and TZG07 geoid models, but the models are not within our reach. Evaluation of the GGMs in Sects. 4.3.3 and 5.2.3 based on the reference and terrestrial point gravity data respectively, will be complemented in Sect. 7.2 along with the evaluation of TZG08 using GPS/levelling.

7.1 Assessment of TZG08 Accuracy by Error Propagation

In this section errors from different sources of determining geoid heights are propagated and expressed in the form of RMS values. From Sect. 3.1, we saw that the LSMS depends on the optimization of Eq. (3.19), and based on this approach we get the modification parameters. Eq. (3.19) is a function of data input which are the pure GGM; ITG-GRACE03S to degree and order 120 and terrestrial surface gravity anomaly. Moreover it requires signal and error degree variances of the GGM and terrestrial gravity anomaly, both at $1' \times 1'$ resolution grid, this was carried out in Sect. 5.3.3 after close analysis of the best error model in Sect. 5.3.2. The results are given in Table 5-10 based on the least squares optimization of Eq. (3.19), and computed for three error models, namely band limited white noise (BLWN), reciprocal distance (RD) and combined BLWN_RD. The results are given as RMS values for the different contributors at different spectral degrees, where degree 21,600 is regarded as infinity. Lastly all are put together as the total RMS error budget in millimetre. Despite the lowest RMS values from the BLWN, the combined BLWN_RD is the one selected for the development of TZG08 given its overwhelmingly properties when compared to the other two separately as discussed in Sect. 5.2.3. From Table 5-10, we get the overall RMS values for the TZG08 with respect to the three error models above in the same order of appearance as 5.1 mm, 49.3 mm and 49.2 mm. The 5 mm RMS error from the BLWN is surely unrealistic. Although the combined error model has slightly smaller RMS value, still the ~ 5 cm RMS is being optimistic, foremost, because it does not involve the errors of the

additive corrections (AC). Therefore for more realistic evaluation, we have to depend on independent external measure, the practice is to compare gravimetric and GPS/levelling geoid heights, and this is continued in the next section.

7.2 External Accuracy Assessment of GGMs and the Geoid Model

Combination of three heights from GNNS e.g. GPS, levelling and a gravimetric geoid model, continuously is finding useful applications in various geodetic practices although basically the three heights are different in many ways, ranging from physical meaning, reference surface, realization to accuracy. The basic geometrical formula which unite them is

$$h - H - N^G = 0, \tag{7.1}$$

where h is ellipsoidal height from, say GPS, H is orthometric height from levelling and N^G is geoid height usually from gravimetry. In practice Eq. (7.1) is never satisfied due to a number of factors like:

a) Random errors of the three heights h, H and N^G.
b) Datum and other deficiencies in the systems of the three heights.
c) Failure to model adequately the intended situations including approximations thereof.
d) Different type of deformations which can affect the coordinate reference systems, datums and monuments.

Close analysis of misclosure of Eq. (7.1) can lead to different geodetic applications (Fotopoulos 2003). For our immediate interest, we will use it for

- Evaluation of local and regional gravimetric geoid model performance.
- Evaluation and selection of a suitable GGM in the AOI.
- Determination of optimal height transformation parameters (corrector surface) for conversion of GPS height to orthometric height i.e. between geoid model surface and the existing levelling datum.

Bullets 1 & 2 are subjects of this section, and the last bullet is dealt with in Ch.8.

For a given network with triple data h, H and N^G in each of its n points we can write

$$\Delta N_i = N_i^{GL} - N_i^G = \left(h_i - H_i\right) - N_i^G = \mathbf{a}_i\mathbf{x} + \varepsilon_i;\ \ i = 1, 2, ..., n \tag{7.2}$$

or in matrix form as

$$\Delta\mathbf{N} = \mathbf{A}\mathbf{x} + \boldsymbol{\varepsilon}, \tag{7.3}$$

where ΔN_i is the difference between geometrical geoid height N_i^{GL} (i.e. ellipsoidal height h_i minus levelled/orthometric height H_i) and gravimetric geoid height N_i^G or in short $\Delta\mathbf{N}$ is the $n \times 1$ misclosure vector. $\mathbf{A}$ is a $n \times m$ matrix of known coefficients, $\mathbf{x}$ is a $m \times 1$ vector of unknown parameters, $\boldsymbol{\varepsilon}$ is a random noise vector,

ε_i is combined random error for the triple heights $\left(h_i, H_i, N_i^G\right)$ at a particular point p_i. Systematic effects including datum inconsistencies are assumed to be contained in the parametric part of Eq. (7.3) i.e. in $\mathbf{Ax}$. Depending on the cited or intended systematic effects to be explored, 3-, 4-, 6- and 7- similarity transformation parameter models are often used to map the situation. The model equations are as follows (Benahmed-Daho et al. 2005); the 3-parameter model is given as

$$\mathbf{a}_i\mathbf{x} = \left(\cos\phi_i \cos\lambda_i\right) x_1 + \left(\cos\phi_i \sin\lambda_i\right) x_2 + \left(\sin\phi_i\right) x_3 , \tag{7.4}$$

whereas the 4-parameter model is given by

$$\mathbf{a}_i\mathbf{x} = \left(\cos\phi_i \cos\lambda_i\right) x_1 + \left(\cos\phi_i \sin\lambda_i\right) x_2 + \left(\sin\phi_i\right) x_3 + x_4 , \tag{7.5}$$

the 5-parameter model is

$$\mathbf{a}_i\mathbf{x} = \left(\cos\phi_i \cos\lambda_i\right) x_1 + \left(\cos\phi_i \sin\lambda_i\right) x_2 + \left(\sin\phi_i\right) x_3 + \left(\sin^2\phi_i\right) x_4 + x_5 , \tag{7.6}$$

while the 7-parameter model is

$$\begin{aligned}\mathbf{a}_i\mathbf{x} = {} & \left(\cos\phi_i \cos\lambda_i\right) x_1 + \left(\cos\phi_i \sin\lambda_i\right) x_2 + \left(\sin\phi_i\right) x_3 + \\ & \left(\frac{\cos\phi_i \cos\lambda_i \sin\phi_i}{\sqrt{1 - e^2 \sin^2\phi_i}}\right) x_4 + \left(\frac{\cos\phi_i \sin\phi_i \sin\lambda_i}{\sqrt{1 - e^2 \sin^2\phi_i}}\right) x_5 + \left(\frac{\sin^2\phi_i}{\sqrt{1 - e^2 \sin^2\phi_i}}\right) x_6 + x_7 ,\end{aligned} \tag{7.7}$$

where $\left(\phi_i, \lambda_i\right)$ are geodetic coordinates of mesh of points p_i with triplet height data h_i, H_i *and* N_i^G and e is the first eccentricity of the reference geodetic surface, in our case GRS80. The parameters $x_1 \rightarrow x_7$ constitute the vector $\mathbf{x}$ of the sought systematic effects. By using one of the opted transformation model of Eqs. (7.4) to (7.7) in Eq. (7.3) we get

$$\mathbf{Ax} = \Delta\mathbf{N} - \boldsymbol{\varepsilon} \tag{7.8}$$

Eq. (7.8) can be solved by least squares technique (LS). This is by optimizing the least squares criterion $\boldsymbol{\varepsilon}^*\boldsymbol{\varepsilon} = minimum$, constrained by the observation Eq. (7.8). Ideally, the individual residuals should be weighted, but this is hardly carried out. For uniformly weighted errors, the LS gives the best estimates for the parameters and errors (i.e. $\hat{\mathbf{x}}$ and $\hat{\boldsymbol{\varepsilon}}$) as

$$\hat{\mathbf{x}} = \left(\mathbf{A}^*\mathbf{A}\right)^{-1} \mathbf{A}^*\Delta\mathbf{N} \tag{7.9}$$

and

$$\hat{\boldsymbol{\varepsilon}} = \left(\mathbf{I} - \mathbf{A}\left(\mathbf{A}^*\mathbf{A}\right)^{-1} \mathbf{A}^*\right)\Delta\mathbf{N} , \tag{7.10}$$

where $\mathbf{I}$ is compatible identity matrix and * means transpose of a matrix.

The adjusted errors $\hat{\boldsymbol{\varepsilon}}$ show the level of absolute agreement between gravimetric and GPS/levelling geoid models, the disagreement between the geoid models is a function of errors of all the involved height systems, i.e. errors of gravimetric geoid model, GPS heights and orthometric heights, including levelling. The fit is nicely expressed by aposterior unit weight variance factor $\hat{\sigma}_0^2$ computed from

$$\hat{\sigma}_0^2 = \frac{\hat{\boldsymbol{\varepsilon}}^* \hat{\boldsymbol{\varepsilon}}}{df}, \tag{7.11}$$

where df the degrees of freedom is the number of over-determinations. The standard error of Eq. (7.11) expresses the combined accuracy of the gravimetric and GPS/levelling system. It is only possible to obtain accuracy of the gravimetric geoid, if the accuracies of GPS and orthometric height systems are known. Often accuracies of GPS and orthometric height systems are only approximately known unless it has been possible to conduct variance components estimation, (Kotsakis and Sideris 1999), whichever way, accuracies of ellipsoidal height system σ_h, and orthometric height system σ_H, would be known at least approximately. Once systematic effects $\mathbf{Ax}$, have been removed from the misclosure vector $\Delta\mathbf{N}$, by a suitable model say a 5-parameter transformation, accuracy of the gravimetric geoid model can be propagated from the combined system accuracy, i.e. $\hat{\sigma}_0^2$, as

$$\sigma_N = \sqrt{\sigma_0^2 - \sigma_h^2 - \sigma_H^2} \tag{7.12}$$

The information we could obtain, only lead to approximate estimation of accuracies of GPS positioning on FBM/IBM and the TNHD i.e. we managed to obtain approximately $\sigma_h = 0.028\,m$ and $\sigma_H = 0.098\,m$. We start with assessment of Tanzania geoid model TZG08, and the GGMs deployed in this research will come after.

Accuracy Assessment of TZG08 With Respect to GPS/Levelling in Tanzania

Figure 4-25 in Sect. 4.3.3 portrays locations of the GPS/levelling data collected for this research in 2007; some are too close and appear as one. More data has been acquired recently, but could not be processed. In total 37 co-located GPS observations, mostly on fundamental benchmarks (FBM) and a few on intermediate benchmarks (IBM), seemed qualified for this undertaking, but during the process, 18 proved to be unsuitable. Most of the data rejected refer to those GPS observations that used reference stations from a geodynamic research project going on in Tanzania, and a few could not pass global chi-square test at 1 % significant level. Until now our efforts to obtain better data have been unfruitful. As for the recently collected (September 2008) GPS on FBM/IBM data, this has not been processed yet as explained in Sect. 4.3.3. Consequently, only 19

GPS/levelling stations will be used in the evaluation/assessment process, and they are depicted in Figure 7-1.

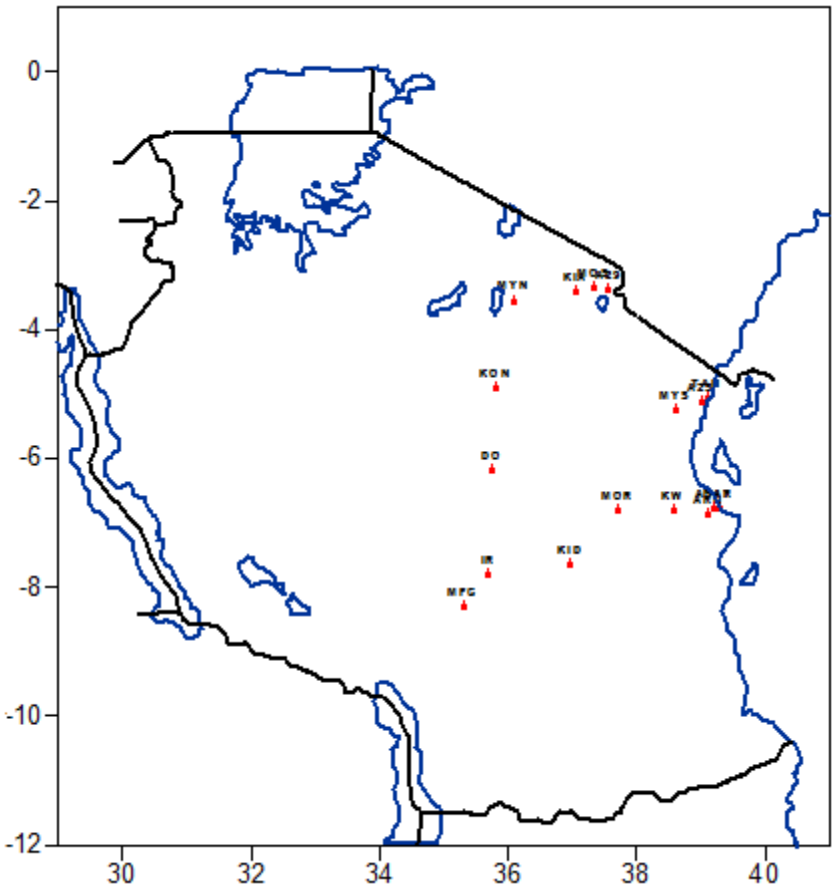

Figure 7-1: The 19 GPS/Levelling stations that qualified for the evaluation of TZG08 and the GGMs

Evaluation of the TZG08 for agreement with the GPS/levelling was conducted first by removing the systematic effect of a datum shift, i.e. 3-parameters only. Then shift and scale effects were applied, i.e. 4-parameters. This continued to five and 7-parameters according to the systematic effect models in Eqs. (7.4) to (7.7).

Reliability on the accuracy estimation of geoid height depends very much on the ability of the parametric part i.e. $\mathbf{Ax}$ to model the systematic effects effectively. Furthermore, in the event weights are assigned to the observations, they must be correct, at least relatively.

Prior to accounting for any systematic effect or adjustment, statistics of the geoid height from GPS/levelling $\mathbf{N}^{GL} = \mathbf{h} - \mathbf{H}$, gravimetric geoid model $\mathbf{N}^{G}$ and their difference or misclosure vector $\mathbf{\Delta N} = \mathbf{N}^{GL} - \mathbf{N}^{G}$ are computed. These are given in Table 7-1 below.

Table 7-1: Statistics of the misclosure vector of GPS/Levelling and gravimetric geoid models before adjustment in metre.

	Min.	Max.	Mean	SErr
N-GPS/Levelling - $\mathbf{N}^{GL}$	-27.222	-16.661	-20.418	4.074
N-Gravimetric - $\mathbf{N}^{G}$	-27.332	-16.985	-20.616	4.003
Difference - $\mathbf{\Delta N}$	-0.550	0.725	0.198	0.405

From Table 7-1, before accounting for any systematic effect inherent in the height systems, TZG08 gravimetric geoid model and geometrical geoid model from GPS/levelling fit with a standard error of 41 cm.

Table 7-2 displays the results of adjusted parameters according to Eq. (7.9), including their standard errors. Due to the small size of the area with GPS/Levelling data, compared to the TZG08 geoid model, see Figure 8-1, also the low distribution and small density, the standard errors of 7-parameter model results are out of range because the standard errors are significant for almost all parameters except the scale factor. In spite of this poor performance of the 7-parameter model, in accounting for systematic errors inherent in the systems, it will continue to be involved in the computations, but its outcome will not be used for any assessment; it is there for curiosity only.

Table 7-2: Estimates of systematic model parameters of Eqs. (7.4) to (7.7) according to Eq. (7.9) together with their associated standard errors. Unit is metre for all except for SF, which is unit less

MODEL	1-PARAMETER		3-PARAMETERS		4-PARAMETERS		5-PARAMETERS		7-PARAMETERS	
Adjusted Parameter	Value (m)	SErr ± (m)	Value (m)	SErr ± (m)	Value (m)	SErr ± (m)	Value (m)	SErr ± (m)	Value (m)	SErr ± (m)
x_1	0.198	0.405	5.292	0.278	454.502	35.997	161.040	55.588	-596.4	480.888
x_2			-7.258	0.364	332.432	27.222	107.174	42.401	-460.9	362.556
x_3			-4.339	0.334	-59.727	4.45	-61.722	4.498	7739.2	4929.71
x_4					-565.501	7E-6	-203.926	1.1E-5	-6160.6	9.5E-5
x_5							-195.658	29.248	-4601.0	3884.227
x_6									483.5	2918.853
x_7									754.5	438.099

Table 7-3 displays the range (minimum and maximum) and mean of the residual vector obtained according to Eq. (7.10) i.e. without the systematic effects. The standard error (SErr) is the square root of the aposterior unit weight variance factor $\hat{\sigma}_0^2$ according to Eq. (7.11).

Table 7-3: Statistics of residual vector of fitting TZG08 gravimetric geoid model and GPS levelling, upon accounting for systematic effects inherent in the system by a range of models. Unit is metre.

Residual Vector	1-parameter		3-parameter		4-parameter		5-parameter		7-parameter	
	Before	After	Before	After	Before	After	Before	After	Before	After
Min.	-0.550	-0.748	-0.550	-0.599	-0.550	-0.559	-0.550	-0.530	-0.550	-0.508
Max.	0.725	0.527	0.725	0.542	0.725	0.576	0.725	0.626	0.725	0.629
Mean	0.198	0.000	0.198	0.000	0.198	0.000	0.198	0.000	0.198	0.000
SErr	0.405	**0.405**	0.405	0.328	0.405	0.305	0.405	**0.297**	0.405	0.296

Comments on Table 7-3

i. Mean of the residual vector equals the bias, i.e. systematic effects which are mainly of non-zero mean character.
ii. Gradually the accuracy of gravimetric geoid model improves as the level of accounting for systematic effects gets better; from simple bias (1-parameter) to 5-parameters account, the overall accuracy moves from about 41 cm to about 30 cm,

The accuracy of TZG08 gravimetric geoid model relative to GPS/levelling has been established by the residual vector standard error. When systematic effects are removed from the total misclosure vector by the 5-parameter model, the accuracy is **29.7 cm.** Note that this accuracy estimate incorporates residuals from all the three height systems. By removing the influence of the other two systems using the standard error estimates arrived at earlier, i.e. $\sigma_h = 0.028\,m$, and $\sigma_H = 0.098\,m$ as per Eq. (7.12), accuracy estimate of TZG08 is obtained as

$$\sigma_N = 27.8\,\text{cm} \tag{7.13}$$

The accuracy estimate of the geoid model is very much dependent on the ability to assign weights to the observations or systems involved and also on how far the systematic effects have been removed. In turn, the reliability of systematic models to correctly account for the effects, is not only or always a function of the model type and the number of parameters involved, but also depends much on the GPS/Levelling network accuracy, distribution, coverage and density

Of the four systematic models used in this study (the 7-parameter model was disqualified), the 5-parameter transformation model has the smallest standard error of the geoid height residual vector (cf. Table 7-3). For the GGM evaluation, the relative performance suffices to select a suitable local/regional GGM model (pure or combined), thus only 5-parameter model will be used in the process of evaluation and selection of suitable GGM in the next stage.

Evaluation of Suitable GGMs by GPS/Levelling Approach

As recommended above, the 5-parameter transformation is used to separate systematic and random effects from misclosure between GGM and GPS/levelling geoid heights. The same GGMs of Sect. 4.3 are involved with their results given in Table 7-4

Table 7-4: Statistics of residual vector upon fitting of GGM and GPS/levelling geoid heights, 5-parameter transformation is used to remove systematic effects. Equal accuracy is accorded to h, H and N, Unit is metre.

WITHOUT ERROR ESTIMATES									
	PURE SATIELITE GGMs				**COMBINED GGMs**				
Systematic Effect	**5-parameterS**				Systematic Effect	**5-parameterS**			
	ITG_GRACE03S_180					**EIGEN-CG01C_360**			
Fitting_	Min.	Max.	Mean	SErr	Fitting_	Min.	Max.	Mean	SErr
Before	-0.906	1.737	0.225	0.698	Before	-0.973	1.707	0.390	0.713
After	-0.730	0.758	0.000	0.372	After	-0.964	0.913	0.000	0.499
	ITG_GRACE03S_120					**EIGEN-CG03C_360**			
Fitting_	Min.	Max.	Mean	SErr	Fitting_	Min.	Max.	Mean	SErr
Before	-1.068	1.784	0.366	0.757	Before	-0.663	1.117	0.218	0.514
After	-0.995	0.914	0.000	0.512	After	-0.409	0.611	0.000	**0.245**
	ITG_GRACE03S_110					**EGM96_360**			
Fitting_	Min.	Max.	Mean	SErr	Fitting_	Min.	Max.	Mean	SErr
Before	-3.285	1.652	-0.412	1.282	Before	-1.283	2.679	0.489	1.276
After	-2.273	1.580	0.000	1.085	After	-1.347	1.015	0.000	0.671
	ITG_GRACE02S_170					**EIGEN-GL04C_360**			
Fitting_	Min.	Max.	Mean	SErr	Fitting_	Min.	Max.	Mean	SErr
Before	-0.958	1.770	0.237	0.712	Before	-0.885	1.668	0.312	0.672
After	-0.790	0.786	0.000	0.399	After	-0.792	0.788	0.000	0.419
	ITG_GRACE02S_110					**GGM02C_200**			
Fitting_	Min.	Max.	Mean	SErr	Fitting_	Min.	Max.	Mean	SErr
Before	-1.062	1.764	0.401	0.769	Before	-0.982	1.761	0.353	0.717
After	-1.069	0.960	0.000	0.549	After	-0.936	0.845	0.000	0.475
	GGM02S_110								
Fitting_	Min.	Max.	Mean	SErr					
Before	-1.045	1.743	0.404	0.767					

After	-1.072	0.962	0.000	0.551
	EIGEN-GL04S1_150			
Fitting_	Min.	Max.	Mean	SErr
Before	-0.997	1.788	0.365	0.729
After	-0.929	0.842	0.000	0.473
	EIGEN-GL04S1_110			
Fitting_	Min.	Max.	Mean	SErr
Before	-1.030	1.792	0.431	0.768
After	-1.071	0.959	0.000	0.550

Comments on Table 7-4:

Pure GGM evaluation/selection

With reference to Figure 4-23 we observe that for most of the pure satellite GGMs, the three signals in the graph show better agreement between spectral degree 110 to 120, above the degree, the situation is unclear, this observation coupled by the recommendations in the GGMs documents from the International Centre for Global Earth Models, (http://icgem.gfz-potsdam.de/ICGEM/evaluation/evaluation.html, 10.05.08) on the degree at which the GGM shows maximum gravity signal power retention, lead us to decide not to use the maximum spectral degree of pure GGMs but to go by the degree recommended in the ICGEM or similar research. Though from Table 7-4 at maximum degree of pure GGMs, the GPS/levelling fit is better compared to the lower degrees for the respective GGM, all these are discarded in the evaluation and nomination of suitable pure GGM. In view of the decision, in Table 7-4 the pure GGMs rank as follows with accuracies in brackets: ITG_GRACE03S_120 (0.512 m), ITG_GRACE02S_110 (0.549 m), EIGEN-GL04S1_110 (0.550 m), GGM02S_110 (0.551 m) and ITG_GRACE03S_110 (1.085 m), thus the **ITG_GRACE03S_120 (0.512 m)** excels as the best pure GGM in the AOI.

Combined GGM evaluation/selection

For the combined GGMs, the weak power in the pure GGM involved at higher degrees is enhanced by the presence of terrestrial gravity data, therefore all the spectral range is used which is degree 360 for all except GGM02C which is degree 200. They rank as follows, with accuracy in bracket: EIGEN-CG03C_360 (0.245 m), EIGEN-GL04C_360 (0.419 m), GGM02C_200 (0.475 m), EIGEN-CG01C_360 (0.499 m) and EGM96_360 (0.671 m), in this case **EIGEN-CG03C_360 (0.245 m)** has emerged the most suitable combined GGM for this research area (AOI).

Conclusion on GGM Selection Using GPS/Levelling.

The same pair of pure and combined GGMs selected in Sect. 4.3.4, cf. Table 4-17 also in Sect. 5.2.3 i.e. ITG_GRACE03S_120 and EIGEN-CG03C has once again been qualified by a very independent method and approach as the most suitable for the AOI. Unfortunately the pattern of Table 4-17 is not adhered to exactly, as commented earlier,

the GPS/levelling approach was discouraged because the data density and distribution is low, moreover it is confined to one locality in the AOI as witnessed in Figure 7-1, while for the first approach of using absolute and observed point surface gravity anomaly, the density, distribution and coverage is much better, cf. Sect. 4.1.4 Figure 4-8 for absolute gravity, and Figure 4-9 for surface point gravity. Evaluation of gravimetric geoid models and GGM by GPS/levelling has been used extensively, but not the absolute and surface point gravity data approach, recommended and used in this study, cf. Sects. 4.3 and 5.2. The data for this approach covers better the AOI, and will many times be available and does not need extra different data observation e.g. GPS on benchmarks, in addition the evaluation process is much easier. Therefore with further counter checks, the method is likely to be a potential alternative for GGM qualification for local/regional geoid model determinations in future.

Chapter Eight

ORTHOMETRIC HEIGHT FROM GNSS

8.1 TZG08 Geoid model as Vertical Datum

The definition of the geoid and some of its uses were given in Sects. 1.1 and 1.1.1. Ideally a geoid model of a country is expected to be its vertical height datum and by definition the datum for orthometric heights (Heiskanen and Moritz 1967 p 50). Our physical visualization of a geoid model is by the mean sea level (MSL) i.e. sea surface in the absence of disturbing factors like tsunamis, ocean currents, salinities, wind, etc., extended through the continents (Vaníček and Krakiwsky 1986). The practical realization of the two surfaces (namely a geoid model and MSL) render them neither coincident with one another nor with the geoid, as many factors inherent in the processes of realizing a geoid model and MSL lead to the departures. One of the most important uses of a geoid model in this era is the conversion of a GNSS (e.g. GPS) ellipsoidal height h into an orthometric height H obtained according to Eq.(7.1), which is very useful for daily uses and has physical meaning. The importance is due to the speed, cost effectiveness and provision of horizontal and vertical coordinates at one go from a GNSS positioning as opposed to the conventional surveying methods, where often horizontal and vertical information are obtained differently at much slower speed and more costly for the same accuracy. As we saw in Sect. 7.2, Eq. (7.1) is never satisfied, and four broad factors were given as the cause of the failure. We further saw that misclosure of Eq. (7.1) can be quantified into two parts: systematic and random parts according to Eq. (7.3). If we manage to reduce the amount of residual effects (random effects), then most of the departure (difference) of the geoid model and MSL will be contained in the systematic part.

8.1.1 Spirit Levelling and Orthometric Height

Spirit levelling is a process of determining height difference between two points, usually using a level instrument which responds to the pull of Earth's gravity field. Due to the limitation of horizontal line of sight, in hilly terrain the process becomes time consuming, tedious and expensive. Moreover, if a closed circuit is levelled, normally it does not rigorously close to zero, thus we usually have a misclosure which in practice is determined from known orthometric height (s) depending on the observation setup. By definition, orthometric height of a point is its elevation, above the geoid (MSL) measured along the curved plumb line of the point. Determination of the orthometric height involves a level surface (equipotential surface) and a plumb line (gravity vector). Consequently the orthometric height system has physical meaning and finds many useful applications, mainly in engineering, science and technology. The process of obtaining an orthometric height from levelled height differences is rigorous as it involves gravity and topographic density above the geoid model, and all these make it expensive and to some

extent not very versatile. Notwithstanding the rigor and difficulties involved, daily needs of orthometric heights are usually on the increase.

Realization of orthometric height involves many processes, with some degree of uncertainty. For example, determination of tide gauge stations which establish MSL, levelling using horizontal line of sight on a curved Earth, elevation along a curved gravity vector from surface to the geoid model (MSL) inside topographic masses of varying mass density to mention a few. An alternative approach which is less involving and less rigorous, would be a big advantage. It is the purpose of this chapter to pursue this alternative method of realizing orthometric height.

8.1.2 Orthometric Height from GNSS-Ellipsoidal Height

The most viable alternative or complementary to orthometric heighting is by use of Eq. (7.1). Unfortunately in the introduction we saw that the geoid model and MSL surfaces usually do not coincide, and consequently Eq. (7.1) is not satisfied. This problem can be tackled from three perspectives (Featherstone 1998, 2002):

- Re-definition and re-adjustment of the existing National Height Datum (NHD) so that it coincides better with the geoid model. For a big country, this option is expensive to implement, in addition it would call for frequent updates as the geoid model improves, thus it is not feasible at all for a big and a developing country.
- Establishment of a new NHD based solely on GPS and geoid heights, i.e. based on $(h - N)$ only. This requires very accurate geoid model and GPS network, and therefore sounds hypothetical for the time being.
- To construct a corrector surface so that the transformation of GNSS ellipsoidal height to orthometric height referred to NHD is direct. In this way the need to carry out separate adjustment every time a GNSS–height is needed to be fitted into the NHD would be avoided. This option is more feasible and conducive, and it is the one which will be followed here, i.e. establishment of a corrector surface to the Tanzania National Height Datum (TNHD), for conversion of GPS ellipsoidal heights to orthometric heights through the TZG08 geoid model.

8.2 Corrector Surface

Combination of gravimetric geoid model with GNSS (GPS), and a NHD orthometric height, when handled appropriately, can produce a surface that allows direct determination of NHD-heights from GNSS, and the surface is hereby referred to as a "Corrector Surface, (CS)". Thus we can say that a CS aims at providing GNSS/GPS users with transformation model between ellipsoidal heights h and NHD-heights H (orthometric). Our fundamental model is Eq. (7.2) with its parametric part given by one of Eqs. (7.4) – (7.7). In Sect. 7.2 we saw that when the aim is to know the accuracy of the geoid model, then $\boldsymbol{\varepsilon}$ (the residual vector) should be the concern, but CS is formed from the parametric part as

$$H_i^{CS} = \mathbf{a}_i \hat{\mathbf{x}} \text{ and in vector form as } \mathbf{H^{CS}} = \mathbf{A}\hat{\mathbf{x}}, \tag{8.1}$$

where H_i^{CS} is a corrector height at a point with GPS/levelling N_i^{GL} and gravimetric geoid height N_i^G. The idea of using H_i^{CS} to convert ellipsoidal and geoid heights into orthometric height, originates from Eq. (7.2), and it is shown below,

$$\begin{aligned} &\Delta N_i = N_i^{GL} - N_i^G = \left(h_i - H_i\right) - N_i^G = \mathbf{a}_i\mathbf{x} + \varepsilon_i;\ i = 1,2,...,n \\ &\therefore\ H_i = h_i - \mathbf{a}_i\mathbf{x} + \varepsilon_i - N_i^G = \left(h_i - N_i^G\right) - H_i^{CS} + \varepsilon_i \end{aligned}, \tag{8.2}$$

where the symbols have the same previous meaning. Since the term in the bracket is known from GNSS/GPS and the geoid model, and H_i^{CS} is obtained from Eq. (8.1) after adjustment according to Eq. (7.9), then orthometric height H_i at the point is obtained with usual random error ε_i. To enable determination of orthometric height from GPS height at any point within the limits of the geoid model, CS is formed out of H_i^{CS} at all the GPS observations on FBM/IBM network points $p_i\left(\varphi, \lambda, H_i^{CS}\right)$, spread preferably all over the limits of the geoid model, with φ and λ as the latitude and longitude coordinates of the network point. The quality of the corrector surface depends on many factors, some of the main ones are:

1. Density, distribution, coverage and quality of the data used, i.e. co-located h, H and N^G.
2. Suitability of the parametric model to account effectively for the systematic effects inherent in the systems.
3. Relative correctness of the observation noises (if applied)
4. Ability of the surface modelling algorithm to map the corrector vector $\mathbf{H^{CS}} = \mathbf{A}\hat{\mathbf{x}}$ onto the corrector surface (CS) i.e. with least changes to vector $\mathbf{H^{CS}}$

This study has 19 effective co-located datasets (triple heights), but confined to one side of the country, cf. Figure 7-1. Therefore the first factor above is highly violated, which means that we can not form a reliable corrector surface for the whole country/geoid model limits, but at most the corrector surface will be effective within the dataset limits. For further reading on modelling of observation noises in GPS/levelling for gravimetric or GGM assessment, consult (Fotopoulos 2003, Kotsakis and Sideris 1999, and Kotsakis et al. 2001). The adjusted parameters $\hat{\mathbf{x}}$ are used to compute the corrector vector $\mathbf{H^{CS}}$ according to Eq. (8.1). In forming the CS, all the zero mean random noise effects (residual vector $\boldsymbol{\varepsilon}$) are filtered out to allow the CS to absorb the long-wavelength errors which usually do not comply with mean-zero error probabilistic behaviour. Eq. (8.1) is tested using the parametric models of Eqs. (7.4) – (7.7) for the one with minimum standard and residual errors. From Table 7-2, it was concluded that the 7-parameter model does not qualify to take care of the systematic effects in this study with the current situation of the GPS/levelling points. Although the 7-parameter model is included in Table 8-1, it is not involved in the assessment; it is there for curiosity only.

Table 8-1: Statistics of corrector vector for different parametric models. Unit is metre.

1-PARAMETER (BIAS)				
	H-Orig	H_Comp	Res.	Corr
Min	10.513	10.425	-0.748	0.198
Max	1552.387	1552.068	0.527	0.198
Mean	756.241	756.241	0.000	0.198
SErr	548.696	548.816	**0.404**	**0.000**

4- PARAMETER				
	H-Orig	H_Comp	Res.	Corr
Min	10.513	10.729	-0.559	-0.106
Max	1552.387	1552.189	0.576	0.741
Mean	756.241	756.241	0.000	0.198
SErr	548.696	548.672	**0.304**	**0.266**

5- PARAMETER				
	H-Orig	H_Comp	Res.	Corr
Min	10.513	10.677	-0.530	-0.054
Max	1552.387	1552.224	0.626	0.811
Mean	756.241	756.241	0.000	0.198
SErr	548.696	548.668	**0.297**	**0.275**

7- PARAMETER				
	H-Orig	H_Comp	Res.	Corr
Min	10.513	10.696	- 0.508	- 0.073
Max	1 552.387	1 552.228	0.629	0.848
Mean	756.241	756.241	- 0.000	0.198
SErr	548.696	548.669	**0.296**	**0.276**

Para=Parameter, Orig=Original, Comp=Computed, Res.=Residual, Corr=Corrector, H=Height

We observe from Table 8-1 that the mean correction for all the models equals the bias. After excluding the 7-parameter model, 1-, 4- and 5-parameter models are left. The statistical properties of 4- and 5-parameter models are very close, except the magnitude of the residual standard error is slightly bigger for 4-parameter model; as a result the **5-parameter model** has a bit extra advantages in the evaluation area over the others and thus the one chosen to determine the corrector surface parameters. Residual standard error consideration is important because in forming the CS, residuals were not involved; Eq.(8.1), but will always affect the quality of the computed heights above the NHD based on ellipsoidal and geoid heights. Hence a model which maintains minimum residuals and corrections should be preferred to the others. With more evaluation points and preferably bigger area, it would be of interest to check on how the 4- and 7-parameter models perform. Now that in Eq. (8.1) vector $\hat{\mathbf{x}}$ is known from the 5-parameter model, coefficients a_i are computed from geodetic coordinates of the network points $p_i(\varphi,\lambda)$. In forming CS, a surface which fits better the vertical distances of the corrector vector $\mathbf{H}^{\mathbf{CS}}$ i.e. $\mathbf{H}^{\mathbf{CS}} = \left[H_i^{CS}\right] = \left[\mathbf{a}_i\hat{\mathbf{x}}\right]$, is the one which portrays minimum deviations. Several methods tested for the minimum (deviation and mean) are portrayed in Table 8-2. Statistics of the methods used to create the CS are given, including the original corrector vector from the 5-parameter model. Statistics of the differences are computed to get the one out of ten tested methods with minimum deviation from the original corrector vector. The conclusion is arrived at by ranking the standard error and mean of the differences. Inverse distance to power (ID2P) has the minimum standard error and minimum mean deviation of all the ten methods in this area. Thus ID2P is selected to create the CS, which is shown in Figure 8-1; first as an insert within the whole geoid model area and then alone at a bigger scale. Contour interval is 5 cm.

Table 8-2: Selection of suitable method for creating "Corrector Surface". Statistics of the ten selected methods after interpolation are given, and then standard error and mean difference from the original corrector vector are compared. The unit is metre.

Inter-Method		Kriging	Inv Dist 2Power	Natural Neghbor	Minimm Curvture	Modified Shepard	Simple Poly Regresn	Cubic Poly Regresn	Radial Bas Funct	Triang Linear Interpol	Moving Average
Stats	**Original Corr. Vector**	**Krgng**	**ID2P**	**NN**	**Min_ Curv**	**Mod_ Sheprd**	**SPR**	**CPR**	**RBF**	**TwLI**	**Mv Av**
Min	-0.054	-0.101	-0.054	-0.043	-0.625	-0.288	-0.231	-0.574	-0.101	-0.044	-0.001
Max	0.811	0.811	0.811	0.800	1.059	0.822	0.646	0.826	0.783	0.802	0.541
Mean	0.211	0.292	0.235	0.345	0.285	0.327	0.208	0.322	0.287	0.359	0.216
SErr	0.269	0.230	0.182	0.203	0.300	0.236	0.188	0.285	0.228	0.207	0.126
Variance	0.072	0.053	0.033	0.041	0.090	0.056	0.035	0.081	0.052	0.043	0.016
Coef_Var	1.275	0.788	0.774	0.589	1.050	0.723	0.905	0.886	0.792	0.577	0.581
Coef_Skw	0.866	0.269	0.730	0.122	-0.001	0.020	0.000	-0.352	0.262	0.031	0.885

Difference of original corr. vec with inter-polatn method		**Diff Krgng**	**Diff ID2P**	**Diff NN**	**Diff Min_ Curv**	**Diff Mod_ Sheprd**	**Diff SPR**	**Diff CPR**	**Diff RBF**	**Diff TwLI**	**Diff Mv Av**
Stats of Differences	Min	-0.082	-0.024	-0.134	-0.248	-0.116	0.003	-0.111	-0.077	-0.148	-0.053
	Max	0.598	0.501	0.745	0.867	0.846	0.866	1.218	0.604	0.836	0.695
	Mean	0.158	**0.106**	0.199	0.185	0.222	0.243	0.283	0.164	0.211	0.155
	SErr	0.268	**0.183**	0.359	0.400	0.353	0.301	0.476	0.265	0.388	0.263

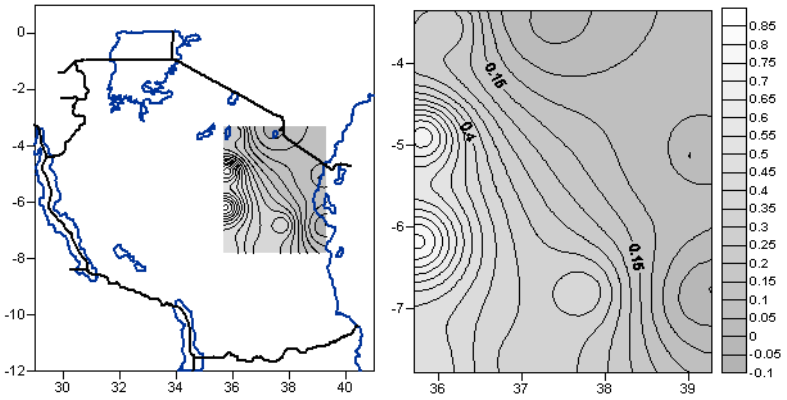

Figure 8-1: Corrector Surface for orthometric height from GPS and TZG08 geoid model to conform to TNHD. Contour interval 0.05 m

The corrector surface (CS) is given in grid format whose limits in longitude λ are $35^{\circ}.6986$ to $39^{\circ}.2853$ and in latitude φ are $-7^{\circ}.7943$ to $-3^{\circ}.3470$. Grid spacing in longitude $\Delta\lambda$ is $0^{\circ}.0448$ and in latitude $\Delta\varphi$ is $0^{\circ}.0449$.

Now we can use Eqs. (8.2) to convert GPS-ellipsoid height at surface position $p_i(\varphi,\lambda)$, $h_i^{GPS}(\varphi,\lambda)$ into equivalent orthometric height referred to TNHD; $H_i^{P,TNHD}(\varphi,\lambda)$ using

the value of TZG08 gravimetric geoid model at p_i, $N_i^G(\varphi,\lambda)$ and the correction from CS $p_i(\varphi,\lambda)$, $CS_i(\varphi,\lambda)$ as follows:

$$H_i^{P,TNHD}(\varphi,\lambda) = h_i^{GPS}(\varphi,\lambda) - N_i^{TZG08}(\varphi,\lambda) - CS_i(\varphi,\lambda) + \varepsilon_i(\varphi,\lambda), \quad (8.3)$$

where $\varepsilon_i(\varphi,\lambda)$ is the mean zero error/residual at $p_i(\varphi,\lambda)$. By having a few benchmarks (BM) observed in the GPS network (elevations) and converted to TNHD using Eq. (8.3), the LS adjustment constrained by the BM orthometric heights improves the quality of $H_i^{P,TNHD}(\varphi,\lambda)$ and that way take care of residual errors $\varepsilon_i(\varphi,\lambda)$.

8.3 Hybrid Geoid Model as Datum for GNSS Orthometric Height

If we had quality high density GPS observations on benchmarks referred to high density TNHD (GPS/levelling) points, well distributed over the entire TZG08 limits, a hybrid geoid model could be formed to reap the advantage of both the geometrical and physical geoid models constrained to TNHD by say the FBM-orthometric heights. The geometric geoid height $N_i^{GL} = (h_i - H_i)$ would be combined with N_i^G from the gravimetric geoid model to form a hybrid geoid model. Unfortuantely neither a suitable GPS system nor a quality NHD orthometric system exists at the moment. Fortunately a project to establish a dense zero, first also tertiary orders of GPS and gravity networks in Tanzania is at advanced stage. The project is jointly funded by the World Bank and the government of Tanzania. Adjunt Professor Peter Morgan from Australia is the technical consultant of the project. Therefore formation of a hybrid geoid model for Tanzania is likely to be a feasible undertaking in the near future if all go according to the GPS and Gravity project.

8.4 Application of Corrector Surface to Mt. Kilimanjaro

Mountain Kilimanjaro is found on the Northern border of Tanzania and Kenya. The mountain is the highest in Africa. The official height of the mountain since 1952 is 5,895 m above MSL. In 1952 trigonometric heighting was used to height the highest peak; Uhuru Peak from two ground stations situated around 55 km away and about 4,000 m below the peak, (Angelakis 1999). In 1999 Mt. Kilimanjaro, was re-heighted using modern GPS technique, (Kil99_Campaign). Leica system 500 and 200 dual frequency receiver sets were deployed and the processing was by Bernesse v4.2 and SKI-Pro software. GPS reference stations were from the International GNSS (IGS) stations at Ascension Islands, Haartebeesthoek, Malindi, Seychelles and Sutherlands. To obtain orthometric height of Uhuru Peak, ITRF ellipsoidal height above EGM96 global geoid model and a mean shift of 0.591 m obtained from two BMs and one triangulation control point (Domberg), involved in the campaign were used. The new height after the processing at Fachhochschule Karlsruhe - University of Technology and University Karlsruhe both of Germany was obtained as 5,892.366 m. The network used to obtain the new height of Mt. Kilimanjaro is on the edge of CS computed in this study. By using geodetic coordinates and ITRF-ellipsoidal height from the Kil99_Campaign, and the corresponding TZG08-geoid heights, and corrections from CS in Eq. (8.3), orthometric heights of Kil99_Campaign controls referred to TNHD i.e. MSL as established from tide gauges in Dar Es Salaam, Tanga and Mtwara are

determined. Table 8-3 contains control stations and estimated orthometric height above EGM96 geoid model from the Kil99_Campaign.

Table 8-3: Control stations of Mt. Kilimanjaro re-heighting campaign in 1999 with orthometric heights referred to EGM96 geoid model, (Angelakis 1999).

Kil99_Campaign Controls	Lat (deg)	Lon (deg)	h (m)	H_egm96 (m)
Moshi ITRF (Philip Hotel)	-3.3474752	37.3424049	827.7729	844.8479
Himo	-3.3824181	37.5665664	869.5326	887.7996
Marangu 2	-3.2401365	37.5146324	1867.2918	1884.7608
Mandara Juu	-3.1778805	37.5119253	2827.8405	2845.0985
Mandara Hut	-3.1816379	37.5133835	2686.9199	2704.1959
Horombo 1	-3.1404775	37.4388836	3683.3668	3700.1498
Horombo Hut	-3.1395149	37.4389354	3698.5793	3715.3603
Kibo Hut	-3.0819293	37.3894249	4682.9378	4699.3638
Gillman's Point	-3.0746907	37.3679187	5691.2948	5707.6188
KIA1	-3.427171	37.0574507	881.2636	898.1926
Uhuru Peak	-3.0763586	37.3539608	5875.502	5891.775
Uhuru Peak		5891.775		5892.366 **

** **Uhuru Peak** (the highest peak of Mt. Kilimanjaro) after applying a shift of 0.591 m to orthometric height above EGM96 geoid model (5,891.775 m) is obtained as **5,892.366** m aMSL.

Comparison of orthometric heights of controls of 1999 Mt. Kilimanjaro re-height campaign referred to EGM96 global geoid model and the new TZG08 geoid model are given in Table 8-4. The difference is appreciable; it ranges from about 1 dm to about 32 dm as height increases from 845 m to 5,895 m above the TNHD (MSL). Take note, that although the orthometric height of Mt. Kilimanjaro highest peak referred to TZG08 geoid model is not yet corrected to fit into TNHD, its value is practically the same as the prevailing official height of the mountain i.e. 5,895 m.

Table 8-4: Comparison of orthometric heights referred to Kil_1999 EGM96 global geoid model and new Tanzania geoid model 2008, TZG08; heights are in unit of metre.

Kil99_Controls	Lat. deg	Lon. deg	h	N-TZG08	**H_TZG08**	H_EGM96_Kil_1999	Diff.
KIA1	-3.427171	37.057451	881.264	-17.024	898.288	898.193	0.095
Philip Hotel	-3.347475	37.342405	827.773	-17.576	845.349	844.848	0.501
Himo	-3.382418	37.566566	869.533	-18.458	887.991	887.800	0.191
Marangu 2	-3.240137	37.514632	1867.292	-17.799	1885.091	1884.761	0.330
Mandara Juu	-3.177881	37.511925	2827.841	-17.996	2845.837	2845.099	0.738
Mandara Hut	-3.181638	37.513384	2686.920	-17.985	2704.905	2704.196	0.709
Horombo 1	-3.140478	37.438884	3683.367	-18.181	3701.548	3700.150	1.398
Horombo Hut	-3.139515	37.438935	3698.579	-18.196	3716.775	3715.360	1.415
Kibo Hut	-3.081929	37.389425	4682.938	-18.772	4701.710	4699.364	2.346
Gillman's Point	-3.074691	37.367919	5691.295	-19.520	5710.815	5707.619	3.196
Uhuru Peak	-3.076359	37.353961	5875.502	-19.430	**5894.932**	5891.775	3.157

Unfortunately, most of the Kil99_Campaign controls (insert on top of CS in the map of Tanzania in Figure 8-2) are outside the CS except three. The three points are not adequate to establish a reliable trend and thus not easy to project for the corrector to Uhuru Peak height with geoid height -19.430 m. Moreover, it should be underscored here that it is not appropriate to extrapolate outside the corrector surface limits.

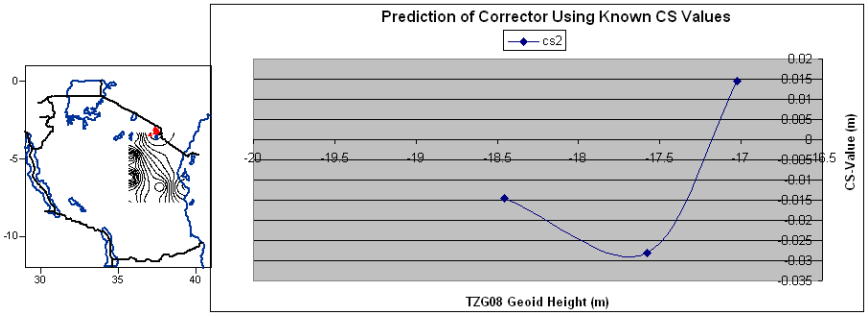

Figure 8-2: Corrector trend for Kil99_Campaign controls which appear on top of CS insert in the map of Tanzania on the left hand side. Only 3 out of 11 controls are within the CS as shown on the right hand side graph of geoid height versus corrector value.

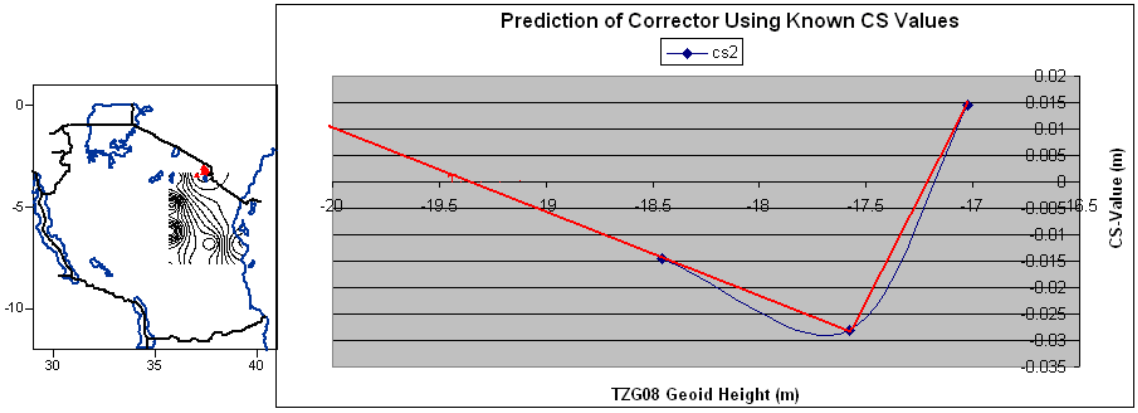

Figure 8-3: Extrapolation of corrector for conversion of orthometric height from TZG08 geoid model to TNHD; a linear correlation between geoid height and corrector value is assumed.

If we opt to project the trend by a straight line using Figure 8-3, corrector value for Uhuru Peak with geoid height -19.430 m, is about +1mm which leaves the orthometric height almost unchanged i.e. at **5,894.931 m aMSL**, and therefore to zero decimal place as is usually presented, **height of Mt. Kilimanjaro is obtained as 5,895 m aMSL,** as it was established in 1952. “Bravo geodetic methods”.

Chapter Nine

DISCUSSION, CONCLUSIONS AND RECOMMENDATIONS

9.1 Discussion

TZG08, Tanzania geoid model (2008) is essentially the second dedicated geoid model of Tanzania which fully covers the country. The first is the TZG07 (Olliver 2007). Although geoid model of Tanzania is also part of AGP2003 and AGP2006, the missing assessment and quality performance greatly limit their usage, besides, the models are still preliminary (Merry et al. 2005) and (Parker et al. 2007). The same argument applies to EGM96 and EGM2008 geoid models as discussed in Sects. 1.1.2 and 1.4. The external assessment of TZG07 based on astro-geodetic geoid model profile is feasible approach, whose fit to TZG07 is 47 cm and we regard this as comprised of errors of both geoid models. Therefore it is possible that the accuracy of TZG07 is slightly better than 47 cm if the residual vector would be distributed between the contributing sources. Notwithstanding, the inability to give the right accuracy of the TZG07 is still a dilemma to users.

Confronted by the above ambiguities, and inspired by the new opportunities of Sect. 1.3, this study set out to determine a new geoid model of Tanzania of better quality and accuracy than any of the existing cf. Sect. 1.4, in spite of the sparse gravity data coverage of varying density, quality and distribution (as seen in Figure 4-11, Figure 4-13 and Figure 4-16b).

Close examination of the three prominent methods of local/regional geoid model determination, which use modern approaches namely RCR, Stokes Helmert of UNB-Canada and LSMS with AC (cf. Chs. 2 and 3), helped to come to a conclusive decision that the most viable method to undertake this study is the LSMS with AC of KTH. The option of the method used in this study is the one which avoids gravity reductions to the geoid, by adding corrections externally to the approximate geoid height determined by the LSMS using unreduced surface gravity anomalies.

One of the major contributions of this study to the geodetic community and especially the developing countries with similar gravity data situation is creation of clean and realistic dense grid of terrestrial surface gravity anomaly Database (DB), from sparse surface gravity data of variable density, quality and distribution. Foremost, only point gravity and gravity anomalies have been used in this research for all the land areas and a mixture of dense point and grid of $2' \times 2'$ data in the Ocean area. Mean data has been avoided as much as possible because mostly it is not accompanied by the procedure followed to create the mean grid data, besides most of the mean gravity data obtained are $5' \times 5'$ grids, which smooth and remove the original high frequencies of the actual gravity data

too far from the $1' \times 1'$ intended in this study. The point gravity data, mostly referenced to the GRS67, and variable calibration datums were converted to IGSN71 and GRS80. Upon cross validation using the Kriging method and statistical testing at 99 % confidence level of 40,350 land surface point gravity anomalies, 39,677 were retained for this study. In the sea, out of 59,778 original data points 57,723 were left.

Due to the absence of accuracy information, methodology was used to arrive at accuracy estimate for the surface gravity anomaly data. Among other things, gravity accuracy information is used in the determination of LS-modification parameters. Thus by using only the point gravity data and in addition methodology to assign accuracy to the observed gravity data, the problem of varying data quality in the AOI has been relieved substantially. Pure GGM, SRTM-DEM and combined GGM have been used to patch up the voids and thus eliminate completely the problem of sparse and variable data density and distribution. A specially designed kind of remove-compute-restore (r-c-r) approach was developed and used (cf. Sect. 5.2 for further enlightenment).

New method of GGM qualification for local/regional geoid model determination, using reference surface terrestrial gravity has been developed and used in this study. Countercheck of the method with the more preferred and commonly used GPS/levelling, showed that the method is equally good since the same pair of pure and combined GGM was passed (cf. Sects. 4.3.3, 5.2.3 and 7.2). Further countercheck of the method using better distribution and coverage of terrestrial surface gravity data and GPS/levelling on FBM/IBM, is likely to prove the method to be a potential GGM qualifier for similar works in future. If it is proved, the method has added advantages over the GPS/levelling.

The LS modification parameters s_n require knowledge of gravity anomaly signal (c_n) and error (σ_n^2) degree variances to infinity. Tscherning and Rapp (1974) error model and a composite error model developed out of band limited white noise and reciprocal distance error models have been used to get the c_n and σ_n^2 in which spectral degree 21,600 was regarded to be the infinity, cf. Sect. 5.3.2 for more insight. Through error propagation of Eq. (3.19), the RMS error of the approximate TZG08 is obtained as 49 mm. i.e. about 5 cm. This value is regarded to be optimistic probably because it does not involve the error sources from the additive corrections.

The approximate geoid model $\tilde{N}$ computed from the LSMS using terrestrial and pure satellite gravity anomaly data, has the following statistics in metre, mean -17.900, minimum -34.122, maximum -5.803, standard error 6.114 and RMS 18.915. The AC statistics in metre are: mean -0.144, minimum -3.516, maximum 1.174, standard error 0.132 and RMS 0.195. TZG08 is assembled out of the approximate geoid model $\tilde{N}$ and the AC leading to the following statistics in unit of metre: mean -18.044, minimum -34.122, maximum -6.115, standard error 6.031 and RMS 19.025, and is displayed in Figure 6-11 and Figure 6-12. We observe that Tanzania geoid model is throughout below the GRS80. The TZG08 geoid model shows strong correlation with conspicuous topographic features like mountains, crater and the EARVS.

GPS/levelling is used as external method to assess the accuracy of the TZG08, also as an alternative method for the selection of most suitable pure and combined GGM for the study area. This assessment is somehow partial since the GPS/levelling data which qualified for this task is located on one part of the geoid model area. Upon separation of systematic effects by 5-parameter model, accuracy of TZG08 while incorporating residuals from GPS and orthometric (levelling) heights is obtained as 29.6 cm. When residual errors from GPS and orthometric heights are approximately removed by error propagation using approximate standard errors of the two systems, the accuracy of TZG08 geoid model is obtained as 27.8 cm. One of the most important applications of geoid model is conversion of GNSS ellipsoidal height to orthometric height. This has been done in Ch. 8, in which a corrector surface (CS) was created to convert GPS ellipsoidal height to orthometric height, but the CS is confined to the area with suitable GPS/levelling points. Application of the CS reconfirmed the height of Mt. Kilimanjaro to be 5,895 m, the same as it was established in 1952 by trigonometric heighting and not the one re-established in 1999 based on EGM96 geoid model and a correction which lowered the height of the mountain by about 3 m!

9.2 Study Limitations

i. Data Quality

Most of the terrestrial gravity data used was not meant for geodetic purposes, consequently vital information is missing, e.g. accuracy of the gravity data, accurate height and positional coordinates, also the positional accuracy. Estimation conducted, based on the field procedures and instruments used to obtain a single overall accuracy of all the data, surely degrades the end geoid model quality.

ii. Data Correlation

Use of pure GGM in the determination of the approximate geoid model and filtering of the same frequencies from the terrestrial gravity data, had the intention to eliminate correlation between the datasets. Combined GGM constitutes ground gravity data frequencies, and most probably from the same data as the one in use. All the effort has been exercised to minimise the correlation of the combined GGM with the existing terrestrial surface point gravity data. First by removing the long and short-wavelengths through pure GGM and RTE (cf. Sect. 5.2) and minimizing the interaction of the ground residual data $1' \times 1'$ grids with similar grids from combined GGM, and whenever necessary the overlap was reduced to about 25 % of the $1' \times 1'$ grid area for two adjacent grids.

iii. Topographic Density Model

Elevation range in the AOI is about 6 km, and it is very erratic especially along the EARVS and mountainous areas, cf. Sect. 4.6. To use single mean density model of $2.67 g\,cm^{-3}$ for the whole of the AOI of about $19^{\circ} \times 18^{\circ}$, introduces biases which are undoubtedly not insignificant especially in high and rough elevation areas (Sjöberg 2004b, and Kiamehr 2006b). Our effort to obtain topographic density model for the East African region has not been fruitful.

iv. Management of SRTM DEM

The 3 arc seconds SRTM DEM (SRTM3) is surely dense DEM and a good representative of the actual topography, but its management in the computer proved to be too involving and cumbersome for the whole AOI of about $19^{\circ} \times 18^{\circ}$. As a result the SRTM3 was averaged to 15", 30", 1' and 6' for different uses as explained in Sects. 4.4 and 5.1.1. In some areas of this study, ability to use SRTM3 would have improved the computed geoid model.

v. Gravity Anomaly Error Model

Since 1974 when C.C. Tscherning and R.H. Rapp developed the gravity anomaly covariance function model, the world has accumulated a lot more of terrestrial gravity data, very likely with improved density, quality and distribution. Better storage and dissemination facilities are available now and easily accessible. The same applies to GGMs gravity anomaly. Availability of improved gravity anomaly signal and error degree variances error model is very much likely would improve substantially the performance of the LSMS and hence geoid model determined from it.

vi. DEM Quality

The original USGS SRTM3-DEM had too many voids and spikes that is why we opted to use CGIAR SRTM3 instead, cf. Sect. 4.4. The CGIAR uses statistical and mathematical procedures which take into account natural trends to eliminate outliers from the USGS SRTM3 $1' \times 1'$ tiles. Although the approach improves the situation appreciably, it is still not the best; a better way would be to use photogrammetric or GPS method. Some sites are doing this e.g. the Jonathan de Ferranti site, cf. Sect. 4.4.1, but the speed is very slow. For the AOI only six $1' \times 1'$ tiles were obtained, which had a slight problem of having all the elevations along the southern borders of the tile set to zero in an area where they should be above 1400 m. Since the DEM is used in many instances, including gravity anomaly gradient determination, to have realistic SRTM3 DEM is surely very important.

vii. GPS/Levelling Data Density and Distribution

GPS/levelling data is essential for the assessment of accuracy of a geoid model and or GGM, also establishment of CS or hybrid geoid model to be a datum for conversion of ellipsoidal height to the corresponding orthometric height. For impartial and accurate results, at least the following data/information which covers fully the geoid model area ought to be in place:

- Well distributed network of FBM/IBM with correctly reduced orthometric height and their accuracies. This is not the case for Tanzania. The network of FBM/IBM is old and covers only a small part of the country, see Figure 4-24, besides most of the monuments and the respective data are missing or misplaced, see the last paragraph of Sect.4.3.3 for elaboration. In addition, the heights are not proper orthometric heights (Saburi et al. 1991).
- Accurate ellipsoidal heights observed/given, at minimum, on all the FBM/IBM monuments, together with accurate horizontal geodetic coordinates and the associated variance covariance matrix (VCM). Accurate reference GPS points say referenced to the International Terrestrial Reference Frame are a problem. Tying

GPS observations to distant reference stations e.g. IGS stations imposes a software processing problem, moreover the density, distribution and coverage is dictated by the in situ FBM/IBM points with right data.

- Geoid model/GGM height accurately estimated on the available FBM/IBM position with right data including its VCM. To obtain correct VCM is not straight forward.

9.3 Conclusion and Recommendations

9.3.1 Conclusion

Collection, cleaning and creation of a new gravity database for Tanzania has been given the highest priority in this study. In addition, patching of sparse gravity data area and voids was carefully studied and implemented using SRTM3 from CGIAR, pure GRACE GGM ITG-GRACE03S to degree and order 120 and combined CHAMP and GRACE GGM EIGEN-CG03C to its maximum degree and order 360; see Ch. 4 and Sect. 5.2. The reputation of the KTH LSMS with AC to determine precise local and regional gravimetric geoid models is now a state of the art as has gradually evolved and become proven in many scientific undertakings since 1989; cf. Sect. 2.3 for the examples of application of the KTH method. Determination of TZG08 geoid model of Tanzania 2008 has adhered to the requirements of the KTH method of LSMS with AC closely. For example, data correlation has been reduced to minimum as explained in Sect. 5.2 and underscored in Sect. 9.2 (ii). By use of dense SRTM DEM, and pure and combined GGM, data voids were completely eliminated, and the quality was highly improved by the tailored r-c-r approach developed in this study. Error model was carefully studied and improved for this study, see Sect. 5.3.2. Radius of the MES was determined to coincide with the GRS80 at more or less the middle of the AOI; this reduced many corrections to minimum (e.g. ellipsoidal corrections which are completely insignificant cf. Sect. 6.2.4 and Figure 6-9). Thus, in spite of the data sparseness, poor distribution and variable quality and density and other problems which existed before this research, we have managed to compute a new Tanzania geoid model (TZG08) of combined accuracy 2**9.7 cm (**cf. Sect. 7.2, Table 7-3). Had the actual observation weights been applied or at least correct relative accuracies of the GPS and TNHD orthometric height system, the actual accuracy of TZG08 is likely to be much better than 29.6 cm. Upon using approximate accuracies for GPS and TNHD, the accuracy of TZG08 is established as **27.8 cm.** The quoted 0.098 m accuracy of TNHD is very much questionable (much underrated) given its background methodology and age, (Saburi et al. 1991, Angelakis 1999).

Given the qualities of the KTH LSMS with AC and the its implementation in this study, the improved GDB used and the quality assessment carried out, the quality and accuracy of TZG08 geoid model is much better than any existing geoid model for Tanzania.

Even without consideration for the improvement to the clean and validated terrestrial gravity database of Tanzania, comparison of Figure 5-2 and Figure 8-1, shows that the original terrestrial gravity data in the area, where the external GPS/levelling assessment has been carried out, is more or less the average of high and low density gravity data in the AOI. Therefore the combined accuracy of 29.6 cm is very probably the overall representative accuracy of TZG08. It is our hope that the TZG08 will be fully utilized to

address some of the orthometric height needs of scientists and engineers in general, but more so construction engineers, planners and mapping agencies with interest in the TZG08 geoid model area $-12^{\circ} \leq \varphi \leq 1^{\circ}$ and $29^{\circ} \leq \lambda \leq 41^{\circ}$. Until the rest of the TZG08 geoid model has been assessed, we recommend that the CS should not be used outside the CS limits.

9.3.2 Recommendations

The importance and necessity of quality terrestrial gravity data of sound distribution, for the determination of accurate precise geoid model has neither changed nor expected to be replaced in the near future. In Sect. 1.2, we explained some of the major factors which hindered Tanzania from determining its own geoid model, until it was done so from outside in 2007. It came out, that the reasons are centred on the: i) lack of relevant, quality and well distributed gravity data, ii) little awareness of the nation (policy makers and fund holders) on the importance of a good geoid model for among other things, economic prosperity and social wellbeing. If ii) above is observed, funds for geodesy infrastructure and development could be obtained from the government. On top of funds for geodesy, the government is urged to establish an organ, which will be the custodian of all gravity data records observed in its territory, under terms and conditions mutually feasible and conducive to both parties. Furthermore the government should discuss with the neighbouring countries in the region for similar establishment in their countries. The reason is that accurate geoid determination needs data from a larger regional area. Henceforth, chart out suitable ways of scientific data exchange for regional cooperation and benefits.

Recommendations for the improvement of the Tanzania geoid model which follow, are charted out mostly in view of the limitations cited in Sect. 9.2.

1. To alleviate gravity data problems cited earlier, the government is urged to look into a possibility to conduct airborne gravimetry, if possible beyond the borders, by having bilateral discussions with the neighbour countries. Airborne gravimetry is likely to be cheaper compared to ground gravity observations, besides it can access almost all types of relief.
2. Assessment of TZG08 by GPS/levelling should be continued as soon as possible to the rest of the country. This will encourage and raise user's confidence to use the geoid model for developmental activities.
3. Ministry of Lands is urged to recover all possible fundamental and primary levelling network points. In addition, the network should be completed as earlier proposed (see Figure 4-24), and continue it to cover the entire country. While doing so, new locality sketches which include GPS coordinates, should be produced; the present sketches are without coordinates and they are over 40 years old. On top of that, precise GPS network on all the FBM/IBM tied to highly accurate and stable International Terrestrial Reference Frame stations should be observed and processed. Thus, VCM for the GPS and levelling networks will be obtained. The VCM are important for proper establishment of geoid model accuracy and ellipsoidal height conversion to orthometric height.
4. Effort to obtain topographic density model of the AOI should be continued for a better geoid model. Kiamehr (2006b) demonstrated the danger of using the present

constant density for topographic masses in mountainous areas such as in Iran, which are very similar to Tanzania.

5. Now that GOCE has taken place recently (March 2009), ARU and MLHSD-Tanzania are urged to commence as soon as it is practically possible, preparation for computation of improved version of TZG08 out of pure GOCE GGM (expected out in the near future), EGM2008 and the new TGDB.

In the meantime, TZG08, the new geoid model of Tanzania, should be publicised to the potential users and stakeholders to enhance economic development and social welfare.

REFERENCES

Andersen OB and Knudsen P (2003): Global marine gravity field from the ERS-1 and Geosat geodetic mission altimetry, J. Geophys. Res. Vol. 103, No. C4, p. 8129 (97JC02198). Further reading: http://www.agu.org/pubs/abs/jc/97JC02198/97JC02198.html

Andritsanos VD, Fotiou A, Paschalaki E, Pikridas C, Rossikopoulos D and Tziavos IN (1999): Local geoid model computation and evaluation. Phys. Chem. Earth (A) Vol. 25, No. 1, pp 63-69

Angelakis N, (1999): Mt Kilimanjaro expedition 1999 GPS data processing and evaluation of the ITRF position and height of Mt Kilimanjaro. First workshop on GPS and mathematical geodesy in Tanzania; October 4, 1999.

Benahmed-Daho SA, Kahlouche S and Fairhead JD (2005): A procedure for modelling the differences between the gravimetric geoid model and GPS-levelling data with an example in the north part of Algeria. Computers and Sciences 32:1733-1745.

Berry PAM, Garlick JD and Smith RG (2006): Near-global validation of the SRTM DEM using satellite radar altimetry. Earth and Planetary Remote Sensing Laboratory, De Montfort University, The Gateway, Leicester, LE19BH, UK.

Claudia CC and David JH (2005): ICESat validation of SRTM C-band digital elevation models, Geophysical Research Letters, Vol. 3

Christopher B (2006): Validation of SRTM, GLOBE and GTOPO3 in Tanzania, a BSc. dissertation in the department of Geomatics, UCLAS, University of Dar Es Salaam, 2006.

Dahl OC and Forsberg R (1999): Different ways to handle topography in practical geoid model determination. Phys. Chem. Earth (A) Vol. 24, No. 1, pp 41-46

Ellmann A (2003): On the Numerical Solutions of Parameters of the Least Squares Modification of Stokes' Formula. IAG Symp. Series 126, IUGG, Springer Verlag

Ellmann A (2004): The geoid model for the Baltic countries determined by the least squares modification of Stokes' formula. Doctoral dissertation in Geodesy No. 1061, Royal Institute of Technology (KTH), Stockholm

Ellmann A and Sjöberg LE (2004): Ellipsoidal correction to the modified Stokes formula. Boll. Geod. Sci. Aff., LXIII, 3, 153-172

Ellmann A and Vaníček P (2006): UNB application of Stokes-Helmert's approach to geoid model computation. Journal of Geodynamics 43(2007):200-213

Fan H (1989): Geoid model determination by Global Gravitational Models and integral formulas. Doctoral thesis in geodesy, department of geodesy report no. 19, KTH, Stockholm, Sweden

Fan H (1997): Theory of errors and least squares adjustment. Division of Geodesy report No. 2015 TRITA-GEOFOTO 1997:21, KTH, Sweden

Featherstone WE (1998): Do we need a gravimetric geoid model or a model of the Australian height datum to transform GPS heights in Australia? The Australian Surveyor vol. 43 No. 4

Featherstone WE (2002): Prospects for the Australian height datum and geoid model. Departmental paper, Dept. of Spatial Sciences, Curtin University, Australia.
Featherstone WE and Kirby JF (1998): Estimates of the separation between the geoid model and the quasigeoid model over Australia. Geomatics Research Australasia No. 68
Forsberg R (1984): Local covariance functions and density distributions. Rep 356, Dep Geod Sci Surv, The Ohio State University, Columbus
Forsberg R (1994): Terrain effects in geoid model computations. - lectures notes. International school for the determination and use of the geoid model. - International Geoid model Service. DIIAR, Milan, Italy.
Forsberg R (1998): The use of spectral techniques in gravity field modelling: trends and perspectives. Phys. Chem. Earth, vol. 23 No. 1, pp. 31-39
Forsberg R (2003): An overview manual for the Gravsoft Geodetic Gravity Field Modelling Programs, KMS - National Survey and Cadastre of Denmark including comments to programs by Tscherning CC (Univ. Cph) and Knudsen P (KMS)
Fotopoulos G (2003): An analysis on the optimal combination of geoid model, orthometric and ellipsoidal height data. PhD thesis, Department of Geomatics Engineering, University of Calgary, Alberta Canada.
Förste C, Flechtner F, Schmidt R, Meyer U, Stubenvoll R, Barthelmes F, König R, Neumayer KH, Rothacher M, Reigber C, Biancale R, Bruinsma S, Lemoine JM and Raimondo JC (2005): A new high resolution global gravity field model derived from combination of GRACE and CHAMP mission and altimetry/gravimetry surface gravity data (EIGEN-CG03C) European Geosciences Union (EGU05-A-04561), General Assembly Vienna, Austria, 24 - 29 April 2005.
Gachari MK and Olliver JG (1998): A high resolution gravimetric geoid model of the Eastern Africa region. Survey review, 34,269,421-436
Golden S (2002): Surfer 8 contouring and 3D surface mapping for scientists and engineers user's guide. Golden Software, Inc., Colorado USA, www.goldensoftware.com
Haagmans R, de Min Evan and Gelderen M (1993): Fast evaluation of convolution integrals on the sphere using 1-D FFT, and a comparison with existing methods for Stokes' integral. Manuscr. Geod 18(5): 27-241
Harold LH, II (2003): Cygwin User's Guide, Red Hat, Inc.
Heiskanen WA and Moritz H (1967): Physical geodesy. W.H. Freemann and Company, San Francisco, USA.
Hofmann-Wellenhof B and Moritz H (2005): Physical geodesy. Springer Wien New York
Hofmann J and Walter D (2006): How complementary are SRTM-X and -C Band Digital Elevation Models? Photogrammetric Engineering & Remote Sensing Journal of the American Society for Photogrammetry and Remote Sensing
Hunegnaw A (2001): Geoid model determination over Ethiopia with emphasis on downward continuation of gravity anomalies. Royal Institute of Technology, Division of Geodesy report No. 1057. PhD thesis, Stockholm Sweden.

Ilias D (2008): Determination of a gravimetric geoid model of Greece using the method of KTH. MSc. thesis in Geodesy, Division of Geodesy, Sch. of Arch. & Built Env. KTH – Stockholm Sweden.
Jarvis A, Reuter HI, Nelson A and Guevara E (2006): Hole-filled SRTM for the globe Version 3, available from the CGIAR-CSI SRTM 90m Database: http://srtm.csi.cgiar.org.
Kaula WM (1966): Theory of Satellite Geodesy. Blaisdell Publ., London
Kellogg OD (1929): Foundations of potential theory. Springer. Berlin.
Kiamehr R (2005): Qualification and refinement of the gravity database by cross validation approach, a case study of Iran, Proc. Geomatics 2004 (84), Conference, National Cartographic Centre of Tehran, Iran.
Kiamehr R (2006a): Precise gravimetric geoid model for Iran based on GRACE and SRTM data and the least squares modification of Stokes' formula with some geodynamics interpretations. Doctoral thesis in Geodesy, KTH – Division of Geodesy, Stockholm Sweden.
Kiamehr R (2006b): The impact of lateral density variation model in the determination of precise gravimetric geoid model in mountainous areas; a case study of Iran. Geophys. J. Int. (2006)
Kiamehr R and Sjöberg LE (2005): Effect of the SRTM global DEM on the determination of a high-resolution geoid model: a case study in Iran, J Geodesy Vol 79 No. 9; pp 540-551.
Kiamehr R and Sjöberg LE (2006): KTH-GEOLAB Scientific software for precise geoid model determination based on the least squares modification of Stokes formula (LSMS), Technical manual, KTH, Division of Geodesy
Koch KR (1999): Parameter estimation and hypothesis testing in linear models. 2nd Ed. Springer, Berlin Heidelberg New York.
Kotsakis C, Fotopoulos G, Sideris MG (2001): Optimal fitting of gravimetric geoid model undulations to GPS/levelling data using an extended similarity transformation model. Proceedings of the annual scientific meeting of the Canadian Geophysical Union of Ottawa, Canada, May 14-17.
Kotsakis C and Sideris MG (1999): On the adjustment of combined GPS/levelling/geoid model network. J Geod 73: 412-421
Kuhn M (2003): Geoid model determination with density hypotheses from isostatic models and geological information. J Geod (2003) 77: 50–65
Lemoine FG, Kenyon SC, Factor JK, Trimmer RG, Pavlis NK, Chinn DS, Cox CM, Klosko SM, Luthcke SB, Torrence MH, Wang YM, Williamson RG, Pavlis EC, Rapp RH and Olsen TR (1998): The development of the joint NASA GSFC and NIMA geopotential model EGM96. NASA Technical Publication
Li Xiong and Götze Hans-Jurgen (2001): Tutorial, Ellipsoid, Geoid model, Gravity, Geodesy and Geophysics. Geophysics 66, 1660-1668.
Ludwiga R and Schneiderb P (2006): Validation of digital elevation models from SRTM X-SAR for applications in hydrologic modelling, ISPRS Journal of Photogrammetry and Remote Sensing Vol 60, Issue 5, August 2006, Pages 339-358
Mark R, Drinkwater R, Haagmans D, Muzi A, Popescu R, Floberghagen M, Kern

and M. Fehringer (2007): The GOCE Gravity Mission: ESA's First Core Earth Explorer, Proceedings of 3rd International GOCE User Workshop, 6-8 November, 2006, Frascati, Italy, *ESA SP-627*, ISBN 92-9092-938-3, pp.1-8.
Martinec Z (1998): Boundary value problems for the gravimetric determination of a precise geoid model. Lecture notes in Earth Sciences No. 73. Springer Verlag
Martinec Z, Matyska C, Grafarend EW and Vaníček P (1993): On Helmert's 2nd condensation method. Manuscr Geod No.18. Springer.
Mayer-Guerr T (2006): Gravitationsfeldbestimmung aus der analyse kurzer bahnbögen am beispiel der satellitenmissionen CHAMP und GRACE. Dissertation University of Bonn.
Mayer-Guerr T (2007): ITG-Grace03s; The latest GRACE gravity field solution computed in Bonn. Joint International GSTM and DFG SPP Symposium, 15-17 Oct 2007, Potsdam.
Mayer-Guerr T, Eicker A and Ilk KH (2006): ITG-GRACE02S, a GRACE Gravity field derived from short arcs of the satellite's orbit. Proceedings of the first symposium of International Gravity Field Service, Istanbul Turkey, 2006.
Meissl P (1971): Preparation for the numerical evaluation of second order Molodenskii type formulas. Dept. of Geodetic Science, OSU Report No. 163, Columbus, Ohio.
Merry CL (2003a): The African Geoid model Project and its relevance to the unification of African vertical reference frames (AFREF). 2nd FIG Regional conference, Marrakech, Morocco, December 2-5, 2003
Merry CL (2003b): DEM-induced errors in developing a quasi-geoid model for Africa. J Geodesy vol. 77, No. 9 pp 537-542
Merry CL (2005): Report of Commission Project 2.3: The African Geoid model Project, part of sub-commission 2.4: Regional geoid model determination for interim activity report for IAG commission 2; The Gravity field for the period: January 2005 - December 2005
Merry CL, Blitzkow D, Abd-Elmotaal H, Fashir HH, John S, Podmore F and Fairhead JD (2005): A preliminary geoid model for Africa. In: A Window on the Future of Geodesy (Ed: Sanso, F.). Springer, Berlin.
Mikhail EM and Gracie G (1981): Analysis & adjustment of survey measurements. Van Nostrand Reinhold Company, ISBN-10: 0442253699; ISBN-13: 978-0442253691.
Molodensky MS, Eremeev VF and Yurkina MI (1962): Methods for study of the external gravity field and figure of the Earth. Translation from Russian (1960), Israel program for scientific translation, Jerusalem.
Moritz H (1980a): Advanced physical geodesy. WH Freeman, San Francisco
Moritz H (1980b): Geodetic Reference System 1980. XVII IUGG General assembly, Canberra, December 1979. Resolution No 7.
Nahavandchi H (1998): Precise Gravimetric-GPS geoid model determination with improved topographic corrections applied over Sweden. PhD Thesis, Division of Geodesy report No. 1050 KTH Stockholm Sweden.
Novak P, Vanicˇek P, Martinec Z, Ve´rroneau M (2001b): Effects of the spherical terrain on gravity and the geoid model. J Geod 75: 491–504

Novak P, Vanicˇek P, Ve´rroneau M, Holmes S and Featherstone W (2001a): On the accuracy of modified Stokes's integration in high-frequency gravimetric geoid model determination. J Geod 74: 644-654

Nsombo P (1996): Geoid model determination over Zambia, PhD Thesis in Geodesy, KTH – Division of Geodesy, Stockholm Sweden.

Olliver JG (2007): The gravimetric geoid model of Tanzania. Survey review, 39,305,212-225

Omang OCD and Forsberg R (2000): How to handle the topography in geoid model determination: three examples. J Geod 74:458–466

Parker A, Merry CL, Combrinck WL, Combrink A and Wonnacott RT (2007): Review of recent research in geodesy in South Africa; 2003 – 2006. Proceedings of the IUGG General Assembly in Perugia, Italy, 2-13, July 2007

Parker M and Marobhe I (1991): Review of gravity survey in Tanzania. Eastern and Southern African Mineral Resource Development Centre report ESAMRDC/91/TECH/68 to Tanzania Petroleum Development Corporation (TPDC)

Paul MK (1973): A method for evaluating the truncation error coefficients for geoid heights. Bull Geo 110: 413-425.

Pavlis, NK, Holmes SA, Kenyon SC and Factor JK (2008): An Earth Gravitational Model to degree 2160: EGM2008, presented at the 2008 general assembly of the European Geosciences Union, Vienna, Austria, April 13-18, 2008.

Press WH, Teukolsky SA, Vetterling WT, Flannery BP (1992): Numerical recipes in Fortran, 2nd ed. Cambridge University Press, Cambridge UK.

Reigber CH, Schwintzer P, Stubenvoll R, Schmidt R, Flechtner F, Meyer U, König R, Neumayer H, Förste CH, Barthelmes F, Zhu SY, Balmino G, Biancale R, Lemoine JM, Meixner H and Raimondo JC (2004): EIGEN-CG01C; A high resolution Global Gravity field Model combining CHAMP and GRACE satellite mission and surface gravity. Data joint CHAMP/GRACE science meeting, GFZ, July 5-7

Saburi J, Laswai ZJM, Richard BK, Stephen DM and Msemo HO (1991): Proposal for rigorous systems of heights for East Africa. Technical report no. 90-1, Department of Land Surveying Ardhi Institute Dar Es Salaam Tanzania.

Sjöberg LE (1977): On the errors of spherical harmonic developments of gravity at the surface of the earth. Rep 257, Department of Geodetic Science, The Ohio State University, Columbus

Sjöberg LE (1984a): Least squares modification of Stokes' and Venning-Meinesz' formulas by accounting for truncation and potential coefficients errors. Manuscr Geod: 9, 209-229

Sjöberg LE (1984b): Least squares modification of Stokes and Venning-Meinesz formulas by accounting for errors of truncation, potential coefficients and gravity data. Department of Geodesy, report no. 27, University of Uppsala, Institute of Geophysics.

Sjöberg LE (1985): Some methods of estimating geoid model undulations by Least squares combination of Stokes's and geopotential coefficients. The Royal Institute of Technology (KTH), Department of Geodesy, Report No. 1, KTH

Stockholm.
Sjöberg LE (1986): Comparison of some methods of modifying Stokes' formula using GEM 9 potential coefficients. Boll. Geod. Sci. Aff., 45, 3, 229-248
Sjöberg LE (1991): Refined least squares modification of Stokes' formula. Manuscripta geodaetica 16: 367-375
Sjöberg LE (1994a): The total terrain effects in the modified Stokes' formula. In: Sünkel H, Marson I (eds) Gravity and geoid model. International Association of Geodesy Symposia, vol. 113. Springer, Berlin Heidelberg New York, pp 616-623
Sjöberg LE (1994b): On the terrain effects in geoid model and quasigeoid model determinations using Helmert's second condensation method. Division of Geodesy Res Rep 36, The Royal Institute of Technology, Stockholm
Sjöberg LE (1995): On the quasigeoid model to geoid model separation. Manuscripta geodaetica 20:182–192
Sjöberg LE (1998a): The exterior Airy/Heiskanen topographic-isostatic gravity potential, anomaly and the effect of analytical continuation in Stokes' formula. J Geod, 72: 654-662.
Sjöberg LE (1998b): The atmospheric geoid model and gravity corrections. Bolletino di Geodesia Scienze Affini, 57, 4, 421- 435
Sjöberg LE (1999): The IAG approach to the atmospheric geoid model correction in Stokes' formula and a new strategy. J Geod 73(7):362–366
Sjöberg LE (2000): Topographic effects by the Stokes–Helmert method of geoid model and quasi-geoid model determinations. J Geod 74(2):255–268
Sjöberg LE (2001a) The effect of downward continuation of gravity anomaly to sea level in Stokes' formula. J Geod, 74: 790-804.
Sjöberg LE (2001b): Topographic and atmospheric corrections of gravimetric geoid model determination with special emphasis on the effects of harmonics of degree zero and one. J Geod 75: 283-290
Sjöberg LE (2003a): A general model of modifying Stokes formula and its Least squares solution. J Geod 77:459–464
Sjöberg LE (2003b): A Computational scheme to model the geoid model by the modified Stokes' formula without gravity reductions. J Geod 77:423-432
Sjöberg LE (2003c): A solution to the downward continuation effect on the geoid model determined by Stokes' formula. J Geod
Sjöberg LE (2003d): The correction to the modified Stokes formula for an ellipsoidal earth. In: Santos M. (ed.): Honoring the academic life of Petr Vanic˘eck. Tech. rep. no. 218, dept. of Geodesy and Geomatics Engineering, the University of New Brunswick (UNB), Fredericton, Canada. pp. 99–110.
Sjöberg LE (2003e): Ellipsoidal corrections to order e2 of geopotential coefficients and Stokes formula. J Geod (2003) 77
Sjöberg LE (2004a): The ellipsoidal corrections to the topographic geoid model effects. J Geod (2004) 77: 804–808
Sjöberg LE (2004b): The effect on the geoid model of lateral topographic density variations. J Geod (2004) 78: 34–39
Sjöberg LE (2004c): A spherical harmonic representation of the ellipsoidal correction to the modified Stokes formula. J Geod (2004) 78: 180–186

Sjöberg LE (2005a): A discussion on the approximations made in the practical implementation of the remove–compute–restore technique in regional geoid modelling. J Geod (2005) 78: 645–653
Sjöberg LE (2005b): A local least squares modification of Stokes' formula. Stud Geophys Geod (49)23-30
Sjöberg LE (2006a): The effects of Stokes formula for an ellipsoidal layering of the Earth's atmosphere. J Geod (2006) 79: 675–681
Sjöberg LE (2006b): From normal height to orthometric height, from quasi-geoid model to geoid model. Paper presented to the NKG General meeting in Copenhagen, May 2006
Sjöberg LE (2007): The topographic bias by analytical continuation in physical geodesy. J Geod 81:345-350
Sjöberg LE and Featherstone WE (2004):Two-step procedures for hybrid geoid modelling. J Geod (2004) 78: 66–75
Sjöberg LE and Hunegnaw A (2000): Some modifications of Stokes' formula that account for truncation and potential coefficient errors J Geod (2000) 74: 232-238
Sjöberg LE and Nahavandchi H (2000): The atmospheric geoid model effects in Stokes' formula. Geophys. J. Int.140 (1):95-100
Sjöberg LE and Ågren J (2002): Some problems in the theory used for the NKG geoid model. In M Poutanen (Ed.): Proc. Nordic Geodetic Commission General Meeting, Helsinki 1-5 October 2002.
Stokes GG (1849): On the variation of gravity on the surface of the Earth. Trans Camb Phil Soc 8: 672-695
Tenzer R, Novák P, Janák J, Huang J, Najafi-Alamdari M, Vajda P, Santos M (2003): A review of the UNB approach for precise geoid model determination based on the Stokes-Helmert method. In: Santos M. (ed.): Honoring the academic life of Petr Vanic˘eck. Tech. rep. no. 218, dept. of Geodesy and Geomatics Engineering, the University of New Brunswick (UNB), Fredericton, Canada.
Tscherning CC, Knudsen P and Forsberg R (1992): Description of the Gravsoft package, in proceedings of the 1st continental workshop on the geoid model in Europe, Prague. May 11-14.
Tscherning CC, Knudsen P and Forsberg R (1994): Description of the Gravsoft package. Geophysical Institute, University of Copenhagen, Technical Report ed, 1994.
Tscherning CC and Rapp RH (1974): Closed covariance expressions for gravity anomalies, geoid model undulations, and deflections of the vertical implied by anomaly degree variance models. Report No. 355, Dept. of Geod Sci, Ohio State Univ, Columbus, Ohio.
Vaníček P and Featherstone WE (1998): Performance of three types of Stokes's kernel in the combined solution for the geoid model. J Geod 72
Vaníček P, Huang J, Novák P, Pagiatakis SD, Véronneau M, Martinec Z and Featherstone WE (1999): Determination of the boundary values for the Stokes-Helmert problem, Journal of Geodesy, Vol.73, Springer.
Vaníček P and Kleusberg A (1987): The Canadian geoid model – Stokesian

approach. Manuscr Geod 12: 86-98
Vaníček P and Krakiwsky EJ (1986): Geodesy the concepts. Elsevier Science Pub. Co.
Vaníček P and Martinec Z (1994): The Stokes-Helmert scheme for the evaluation of a precise geoid model. Manuscr Geod 19: 119-128
Vaníček P and Sjöberg LE (1991): Reformulation of Stokes's theory for higher than second degree reference field and modification of integration kernels. Journal of Geophysical research, Vol. 96, No.B4.
Vaníček P, Sun W, Ong P, Martinec Z, Najafi M, Vajda P and Horst B (1996): Downward continuation of Helmert's gravity. J. Geodesy 71, 21–34.
Wells DE and Krakiwsky EJ (1997): The method of least squares, Lecture notes no.18 (original 1971, reprint 1997), Department of Geodesy and Geomatics Engineering, University of New Brunswick (UNB), Canada.
Wenzel G (1981): Zür Geoid modelbestimmung durch Kombination von Schwere anomalien und einem \kunglfunktionsmodell mit Hilfe von integralformeln. ZfV., 106, 3, 102-111.
Wenzel G (1982): Geoid model computation by least squares spectral combination using integral kernels. Presented to symposium 4b "Geoid model Definition and Determination" General Meeting of IAG, Tokyo 1982.
William J (revised for 4.3BSD by Mark Seiden) (1998): An Introduction to the C-shell, Computer Science Division Department of Electrical Engineering and Computer Science University of California, Berkeley, California 94720
Wong L and Gore R (1969) Accuracy of geoid heights from modified Stokes kernels, Geophysical Journal of the Royal Astronomical Society 18, 81-91.
Ågren J (2004a): The analytical continuation bias in geoid model determination using potential coefficients and terrestrial gravity data. Accepted for publication in Journal of Geodesy
Ågren J (2004b): Regional geoid model determination methods for the era of satellite gravimetry. (Numerical investigations using synthetic earth gravity models). Doctoral thesis, KTH – Division of Geodesy, Stockholm Sweden.
Ågren J Kiamehr R and Sjöberg LE (2006a): Progress in the determination of a gravimetric quasi-geoid model over Sweden, Nordic geodetic commission general assembly, May 29 to June 2, 2006, Copenhagen, Denmark.
Ågren J Kiamehr R and Sjöberg LE (2006b): The Swedish geoid model as evaluated by the method of least squares modification of Stokes with additive corrections, the first international symposium of the International Gravity Field Service (IGFS), August 28 – 1st September 2006, Istanbul, Turkey.
Ågren J and Sjöberg LE (2004): Comparison of some methods for modifying Stokes' Formula in the GOCE Era. Proc. 2nd International GOCE user workshop "GOCE, The Geoid model and Oceanography" ESA-ESRIN, Frascati, Italy 8-10 March, 2004.